SSC-SR-1032

The Superconducting Super Collider

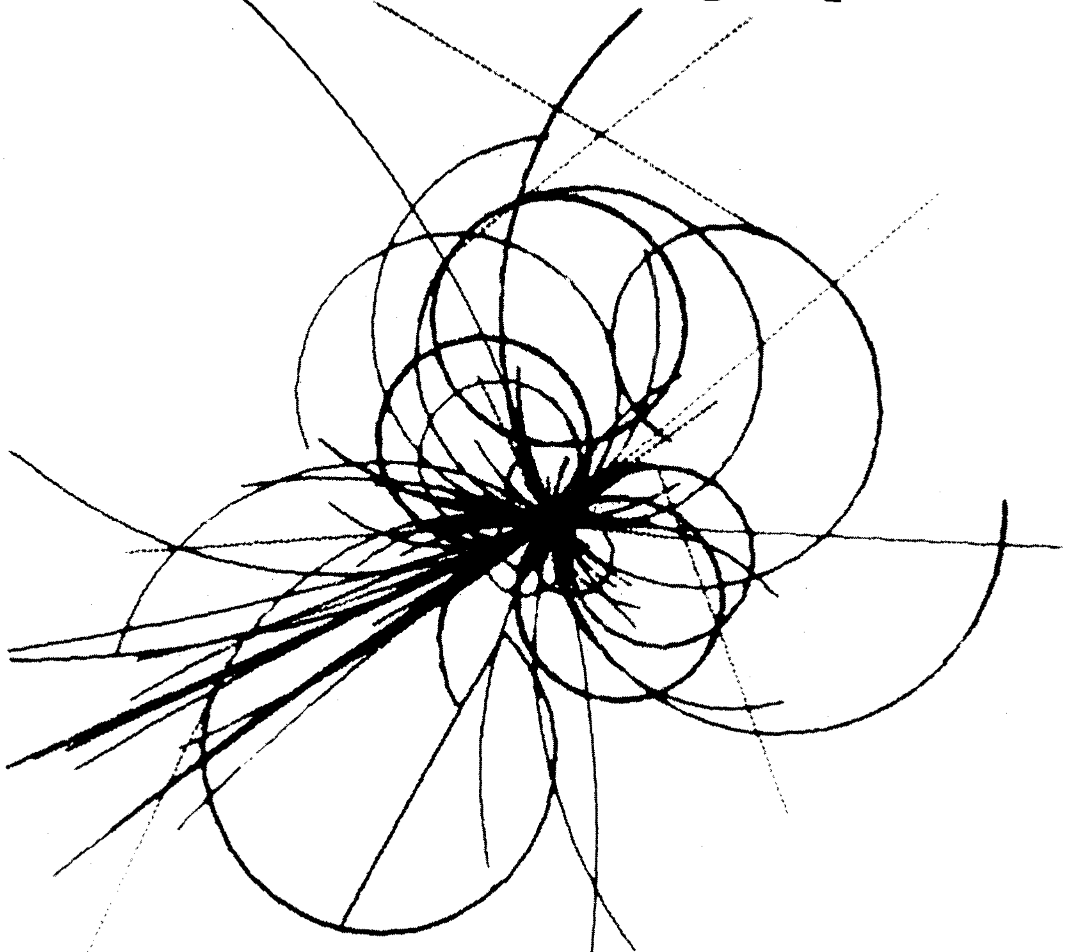

Report of the SSC Workshop on Distributed Multipole Correction Coils

Task Force Report

R. Sah, Editor
SSC Central Design Group

January 1988

SSC-SR-1032

Report of the SSC Workshop on Distributed Multipole Correction Coils

R. Sah, Editor

SSC Central Design Group*
c/o Lawrence Berkeley Laboratory
Berkeley, California 94720

January 1988

* Operated by Universities Research Association for the U.S. Department of Energy

Executive Summary

The SSC Workshop on Distributed Multipole Correction Coils was held at Brookhaven National Laboratory on October 13 and 14, 1987. This Workshop was organized by the SSC Central Design Group, and its purpose was to discuss the present status of specifications, designs, and R&D plans for distributed, actively-powered multipole correction coils (i.e., bore tube windings) for the SSC. The Workshop had 25 participants, including seven from industry and one from DESY, in Germany. A list of participants is included as part of this report.

The Workshop was organized into four consecutive sessions to discuss the following topics: requirements for distributed correction coils, distributed correction coil designs, materials issues, and plans for future R&D. The Workshop agenda is included as Appendix A. The following conclusions were drawn from the workshop:

(1) Accelerator physics considerations indicate that distributed multipole correction coils represent a feasible and flexible method to correct magnetic field errors in the SSC.

(2) Considerable progress has been made by Brookhaven National Laboratory in collaboration with industry to develop a possible fabrication technique for distributed correction coils. This technique consists of imbedding superconducting wire in a flexible plastic substrate. Its feasibility for the SSC still needs to be demonstrated. BNL has presented a preliminary plan for the necessary R&D.

(3) A successful technique has been developed to manufacture distributed correction coils for HERA. The coil performance is excellent. As yet, no plan has been proposed to study this type of correction coil for the SSC.

(4) The results from an experiment to study radiation damage to organic materials, although still preliminary, are providing guidance in selecting the most radiation resistant materials to use in correction coils. The test samples in this experiment were subjected to much larger radiation doses than expected at the SSC. Considerable information on radiation damage is available in the literature.

Table of Contents

Appendix G: BNL 39615, "Development of the SSC Trim Coil Beam Tube Assembly," J. Skaritka et al., March 16, 1987.

Appendix H: "Results to Date: SSC Correction Coil Performance," talk by Peter Wanderer.

Appendix I: "HERA Correction Coil Design and Performance," talk by Peter Schmueser.

Appendix J: "Radiation Damage to Organic Materials," talk by Roger Clough.

Appendix K: "Results of Radiation Damage Experiments at BNL," talk by Al Prodell. Appendix includes summary of experimental results.

Appendix L: "Proposals for New Materials," talk by John Skaritka.

Appendix M: "Cryogenic Performance of Materials," talk by Mort Katz.

Requirements for Distributed Correction Coils

The main function of the distributed correction coils (or bore tube windings) described in SSC-SR-2020, the Conceptual Design Report (CDR) for the Superconducting Super Collider (SSC), is to compensate for the systematic field errors in the SSC magnets, especially the field distortions due to superconductor magnetization currents and due to iron saturation. The correction coils consist of long windings that are attached to the outside of the beam tubes. These coils are located within the main dipole magnets; and, within each dipole magnet, half of the available length along the beam line is devoted to a b_2 coil (sextupole), and the remaining length is divided between b_3 and b_4 coils (octupole and decapole).

The SSC also has "lumped" correctors that are discrete elements not contained within the main dipole magnets. These correction magnets are contained in the spool pieces. From an accelerator physics point of view, this hybrid correction scheme provides a very satisfactory field compensation, assuming that the expected field uniformity is achieved (for example,at injection, $b_2 \leq 4.7$, $b_4 \leq 0.3$, and $b_6 \leq 0.07$, all expressed in standard units of 10^{-4} B_o at 1 cm). (See Appendix B for the projection transparencies from a talk by Richard Talman.) The correction coils can be powered to achieve the required tolerance on tune variation ($\Delta\nu \leq 0.005$ at 5 mm amplitude and 0.001 fractional momentum deviation). They can also be used, via the "binning" technique, to help compensate for random field errors.

Other compensation schemes for field errors are being considered. It is possible that in the final SSC design, some or all of the multipole correction coils will be replaced by lumped correction magnets. Tune shift calculations, described in Appendix B, indicate that such schemes are capable of satisfactorily compensating substantial systematic field errors. Preliminary tracking studies support the conclusion that lumped correctors can provide satisfactory compensation; however, since relevant studies of the "smear", resonance widths, and other indicators of accelerator performance have not yet been completed, it is not certain whether lumped correctors alone can compensate for very large systematic field errors.

Continuing studies will focus on understanding in detail how well these lumped-corrector compensation schemes would work. Although completed after the Workshop, SSC-N-401, "A Design for SSC Multipole Correction Coils," by Richard Talman, is included as Appendix C. Other SSC Notes on this subject include SSC-N-383 by E. Forest and J. Peterson, SSC-N-413 by R. Talman, and SSC-N-417 by D. Neuffer.

Distributed Correction Coil Designs

This workshop session included the following topics:

(1) Magnetic Design
(2) Engineering Design and Multiwire Techniques
(3) Results to Date: SSC Correction Coil Performance
(4) HERA Correction Coil Design and Performance

Magnetic Design

The magnetic design of the distributed multipole correction coils were discussed in a talk by Pat Thompson. See Appendix D.

Conductor Parameters

The conductor requirements for the distributed correction coils are much less severe than those for the main dipole windings. The new parameters for the conductor (single-strand conductor; 0.014 in. or 356 μm strand diameter; 54 filaments per strand; 27 μm filament diameter; and $J_c > 2.2$ kA/mm^2) were selected primarily on the basis of the following major criteria:

(1) The wire diameter must be small enough so that the wire can be "written" with the Multiwire machine. (See Appendices F and G.)
(2) It was desired that the "short sample" current for the conductor be greater than 4 times the desired operating current.
(3) The field distortions due to superconductor magnetization currents in the correction coils must be much less than those from the main dipole coils.

Although the above criteria certainly lead to a workable correction coil design, two possible modifications to these criteria should be considered. The factor of 4 margin in the short sample current might be reduced, thus permitting an attractive decrease in the wire size. The thinner conductor, of course, would be easier to form into correction coils using the Multiwire machine. The choice of a different conductor might reduce the field distortions due to superconductor magnetization currents by perhaps a factor of two. However, an adequate margin in the current density must be provided to accommodate energy deposition in the correction coils due to beam loss and hadronic cascades.

Automation of Coil Wiring Process

An automated system has been developed to wind the correction coils. The Multiwire Division of Kolmorgan Corporation has adapted a machine to wind correction coils directly onto a flexible plastic-foil substrate. In addition, outlines of the coils are drawn onto transparent plastic sheets, which can be used as templates for visually checking the accuracy of the finished coil assembly. The coil assembly is then wrapped around the bore tube of a dipole magnet and is tightly bound to it. In this way, the desired wire placement, determined on the basis of magnetic field requirements, can be accurately and largely automatically achieved during the manufacture of the correction coils.

Construction Accuracy and Field Errors

Included in Appendix D is SSC-N-226, "Field Quality for SSC Internal Trim Coils," Pat Thompson, August 20, 1986. This paper discusses the magnetic field errors which would result from construction inaccuracies in the multipole correction coils and presents an estimate of the field accuracy that can be readily achieved, given the present state of technology. The construction errors considered were the following:

(1) Displacement of a correction coil as a whole, transverse to the beam direction.

(2) Rotation of a coil, about its central axis.

(3) A gap in the coil, generated by wrapping the correction coil assembly around a bore tube that has an incorrect diameter.

(4) Elliptical distortion of the bore tube.

(5) Random wire displacements.

(6) Displacements of "blocks" of wires. For example, a sextupole coil is considered as 12 separate blocks or groups of wires.

The rms magnetic field errors expected from *coil* placement errors in the correction coils (in contrast to placement errors of *individual wires*) were about 5 percent of the correction coil field, assuming the following rms construction errors: x displacement of 0.25 mm, y displacement of 0.25 mm, and 0.9° coil rotation error. The magnetic field measurements, discussed in a later section of this report, indicated that the actual accuracies were somewhat better. Wire displacements and block displacements do not tend to generate large field errors.

Appendix E is a note by Jack Peterson and Alex Chao on "Tolerances of Beam-Tube Corrector Errors." This note includes a table on the tolerances for *random* errors of correction coil construction. The first two columns of the table give the type of construction error being considered and the accuracy that must be achieved. The next two columns show the strength of the most important multipole error field which is generated, and the last column identifies the correction coil which generates that error field. The tolerances for *systematic* construction errors are not yet available.

Engineering Design and Multiwire Techniques

The engineering design of the SSC correction coils, discussed briefly above, is described in detail in Appendices F and G. Accurate and rapid conductor placement is achieved by using a Multiwire wiring machine to lay down - or "write" - an insulated superconductor wire in a coil pattern on a flat flexible substrate, which has been coated with a thermosetting adhesive.

Several manufacturers play important roles in the construction of the SSC correction coil prototypes. Du Pont Company bonds a layer of Kapton to a layer of FEP Teflon, and the finished product is laminated at Sheldahl, Inc., with a composite of glass and Multiwire RC205 adhesive. This substrate material is then precision slit at the Metlon Company, and precise sprocket holes and locating slots are punched by the Schneider and Marquard Company. Finally, Multiwire lays the wire in a coil pattern on this finished substrate, and the completed correction coil assembly is delivered to BNL.

The Multiwire machine was originally developed to lay copper wire onto a layer of adhesive on a circuit board, and it has been adapted to construct correction coils for the SSC. The wire can be written to an accuracy of about .001 in. (25 μm), and coated wire with a .008-in. diameter has been written at speeds up to 600 inches per minute (15 m/min). To achieve a production rate of 10 dipoles' worth of coils per day, about 4 wiring machines would be needed. Recently, Kapton-wrapped, .014-in. superconductor wire has been successfully laid down, at about 175 inches per minute (4 m/min). At this speed, about 10 wiring machines would be needed.

When the correction coil assembly is completed, it is wrapped around the insulated beam tube and tightly secured with layers of Kevlar impregnated with FEP Teflon. The materials used in the coil manufacture must exhibit radiation resistance as well as have good mechnical properties over a wide temperature range. A final insulating layer of Kapton is applied to the assembly to prevent shorts to the main dipole coils. Accurate positioning of the coil assembly on the bore tube is provided by guides which fit into slots cut into the coil substrate. The completed correction coil and beam tube assembly is keyed to the dipole magnet collars at the top and the bottom. G-10 spacers between the distributed multipole correction coils and the main dipole coils limit flexure during operation. The evolution of the engineering design during the prototype development is described in Appendix F.

Results to Date: SSC Correction Coil Performance

Four 4.5 m and two 17 m sextupole correction coils have been built using the Multiwire technique and tested within dipole magnets. Useful quench current data were acquired for two of the 4.5 m coils and one of the 17 m coils. The quench currents of the remaining coils were adversely affected by the presence of the warm beam-tube insert containing the magnetic-field measurement coil. The .008-in. superconductor wire used in these model correction coils has a "short sample" current of 16 A at a main dipole field of 6.6 T; the design operating current is 4 A.

The details of the correction coil test data are given in Appendix H. The quench current histories of the two 4.5 m coils, tested in a 5.8 T magnetic field, were similar: all quenches were above 4 A, the coils trained to the short sample current in 5 to 10 quenches for each current polarity, the coils remembered their previous training after a single polarity reversal, and they required retraining after thermal cycling to room temperature. The quench currents for the 17 m coil exhibited an unexpected dependence on history and ramp rate, possibly because of a suspected short circuit in the vicinity of a splice. This coil did reach currents of 7 to 12 A in fields of 4 to 5.5 T, but the quench data were insufficiently repeatable to permit a sensible detailed analysis.

Although the short coils meet specifications, it is troubling that the coils require so much training to reach the short sample current. Considerable development remains before the present performance goals can be achieved (64 A short sample current in a 6.6 T dipole field, 16 A operating current). Serious consideration should be given to reducing the factor of 4 safety margin incorporated in the design operating current: not only does this large safety margin lead to an inefficient use of superconductor in producing a given correction field, but the presence of extra superconductor increases the field distortions due to superconductor magnetization currents. These field distortions are particularly serious at low field (i.e., during SSC injection). The HERA experience with correction coils (discussed later in this report and in Appendix I) indicates that routine operation at a large fraction of the short sample current is possible, if the superconducting wires are firmly supported mechanically, so that they do not move under the influence of Lorentz forces. However, the operating margin must be set high enough to deal with hadronic showers in the coils.

When superconducting wires are immersed in an external magnetic field, that field can generate magnetization currents and field distortions. In Appendix H, the measured multipole fields are given for the correction coil operating at 2 A while immersed in a 2 T dipole field, because these conditions correspond roughly to the largest fractional magnetic field correction which is required from the coils. In the last table of Appendix H, the measured multipole fields are presented. For comparison, the field accuracy requirements for the SSC dipoles are also given. When the measured multipole fields are compared with the requirements for the correction coil field accuracies (given in Appendix E), it can be seen that the construction accuracies appear to be about what is required: many *random* multipole tolerances have been met. Not much can be said at this point about the *systematic* field errors. The requirements have not been determined precisely, and not enough coils have been measured to shed much light on this issue.

HERA Correction Coil Design and Performance

Appendix I consists of the projection transparencies from Peter Schmueser's talk on the HERA correction coils. Care must be taken when using this Appendix, because the notation used at HERA to describe multipole fields differ from that used at the SSC: the indices differ by one (at HERA, "b_2" means the quadrupole field, not the sextupole field), and the reference radius is 25 mm. A successful method to fabricate correction coils has been developed at HERA. This design is an extension of the design of the correction coils in CBA magnets. The HERA correction coils are about 6 m long and have an outer diameter of 67 mm. For comparison, the corresponding dimensions for the SSC coils are 8 m and 36.3 mm.

HERA has distributed correction coils which produce quadrupole fields and sextupole fields. A pair of 6 m coils is mounted on the cold beam pipe, within the main dipoles, near each quadrupole magnet. Each correction coil assembly consists of 3 sextupole subcoils mounted on the beam pipe and 2 quadrupole subcoils wrapped around the sextupole subcoils. The quadrupole correctors have a design field strength of 0.048 T at a radius of 25 mm, and the sextupole correctors have a strength of 0.03 T at the same radius. The technique used to fabricate the HERA correction coils is very different from that proposed by BNL for the SSC correction coils. Single-strand, multifilament superconductor wire with a diameter of .028 in. (0.70 mm) is wrapped with Kapton film and with a glass-fiber and epoxy layer. This insulated wire is wound into a subcoil, and the subcoil is cured in a press. The various subcoils are then mounted on the beam tube and are lashed tightly to the tube with a compression wrapping of glass fiber. Early prototypes using a compression wrapping of aramid fibers exhibited an unacceptable loss of tension during cooldown. The field quality of the HERA correction coils significantly exceeds the accelerator physics requirements.

The HERA correction coils are designed to operate at a nominal current of 85 A, and the acceptance limit was set at 230 A (about 79 percent of the short sample current of 290 A). In the first production series of 61 coils, all made with BBC conductor, all but one coil exceeded the acceptance limit. However, of the first 148 coils, about 10 percent failed the acceptance limit. This problem was traced to the superconducting wire, which had flaws which could be located using an eddy current technique. Since this problem came to light, only eddy-current tested superconductor has been used in HERA correction coils.

The alignment scheme for the HERA correction coils depends on sensing induced signals in the correction coils, when the main dipole coils are excited with a 500 Hz ac waveform. The alignment is accurate to about 1 mrad.

The HERA correction coils are being constructed using a simple and proven technique which may possibly be adapted for the SSC. However, no proposals have been made at this time to study the use of HERA style correction coils at the SSC.

Materials Issues

This workshop session included the following topics:

(1) Radiation Damage to Organic Materials
(2) Results of Radiation Damage Experiments at BNL
(3) Proposals for New Materials
(4) Cryogenic Performance of Materials

Radiation Damage to Organic Materials

Appendix J consists of the projection transparencies from the introductory talk on this topic given by Roger Clough. Some of the presented material will be contained in a future publication.*

Much of the data comes from experiments conducted at Sandia, where there is a swimming-pool radiation-exposure facility for subjecting samples to ionizing radiation (gamma rays) from a Cobalt 60 source. This facility permits the simultaneous exposure of many samples at different conditions of dose rate, temperature, and atmospheric environment. In general, there are two major mechanisms of radiation damage to polymers. *Cross linking* of molecular chains tends to harden materials, while *scission* of chains leads to softening. The dominance of one mechanism over the other controls the type of radiation damage which is observed.

Many radiation degradation effects in organic materials can be understood in terms of the following model:

(1) The radiation exposure creates highly-reactive free radicals in the material.
(2) In the presence of oxygen, the free radicals undergo oxidation reactions. As these reactions go to completion, the degradation of material properties occurs.
(3) In an inert environment (nitrogen, helium, vacuum, etc.), the oxidation reactions cannot go to completion, so the free radicals remain in the material. Generally, much less radiation damage is apparent. If the sample is exposed to oxygen at a later time, the oxidation occurs and the radiation damage becomes much more pronounced.

* R.L. Clough, "Radiation Resistant Polymers," **Encylopedia of Polymer Science and Engineering** (John Wiley & Sons), to be published.

Appendix J contains some experimental data on radiation degradation; these examples can be understood in terms of the above model.

(1) One experiment shows the *oxygen effect* on the radiation degradation of PVC. See page J-7. The capacity for tensile elongation is the ability of a material to be stretched before it breaks. In this experiment, the capacity for tensile elongation, relative to its initial value, is used as a measure of mechanical elasticity. Under simultaneous conditions of radiation and elevated temperature, the PVC is found to degrade quickly in air, while the same material largely retains its original properties in a nitrogen atmosphere.

(2) A second experiment (in air) illustrates the *dose-rate effects* of radiation damage to PVC. See page J-8. Again, the loss of the capacity for tensile elongation is used as a measure of radiation damage. When tensile elongation is plotted against total radiation dose (in Mrad), for different dose rates, it can be seen that low dose rates lead to greater apparent damage at a given total dose. This dose-rate effect can be understood in terms of the time that is required for the oxidation reactions to go to completion, and indeed this effect is not observed in experiments conducted in an inert atmosphere.

(3) The *radiation sensitization* of polyethylene to thermal degradation is demonstrated in an experiment (page J-9) where the degradation of tensile elongation due to elevated temperatures is found to be much faster in a sample that had previously been irradiated. This effect can be understood in terms of the free radicals (or peroxides) that were created in the material during irradiation and that did not react until the sample was exposed to high temperatures.

(4) On Page J-10 is shown experimental data that illustrate the *inhomogeneous degradation* of a test sample. Here, the hardness of a sample is quantified by measuring the penetration of a sharp probe. The circular data points show the uniform initial hardness of the sample, and the squares show the radiation hardening which is observed in an inert atmosphere. The triangles, however, show that the hardness of the sample undergoes inhomogeneous changes when the sample is irradiated in air. The sample surfaces, exposed to oxygen, have softened while the core of the sample has hardened in the absence of oxygen.

As discussed earlier, the radiation degradation of organic materials often exhibits significant dose-rate effects. In particular, low dose rates can lead to high levels of degradation for a given total dose, so it is important to estimate the damage that occurs at very low dose rates. Because it is very time consuming to irradiate samples to large total doses while maintaining a very low dose rate, an **accelerated aging method** has been developed in which irradiation at elevated temperatures is used to simulate irradiation at low dose rates. Page J-12 shows the total dose required to reduce the tensile elongation capacity by 40 percent at various conditions of temperature and dose rate. It can be seen that low dose rates and high temperatures lead to greater radiation damage. The data points for which the samples became heterogeneous are discarded. Then the 43°C data are held fixed, while the data points for each high temperature condition are shifted to the left until a single curve is created, as shown on page J-13.

When an organic compound is being selected for applications requiring radiation resistance, several issues must be considered. The inherent radiation resistance of the compound for the relevant conditions (inert environment vs. oxidizing atmosphere) should be considered. The data given in Appendix J show that some organic compounds, such as aromatic compounds (i.e., those containing an unsaturated ring of carbon atoms), are especially radiation resistant. Note that chemical stability is not a good indication of radiation resistance.

The inherent radiation resistance of an organic compound can be increased through the use of additives such as antioxidants. Even small proportions of additives can have a major effect.

Results of Radiation Damage Experiments at BNL

Appendix K contains the projection transparencies from a talk by Al Prodell on this subject. Also included is a tabular summary of the results of the experiments. The test samples used in the radiation damage experiments were fabricated from various combinations of materials, including organic materials being considered for correction coil construction. The 3.8 to 7.3-cm diameter samples were exposed to 193 MeV protons at the Brookhaven Linac Isotope Producer (BLIP) beam line. Every 200 ms, the linac produced a 22 mA proton pulse which had a duration of 420 μs. Since the BLIP beam line received 12 out of every 13 linac pulses, the average BLIP beam current was 42 μA. Each sample was exposed for about one half hour, so the dose was 21 μA-hr. The beam size was about 2.1 cm (full-width, half-maximum), so the effective beam area was about 3.5 cm^2. The exposures had been designed to provide a total dose of 40 MGy, assuming a 6.9 cm^2 beam area, so the actual total dose was about 80 MGy. A preliminary estimate of the total radiation dose to the correction coils during the lifetime of the SSC is on the order of 1 MGy, as described in SSC-N-439 by Don Groom.

Over 50 samples were studied in this irradiation experiment, and the results are summarized in Appendix K. Some samples survived the radiation well, but others clearly were damaged. For example, RX630 swelled about 6 percent and lost considerable compressive strength; RC205 Multiwire adhesive became brittle and lost most of its wire peel strength; FEP Teflon lost much of its bond strength and became brittle after exposure to air; and Kevlar fibers became brittle and weak. Although this experiment exposed test samples to much greater total radiation doses than anticipated at the SSC, the preliminary results of the experiment will be used to select more radiation-resistant materials to be used in future correction coil models. This strategy will ensure, at no increase in cost, that the materials used in the correction coils will survive, even if considerably higher total irradiation doses were encountered at the SSC than is presently expected.

The results of this experiment are providing valuable guidance in the selection of materials with greater radiation tolerance; however, it would be desirable to make a more accurate estimate of the total radiation dose which the SSC correction coils must withstand. Peter Schmueser commented that DESY has a modeling program which can be used to perform the SSC calculation.

Proposals for New Materials

Appendix L consists of the projection transparencies from a talk by John Skaritka on the choice of improved materials to be used in future models of correction coils. The proposed changes are listed, and the reasons for the changes are given. For example, the compressive wrapping of Kevlar fiber will be replaced by glass fiber, because glass has a better thermal contraction coefficient, has greater radiation resistance, and is less costly. Appendix L includes a schematic diagram of the current choices for construction materials for the correction coils, and it discusses possible additional changes.

Cryogenic Performance of Materials

Appendix M consists of the projection transparencies from a talk by Mort Katz on the mechanical and electrical properties of various organic materials at low temperatures. Also included were some data on the radiation resistance of these materials. The following topics were discussed:

(1) Some properties of Du Pont fluoroplastic resins.
(2) Experimental data on mechanical properties of these materials down to about 77 K.
(3) Electrical properties of various organic materials at liquid helium temperatures and above.
(4) Radiation damage data on Kapton (Du Pont trademark) polyimide film.

Generally speaking, there is not a great deal of experimental data on the cryogenic properties of the organic materials which have been considered for correction coil construction, partly because some materials, such as Kapton, are especially valued for their excellent *high temperature* properties. However, Du Pont Company might be willing to measure materials properties at conditions that are important for SSC applications.

What's Next ?

The last session of the workshop was devoted to a discussion of future plans for R&D on distributed correction coils for the SSC. A plan to build and test short correction coil models is outlined on the last page of Appendix L. Briefly, 0.6-meter models will be built to test new construction methods and materials before longer models are attempted.

Leonard Schieber presented some preliminary thoughts on using the Multiwire technique to build correction coils directly on the surface of the bore tube, rather than fabricating the coils on a flexible substrate. He felt that this process would be feasible. One major advantage of applying the coils directly onto the bore tube is a possible improvement in the accuracy of conductor placement: specifically, this technique may provide a straightforward way to accommodate small variations in the diameter of the beam tube. In the present method of correction-coil fabrication, the coil assembly is wrapped around the beam tube, so any variation in tube diameter leads to a poor mechanical fit and to magnetic field errors. (It is possible, however, that the present technique might be modified to compensate for bore-tube diametric variations. One scheme would be to select individually the thickness of the Kapton wrapping for every bore tube, so that all the wrapped tubes would have identical diameters.) Two fabrication concepts were presented for applying the correction coils directly onto the beam tubes. The tube can move back and forth under the wiring head, or the wiring head can be mounted on a moving carriage for building the coils. Clearly there are many tooling design issues to be addressed should it be decided to pursue this new fabrication technique. It is possible that 10 or more wiring machines would be required for the SSC, and each machine for building correction coils directly on beam tubes can cost many hundreds of thousands of dollars.

Workshop Conclusions

Requirements for Correction Coils

There are a number of possible ways to compensate for field errors in the SSC. Accelerator physics studies indicate that the use of distributed multipole correction coils (with some additional "lumped" correctors located in spool pieces) is a flexible method to correct for systematic field errors, including magnetization effects. This scheme will certainly provide adequate corrections, assuming that the multipole specifications for the main SSC magnets are met. In addition, distributed correction coils permit the compensation of random field errors, if the "binning" technique is used. At least two methods are presently being used to fabricate distributed correction coils: BNL is investigating the Multiwire technique, and HERA is winding coils from strand. Other methods involving shunting current in the main magnet coils or powering the coil wedges might also be possible.

Among other field-error correction schemes currently under study are ones in which the distributed correction coils are entirely replaced by lumped correctors. These ideas require more study before the trade-offs are understood.

General Conclusions

The Workshop was very successful in providing an effective forum for information to be exchanged. The presentations were informative, and it was clear that the industrial collaborators are deeply involved. The present design for the magnetic-field-error correction system, as described in the Conceptual Design Report, makes use of distributed multipole correction coils as well as lumped correctors. This design is powerful and flexible, and the correction system will surely perform its required task. However, more accelerator physics studies and much more engineering development are required before a functioning, reliable correction system is in hand.

Encouraging progress has been made in the R&D effort to adapt the Multiwire technique to build SSC correction coils:

(1) The newly proposed testing and development program, as described in Appendix L, provides a potentially quick and orderly method to investigate possible improvements in the fabrication of correction coils. Many short coils will be built and tested, in order to evaluate alternative designs, before long coils are built. The overall feasibility of using the Multiwire technique to build distributed correction coils for the SSC must be established. Other design issues that require study are the glass-fiber compression

wrapping, film insulation of the wire, and new adhesives.

(2) Multiwire and the other industrial collaborators have responded impressively. They have played a crucial role in developing the design for the correction coils and a sensible construction method for these coils.

(3) A rational plan has been developed to build future models of correction coils using more radiation-resistant materials. The SSC Central Design Group must provide a more precise estimate of the total radiation dose to be withstood by the correction coils. The radiation resistance of the organic materials, especially the adhesives, must be better understood. Other materials properties, such as the thermal conductivity of Kapton, need to be measured.

A successful technique has been developed to manufacture distributed correction coils for HERA. The coil performance is excellent. As yet, no plan has been proposed to study this type of correction coil for the SSC.

Other Issues

(1) The testing and development program for correction coils must be spelled out in more detail, including estimates for the cost and schedule.

(2) The superconducting wire parameters need to be optimized further. How large are the magnetization effects? Is it true that the b_4 field distortions from magnetization currents in the correction coils tend to *cancel* those from the main coils of the dipoles? Other wire issues are the mechanical flexibility of the wire, the insulation technique, and quality control.

(3) The alignment of the correction coil is an important and difficult issue which can be adequately investigated only by building and testing full-length models.

(4) Complete magnetic measurements require the development of an improved measuring apparatus. It is necessary to develop a smaller field-measurement coil and a low heat leak warm beam tube insert.

(5) The CDG must provide detailed requirements for the magnetic field accuracy that must be achieved by the correction coils.

LIST OF PARTICIPANTS

WARREN LARSON
SUPERCON CO.
830 BOSTON TURNPIKE
SHREWSBURY, MA 01545

TOM CAMPBELL
TENSOLITE
DIVISION OF CARLISLE CORPORATION
OLD POST ROAD
ROUTE 9A
BUCHANAN, NY 10511
(914) 737-5600

LEONARD SCHIEBER
PCK TECHNOLOGY
MULTIWIRE EED
322 SOUTH SERVICE ROAD
MELVILLE, NY 11747
(516) 454-4496
FTS (516) 454-4496

ANDREW J. FELDMAN
BROOKHAVEN NATIONAL LABORATORY
UPTON, NY 11973

ARTHUR F. GREENE
BROOKHAVEN NATIONAL LABORATORY
BUILDING 902B
UPTON, NY 11973

EUGENE R. KELLY
BROOKHAVEN NATIONAL LABORATORY
BLDG. 902B
UPTON, NY 11973

CARL KLAMUT
BROOKHAVEN NATIONAL LABORATORY
UPTON, NY 11973

ALBERT G. PRODELL
BROOKHAVEN NATIONAL LABORATORY
BUILDING 911-B
UPTON, NY 11973

JOHN SKARITKA *(Session Leader)*
BROOKHAVEN NATIONAL LABORATORY
UPTON, NY 11973

PATRICK THOMPSON
BROOKHAVEN NATIONAL LABORATORY
BLDG. 902B
UPTON, NY 11973

PETER WANDERER *(Session Leader)*
BROOKHAVEN NATIONAL LABORATORY
BLDG. 902B
UPTON, NY 11973

ERICH H. WILLEN
BROOKHAVEN NATIONAL LABORATORY
BUILDING 902A
UPTON, NY 11973

RICHARD TALMAN
CORNELL UNIVERSITY
NEWMAN LABORATORY
ITHACA, NY 14853

JIM OCHNER
DUPONT CO.
213 HITCHING POST DRIVE
WILMINGTON, DE 1980
(302) 992-5388

MORT KATZ
DUPONT CO.
P.O. BOX 89
CIRCLEVILLE, OH 43113
(614) 474-0341
FTS (614) 474-0341

BRENT SWEITZER
SHELDAHL INC.
1150 SHELDAHL ROAD
NORTHFIELD, MN 55057
(507) 663-8518

JOHN PEOPLES
FERMILAB
MS 341
P.O. BOX 500
BATAVIA, IL 60510

ROGER CLOUGH
DIVISION SUPERVISOR
SANDIA NATIONAL LABORATORIES
CHEM. OF ORGANIC MATERIALS DIV.
1811
ALBUQUERQUE, NM 87185
(505) 844-3492
FTS 844-3492

TOM LEGBANDT
BARCEL WIRE AND CABLE CORPORATION
2851 ALTON AVENUE
IRVINE, CA 92714
(714) 863-0300
FTS (714) 863-0300

ALEX CHAO *(Session Leader)*
SSC CENTRAL DESIGN GROUP (CDG)
LAWRENCE BERKELEY LABORATORY
90 - 4040
1 CYCLOTRON ROAD
BERKELEY, CA 94720

PETER LIMON *(Organizer, Session Leader)*
SSC CENTRAL DESIGN GROUP (CDG)
LAWRENCE BERKELEY LABORATORY
90 - 4040
1 CYCLOTRON ROAD
BERKELEY, CA 94720
PJLIMON@LBL

RICHARD SAH *(Asst. Organizer, Editor)*
SSC CENTRAL DESIGN GROUP (CDG)
LAWRENCE BERKELEY LABORATORY
90 - 4040
1 CYCLOTRON ROAD
BERKELEY, CA 94720
SAH@LBL

MAURY TIGNER
DIRECTOR
SSC CENTRAL DESIGN GROUP (CDG)
LAWRENCE BERKELEY LABORATORY
90 - 4040
1 CYCLOTRON ROAD
BERKELEY, CA 94720
TIGNER@LBL

JOHN ZBASNIK
LAWRENCE BERKELEY LABORATORY
46 - 161
1 CYCLOTRON ROAD
BERKELEY, CA 94720

PETER SCHMUESER
DEUTSCHES ELEKTRONEN SYNCHROTRON
F35H
NOTKESTRASSE 85
2000 HAMBURG 52
WEST GERMANY
011- 49-8998-3887

APPENDIX A

Workshop Agenda

Agenda for

Workshop on Distributed Multipole Correction Coils

Tuesday, October 13

Welcome (Limon)	8:30 a.m.
Requirements for distributed multipole correction coils (Session leader: Chao. Speaker: Talman)	8:45
Distributed correction coil designs (Session leader: Wanderer)	
Magnetic design (Thompson)	9:30
Engineering design (Skaritka)	9:55
Coffee Break	10:20
Multiwire techniques (Schieber)	10:35
Results to date: SSC corr. coil performance (Wanderer)	11:00
HERA correction coil design and performance (Schmueser)	11:45
Lunch	12:30 p.m.
Materials issues (Session leader: Skaritka)	
Radiation damage to organic materials (Clough)	1:20
Results of radiation damage experiments at BNL (Prodell)	1:50
Proposals for new materials (Skaritka)	2:10
Cryogenic performance of materials (Katz)	2:30
What's next ? (Session leader: Limon)	
Direct application of coils to bore tubes (Schieber)	2:50
Discussions	3:10
Workshop Dinner	7:00 p.m.

Wednesday, October 14

Write report	8:30 a.m.
Lunch	12:00 noon
Summary session	1:00 p.m.
Close of workshop	2:00 p.m.

APPENDIX B

"Requirements for Distributed Multipole Corrections Coils,"

Talk by Richard Talman

Requirements for Distributed Multipole Correction Coils. BNL Workshop. R. Talman 13 Oct. 1.

1. Compensation of field errors
   (i) random
   (ii) systematic
2. Sample calculation to illustrate convergence and consequences.
3. Tune dependence on amplitude due to nonlocal compensation.
4. Analytic formulas for leading terms of tune dependence; numerical values
5. Investigation using tracking with TEAPOT
6. Possible variants of CDR plan
   i) use only b_2 bore tube windings
   ii) use no bore tube windings.

1. Compensation of Field Errors

(i) Random field errors THE MAIN PROBLEM (BUT NOT FOR THIS WORKSHOP)

- determines dynamic aperture
- assume active compensation
- assume all multipole coefficients have been measured
- identify most important one (or possibly two) coefficients. b_2 (or b_2 and a_1)

(a) sorting – group magnets in pairs with b_2 approximately canceling.

(b) binning – maintain a "spectrum" of trim currents, and route them appropriately through b_2 bore tube windings.

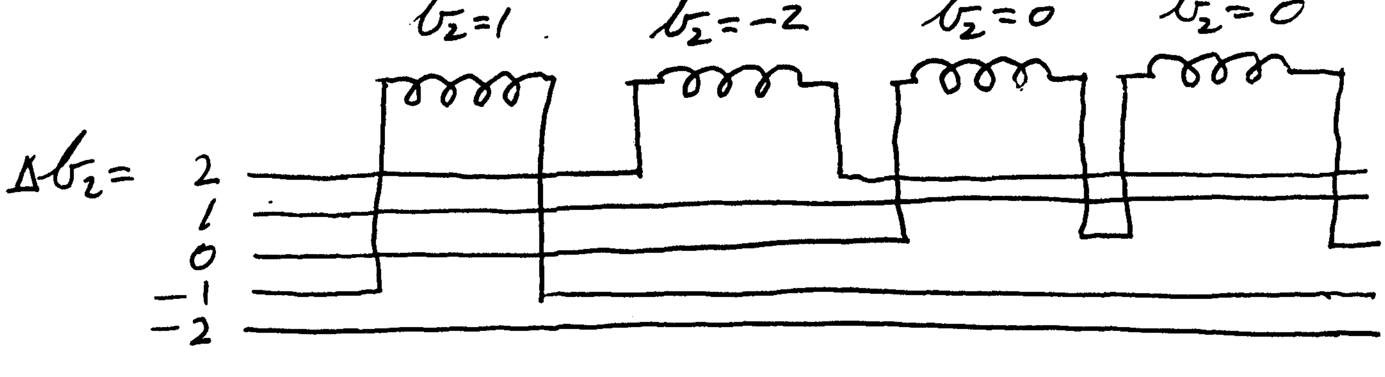

MAIN SUBJECT OF WORKSHOP

ii) Systematic field errors

- cause errors in global accelerator like tune, chromaticity etc.
- for definiteness concentrate on persistent current allowed multipoles $b_2, b_4, b_6 \ldots$
- accelerator performance specification

$|\Delta Q| < 0.005$
for $\delta < 0.001$
ampl $<$ 5 mm

SYSTEMATIC CORRECTION SCHEME	CROSS SECTION	WHAT IS BEING COMPENSATED ?	FLEXIBLE ?	NOTES
bore tube 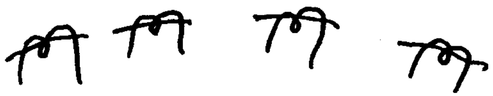	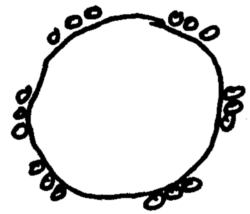	magnet b_2, b_4	no	P. Wanderer CDR-B.8 ↓
bore tube + lumps 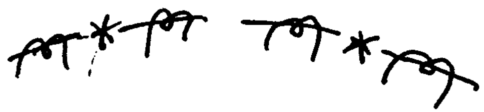		magnet b_2, b_4 + accelerator	yes	CDR
wedges 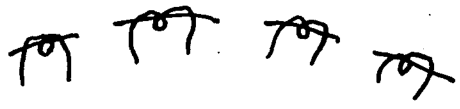	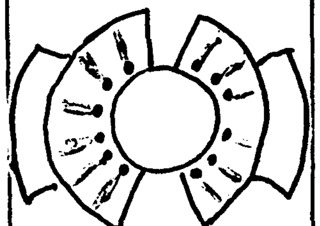	magnet $a_0 - a_5$, $b_0 - b_5$	yes	RT SSC-N-208 M.A. Green SSC-N-319
lumps only 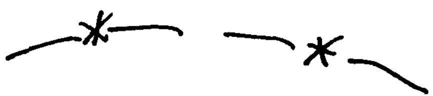		accelerator	yes	D. Neuffer SSC-N-339 etc.

2. Sample Calculation to Illustrate Units, Convergence, Systematics and Operational Consequences of Multipole Errors

Consider N magnets each bending by $\frac{2\pi}{N}$

Particle horizontal displacement $= x + \eta\delta$

Bend error in one magnet $= \frac{2\pi}{N}\left[b_0 + b_1(x+\eta\delta) + b_2(x+\eta\delta)^2 + \cdots\right]$

Keep only "quadrupole" terms

$$= \frac{2\pi}{N}\left[b_1 + 2b_2(\eta\delta) + 3b_3(\eta\delta)^2 + \cdots\right]$$

Use "golden rule" to get tune shift in all N magnets

$$\Delta Q = \frac{1}{4\pi}\sum \beta \frac{2\pi}{N}\left[b_1 + 2b_2(\eta\delta) + \cdots\right]$$

$$= \frac{\langle\beta\rangle}{2}\left[b_1 + 2b_2(\langle\eta\rangle\delta) + 3b_3(\langle\eta\rangle\delta)^2 + \cdots\right]$$

Typical values: $\left.\begin{array}{l}\langle\eta\rangle = 2.07\,m \\ \delta = 0.001\end{array}\right\}$ $\langle\eta\rangle\delta = 0.2\,cm$

$\langle\beta\rangle = 185\,m$

Convergence: with b_n measured in cm units

$$\frac{(\text{term})_{n+1}}{(\text{term})_n} = \frac{n+1}{n}\,\frac{b_{n+1}}{b_n}\,0.2$$

See Table

Table 2

6

Tolerances and estimated strengths of systematic multipole context in the SSC dipoles. All multipole strengths are in units of $10^{-4} cm^{-n}$. The tolerances are obtained from the linearity criteria. Estimated strengths are extrapolated from Tevatron data on calculated from the magnet properties.

Multipole	Tolerance (Conceptual Design)	Tolerance (Current Lattice)	Estimated Random Error (Tevatron)	Estimated Systematic Strength (Tevatron)	Estimated Persistent Current Multipole Strength	Estimated Saturation Multipole Strength
b_2	0.0072	0.0097	2.0	0.45	-4.7	1.2
b_3	0.011	0.017	0.35	-0.14	--	--
b_4	0.016	0.031	0.60	-0.33	0.30	-0.05
b_5	0.024	0.054	0.06	-0.024	--	--
b_6	0.035	0.096	0.08	1.57⁺	0.07	-0.01
b_7	0.051	0.17	0.16	0.009	--	--
b_8	0.074	0.29	0.02	-2.1⁺	<0.02	0.02

⁺ Tevatron magnet design; to be reduced in SSC magnet design.

From Neuffer SSC-132

- convergence for persistent current and saturation is excellent.
- convergence for "geometric" "systematic" terms is not necessarily good. (see Tevatron column)
- convergence was improved in going from 60° lattice to 90° lattice

$$\langle \eta \rangle \propto \frac{1}{Q^2} \qquad \text{magnets}/\tfrac{1}{2}\,\text{cell}$$

$$\frac{\langle \eta \rangle_{new}}{\langle \eta \rangle_{old}} = \frac{Q^2_{old}}{Q^2_{new}} = \left(\frac{60^\circ}{90^\circ}\,\frac{6}{5}\right)^2 = \frac{16}{25}$$

Magnitude

$$\Delta Q = b_2 \beta \eta \delta$$
$$= 4.7\times10^{-4} \times 1.85\times10^{4} \times 2.07\times10^{2} \times 10^{-3}$$
$$= 1.8$$
$$= 360 \text{ times the tolerance}$$

Not to worry

1. Assume this can be compensated to the 10% level by dead reckoning
2. The rest can be compensated empirically

Justification

It is done in existing accelerators e.g. at CESR

$$\xi = \text{chromaticity} = \frac{dQ}{d\delta}$$
$$= b_2 \beta \eta$$

can be set to absolute accuracy of ± 0.5 and controlled to ± 0.1. What is the corresponding systematic compensation of b_2?

$$b_2 \sim \frac{dQ/d\delta}{\beta\eta} \cong \frac{0.1 - 0.5}{10^3 \times 0.3 \times 10^3} \text{ cm}^{-2}$$
$$\cong 10^{-6} \text{ cm}^{-2}$$
$$= 10^{-2} \text{ "units"}$$

Pangloss Principle: if its large enough to be bad then its large enough to be measured and compensated

3. Tune Dependence on Amplitude Due to Nonlocal Sextupole Compensation

Analogy from mechanics

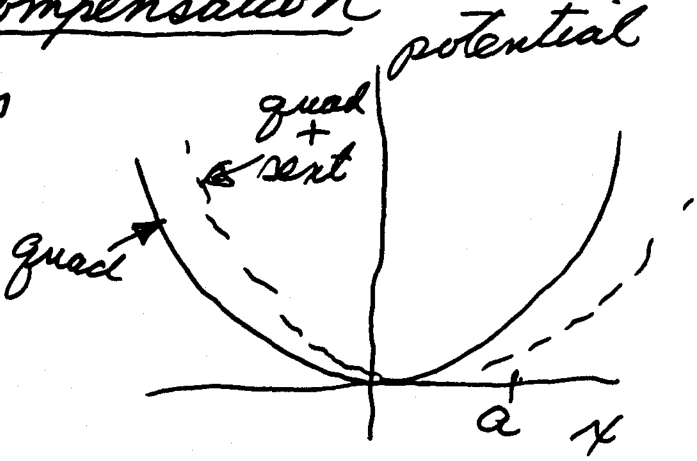

To terms linear in x the freq. shifts on the left and right cancel

$\Delta freq \propto a^2$

Lattice

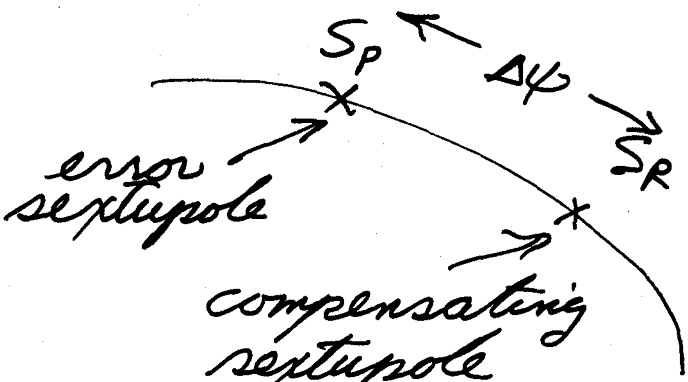

Small amplitude motion μ_0

$$x = a \cos 2\pi Q_0 t$$

Tune shift:

$$\Delta Q = -\frac{a^2}{32\pi}\sum_{P,R}\beta_P S_P \beta_R S_R \left\{\frac{\cos\Delta\psi \sin\mu_0}{1-\cos\mu_0} + \frac{\sin\Delta\psi \sin 2\Delta\psi \sin 2\mu_0 + \cos\Delta\psi}{2(\cos 2\mu_0 - \cos\mu_0)}\right\}$$

$$\cong -\frac{a^2}{32\pi}\beta^2 S^2\left[-1+\cos 2\Delta\psi\right] \quad \text{if } S_P\beta_P = -S_R\beta_R = S\beta$$

$$\cong \frac{a^2}{16\pi}\beta^2 S^2 \Delta\psi^2$$

$$\propto \left(\frac{1}{\#\text{of lumps/cell}}\right)^{3}$$

4. Tune Dependence: Leading Terms

Momentum (δ)

$$\Delta Q_2(\underline{\underline{\delta}}) = b_2(\text{in "units"}) \frac{1}{R}\left(\frac{\ell}{\sin\phi}\right)^3 \delta$$

(ℓ: length of ½ cell; ϕ: phase advance/½ cell; R: gross radius)

$$\Delta Q_4(\delta) = 10^4\, b_4(\text{in "units"}) \frac{2}{R^3}\left(\frac{\ell}{\sin\phi}\right)^7 \delta^3$$

Amplitude (ε)

$$\Delta Q_2(\underline{\underline{\varepsilon}}) = \frac{1}{\pi}\frac{\ell}{R}\left[b_2(\text{in "units"})\right]^2 \cdot \left(\frac{\ell}{\sin\phi}\right)^3 \varepsilon$$

Amplitude and Momentum (ε, δ)

$$\Delta Q_4(\underline{\underline{\varepsilon, \delta}}) = 10^4\, b_4(\text{in "units"}) \frac{3}{2}\frac{1}{R}\frac{\ell}{\sin\phi}\, \varepsilon\delta$$

Residue After Remote Compensation

$$\Delta Q_2(\underline{\underline{\text{remote}}}) \cong \Delta Q_2(\varepsilon)\, \Delta\psi^2$$

($\Delta\psi$: phase interval between error and compensation)

SSC 90° Lattice — Uncompensated Tune Shifts[1]

		filament size				
		2μ	5μ	8.7μ	20μ	
	b_2	−2.0	−4.7	−7.5	−12.4	
	b_4	0.11	0.31	0.65	2.0	
	b_6	0.025	0.066	0.12	0.28	
	b_8	0.02	0.045	0.079	0.16	
MOMENTUM (δ)	$\Delta Q_2(\delta)$	−.57	(−1.33)	−2.12	−3.51	δ
	ΔQ_4	.003	.007	.015	.045	δ^3
	ΔQ_6	.000	.000	.000	.000	δ^5
	ΔQ_8	0.7×10^{-4}				
AMPLITUDE (ε) + MOMENTUM (δ)	$\Delta Q_2(\varepsilon,\delta)$	—	—	—	—	
	ΔQ_4	.014	(.039)	.082	.25	$\delta\varepsilon$
	ΔQ_6	.001	.003	.006	.013	$\delta\varepsilon^2$
	ΔQ_8	.000	.000	.000	.000	$\delta\varepsilon^3$
AMPLITUDE (ε)	$\Delta Q_2(\varepsilon)$	.007	(.038)	.095	.92	ε
	ΔQ_4	.000	.000	.000	.390	ε^2
	ΔQ_6					
REMOTE	$\Delta Q_2(\varepsilon,\Delta\psi)$	.001	.007	.017	.166	

5. Investigation Using TEAPOT Tracking

- define lattice. For present purposes use arcs only
- introduce alignment errors, systematic and random magnet errors. For present purposes only systematic magnetic errors.
- adjust compensating elements.
- track various particles e.g. 256 turns
- perform FFT. For present purposes only the tune of the fundamental is important. (In general dominant nonlinearity can be diagnosed.)
- plot $Q(\delta = \pm 0.001, \varepsilon_x = \varepsilon_y)$ ← or other phase space points.

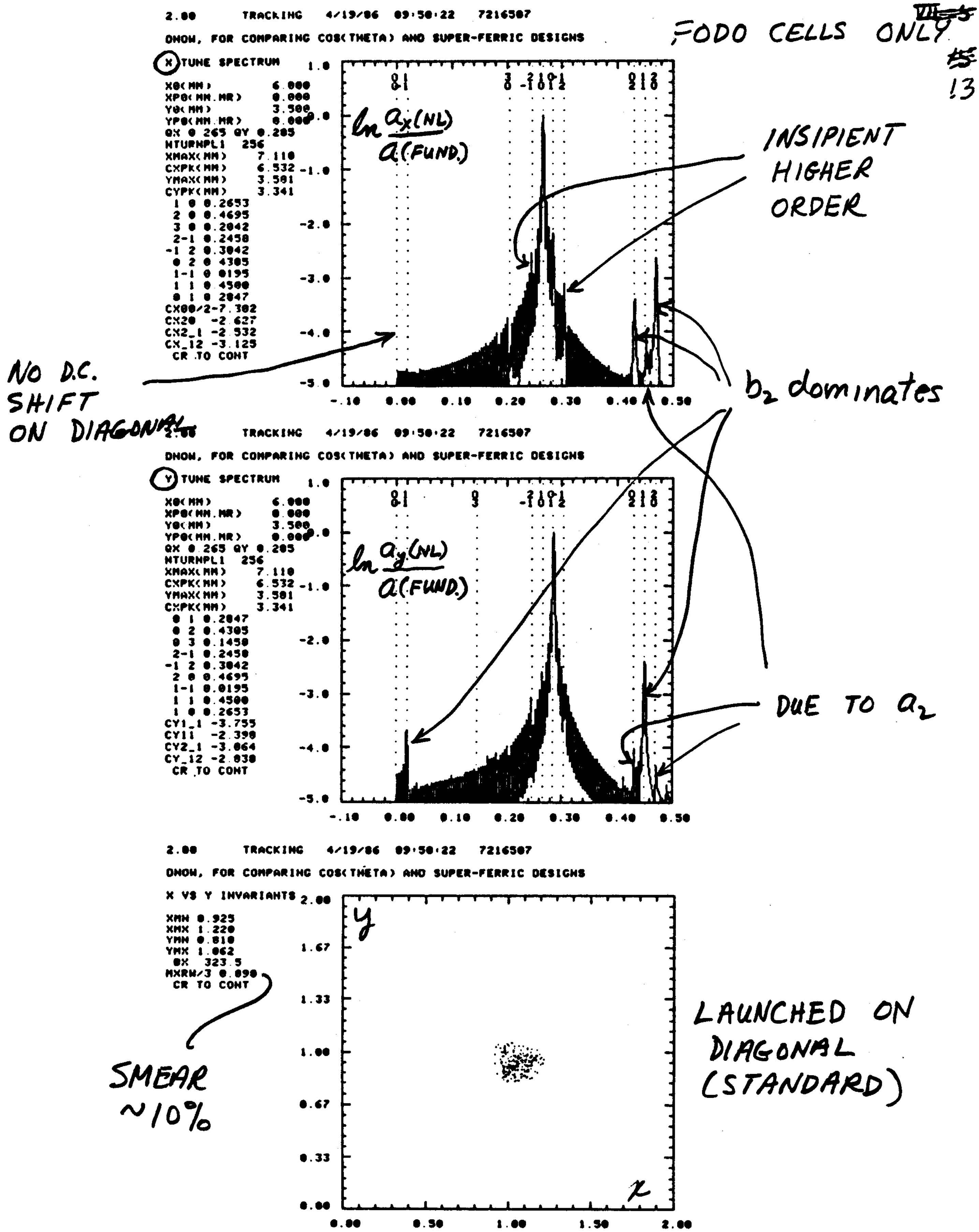
2.00 TRACKING 4/19/86 09:50:22 7216507
DNOW, FOR COMPARING COS(THETA) AND SUPER-FERRIC DESIGNS
X TUNE SPECTRUM
X0(MM) 6.000
XP0(MM.MR) 0.000
Y0(MM) 3.500
YP0(MM.MR) 0.000
QX 0.265 QY 0.205
NTURNPL1 256
XMAX(MM) 7.110
CXPK(MM) 6.532
YMAX(MM) 3.501
CYPK(MM) 3.341
1 0 0.2653
2 0 0.4695
3 0 0.2042
2-1 0.2458
-1 2 0.3042
0 2 0.4305
1-1 0.0195
1 1 0.4500
0 1 0.2047
CX00/2-7.302
CX20 -2.627
CX2_1 -2.532
CX_12 -3.125
CR TO CONT
$\ln \frac{a_x(NL)}{a(FUND.)}$
FODO CELLS ONLY
13
INSIPIENT HIGHER ORDER
NO D.C. SHIFT ON DIAGONAL
b_2 dominates
2.00 TRACKING 4/19/86 09:50:22 7216507
DNOW, FOR COMPARING COS(THETA) AND SUPER-FERRIC DESIGNS
Y TUNE SPECTRUM
X0(MM) 6.000
XP0(MM.MR) 0.000
Y0(MM) 3.500
YP0(MM.MR) 0.000
QX 0.265 QY 0.205
NTURNPL1 256
XMAX(MM) 7.110
CXPK(MM) 6.532
YMAX(MM) 3.501
CXPK(MM) 3.341
0 1 0.2047
0 2 0.4305
0 3 0.1458
2-1 0.2458
-1 2 0.3042
2 0 0.4695
1-1 0.0195
1 1 0.4500
1 0 0.2653
CY1_1 -3.755
CY11 -2.390
CY2_1 -3.064
CY_12 -2.030
CR TO CONT
$\ln \frac{a_y(NL)}{a(FUND.)}$
DUE TO a_2
2.00 TRACKING 4/19/86 09:50:22 7216507
DNOW, FOR COMPARING COS(THETA) AND SUPER-FERRIC DESIGNS
X VS Y INVARIANTS
XMN 0.925
XMX 1.220
YMN 0.810
YMX 1.062
0X 323.5
MXRM/3 0.090
CR TO CONT
y
x
SMEAR ~10%
LAUNCHED ON DIAGONAL (STANDARD)

2.00 tracking 4/19/86 09:50:22 7216507
dnow, for comparing cos(theta) and super-ferric designs
NPART 10 NTURNSIN 256 BETAX 323.46 BETAY 109.67 ALPHX 0.00 ALPHY 0.00
TUNEXT 68.2650 TUNEYT 68.2850
TUNEX 0.2650 TUNEY 0.2850

X0 (mm)	0.5000	1.0000	2.0000	3.0000	4.0000	5.0000	6.0000	7.0000	8.0000	9.0000
XP0 (mm.mr)	0.0000	0.0000	0.0000	0.0000	0.0000	0.0000	0.0000	0.0000	0.0000	0.0000
Y0 (mm)	0.2900	0.5800	1.1600	1.7400	2.3300	2.9200	3.5000	4.0100	4.6700	5.2600
XP0 (mm, mr)	0.0000	0.0000	0.0000	0.0000	0.0000	0.0000	0.0000	0.0000	0.0000	0.0000
XMAX (mm)	0.5033	1.0150	2.0686	3.1722	4.3171	5.5012	7.1096	8.8295	11.0100	12.7432
CXPK (mm)	0.5086	1.0197	2.0527	3.1079	4.1964	5.3318	6.5320	7.8157	9.3217	10.7088
YMAX (mm)	0.2916	0.5871	1.1848	1.7781	2.3959	2.9937	3.5806	4.1182	4.8049	5.4842
CYPK (mm)	0.2904	0.5805	1.1576	1.7269	2.2931	2.8383	3.3414	3.7269	4.1674	4.5550
ν_x → 1 0	0.2650	0.2650	0.2650	0.2650	0.2651	0.2652	0.2653	0.2653	0.2653	0.2651
$2\nu_x$ → 2 0	0.4701	0.4701	0.4700	0.4699	0.4698	0.4697	0.4695	0.4694	0.4694	0.4697
3 0	0.2051	0.2051	0.2050	0.2049	0.2047	0.2045	0.2042	0.2040	0.2041	0.2046
$2\nu_x - \nu_y$ → 2 -1	0.2449	0.2450	0.2450	0.2452	0.2454	0.2456	0.2458	0.2459	0.2457	0.2453
-1 2	0.3050	0.3050	0.3049	0.3047	0.3045	0.3044	0.3042	0.3042	0.3044	0.3049
0 2	0.4300	0.4301	0.4301	0.4302	0.4304	0.4305	0.4305	0.4305	0.4303	0.4300
1 1	0.0200	0.0200	0.0199	0.0198	0.0197	0.0196	0.0195	0.0194	0.0196	0.0199
1 1	0.4501	0.4501	0.4501	0.4501	0.4501	0.4501	0.4500	0.4499	0.4499	0.4498
ν_y → 0 1	0.2850	0.2850	0.2849	0.2849	0.2848	0.2848	0.2847	0.2847	0.2848	0.2850
CX00/2-bknd	0.0000	-0.0013	-0.0013	-0.0012	-0.0011	-0.0013	-0.0017	-0.0020	-0.0016	-0.0021
CX20 "	0.0000	0.0038	0.0131	0.0234	0.0346	0.0467	0.0598	0.0734	0.0878	0.0982
CX2_1 "	0.0000	-0.0005	0.0013	0.0047	0.0092	0.0143	0.0196	0.0269	0.0429	0.0630
CX 12 "	0.0000	-0.0017	-0.0050	-0.0100	0.0157	0.0202	0.0245	0.0271	0.0286	0.0063
CX11 "	0.0000	-0.0012	-0.0021	-0.0028	-0.0036	-0.0033	0.0004	0.0072	0.0175	0.0265
CX1_1 "	0.0000	-0.0007	-0.0007	-0.0002	0.0002	0.0005	0.0056	0.0054	0.0018	0.0036
CY00/2-bknd	0.0000	-0.0015	-0.0019	-0.0018	-0.0018	-0.0019	-0.0022	-0.0026	-0.0027	-0.0014
CY1_1 "	0.0000	0.0002	0.0033	0.0072	0.0114	0.0159	0.0186	0.0223	0.0301	0.0340
CY11 "	0.0000	0.0053	0.0187	0.0328	0.0477	0.0638	0.0815	0.1006	0.1216	0.1388
CY2_1 "	0.0000	-0.0014	-0.0009	0.0011	0.0040	0.0073	0.0109	0.0157	0.0252	0.0342
CY_12 "	0.0000	-0.0013	-0.0003	0.0025	0.0539	0.0512	0.0467	0.0406	0.0315	0.0556
CY02 "	0.0000	-0.0013	-0.0009	0.0002	0.0018	0.0039	0.0066	0.0097	0.0132	0.0134
XMN	0.9901	0.9830	0.9705	0.9616	0.9553	0.9370	0.9252	0.9244	0.8986	0.8524
XMX	1.0080	1.0188	1.0454	1.0804	1.1227	1.1714	1.2201	1.2785	1.3668	1.4373
YMN	0.9855	0.9758	0.9529	0.9254	0.8951	0.8559	0.8096	0.7456	0.6717	0.6181
YMX	1.0009	1.0072	1.0187	1.0309	1.0443	1.0543	1.0615	1.0606	1.0581	1.0852
XRW/3=XSM	0.0060	0.0120	0.0250	0.0396	0.0555	0.0777	0.0977	0.1172	0.1549	0.1932
YRW/3=YSM	0.0051	0.0105	0.0220	0.0352	0.0495	0.0657	0.0834	0.1042	0.1278	0.1543
SMEAREMPIR.	0.0060	0.0120	0.0250	0.0396	0.0555	0.0777	0.0977	0.1172	0.1549	0.1932
SMEARTHEOR1	0.0000	0.0071	0.0233	0.0411	0.0602	0.0809	0.1032	0.1272	0.1546	0.1760
SMEARTHEOR2	0.0000	0.0075	0.0239	0.0427	0.0830	0.0991	0.1181	0.1398	0.1679	0.1981

- X0 … XP0 rows: launching amplitudes
- CXPK, CYPK: "fundamental" amplitudes
- XMAX, YMAX: maximum amplitudes encountered
- Tune rows: tunes of prominent lines
- CX/CY rows: amplitudes of prominent lines
- XMN … YMX: upper and lower limits of "invariants"
- XRW/3=XSM, YRW/3=YSM: X } Y } SMEAR
- SMEAREMPIR.: SMEAR } empirical smear
- SMEARTHEOR1: 1st order lines } FFT smear
- SMEARTHEOR2: 1st + 2nd order lines } FFT smear

Note correspondance between empirical smear and FFT "smear" $= \sqrt{\Sigma (N.L.\,ampl)^2}$

B15

6. Possible Deviation from CDR ; (i) only b_2 distributed bore 15 tube winding

SYSTEMATIC TUNE COMPENSATION

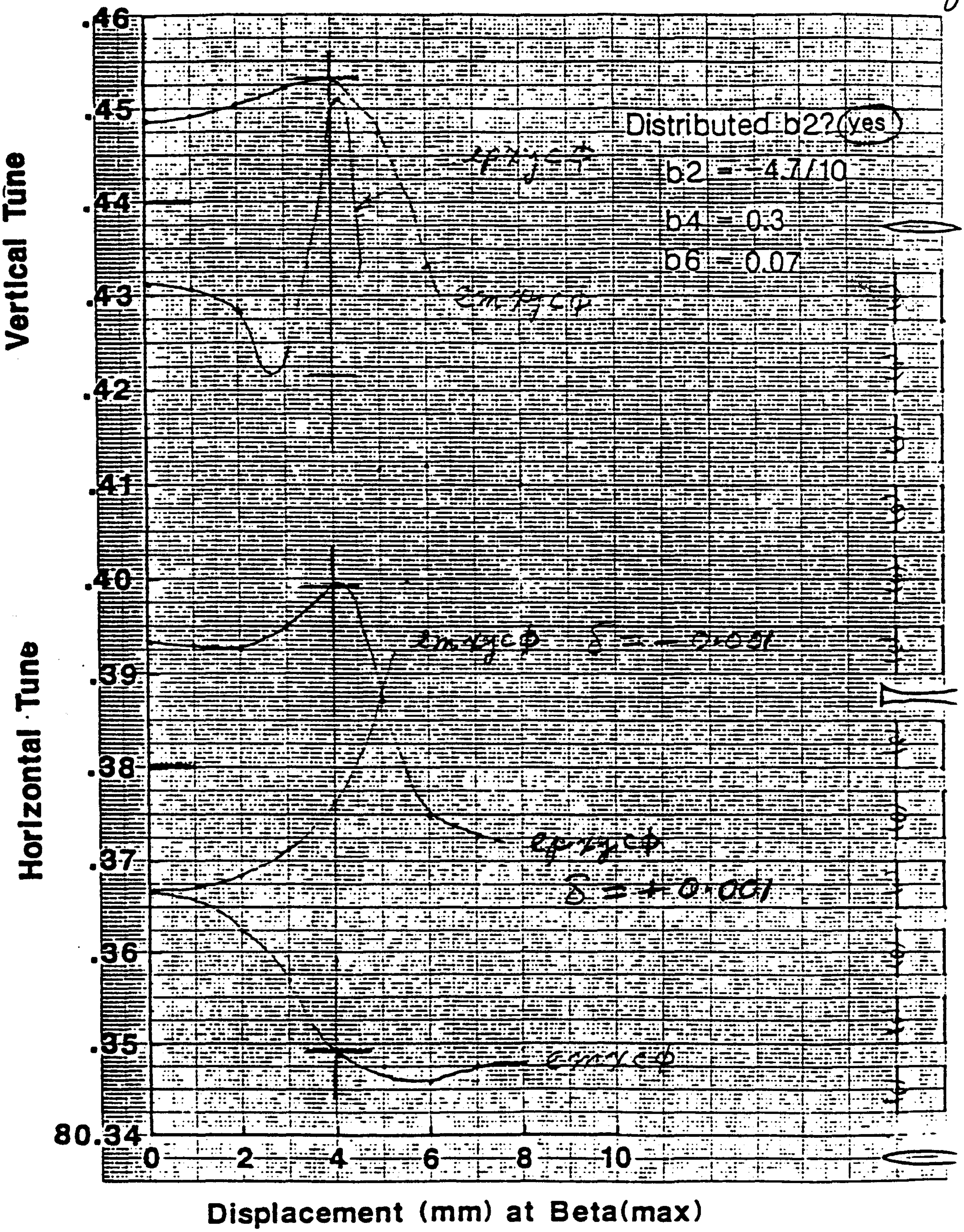

SYSTEMATIC TUNE COMPENSATION

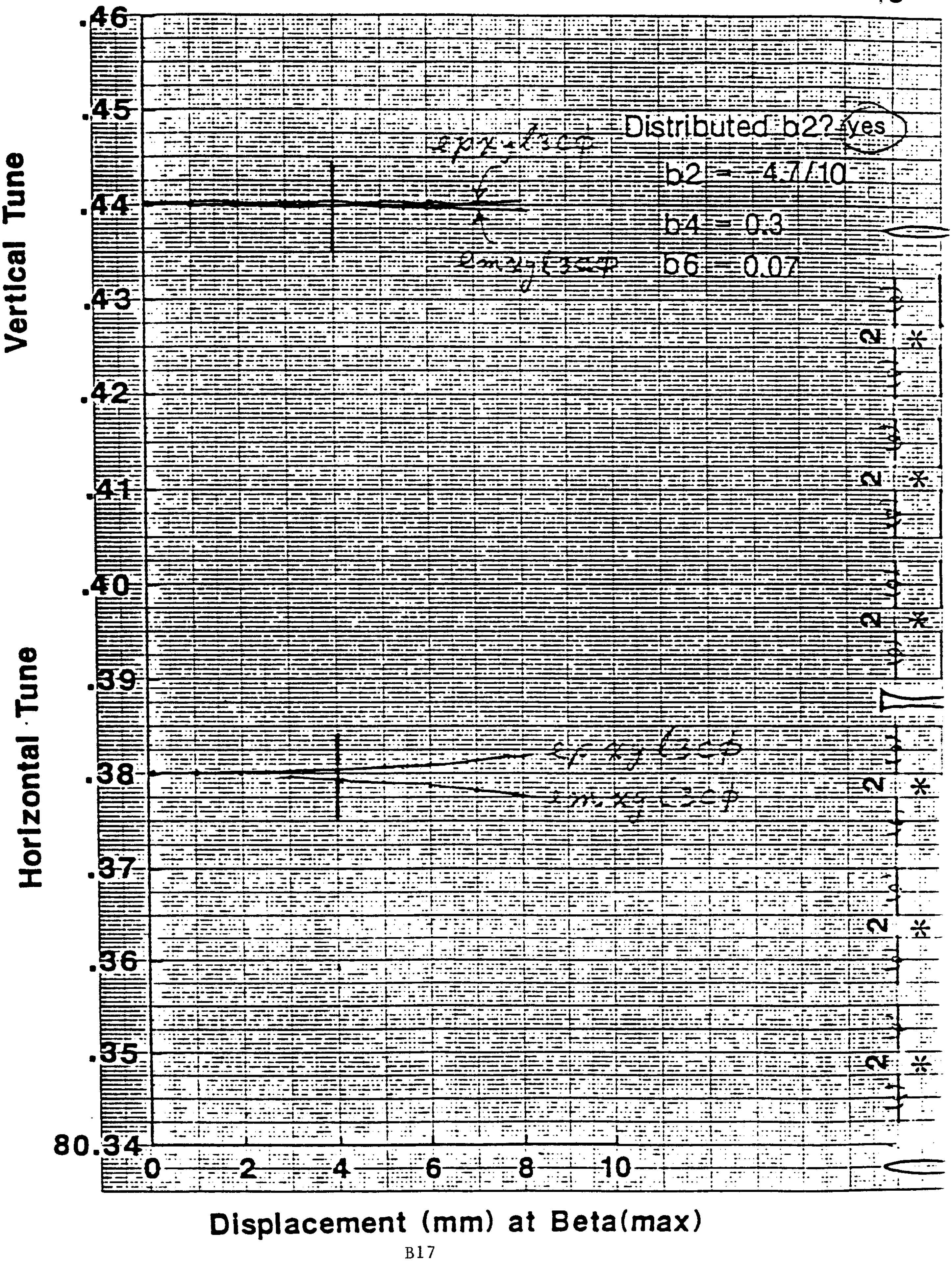

SYSTEMATIC TUNE COMPENSATION

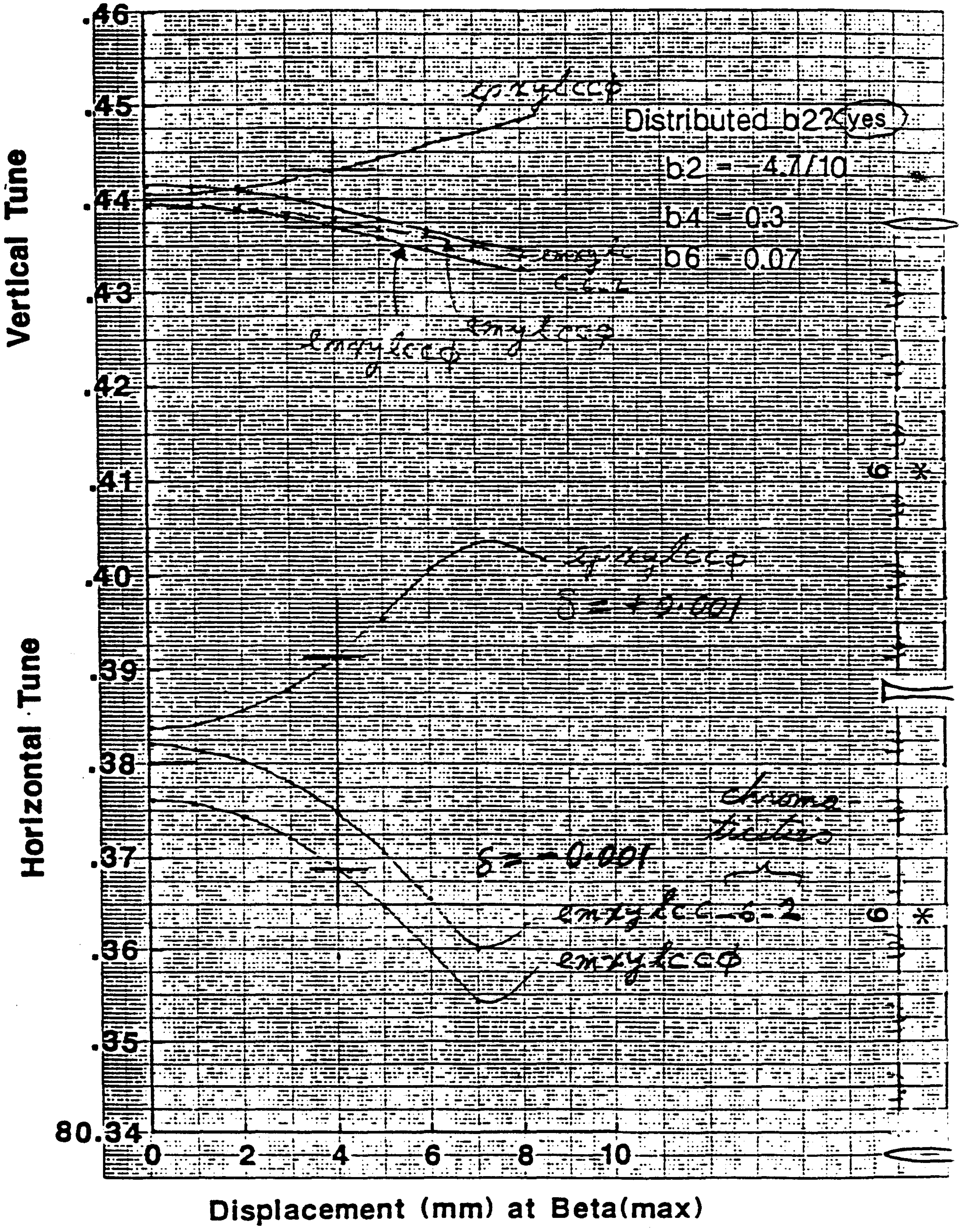

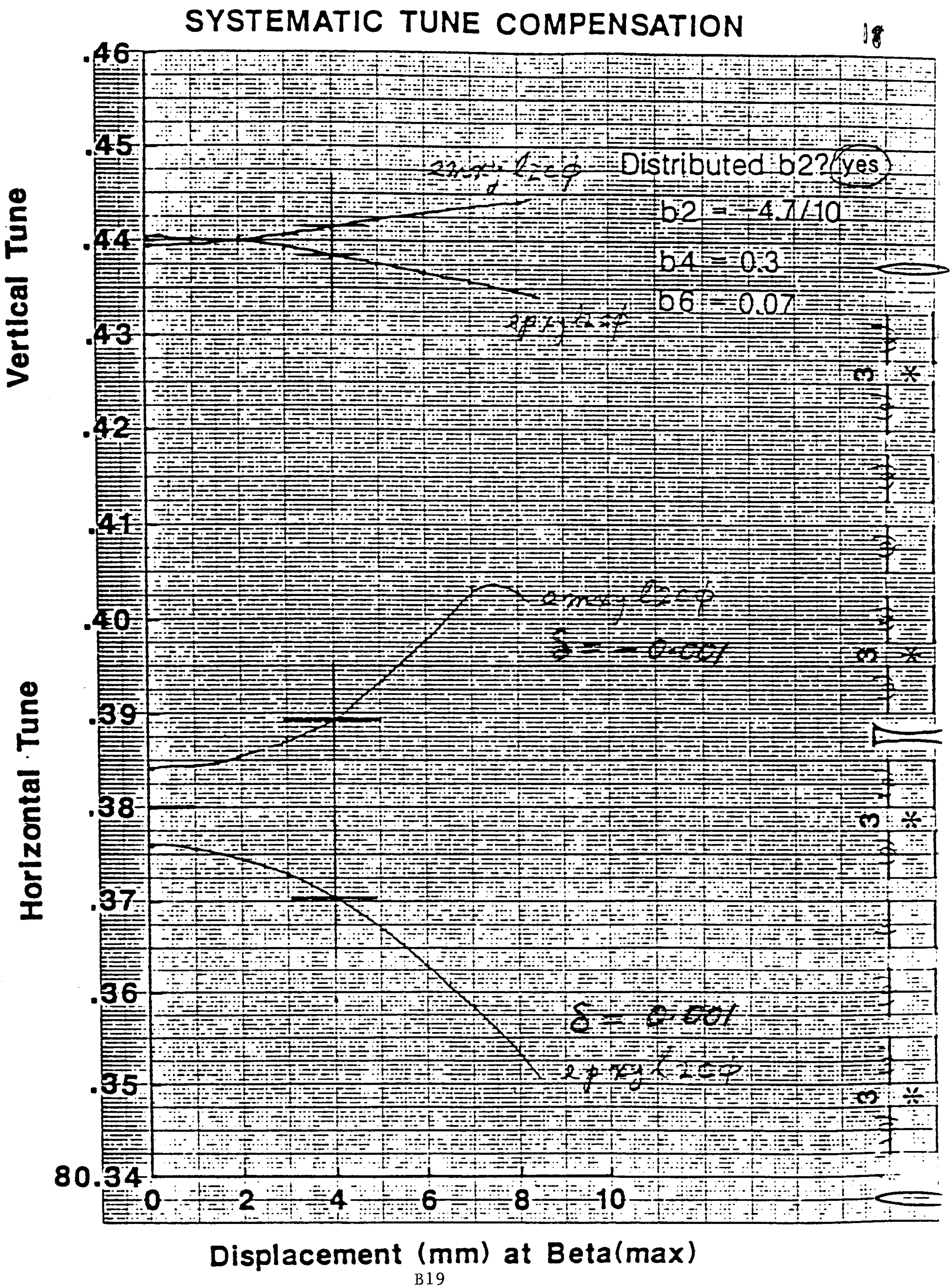

SYSTEMATIC TUNE COMPENSATION
Vertical Tune
Horizontal Tune
.46
.45
.44
.43
.42
.41
.40
.39
.38
.37
.36
.35
80.34
0
2
4
6
8
10
Displacement (mm) at Beta(max)
Distributed b2? yes
b2 = -4.7/10
b4 = 0.3
b6 = 0.07
δ = -0.001
δ = 0.001

SYSTEMATIC TUNE COMPENSATION

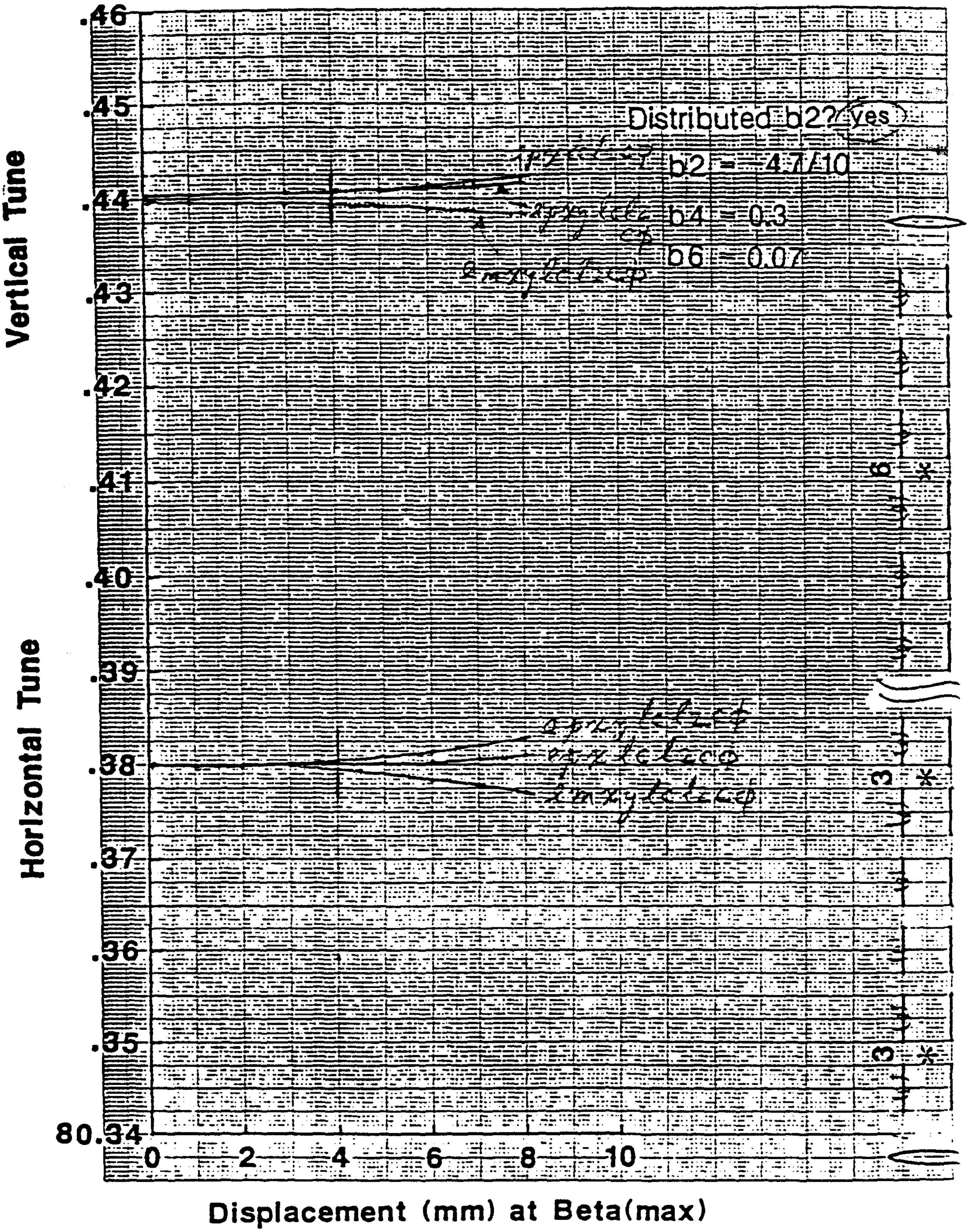

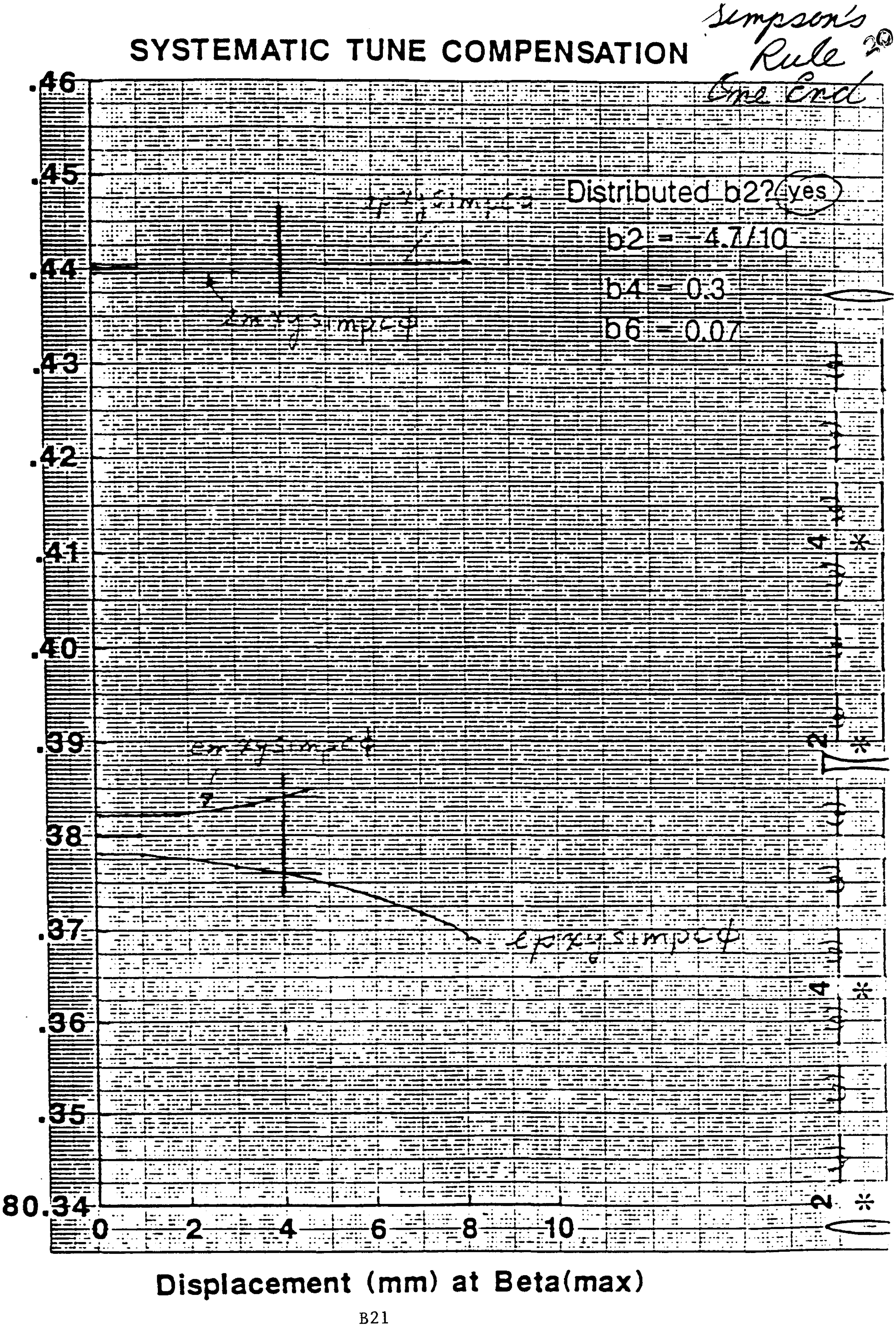
Simpson's Rule
One End
20
SYSTEMATIC TUNE COMPENSATION
Vertical Tune
Horizontal Tune
.46
.45
.44
.43
.42
.41
.40
.39
.38
.37
.36
.35
80.34
Distributed b2? yes
b2 = -4.7/10
b4 = 0.3
b6 = 0.07
0
2
4
6
8
10
Displacement (mm) at Beta(max)

Tolerable Systematic b_2

b_2 Bore Tube Winding Only, b_4, b_6 remote.

		max b_2	extra spools/half cell
chromaticity sextupoles only	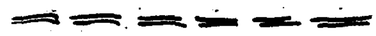	0.94	0
lc	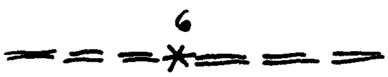	2.1	0
l2		2.5	1
l3	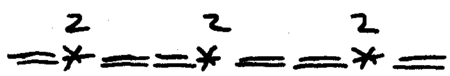	47	2
lc l2	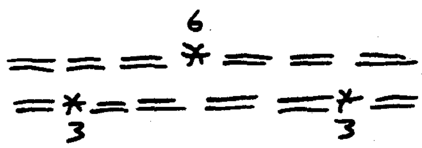	29	0.5
Simpson's rule, One end.	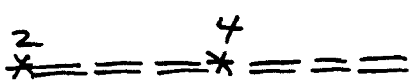	7.2	1

Conclusions.

1. CDR plan with both b_2 and b_4 distributed in every dipole is amply fine-grained.
2. Distributed b_4 could be replaced by lumped quite cheaply.

aside: spool pieces in interior of $\frac{1}{2}$ cells are needed for "local" decoupling.

b.(cont) Possible Deviation from CDR : (ii) no bore tube windings

SYSTEMATIC TUNE COMPENSATION

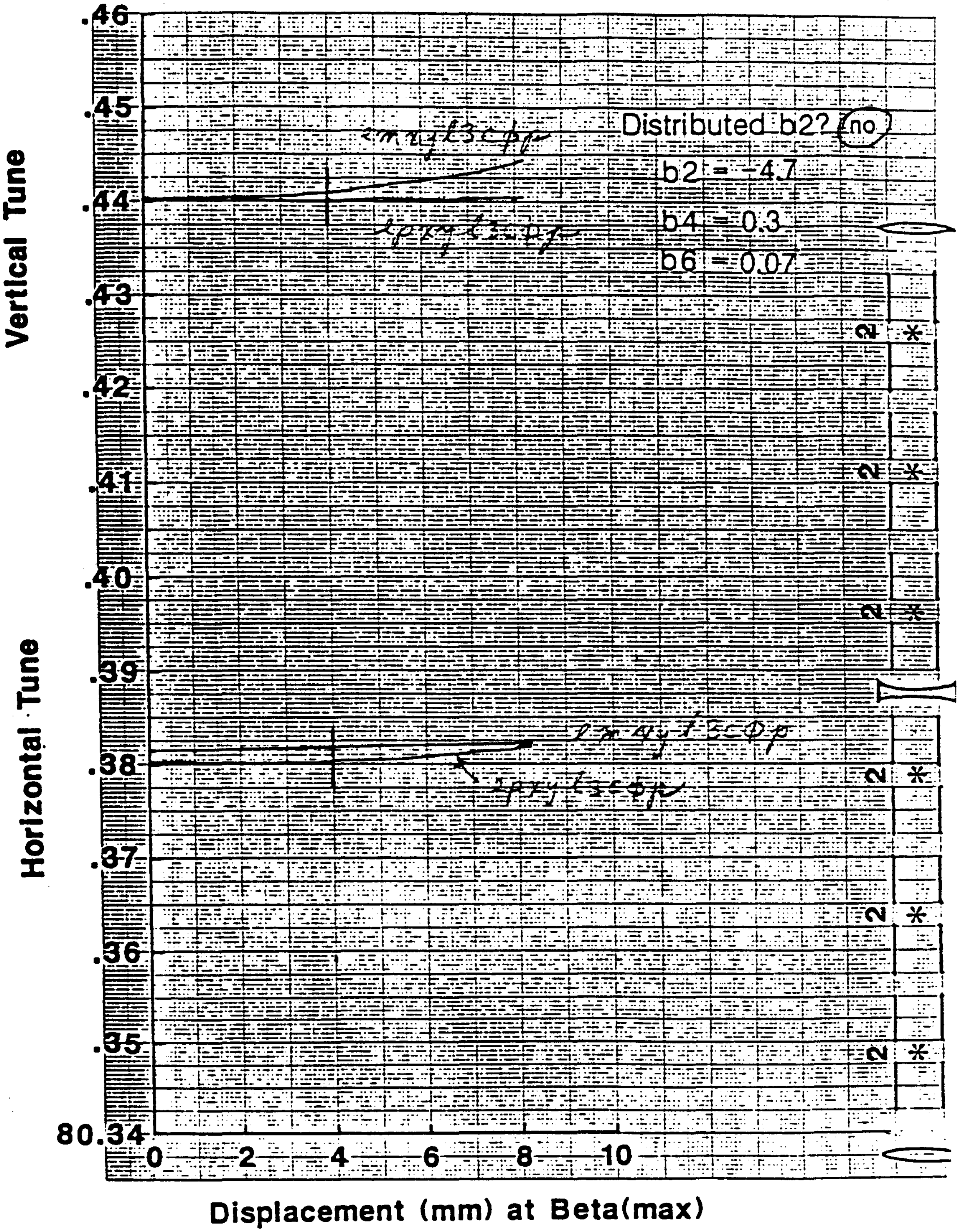

SYSTEMATIC TUNE COMPENSATION

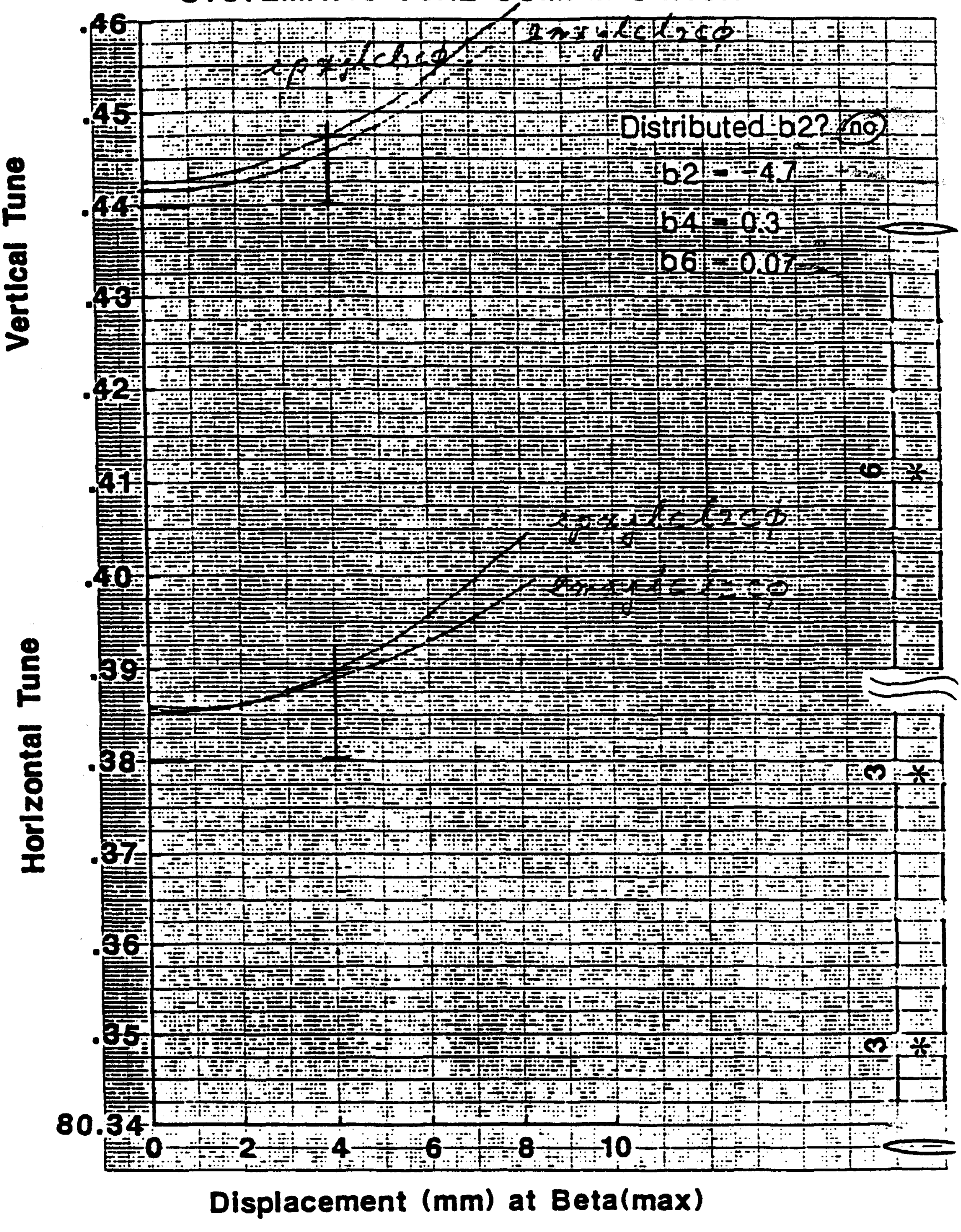

SYSTEMATIC TUNE COMPENSATION

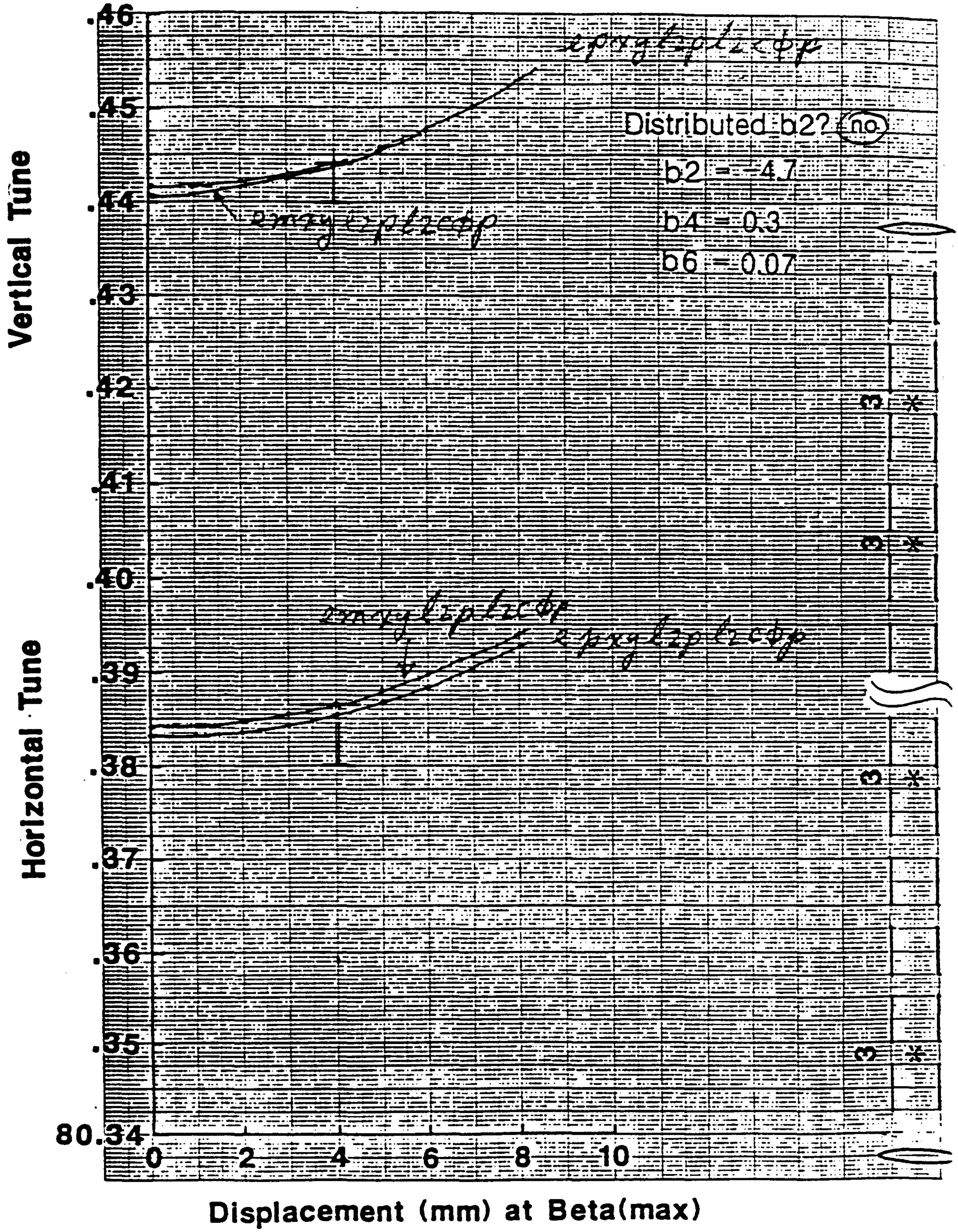

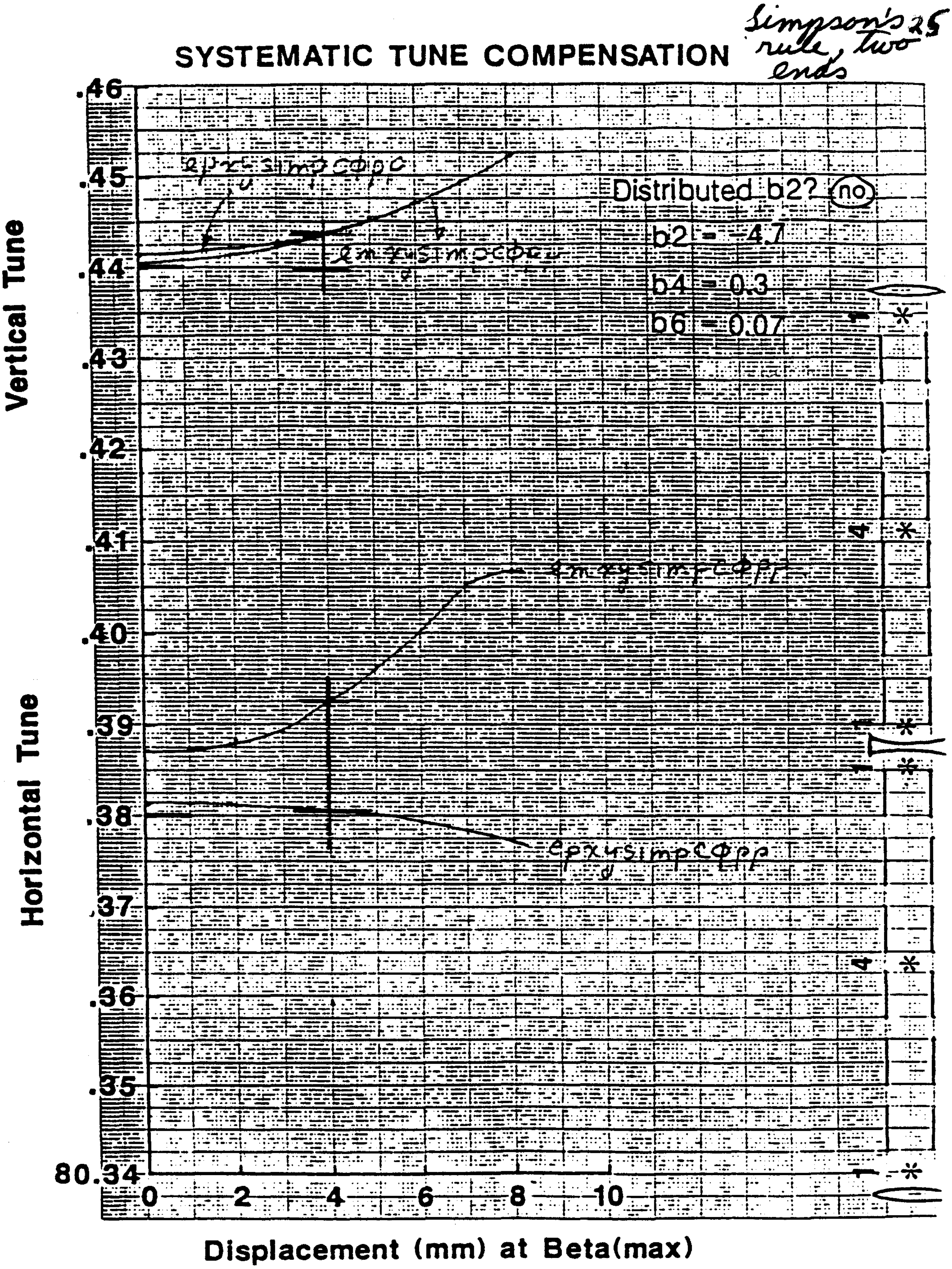

SYSTEMATIC TUNE COMPENSATION
Simpson's rule, two ends 25
Distributed b2? no
b2 = -4.7
b4 = 0.3
b6 = 0.07
.46
.45
.44
.43
.42
.41
.40
.39
.38
.37
.36
.35
80.34
Vertical Tune
Horizontal Tune
0
2
4
6
8
10
Displacement (mm) at Beta(max)

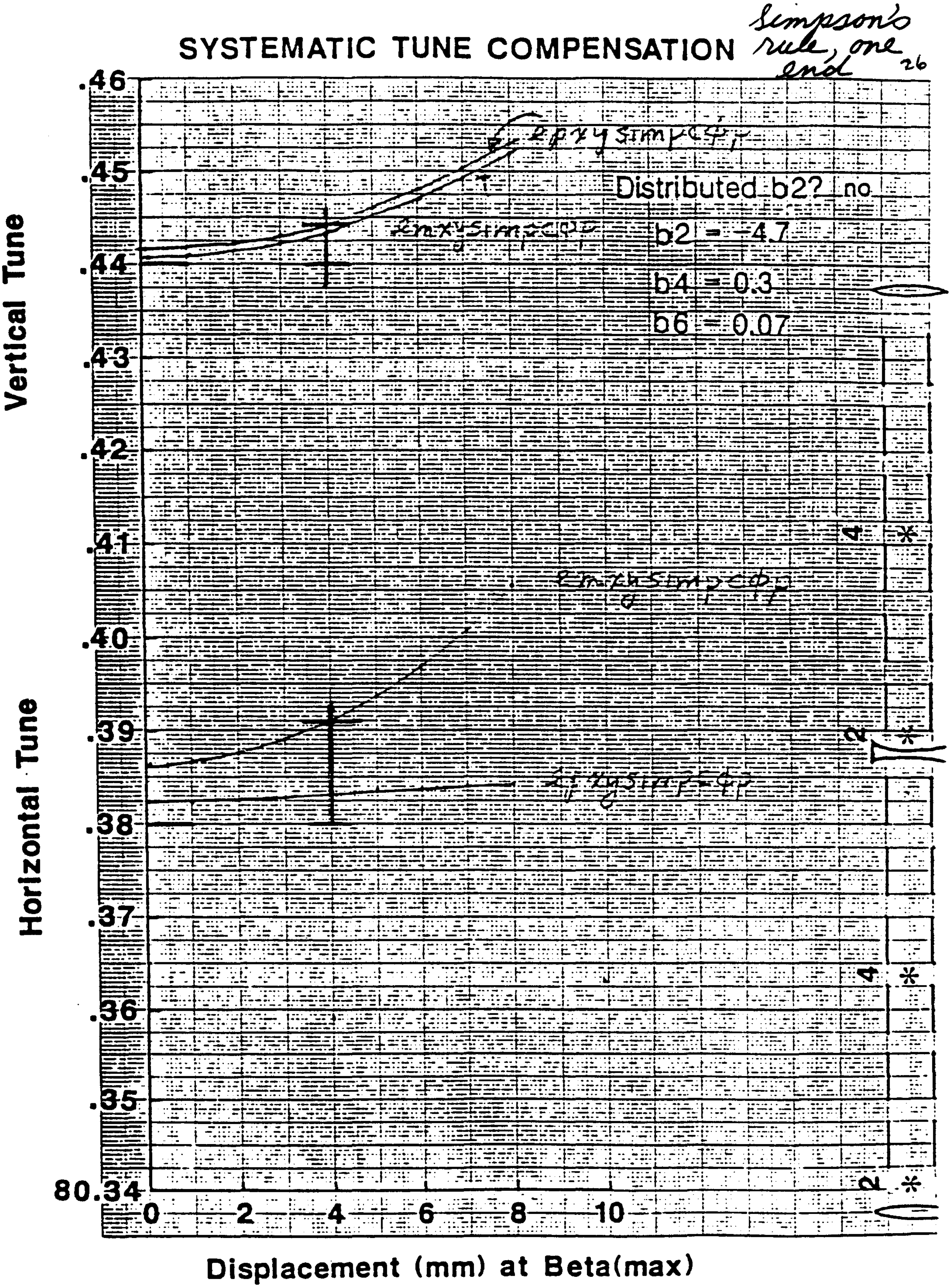

SYSTEMATIC TUNE COMPENSATION
Simpson's rule, one end
26
Distributed b2? no
b2 = -4.7
b4 = 0.3
b6 = 0.07
Vertical Tune
Horizontal Tune
.46
.45
.44
.43
.42
.41
.40
.39
.38
.37
.36
.35
80.34
0
2
4
6
8
10
Displacement (mm) at Beta(max)

Tolerable Systematic b_2
No Bore Tube Windings

		Max. tolerable b_2	Extra spools/ half cell
b_3		26.2	2
lcl2	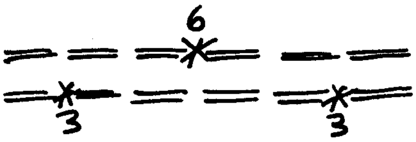	4.9	0.5
l2pl2	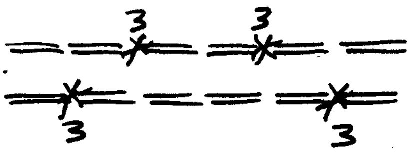	7.2	1
Simpson's rule, one end		3.9	1
Simpson's rule, two ends.		3.8	2

aside: "binning" would still work, though not quite as well.

APPENDIX C

SSC-N-401, "A Design for Multipole Correction Coils,"

Richard Talman, October 26, 1987

Appendix also includes abstract of SCC-N-413, "Systematic Compensation of the SSC with Two Lumped Correctors per Half Cell," Richard Talman, December 1, 1987.

SSC-N-401

A Design for SSC Multipole Correction Coils

Richard Talman
SSC Central Design Group
October 26, 1987

Abstract

Two coil designs are given for SSC correction magnets which generate dipole, sextupole and decupole magnetic fields within a single lumped element. The lengths of these magnets are determined by the dipole steering requirement. The increase in their length due to incorporating sufficient sextupole and decupole capability is negligible.

I. Introduction

In the SSC, multipole correction magnets are needed for various purposes. In the CDR it has been assumed that the correction of any particular multipole requires the corresponding pure single element. For example, b_2 compensation requires a sextupole magnet. Here a design will be given for a single-layer multi-coil magnet which can be used to correct all of b_0, b_2 and b_4. Symmetry makes it natural to correct these particular elements in the same magnet. It is also natural to correct b_1 and b_3 together in a magnet of opposite reflection symmetry, perhaps in the main focusing quads, but that case will not be considered here. Correction of the even skew elements a_{2r} can be performed by rotating the magnets considered here by 90°.

The designs considered here could perfectly well be applied to long bore-tube correction elements inserted into the main dipole magnets but the case of short lumped correctors will be emphasized. It may be that the fabrication techniques developed by Skaritka and others at BNL for fabricating correction coils can be used also for the coils discussed here.

The use for b_0 correction is to trim the closed orbit by local steering. It is assumed in the CDR that there will be one such, independently-powered, dipole correction element in each half cell. It has further been assumed in the CDR that the prototypical use for sextupoles and decupoles is to compensate for persistent current mutlipoles. For this purpose, families of b_2 elements are wired together in series, and similarly for b_4. We will give one design appropriate for such a correction scheme.

Another scheme, which has not previously been considered, and which would require twice as many power supplies, would permit the individual control of b_0 and b_2 elements within each half cell. It is conjectured here (but remains to be exhibited) that such a scheme can both correct the closed orbit and give a large improvement in dynamic aperture for the SSC. Anyway, a design appropriate for such a correction element will be given. This magnet will also contain a decupole coil not necessarily individually controllable. This case, for which the analysis is slightly simpler, will be described first.

II. Theory

Figure 1a shows a current distribution of the symmetry to be considered; symbols defining the geometry are shown there. Assume that the coil is thin and lies on a circle of radius R. To simplify the formulas we will set R = 1 and reintroduce R explicitly only at the end. By Ampere's law the y component of magnetic field at point P due to current in the range dθ is given by:

$$dBy(x,0) = C\frac{\cos\theta - x}{\sin^2\theta + (\cos\theta - x)^2}d\theta \qquad (1)$$

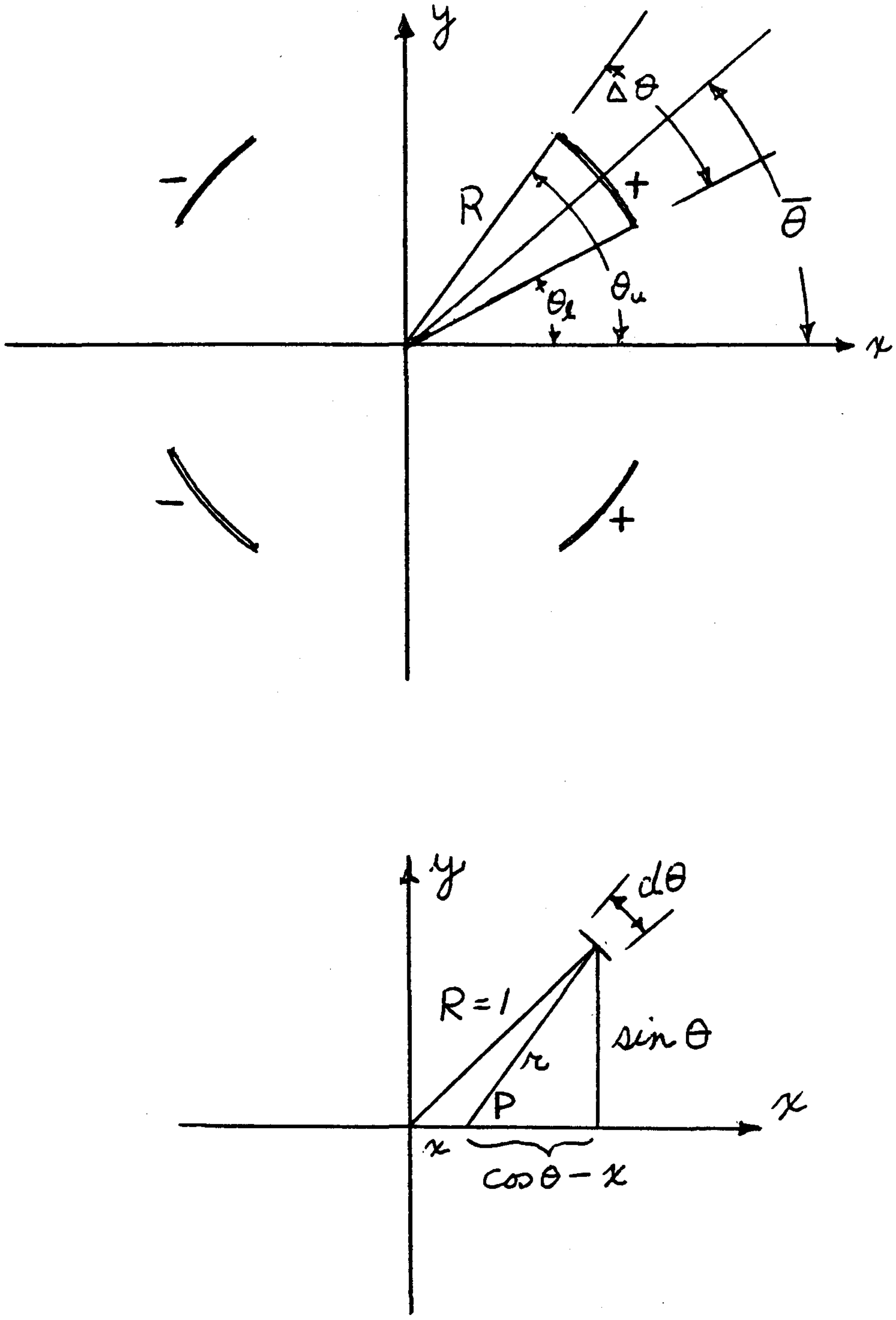

Figure 1. Geometry of coils having the same symmetry as a dipole.

where the constant C will be specified later. Summing and integrating over all four coils. We obtain

$$By(x,0) = 2C \int_{\theta_l}^{\theta_u} \left[\frac{\cos\theta - x}{\sin^2\theta + (\cos\theta - x)^2} + \frac{\cos\theta + x}{\sin^2\theta + (\cos\theta + x)^2}\right] d\theta \tag{2}$$

To study the multipole content we require an expansion in powers of x of the expression in square brackets.

$$2C[\,] = 4C\cos\theta \frac{1 - x^2}{1 - 2\cos 2\theta x^2 + x^4} \tag{3}$$

$$= 4C\cos\theta\left[1 + (-1 + 2\cos 2\theta)\, x^2 + (1 - 2\cos 2\theta + 2\cos 4\theta)\, x^4 + \ldots\right] \tag{4}$$

Finally we get

$$By(x,0) = b_0 + b_2 x^2 + b_4 x^4 + \ldots.$$

where

$$b_0 = 8C \sin\frac{\Delta\theta}{2}\cos\bar{\theta}$$
$$b_2 = \frac{8C}{3}\sin\frac{3\Delta\theta}{2}\cos 3\bar{\theta}$$
$$b_4 = \frac{8C}{5}\sin\frac{5\Delta\theta}{2}\cos 5\bar{\theta} \tag{5}$$

It can be seen that, when expressed in terms of the average coil angle $\bar{\theta}$ and the coil angular extent $\Delta\theta$, certain multipole attributes can be read directly from these analytic expressions for the b_n.

The constant C in (1) is given by

$$C = \frac{10^4}{B_0} 10^2 \frac{\mu_0}{2\pi} \frac{1}{R} \frac{NI}{\Delta\theta} \tag{6}$$

where the coil is assumed to have N turns and to carry current I. The units are MKS except that the factor of 10^2 permits distances to be measured in centimeters, as is coventional. The factor 10^4 is also part of the conventional "units" and B_0 is a reference dipole field; the b_n's are "fractional" errors referred to B_0. Finally in all previous formulas x should be replaced by x/R.

III. A Dipole-Sextupole Coil With a Subsidiary Decupole Winding.

Consider a coil design such as illustrated in Figure 2. There are three independent coils (only a single turn is shown but each coil can have mutliple turns.) For this magnet it is assumed that two currents I_{02} and I'_{02} are individually controlled while I_4 flows through a family of series-wired decupoles which compensates systematic b_4 terms. The currents I_{02} and I'_{02} are to be adjusted to give the desired dipole and sextupole (i.e., b_0 and b_2) fields. Since there is no independent b_4 control these coils must be (and have been) designed so that they give no b_4 contribution. By preference I_4 would not contribute to b_0 and b_2 but that is not really necessary (and is not achieved in the proposed design) because I_{02} and I'_{02} can be adjusted to compensate.

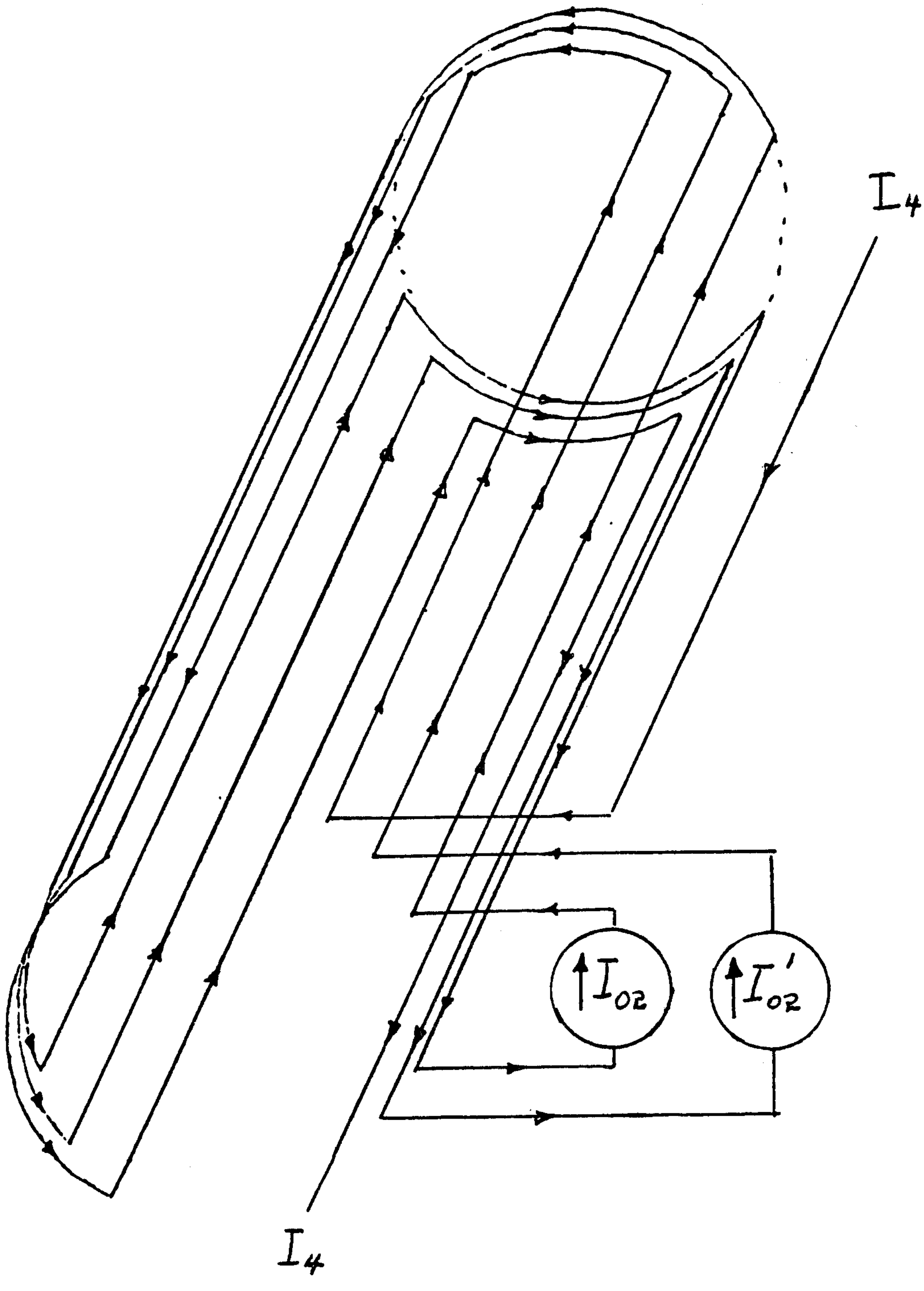

Figure 2. Wiring diagram (copied from M. Green) for a b_0, b_2, b_4 correction magnet with b_0 and b_2 individually controllable.

These conditions can be expressed analytically by introducing a 3 × 3 transfer matrix M which relates the vector $B = (b_0, b_2, b_4)^T$ to the vector $I = (I_{02}, I'_{02}, I_4)^T$ according to

$$B = MI$$
$$I = M^{-1} B \tag{7}$$

For the coil shown in Figure 3 the angles are

$$\theta_0 = 0$$
$$\theta_1 = 0.6284 = 36.00°$$
$$\theta_2 = 1.2565 = 71.99°$$
$$\theta_3 = 1.4 = 80.21° \tag{8}$$

and the matrix and its inverse are given by

$$M = \begin{pmatrix} 0.29392 & 0.18158 & 0.01722 \\ 0.15850 & -0.25641 & -0.04735 \\ 0 & 0 & 0.06577 \end{pmatrix} \tag{9}$$

$$M^{-1} = \begin{pmatrix} 2.4621 & 1.7435 & 0.61061 \\ 1.5219 & -2.822 & -2.4303 \\ 0 & 0 & 15.2045 \end{pmatrix} \tag{10}$$

From the structure of these matrices it can be seen that b_0 and b_2 can be adjusted arbitrarily without influencing b_4. On the other hand, to obtain a pure b_4 field the currents must be in the ratios 0.61:–2.43:15.2.

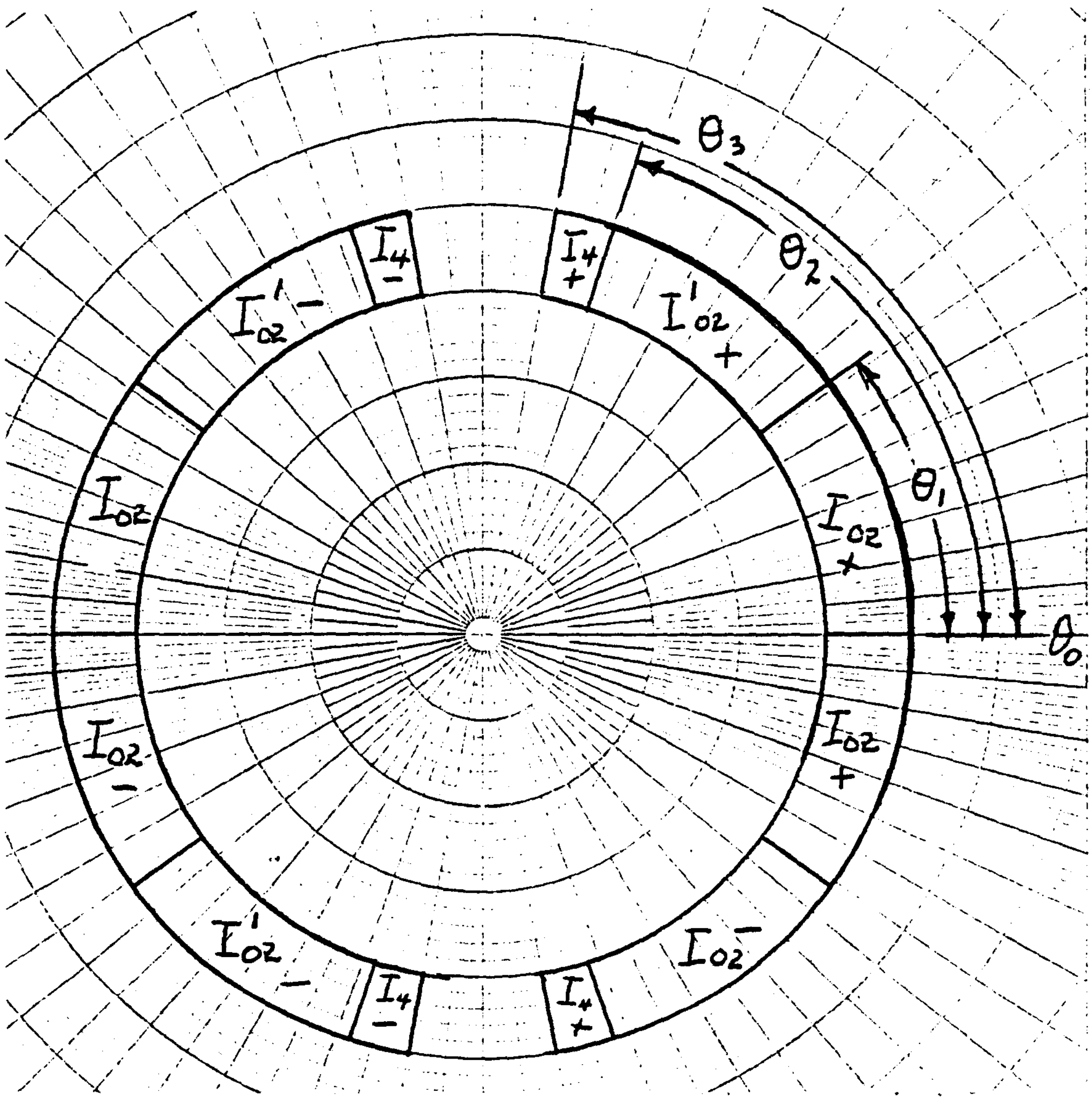

Figure 3. A dipole-sextupole coil with subsidiary decupole winding.

One can inquire whether this design is "inefficient" in the sense that the currents are "bucking" each other, thereby giving a smaller maximum field for a given maximum current than would otherwise be possible. For a pure dipole field the currents are in the ratio $I_{02}:I'_{02}$ = 2.46:1.52. Since the coils subtend equal arcs the current I'_{02} is less than maximum by some 38%, assuming that I_{02} is maximum. On the other hand a single pure dipole coil only subtends 60° instead of the 72° of these two coils. Combining factors the present arrangement is only 3% weaker than a 60° pure dipole coil with the same current limit.

Next we inquire about achievable sextupole strength. This time assume the maximum excitation is set by I'_{02} = 2.46, (the same curent limit but for the other coil). This is 0.87 times the value 2.82 (see formula (10)) and that is one factor by which the maximum value of b_2 will be less than the maximum value of b_0. Now in the CDR the maximum dipole correction field per half cell is 3.1 Tesla-m which can be compared to the full bend field per half cell which is 6 × 16 m × 6.6 T = 634 T-m. Using the conventional "units" (by which fractional fields are quoted in parts per 10^4) this required dipole field for the steering coil being designed can be quoted as $10^4 \times 3.1/634 = 50$ units. Since only horizontal bends can be modified this should be derated to 25 units. Taking the coil radius as 2.2 cm and working in the conventional cm units the maximum sextupole strength would be $b_2 = 0.87 \times 25/(2.2)^2 = 4.5$ units. This is a "full field" value, not an "injection" value. It greatly exceeds the value of 2 units presently specified for distributed bore tube sextupole correctors at full field.

The contents of the previous two paragraphs can be recapitulated as follows: the required integrated sextupole correction field strength per half cell can be achieved in the same elements as are used for steering. The lengths of these elements are determined by steering requirements; they do not need to be lengthened owing to the "piggyback-riding" sextupole coils. Furthermore, the decupole correction can be thrown in also at no cost in length along the beam line.

Before becoming too elated by this result one should be reminded that a lumped sextupole compensation scheme with just one lump per half cell is known to be inadequate. Also schemes which move horizontal steering away from horizontal focusing quads will force the steering correctors to be somewhat stronger. A scheme using two lumps per half cell is being worked on. It will be the subject of a subsequent report.

IV. A Dipole Coil With Subsidiary Sextupole and Decupole Windings.

Consider next the coil shown in Figure 4. This has four windings except that the first and third are wired in series to form a dipole coil which carries a current I_0. This coil has been designed to give zero contribution to both b_2 and b_4. The second winding, carrying current I_4 corrects decupole errors. It has a dipole component which must be compensated with I_0. The fourth winding carries current I_2 and corrects sextupole, with I_0 and I_4 being adjusted to compensate its dipole and decupole fields.

The angles defining the coil are

$$\begin{aligned}
\theta_0 &= 0 \\
\theta_1 &= 24.40^\circ \\
\theta_2 &= 36.10^\circ \\
\theta_3 &= 60.16^\circ \\
\theta_4 &= 74.48^\circ
\end{aligned} \tag{11}$$

and the matrix equation describing its performance is

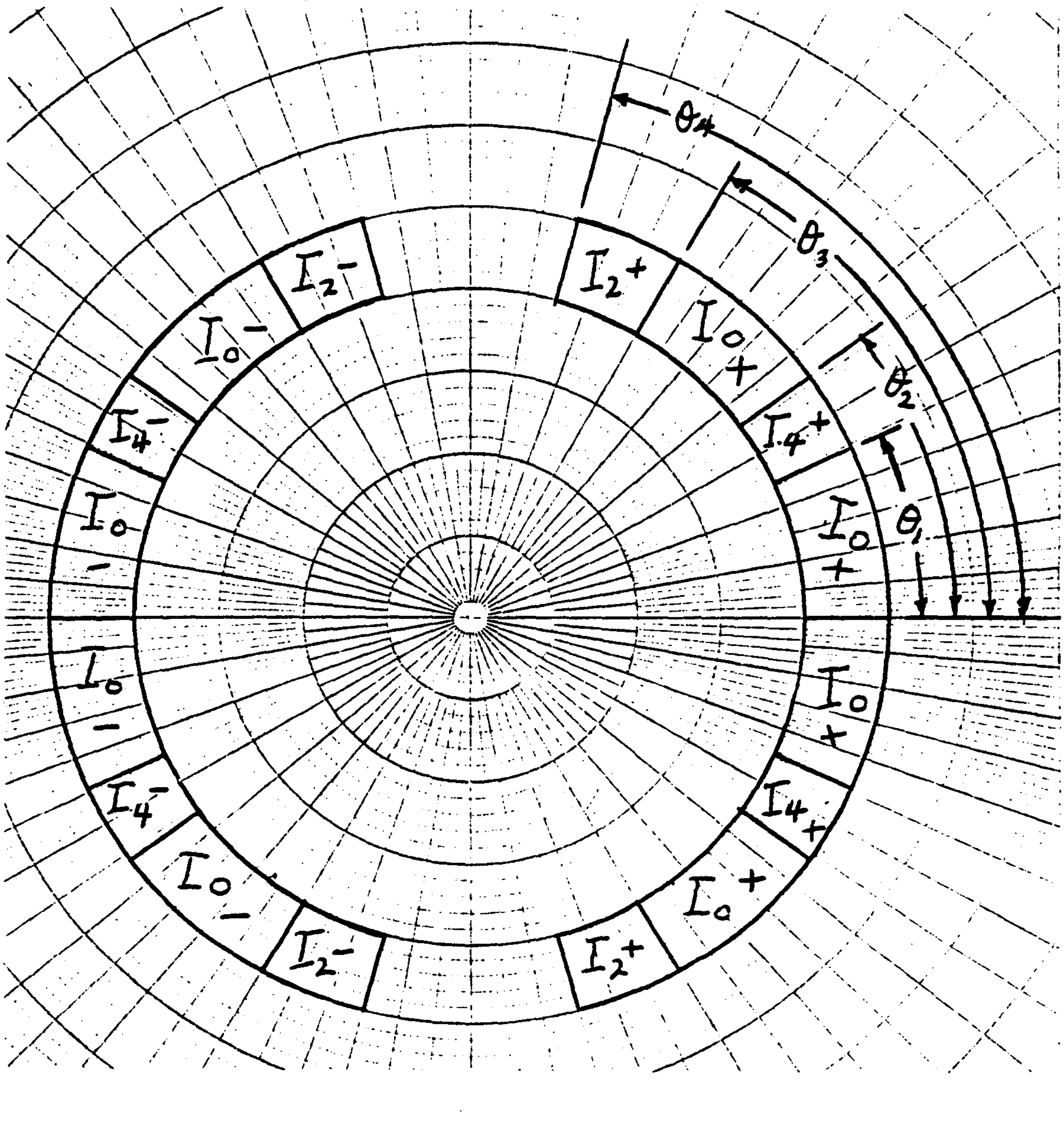

Figure 4. A dipole magnet with subsidiary sextupole and decupole windings.

$$\begin{pmatrix} b_0 \\ b_2 \\ b_4 \end{pmatrix} = \begin{pmatrix} 0.3456 & 0.0481 & 0.0880 \\ 0 & -0.1132 & 0 \\ 0 & 0.1074 & -0.0856 \end{pmatrix} \begin{pmatrix} I_0 \\ I_2 \\ I_4 \end{pmatrix} \tag{12}$$

$$\begin{pmatrix} I_0 \\ I_2 \\ I_4 \end{pmatrix} = \begin{pmatrix} 2.893 & 4.051 & 2.974 \\ 0 & -8.834 & 0 \\ 0 & -11.084 & -11.682 \end{pmatrix} \begin{pmatrix} b_0 \\ b_2 \\ b_4 \end{pmatrix} \tag{13}$$

By introducing a more complicated arrangement with more coils it would be possible to improve the "orthogonality" of these correction coils. Also many other variants are possible.

SSC-N-413

Systematic Compensation of the SSC With Two Lumped Correctors Per Half-Cell

RICHARD TALMAN

SSC Central Design Group

December 1, 1987

ABSTRACT

Lumped systematic field compensation of the SSC is analysed using **teapot** for particle tracking followed by Fourier analysis. The smallest number of correctors per half cell yielding acceptable compensation is at most three, and is probably two; the latter case is studied here. The best scheme found meets the requirement of constancy of the off-momentum, large-amplitude tunes, is sufficiently fine-grained to yield satisfactory improvement of the linear aperture by means of the "binning" compensation of random errors, and has been checked to be satisfactory for chromaticity adjustment and orbit flattening. Only a single point in the tune plane has been studied and the minimum set of multipoles needed in the lumped correctors remains to be determined. Also sensitivity to errors which are partly random, partly systematic has not been studied.

APPENDIX D

"Magnetic Design,"

Talk by Pat Thompson

Appendix includes "Field Quality for SSC Internal Trim Coils," Pat Thompson, August 20, 1986.

MAGNETIC DESIGN OF INTERNAL CORRECTORS

P.A.Thompson(BNL)

Presented at SSC-Workshop on Distributed Correction Coils

13-14-October-1987

I CONDUCTOR SPECIFICATION

The first problem criterion is the neccessary short sample current. For these trim coils we chose to design for Ioperation~ 0.25 Ishort sample. The estimation was that the labor involved in making coils with the mechanical excellence to reach ~100% of short sample would be more expensive than the added superconductor.

Most of the coils of this type made previously have had copper to superconductor ratios of ~2:1 and there are no compelling reasons to change.

The larger the wire diameter, the fewer turns neccessary for a given field strength. Also larger wires are less vulnerable to damage both in manufacture and in wireing. The insulation of the wire is a significant 20-50% fraction of the total cost of small wires.

The Multiwire^R process offers significant savings in labor and improvements in accuracy. The mechanics of this process limit the wire size to 0.006" (previous), 0.014"(under test), 0.020" (soon??).

So current design is 0.014" wire.

Note that the wire specification is conservative both in Jc and in the ratio of operating current to short sample. The coils are 8 meter(B2),3meter(B3), and 5 meter(B4) long. The right hand column in this table gives the field strength in "standard units" (1x10^{-4}' x 6.6 Tesla @ 10 mm) and in parenthesis the required strength. These are values for I = 16 Amps (25% of short sample).

WIRE DIAMETER

AS LARGE AS PRACTICAL

1) LESS LABOR

2) MORE RESISTANT TO DAMAGE

BUT MULTIWIRE TECHNIQUE

$\phi < 0.008''$ BEFORE

$\phi < 0.014''$ NOW

ϕ = 0.014"

$J_c \geq$ 2.2 kA/mm² @5T 4.2K

THEN: $I_c \cong$ 63A @6.6T 4.5K

COIL LIMITS.

$I_o = \frac{1}{4} I_c = 16$ A

COIL	B_N/A	$b'_n \cdot L$/16m-A	$\frac{b'_n \cdot L}{16}$ @I_{op}
B_2	3.6	0.27	4.3 (4)
B_3	2.0	0.057	0.9 (0.4)
B_4	1.1	0.053	0.8 (0.4)
	$\left(\frac{G@10m}{A}\right)$		

At injection, the Jc in the trim conductor is very high and the transport current needed for correction purposes is a very small (<0.5%) fraction of this. Thus large persistent magnetization currents can be induced in the superconducting filaments. Since the trim conductors are much closer to the center of the bore tube than the main coils, the higher multipole contributions from this effect are enhanced,

Two cases have been calculated: 1) the early trim coils in which a single filament (140 um) conductor was used and a later version with a multifilamentary conductor. There is no intention of building further coils with single filament conductor.

MAGNETIZATION

1) EARLY CALCULATION

   $\Rightarrow$ NEGLIGBLE

2) MEASUREMENTS

   $\Rightarrow$ $\approx$ MAIN COIL

CALCULATED MAGNETIZATION @ 0.33T

COIL → B2 B3 B4

b'_N MAGNTZ

	B2	B3	B4
b'_0	17	13	10
b'_2	—	—	—
b'_4	-3.6	—	—
b'_6	1.6	-1.2	—
b'_8	—	0.5	-0.4
b'_{10}	0.13	—	0.2

WIRE $\emptyset$ = 0.008" = 200 μm

FILAMENT ~140 μm

X1

I_c @ 0.5T ~120 A

CALCULATED MAGNETIZATION @ 0.33T

COIL =

b_N'

	B2	B3	B4
b_0'	3.3/1.7 *	2.4/0.5	2.0/0.6
b_2'	—	—	—
b_4'	-0.7/0.35	—	—
b_6'	0.3/0.2	-0.2/0.04	—
b_8'	—	0.09/0.04	-0.08/0.02
b_{10}'	0.02/0	—	0.03/0.01

WIRE ∅ = 0.014" 356 μm

Filament 0.001" 27 μm
× 54

I_c @.3T ~370 A

The multi-wire method of making flat coil patterns has been used because of its low labor cost, accuracay and reproducibility. The block diagram shows the data flow for coil generation with this technique. The input at the start is basic parameters such as wire size, bore tube diameter, and the physics parameters of the desired coil. The computer code then generates the specific commands for the wiring head. These commands are also feed directly into a code which calculates the field harmonics. The resultant data (as well as being printed out for reference), is electronically transported to an on-site Computer-Vision^R CAD system which can produce high quality displays, production drawings and high accuracy (0.001") templates for quality control.

The wiring commands are also transported electronically to the Multi-wire VAX and thence to the wiring head. There is thus ~0 delay between a decision to make a particular coil and when the wiring head can start running. Very few cracks exist in which human errors can result in a different coil being wired from that which was calculated. In principle, one could make individual trim coils in any number- this is probably a dangerous degree of freedom.

Any flat coil pattern needs to be cut so that it can be wrapped around the bore tube. In the obvious way (one coil per pole) of making coils the only place to put these cuts is at the midplane. The midplane is the worst place to remove conductor. Hence these coils have been designed as "double coils", with one coil for every two poles. Then one can cut the pattern at one of the poles where there is an almost arbitrary amount of dead space.

MULTIWIRE

1) ACCURATE
   FAST
   ARBITRARY PATTERN

2) BUT NEED CUT SOMEWHERE

SO

"DOUBLE COILS"

eg. A SEXTUPOLE HAS 3 SEPARATE COILS.

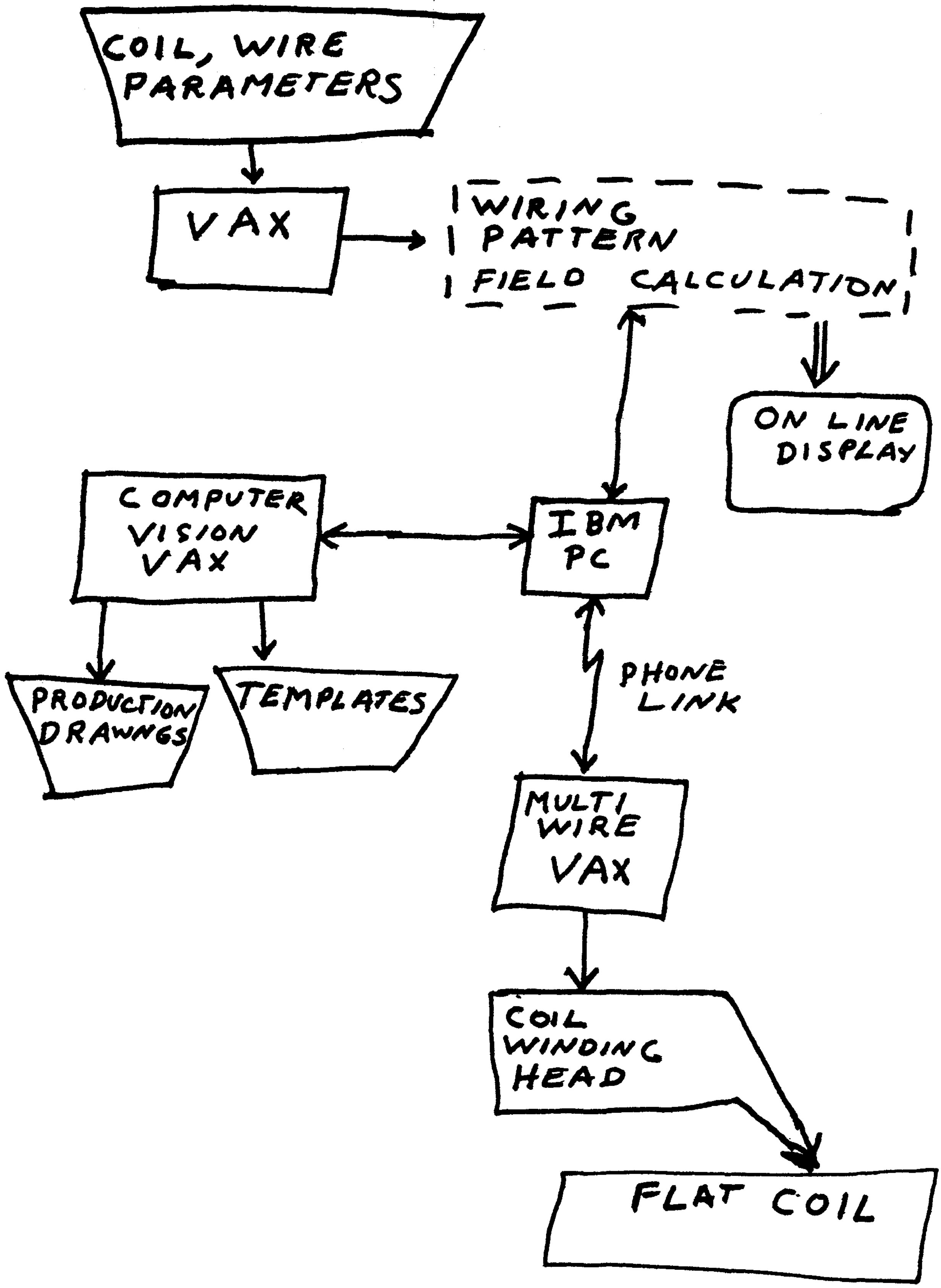

COIL, WIRE PARAMETERS
VAX
WIRING PATTERN
FIELD CALCULATION
ON LINE DISPLAY
COMPUTER VISION VAX
IBM PC
PRODUCTION DRAWNGS
TEMPLATES
PHONE LINK
MULTI WIRE VAX
COIL WINDING HEAD
FLAT COIL

A drawback of the "double coil" concept is that the ends violate the basic symmetry. Most "as built" coils have small deviations- eg. one fewer turns around the lead end than the return end, one leg of each turn slightly longer, interconnections, and the leads. With this completely computer controlled system, it is possible to sum the field produced by each piece of wire to determine the total field and by use of the precision template to insure that the completed coil matches the computer model to high precision.

The tables of harmonics for the coils are calculated in this fashion. The fundamental has been set =10000, thus the impurities are parts in 10^4 of the fundamental which in turn is $4(0.4)\times10^{-4}$ of the dipole field (sextupole/other).
Looking through these tables reveals that the various asymmetries produce $<3 \times 10^{-4}$ of the trim field. And that the second allowed harmonic(the first non-zero harmonic for single block coils) is comparable. Thus worst case results are 10^{-7} of the main field. These could be corrected by very small changes in the trim winding pattern, but are so small compared to both rms and systematic errors from other causes it was not thought worthwhile.

```
Harmonic,Length,Coil length,turns,spacing,circum Xcorner Ycorner
   2    18.000     14.000    20      0.024      4.373
 x Corner  Y corner  overhang   # of blocks
    0.0000       0.0000      0.0080
FILE =DUA0:[THOMPSON.SSC]FOR001.DAT; run on 12-OCT-87
 ZOOM? X,Y lower left(inches),Full Scale(inches)=
```

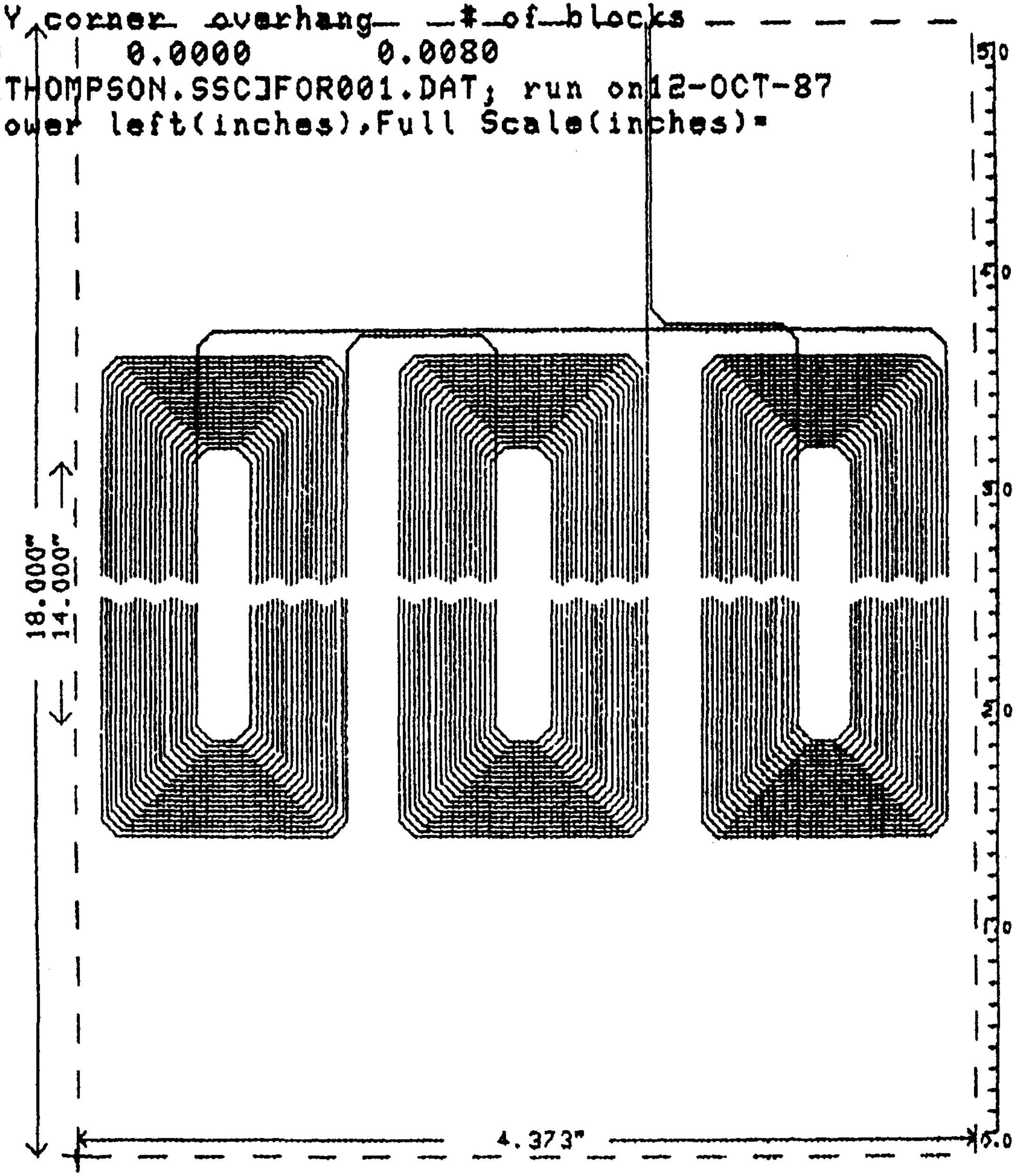

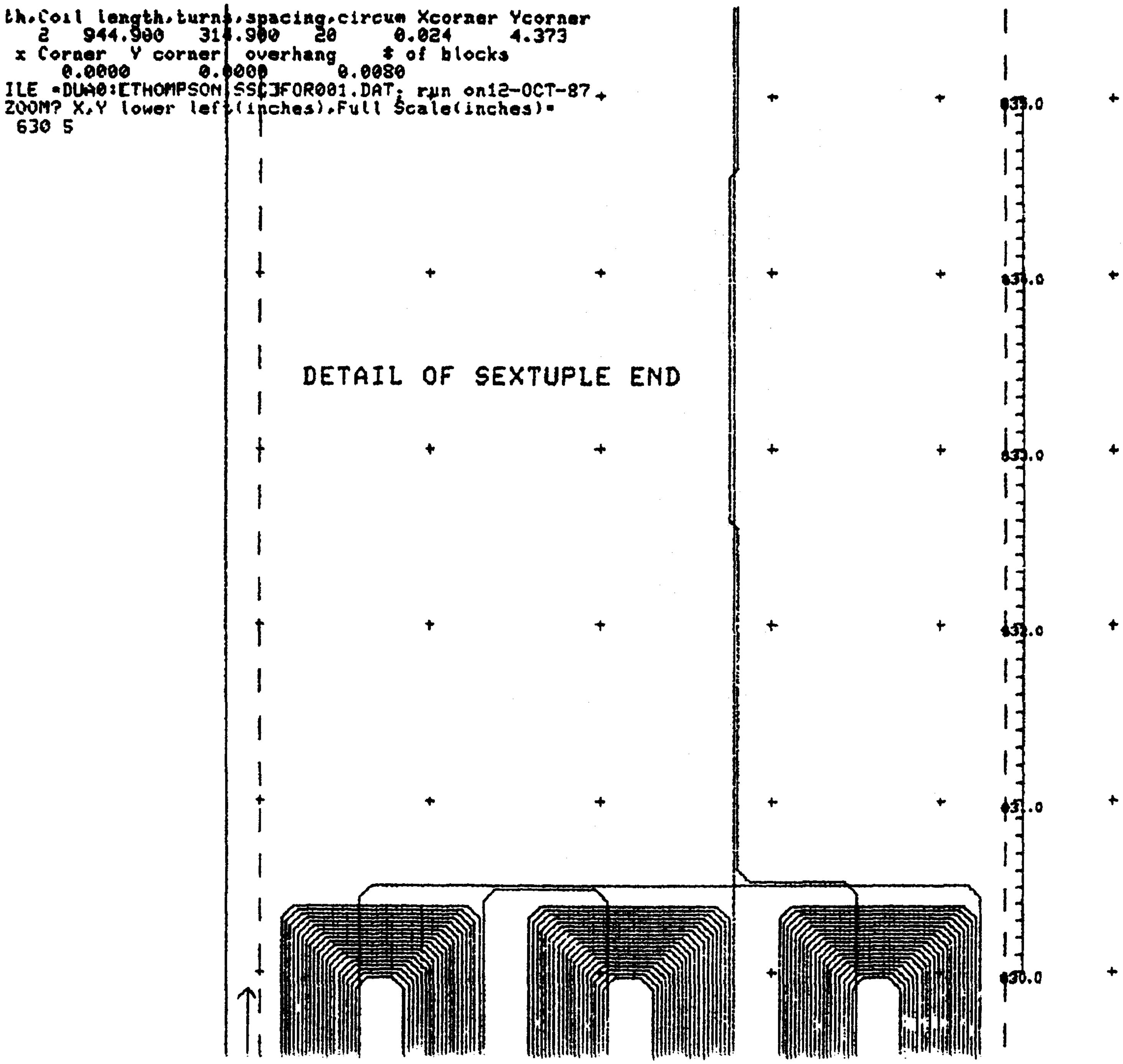

th,Coil length,turns,spacing,circum Xcorner Ycorner
2 944.900 314.900 20 0.024 4.373
x Corner Y corner overhang # of blocks
0.0000 0.0000 0.0080
ILE =DUA0:[THOMPSON.SSC]FOR001.DAT; run on12-OCT-87
ZOOM? X,Y lower left(inches),Full Scale(inches)=
630 5
DETAIL OF SEXTUPLE END

SEXTUPOLE 8 METERS 0.014" wire

Total commands= 802 Feet of wire= 3214.224

All Harmonics integrated for Coil Length = 8.00 m

Harmonic #	B(Nharm) (Tesla,m)	B(Nharm) @ R =(mm)	
2	28.802	0.00288	10.00

Harmonics Normalized(*1e4) at Reference Radius

1	-0.05259	0.20398
2	0.20263	-0.33605
3	-0.93654	10000.00000
4	0.47946	-0.11803
5	-0.42719	-0.03982
6	1.51295	0.08235
7	-0.19809	-0.18415
8	0.09529	0.17306
9	-0.02618	-0.16024
10	-0.01684	0.09761
11	0.03272	-0.05872
12	-0.02081	0.02874
13	0.02768	-0.01174
14	-0.01951	0.00149
15	0.01293	-2.16683
16	-0.00678	-0.00455
17	0.00311	0.00414
18	-0.00152	-0.00304
19	-0.00004	0.00206
20	0.00043	-0.00121

Generated # holes,sizes= 0

```
Harmonic,Length,Coil length,turns,spacing,circum Xcorner Ycorner
   3    18.000     14.000   14     0.026      4.373
 x Corner  Y corner  overhang   # of blocks
     0.0000        0.0000        0.0080
FILE =DUA0:[THOMPSON.SSC]FOR001.DAT; run on12-OCT-87
 ZOOM? X,Y lower left(inches),Full Scale(inches)=
```

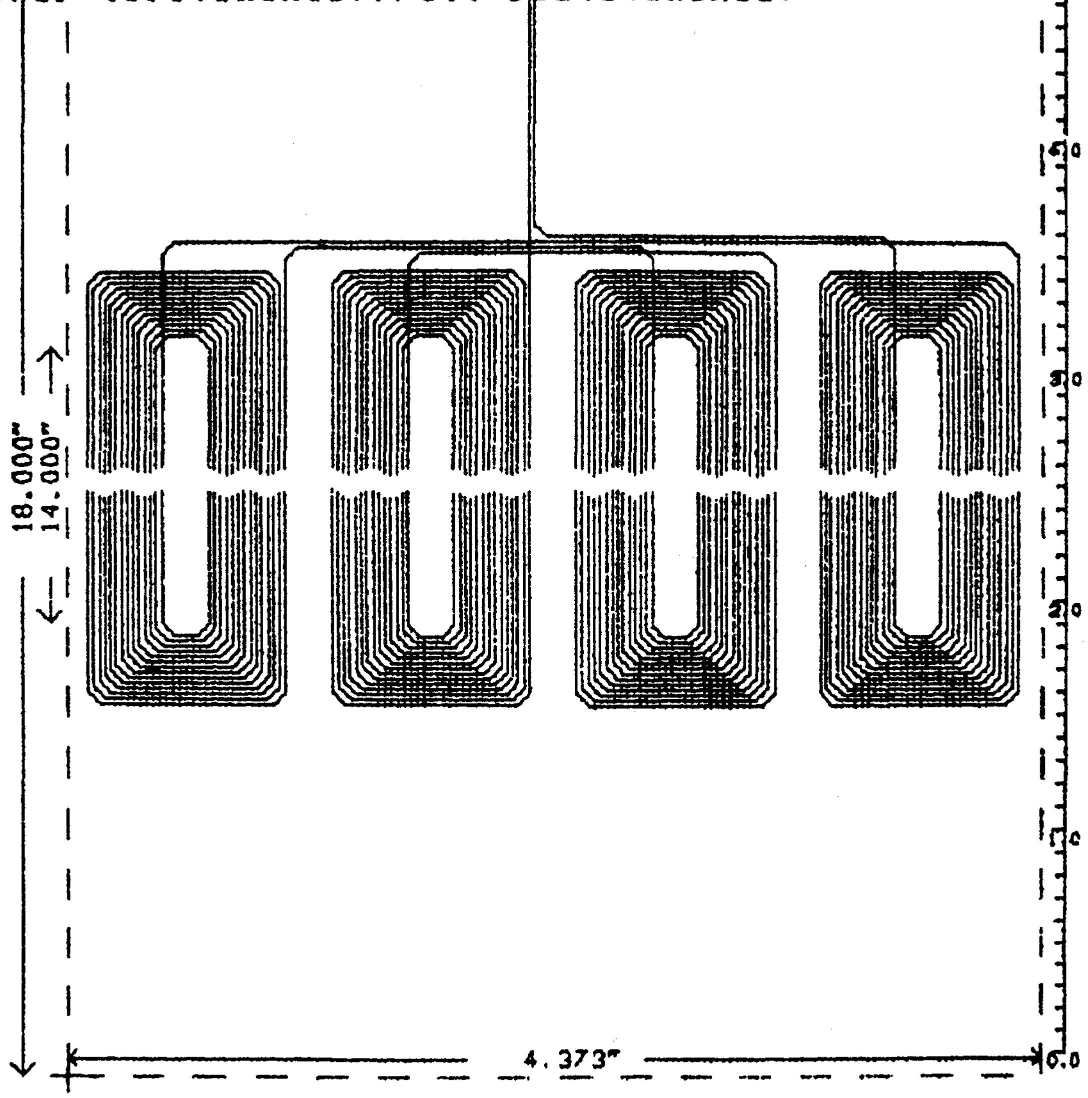

OCTUPOLE 3 meters 0.014" wire

Total commands= 649 Feet of wire= 1180.325

All Harmonics integrated for Coil Length = 3.10 m

Harmonic #	B(Nharm) (Tesla,m)	B(Nharm) @ R =(mm)	
3	590.32	0.00059	10.00

Harmonics Normalized(*1e4) at Reference Radius

1	0.71605	0.64780
2	-1.25665	-0.62678
3	1.35116	-0.10688
4	-2.71742	10000.00000
5	0.54386	-1.17992
6	0.13048	1.07452
7	-0.49870	-0.66177
8	1.73404	0.13535
9	-0.42569	0.07587
10	0.22745	-0.19783
11	-0.06268	0.19180
12	-0.03536	-0.15236
13	0.06332	0.06569
14	-0.05775	-0.01527
15	0.03719	-0.01066
16	-0.01232	0.01738
17	0.00318	-0.01544
18	0.00332	0.00940
19	-0.00479	-0.00396
20	0.00406	-0.22412

Generated # holes,sizes= 0

Harmonic,Length,Coil length,turns,spacing,circum Xcorner Ycorner
4   18.000   14.000   12   0.024   4.373
x Corner   Y corner   overhang   # of blocks
0.0000   0.0000   0.0080
FILE =DUA0:[THOMPSON.SSC]FOR001.DAT; run on12-OCT-87
ZOOM? X,Y lower left(inches),Full Scale(inches)=

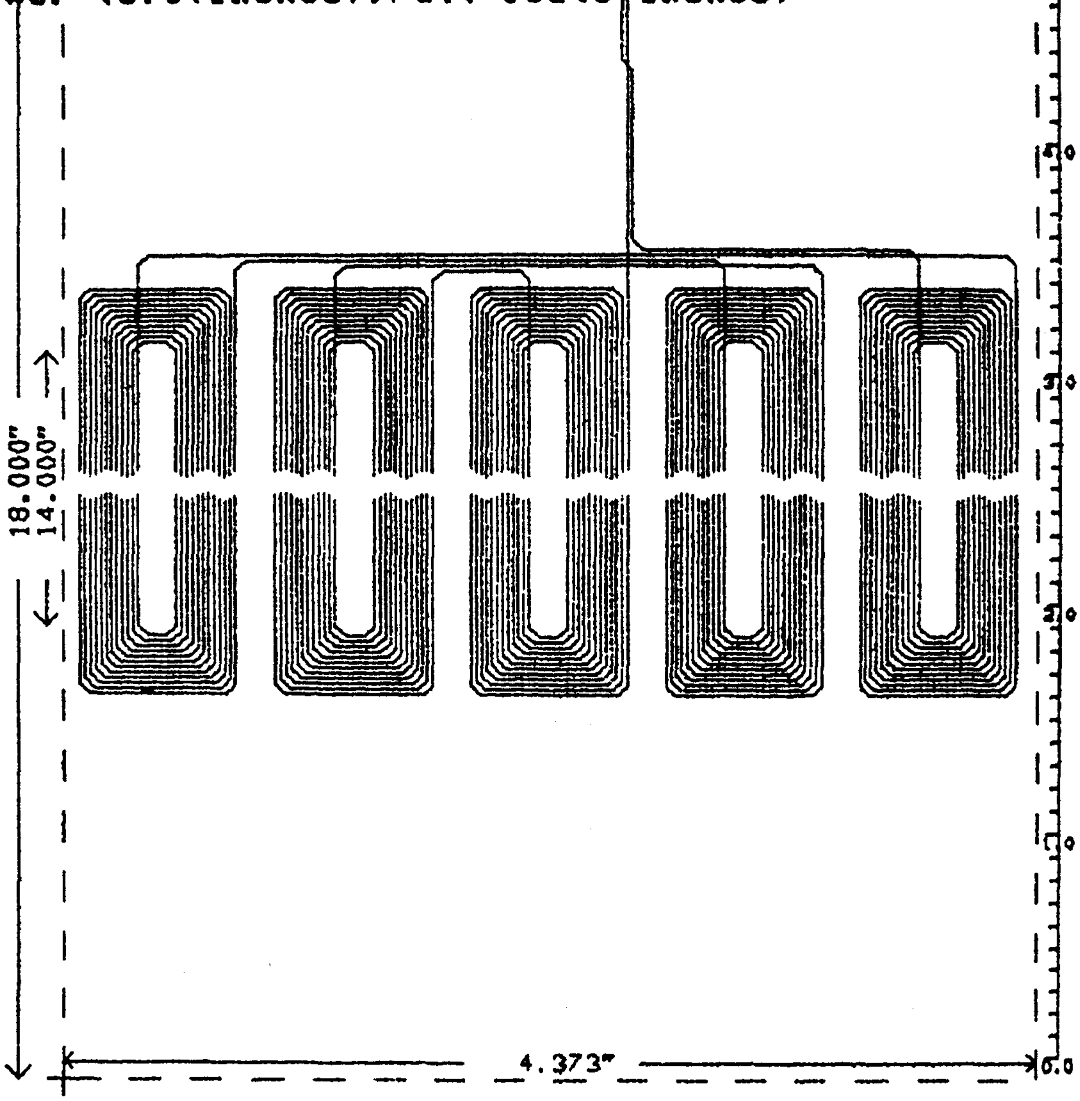

```
Harmonic,Length,Coil length,turns,spacing,circum Xcorner Ycorner
   4   202.000   197.000   12     0.024     4.373
 x Corner  Y corner  overhang    # of blocks
     0.0000     0.0000      0.0080
FILE =DUA0:[THOMPSON.SSC]FOR001.DAT; run on12-OCT-87
 ZOOM? X,Y lower left(inches),Full Scale(inches)=
09898 5
```

DECAPOLE END DETAIL

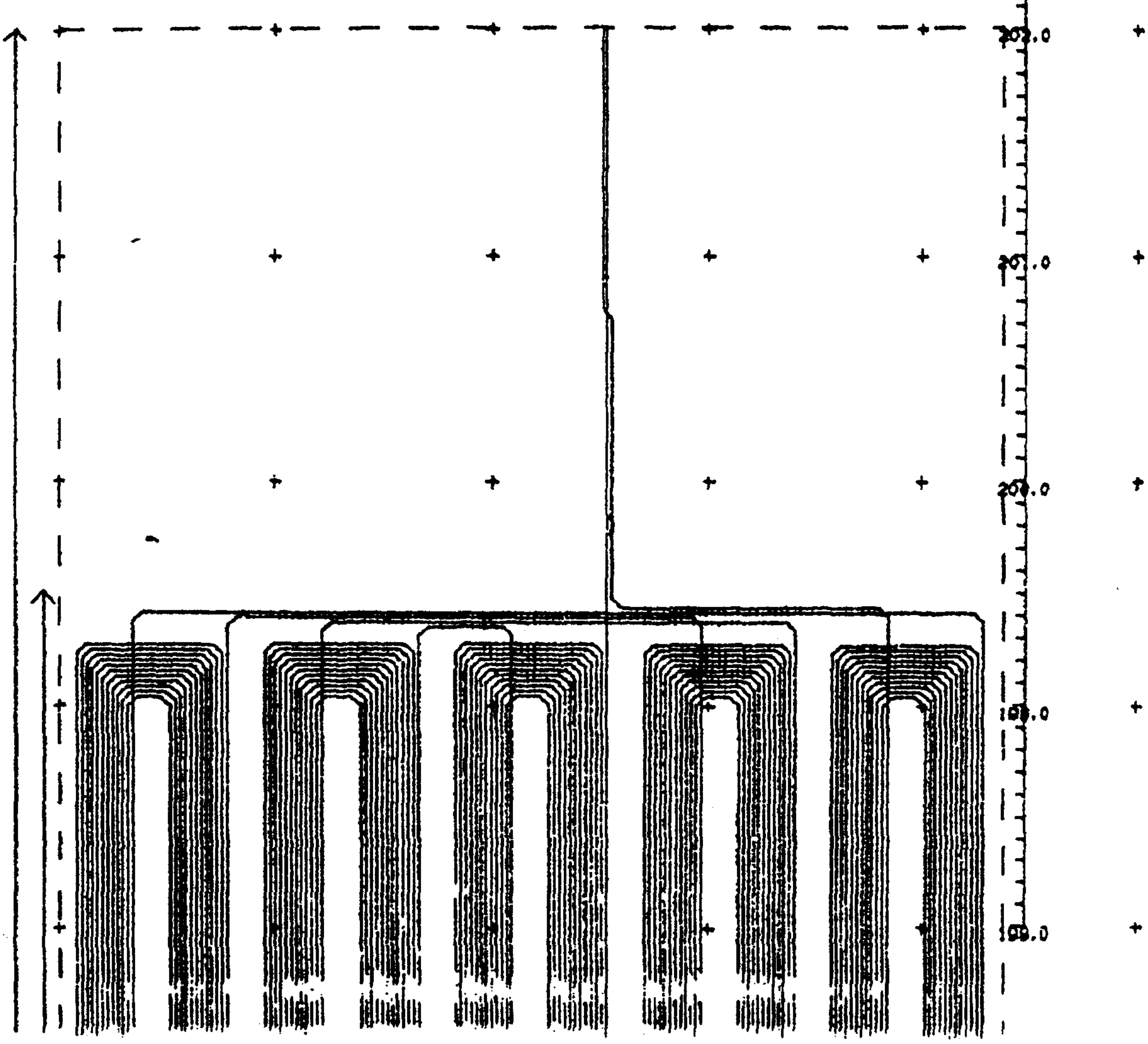

DECAPOLE 5 meters,0.014" wire

Total commands= 490 Feet of wire= 1978.425

Harmonics integrated for Coil Length = 5.00 m

Harmonic #	B(Nharm) (Tesla,m)	B(Nharm) @ R =(mm)	
4	57696.	0.00058	10.00

Harmonics Normalized(*1e4) at Reference Radius

1	0.20353	0.42745
2	0.08864	-0.34930
3	-0.10208	0.16590
4	-0.14027	-0.05525
5	-1.00502	10000.00000
6	0.02009	0.02137
7	-0.02330	0.00870
8	0.01890	-0.00171
9	-0.00846	-0.00466
10	0.35374	-0.02605
11	-0.00424	-0.00166
12	0.00267	0.00174
13	-0.00125	-0.00150
14	0.00073	0.00008
15	-0.00129	-0.00443
16	-0.00001	0.00038
17	0.00001	-0.00026
18	-0.00005	0.00017
19	0.00006	-0.00008
20	0.00040	-0.00005

Generated # holes,sizes= 0

II TRIM COIL FIELD ERRORS

Attached is a note discussing many of the possible errors in trim coils. Presented at the workshop were:

1. The definitions of errors discussed (pages 2,3)

2. The mechanical tolerances page 6

3. Results pages 7,8.

4. A more precise calculation of the systematic field errors in the winding pattern. THIS REPLACES SECTION IV.1. The exact calculation gives values 1-2 orders of magnitude smaller than the estimates in this section.

5. Note that the octupole design has been changed- there are NO POLE LOCATOR pins within these coils. This design turned out to be mechanically undesireable. We may have problems with the coil twisting over its 3 meter length- if so we can make the coil i two pieces with location in between.

6. Magnetization- Section IV.3- This section was in error and should be replaced bv the discussion at the workshop.

Field Quality for SSC Internal Trim Coils

P.A. Thompson

20-August-1986

I INTRODUCTION

This note presents calculations of the field errors induced in the proposed SSC internal trim coils by various construction and assembly errors. Tolerances have been derived from these errors. With tolerances of approximately 10 mils, which is achievable with the present technology, the worst case errors are about 5% of the fundamental harmonic. In may be possible to develop a technology which will produce 4 mil accuracies which correspond to worst case errors of 2 %.

II ERROR MATRICES

The program computes the perturbed positions of the wires of the coil under study. The field is sampled at 64 points around a 10 mm radius and a Complex Fast Fourier Transform is used to obtain the harmonic expansion. For calculation standard perturbations of 1 mm and 5 degrees have been used. These are larger than the tolerances which will be discussed latter. Six basic types of perturbation have been investigated:

1. Displacement, the coil as a whole is displaced in an arbitrary direction from the center of the main dipole coil. For simplicity, results are presented for a 1 mm displacement in the y direction. For small displacements the effects of multiple perturbations add linearly, and the effects of a displacement in x are similar to those in y except for the generation of normal rather than skew harmonics. The dominant effect is the generation of the (m-1)th normal/skew harmonic, with second order terms in (m-2).

2. Rotation, the coil as a whole is rotated about its center relative to the main dipole coil. Results are presented for a standard 5 degree rotation. The dominant effect is the generation of the m-th skew harmonic.

3. A gap in the Coil. If the diameter of the bore tube is larger than the coil, an asymmetric gap will be generated. The results for a 5 degree gap at 22 degrees are presented. 22 degrees is where the cut in the substrate will be made. This generates a very rich harmonic spectrum.

4. Ellipse: In assembly it is likely that the bore tube will be distorted. The simplest distortion is an ellipse. Results are given for a perturbation of 1 mm inward at the pole. This generates a significant normal (m-2)th harmonic. An ellipse with its short axis horizontal has the same harmonics but with the opposite signs.

5. Random Wire displacements. Calculations were done for the case where each wire is allowed to move up to 1 mm azimuthaly from its nominal location. (In the physical coil these wires would often overlap for such a large variation). The disturbution used is flat from -1 mm to + 1 mm of displacement.The field perturbations generated in this manner are small, presumably due to the large number of wires (~200) involved.

6. Random Block displacements. Calculations were done where each block of wires was moved randomly over +-1 mm. For this calculation, a block is the group of wires between each "midplane" and pole. Thus a sextupole coil consists of 12 blocks. The field distortions produced by these displacements are marginally significant. If the two blocks between adjacent poles were displaced as a whole, the field distortions would be approximately twice as large.

The results of these calculations are presented in tables 1-3; one table for b2,b3 and b4 coils. In these tables the perturbations are 1 mm for displacements and 5 degrees for rotations. These values were chosen for ease in comparing data and are larger than reasonable tolerances. A subsequent section of this note develops actual tolerances. The tables are arranged with 12 columns of harmonics subdivided into 6 groups of two. The first column in each group is the Bx or skew harmonic, the second is the normal harmonic. The rows are labeled with the power of R for the harmonic. The values quoted are percent (%) of the fundamental- evaluated at 10 mm radius. Thus the normal fundamental harmonic is usually close to 100%. For the two cases where random perturbations were applied, only the rms variation of the fundamental from 100% is given. This variation is of course unsigned.

Table 1: Field Perturbations for b2 Coil
(as percent of Fundamental)

COIL -- b 2 (C 3) 19 turns 6.70 G/Amp

m-1	displacement dy=1 mm		Rotation 5 deg		Gap 5 deg.		Ellipse dy=-1mm		Wire rms 1 mm		Block rms 1 mm	
0	0	-1.0	0	0	-2.5	1.3	0	-13.2	0.5	0.6	2.1	1.6
1	20.0	0	0	0	-3.1	4.4	0	0	0.7	0.6	1.7	2.4
2	0	100.0	25.9	96.6	-13.6	99.1	0	100.0	0.7	0	2.2	0
3	0	0	0	0	-1.0	-2.9	0	0	0.6	0.3	1.2	2.7
4	0	0	0	0	-0.7	-0.7	0	0	0.2	0.3	0.9	1.2
5	0	0	0	0	-0.4	-0.1	0	-2.2	0	0	0	0
6	0	0	0	0	-0.2	0	0	0	0	0	0	0
7	0	0	0	0	-0.1	0.1	0	0	0	0	0	0
8	0	0	0	0	0	0.1	0	0	0	0	0	0
9	0	0	0	0	0	0	0	0	0	0	0	0
10	0	0	0	0	0	0	0	0	0	0	0	0
11	0	0	0	0	0	0	0	0	0	0	0	0
12	0	0	0	0	0	0	0	0	0	0	0	0
13	0	0	0	0	0	0	0	0	0	0	0	0
14	0	0	0	0	0	0	0	0	0	0	0	0

Table 2: Field Perturbations for b3 Coil
(as percent of Fundamental)

COIL -- b 3 (C 4) 14 turns 3.7 G/Amp

m-1	displacement dy=1 mm		Rotation 5 deg		Gap 5 deg.		Ellipse dy=-1mm		Wire rms 1 mm		Block rms 1 mm	
0	-0.1	0	0	0	-3.2	1.2	0	0	1.3	0.8	3.1	2.0
1	0	-3.0	0	0	-3.9	3.3	0	-26.1	0.9	1.0	7.0	2.7
2	30.0	0	0	0	-3.8	6.6	0	0	0.9	0.8	3.2	3.0
3	0	100.0	34.2	94.0	-17.4	98.5	0	100.0	1.2	0	3.2	0.1
4	0	0	0	0	-0.7	-3.9	0	0	0.9	0.5	2.2	2.0
5	0	0	0	0	-0.6	-1.1	0	-2.6	0	0	0	0
6	0	0	0	0	-0.4	-0.4	0	0	0	0	0	0
7	0	0	0	0	-0.2	-0.1	0	0	0	0	0	0
8	0	0	0	0	-0.1	0	0	0	0	0	0	0
9	0	0	0	0	-0.1	0	0	0	0	0	0	0
10	0	0	0	0	0	0	0	0	0	0	0	0
11	0	0	0	0	0	0	0	0	0	0	0	0
12	0	0	0	0	0	0	0	0	0	0	0	0
13	0	0	0	0	0	0	0	0	0	0	0	0
14	0	0	0	0	0	0	0	0	0	0	0	0

Table 3: Field Perturbations for b4 Coil
(as percent of Fundamental)

COIL -- b 4 (C 5) 11 turns 2.0 G/Amp

m-1	displacement dy=1 mm		Rotation 5 deg		Gap 5 deg.		Ellipse dy=-1mm		Wire rms 1 mm		Block rms 1 mm	
0	0	0	0	0	-4.4	1.2	0	1.3	0.8	1.9	4.1	4.4
1	-0.4	0	0	0	-5.3	3.2	0	0	2.5	2.9	5.5	4.5
2	0	-6.0	0	0	-4.9	5.2	0	-39.0	1.7	1.3	7.1	6.0
3	40.0	0	0	0	-4.6	8.7	0	0	1.0	1.7	4.6	3.5
4	0	100.0	42.3	90.6	-21.2	97.7	0	100.0	1.3	0	1.8	0
5	0	0	0	0	-0.3	-5.0	0	0	0	0	0	0
6	0	0	0	0	-0.5	-1.5	0	-3.0	0	0	0	0
7	0	0	0	0	-0.4	-0.5	0	0	0	0	0	0
8	0	0	0	0	-0.2	-0.2	0	0	0	0	0	0
9	0	0	0	0	-0.1	-0.1	0	0	0	0	0	0
10	0	0	0	0	-0.1	0	0	0	0	0	0	0
11	0	0	0	0	0	0	0	0	0	0	0	0
12	0	0	0	0	0	0	0	0	0	0	0	0
13	0	0	0	0	0	0	0	0	0	0	0	0
14	0	0	0	0	0	0	0	0	0	0	0	0

III TOLERANCES

It seems sensible to discuss two levels of manufacturing tolerances; the level which can be achieved with present technology and careful construction, and the level which could be reached with significantly improved technology. These are summarized below:

Technology Level	I	II
Tolerance		
Displacement of Coil	10 mil=0.25 mm	4 mil=0.10 mm
Rotation of Coil	10 mil=0.9 deg	4 mil=0.4 deg
Gap	10 mil=0.9 deg	4 mil=0.4 deg
Elliptical Deformation	10 mil=0.25 mm	4 mil=0.10 mm
Wire RMS	5 mil=0.12 mm	2 mil=0.05 mm
Block Rms	5 mil=0.12 mm	2 mil=0.05 mm
Coil Length	40 mil=1 mm	

The displacement of the coil comes from the tolerance build up in the locating keys and the uncertainty of the shape of the inner circumference of the main coil. To improve this significantly would require a more sophisticated locating system and a method of measuring the position of the bore tube accurately with respect to the main coil. The rotational uncertainties arise from the same sources. The gap in the circumference arises from uncertainties in the diameter of the bore tube. It may be possible to reach the 4 mil (1.3 mil on the diameter) tolerance by building up the bore tube with Kapton, this is a lengthy procedure.

The elliptical deformation comes from the assembly procedure for the main coils. Ironically, the deformation can be reduced at the expense of increasing the uncertainty in the placement of the coil as a whole. To achieve the 4 mil tolerance would require both a new assembly arrangement and a means of measuring the bore tube shape in situ.

The wire and block internal variations are the easiest to control and have the least effect upon the field quality. One could probably achieve 2 mil tolerances with the present techniques.

The tolerance on the overall length is a nominal one, and represents less than 0.03 % variation in effective length.

III.1 Results For Sextupole (b2) Coil

Refering to table 1, one can determine coefficients for the various harmonics, and multipling them by the tolerances above gives the following field errors:

Tolerance Level		I	II
Perturbation	Coefficient	Amplitude	Amplitude
Displacement	b1/a1 = 20	5 %	2 %
Rotation	a 2 = 26	6 %	2 %
Gap	a2 = 14	2.5%	1 %
Elliptical	b0 = 13	3 %	1.5 %
Wire Rms	b's/a's ~ 0.6	0.1%	0.06 %
Block Rms	b's/a's ~ 2.7	0.7%	0.3 %

It is apparent from the above that the problems with trim coil fields are dominated by the positioning of the coil as a whole. In reading this table, it should be remembered that the harmonics are quoted as a percent of the b2 field which is $<5 \times 10^{-4}$. Hence these fields are <6 ppm of the central dipole field. These field errors will also tend to be fairly random from magnet to magnet and perhaps even within a magnet. The exception is the dipole generated by elliptical squeezing of the coil. Any significant improvement below the 5% level will require an elaborate measurement technique to verify the placement.

III.2 Results For Octupole (b3)

The results for the octupole are of course similar, however because of the higher multipolarity, the coefficients are larger. Fortunately, this coil is only intended to supply 0.4 units of correction (a factor of 10 less).

Tolerance Level		I	II
Perturbation	Coefficient	Amplitude	Amplitude
Displacement	b2/a2 = 30	8 %	3 %
Rotation	a3 = 34	8 %	3 %
Gap	a3 = 17	3 %	1 %
Elliptical	b1 = 26	6 %	3 %
Wire Rms	b's/a's ~ 1.5	0.4%	0.2 %
Block Rms	b's/a's ~ 5.0	1.2%	0.5 %

Although these errors seem large, one should recall that 8% x 0.4 x 10^{-4} is 3 ppm, and that the bulk of them will be random.

III.3 Results For Decapole (b4)

This coil is even more sensitive, but again is only intended for 0.4 units of excitation.

Tolerance Level		I	II
Perturbation	Coefficient	Amplitude	Amplitude
Displacement	b3/a3 = 40	10 %	4 %
Rotation	a4 = 42	10 %	4 %
Gap	a4 = 21	5 %	2 %
Elliptical	b2 = 39	10 %	5 %
Wire Rms	b's/a's ~ 2.5	0.6%	0.3 %
Block Rms	b's/a's ~ 7.0	1.7%	0.7 %

If one takes the worst case of 10 %, at 0.4 units of excitation this becomes 4 ppm of the central field.

III.4 Forces

The Lorentz forces applied to these trim coils are comparatively low: 5 amps x 6.5 Tesla = 32.5 N/meter = 0.2 lbs/inch-wire. If the sextupole coil is unsupported, these forces will produce a maximum radial deflection at the midplane of 0.0009". The higher multipoles will produce even smaller deflections. There also can be collective forces between the trim coil and the main coil. For a pure dipole field, and the trim coils considered, the only force which is not identically zero occurs in the case of a gap in the coil (at 22 degrees). For a five degree gap a tangential force of 0.31 lbs/inch is generated in the sextupole. The equivalent numbers for the octupole and decapole are 0.24 and 0.19. If the bore tube were confined only at one end, this could produce rotations of 30 degrees. In the actual case where the coil is keyed every 24 inches, the accumulated rotation is <0.1 degree. The sideways force on the keys will be 7 lbs.

III.5 Magnetic Coupling

If there are any common harmonics between the trim and main coils, there will be electromagnetic coupling between them. The extreme case is where the trim coil has the same harmonic contentas the main coil. For the coils considered in this note, there are two sources of this coupling. 1) The main dipole has a small sextupole component which couples to the sextupole trim coils. This is dominated by 2) Dipole components in the b2 and b4 coils generated by elliptical deformations. The most serious effect of this coupling is that a quench in the main coil induces a voltage on the trim windings. For the coils considered this coupling coefficient has been calculated to be 0.045 volts/meter/(Tesla/sec) for a 1 mm deflection of the b2 coil. (the equivalent coefficient for b4 is 0.002). For dB/dt = 50 Tesla/sec and a length of 8 meters this gives 18 volts/sextupole coil. If the level I tolerances (0.25 mm) are achieved this becomes 4 volts/coil.

IV MISCELLANEOUS FIELD ERRORS

IV.1 Ends

To eliminate coil-to-coil crossovers and for compatibility with the flat coil manufacturing technique, the coils are wound in pairs. This means (see Figure 1) that a sextupole has only 3 separate coils, rather than the 6 one might expect. The ends of such coils produce a small addition to the fundamental and a skew harmonic at twice the angular frequency. From the dimensions of the coils it is trivial to calculate upper limits on the sizes of these terms. For a Cm (bm-1) coil these limits are:

$C_m <$ theta*R/L and $C_{2m} <$ theta*R/L *$(Ro/R)^m$

where theta = 2*pi/(3*m), R is coil radius, L is coil length and Ro is the 10 mm reference radius.

The Results are:

Sextupole (b2) L=8 meters

$C_3 < 0.14$ %

$C_6 < 0.03$ %

Octupole (b3) L=3 meters

$C_4 < 0.30$ %

$C_8 < 0.04$ %

Decapole (b4) L=5 meters

$C_5 < 0.14$ %

$C_{10} < 0.01$ %

The addition to the fundamental is the same as a small increase in effective length and is unimportant. The skew terms are all <0.1% and can be ignored.

IV.2 Octupole Locator Pins

The pins which locate the trim coil within the main coil must be at 90 and 270 degrees to match the main coil poles. For the octupole trim coil, these pins lie on the midplane of the windings. To allow for this the windings must follow the cutouts around these pins. (This is shown in Figure 2). Because octupole symmetry is maintained for these cutouts, the only harmonics generated are octupole (b3) and 24-pole (b11). The cutouts are spaced 18" apart, giving a reduction in octupole strength of 2.6 % and a b11 of 0.04% of b3 (at 10 mm).

IV.3 Magnetization

The trim coil conductor itself will exhibt magnetization effects, from the interaction of the main dipole field with the superconductor in the trim coils. The volume of superconductor in the trim coils is approximately 0.5% of that in the main coils. The filament size is approximately 120 microns compared with 5 microns for the main coil. Thus the effective magnetization strength is 12 % of that of the main coil. The dominant effect will be a dipole term which will be indistinguishable from the larger dipole magnetization term produced in the main coil. Smaller amounts of the higher dipole allowed harmonics will be produced. These are the same harmonics which are produced by magnetization in the main coil and are factors of four or more smaller, and their effect upon the beam is further reduced by the ratio of their lengths to that of the main coil. Although these field contributions could be reduced by using a multifilamentary wire for the trim coils, the added technical difficulties of using such a wire are not warranted by the negligible improvement in the magnet as a whole. The magnitudes of these perturbations are given in table 4 below.

Table 4: Trim Coil Magnetization
(Prime units at injection)

Trim Coil \ harmonic (m-1)=	0	2	4	6	8
Sextupole	-0.59	+0.08	-0.03	0.00	0
Octupole	-0.59	+0.06	-0.01	-0.00	-0.00
Decapole	-0.60	+0.07	-0.02	+0.00	-0.00

It is also possible for the trim coil to induce magnetization images in the main coil. This effect has a magnitude of 10% of the trim coil strength and can be reduced to a negligible level by careful cycling of the trim coil.

IV.4 Current Tolerances

To achieve 1% field accuracy the current supplied to the coils must be controlled to 1% . At low field the excitation current will be approximately 200 mA requiring a least count of 2 mA or less. Neither of these requirements is difficult to achieve.

APPENDIX E

"Tolerances of Beam-Tube Corrector Construction Errors,"

Jack Peterson and Alex Chao

November 13, 1987.

TOLERANCES OF BEAM-TUBE CORRECTOR CONSTRUCTION ERRORS

J.M. Peterson and A. Chao
13 November 1987

The tolerance to random errors in the manufacture and assembly of the beam-tube correction windings was estimated on the basis of the tolerable error multipoles produced in each winding when energized. The tolerable **random** multipoles for the beam-tube windings were taken as 1/3 of those for the SSC dipoles listed in SSC-N-183 ("Requirements for Dipole Field Uniformity and Beam-Tube Correction Windings," A. Chao and M. Tigner, May 1986) and translated to tolerances on the beam-tube-winding parameters using the error matrices from SSC-N-226 ("Field Quality for SSC Internal Trim Coils," P.A. Thompson, August 1986). The resulting rms tolerances on the coil parameters and the responsible error multipole in each case are as follows:

TOLERANCES FOR RANDOM ERRORS

COIL PARAMETER	RMS TOLERANCE	RESPONSIBLE ERROR MULTIPOLE	TOLERANCE (STANDARD UNITS)	RESPONSIBLE COIL
Displacement $\Delta x, \Delta y$	0.3mm	a_1, b_1	0.23, 0.23	sextupole
Rotation	0.5°	a_2	0.20	sextupole
Gap	0.9°	a_2	0.20	sextupole
Ellipse Δr	0.8mm	b_2	0.13	decapole
Wire Position	0.5mm	a_2	0.20	sextupole
Block Position	0.5mm	a_3	0.23	sextupole

(a_n, b_n represent the skew and normal coefficients of the $2(n + 1)$ multipole.)

Although the listed tolerances lead to acceptable rms multipole strengths, effort should be made to reduce the manufacturing and assembly errors further, if practicable. The smaller the random errors, the smaller the average, or systematic, error will be and the easier they can be dealt with operationally.

The tolerance on the systematic errors depends on the envisioned operational procedure of compensating for the persistent current multipoles. At the moment, this procedure is still being developed by simulations. For this reason, the systematic tolerances for the beam-tube windings are not yet available. A preliminary look indicates, for example, that to fulfill the systematic tolerances specified for the magnet bodies in SSC-N-183 may not be good enough for these windings. It is expected that some tolerance figures would be available in a few months' time.

APPENDIX F

"Engineering Design,"

Talk by John Skaritka

ENGINEERING DESIGN

DESIGN REQUIREMENTS AND CONSTRANTS.

1 BEAM TUBE DIA. 1.360 X ≈60 FT LONG.

2 DIPOLE COIL I.D. 1.564 X "

3. HELIUM PASSAGE .060 X "

4. ALL CORRECTION MUST RESIDE IN A .042" RADIAL GAP AROUND THE BEAM TUBE.

5. ALL COILS WILL BE SYMETRICAL (CLOSE TOLERANCE)

6. ALL WIRE POSITIONS WITH IN COIL BLOCK MUST BE EVENLY DISTRIBUTED (CLOSE TOLERANCE)

7. WIRES MUST BE SECURELY AFFIXED TO THE BEAM TUBE AND PREVENTED FROM HAVING RELATIVE MOTION.

8. ACCUMULATIVE TOLERANCES MUST NOT DISTORT THE OVER ALL COIL DESIGN.

9. A GOOD BOND TO THE BEAM TUBE IS DESIRABLE.

10. THE ASSEMBLY MUST BE ACCURATE AND REPRODUCABLE

11. THE ASSEMBLY MUST BE SUITABLE FOR MASS PRODUCTION TECHNIQUES,

12. IN PRODUCTION QUANTITIES THE ASSEMBLY MUST BE COST EFFECTIVE.

13. A WORKING MODEL MUST BE PRODUCED AS SOON AS POSSIBLE AT LITTLE OR NO COST

14. THOUSANDS OF FT. OF FINE WIRE MUST BE WOUND WITHOUT BREAKING OR SHORTING.

15. MULTIPOLAR CORRECTIONS MUST BE ANTICIPATED AND INCORPORATED WITH NEGLIGABLE TIME AND TOOLING COST

16. TECHNICAL PERSONNEL TO PREFORM ASSEMBLY WILL BE LIMITED TO ONE SENIOR TECH AND ONE HELPER.

17. MAX. TIME ENGINEER CAN SPEND ON WITH THIS JOB IS 30% FULL TIME.

18. CRYOGENIC AND RADIATION EFFECTS MINIMISED

AFTER CAREFUL EVALUATION OF VARIOUS WINDING TECHNIQUES CONCLUSIONS WERE MADE ABOUT THE ENGINEERING DESIGN.

FOR ITEMS 1, 2, 3, 5, 6, 8, 11, 12, 14, 15, 17

THE MULTIWIRE PROCESS WAS THE ONLY POSSIBLE SOLUTION TO IN CORPORATE THE ABOVE ITEMS.

FOR ITEMS 10 12 13 16

THE ASSEMBLY TOOLING MUST BE ACCURATE, SAFE SIMPLISTIC AND EASY TO USE.
A SURFACE TABLE WOULD GIVE THE ACCURACY FIXTURING AND LIGHTWEIGHT TRANSPORT TOOLING WAS DESIGNED.

FOR ITEMS 4, 7, 5, 9, 10, 13, 18.

KAPTON WITH A THERMAL PLASTIC ADHESIVE WAS SELECTED. A STRAPPING OF KEVLAR OR GLASS WOULD BE USED SECURE THE WINDINGS.
IDEAL MATERIALS DIDNOT EXIST YET TOGET STARTED WE HAD TO USE WHAT WAS AT HAND.

FEP COATED KAPTON

EPOXIES AND MATERIALS WE HAD USED BEFORE

* MULTIWIRE STANDARD RC 205 MODIFIED TO SURVIVE LHE TEMPS.

* THE LEAST COSTLY TOOLING WAS PRODUCED FOR USE AT MULTIWIRE AND BNL

A PRODUCTION PROCEDURE WAS DEVISED TO TAKE INTO CONSIDERATION OUR LIMITED FACILITIES, TIME, AND FUNDING.

1 WIRE WOULD BE SPECIFIED, PURCHASED, INSPECTED AND INSULATED.

2. SUBSTRATUM WOULD BE PRODUCED AT SHELDAHL AND SLIT.

3. SUBSTRATUM WOULD BE PRECISION SLIT AT THE METLON COMPANY AND PRECISION PUNCHED AND SLOTED AT THE SCHNEIDER + MARQUARD CO.

4. SUBSTRATUM WOULD BE DELIVERED TO MULTIWIRE ALONG WITH SUPERCONDUCTOR, THERE WIRING WOULD TAKE PLACE. AFTER PROCESSING THE SUBSTRATUM IS DELIVERED TO BNL.

5. THE BEAM TUBE IS INSPECTED AND WRAPED WITH KAPTON. THE KAPTON IS HEAT SEALED ONTO TUBE.

6. USING SPECIAL FIXTURES LOCATION PINS ARE ATTACHED TO THE TUBES SURFACE TO ESTABLISH A PLANE ALONG THE MIDDLE OF THE BEAMTUBE PARALLEL TO THE SURFACE PLATE.

7. PRECISION REFERENCE SLOTS IN THE SUBSTRATUM ARE POSITIONED ON TO THE LOCATION PINS.

8. THE SUBSTRATUM IS WRAPED AROUND THE BEAM TUBE AND LASHED INTO PLACE BY TWO LAYERS OF KEVLAR 1 LAYER CW, 1 LAYER CCW.

9. THE ASSEMBLY IS BAKED AT 300°C TO BOND THE FEP ADHESIVES TOGETHER AND TO THE BEAM TUBE

10. A 50% OVERLAP WRAP OF KAPTON IS APPLIED TO THE TUBE AND HEAT SEALED ON.

11. POLE LOCATION KEYS AND BUMPER STRIPS ARE GLUED INTO PLACE USING THE SAME FIXTURE AS THE LOCATION PINS.
KEYS TRANFER THE COIL POLE POSITION TO OUTSIDE THE ASSEMBLY.

12. POLE BUMPERS ARE RELIEVED TO HANDLE COLLAR DEFLECTIONS, AND TEFLON TAPE IS ADDED AS A SLIP PLANE ON THE MIDPLANE BUMPERS

13. INSPECTIONS, MECHANICAL AND ELECTRICAL ARE PROFORMED, TUBE ENDS ARE FLARED.

14. AFTER INSPECTION IS COMPLETE THE ASSEMBLY IS TRANSPORTED ON A STRONGBACK TO MAIN MAGNET ASSEMBLY AREA. FOR INSTALLATION INTO THE DIPOLE AND END FLANGE WELDING.

☆ A COMPLETE SPECIFICATION OUTLINE WILL BE INCLUDED IN THIS WRITE UP AND THE FINAL TRAVELER WITH COMPLETE SPEC'S WILL BE PART OF THE FINAL REPORT.

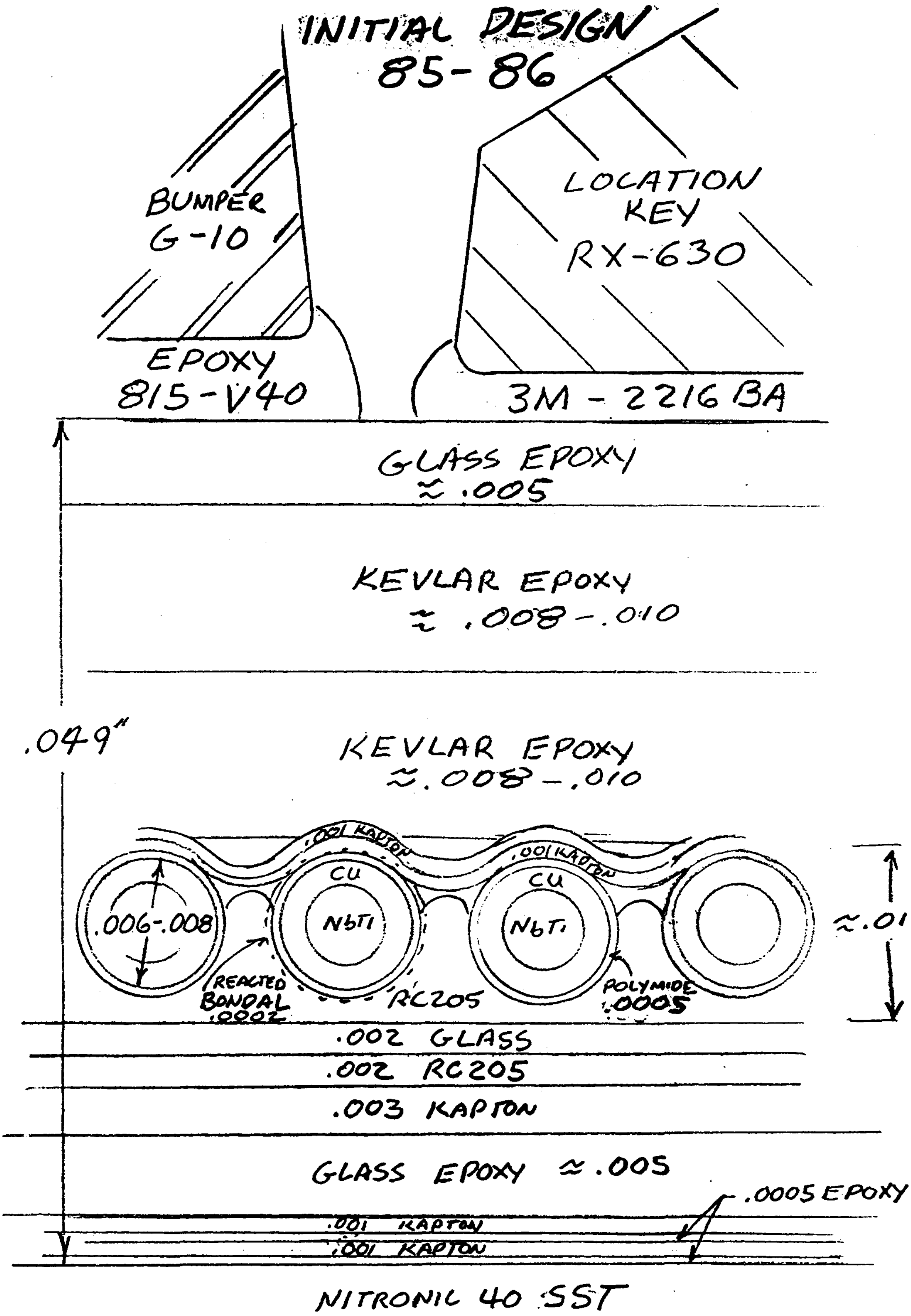
INITIAL DESIGN
85-86
BUMPER
G-10
LOCATION
KEY
RX-630
EPOXY
815-V40
3M - 2216 BA
GLASS EPOXY
≈ .005
KEVLAR EPOXY
≈ .008 - .010
.049"
KEVLAR EPOXY
≈ .008 - .010
.001 KAPTON
.001 KAPTON
CU
CU
.006-.008
NbTi
NbTi
≈ .012
REACTED
BONDAL
.0002
RC205
POLYMIDE
.0005
.002 GLASS
.002 RC205
.003 KAPTON
GLASS EPOXY ≈ .005
.0005 EPOXY
.001 KAPTON
.001 KAPTON
NITRONIC 40 SST

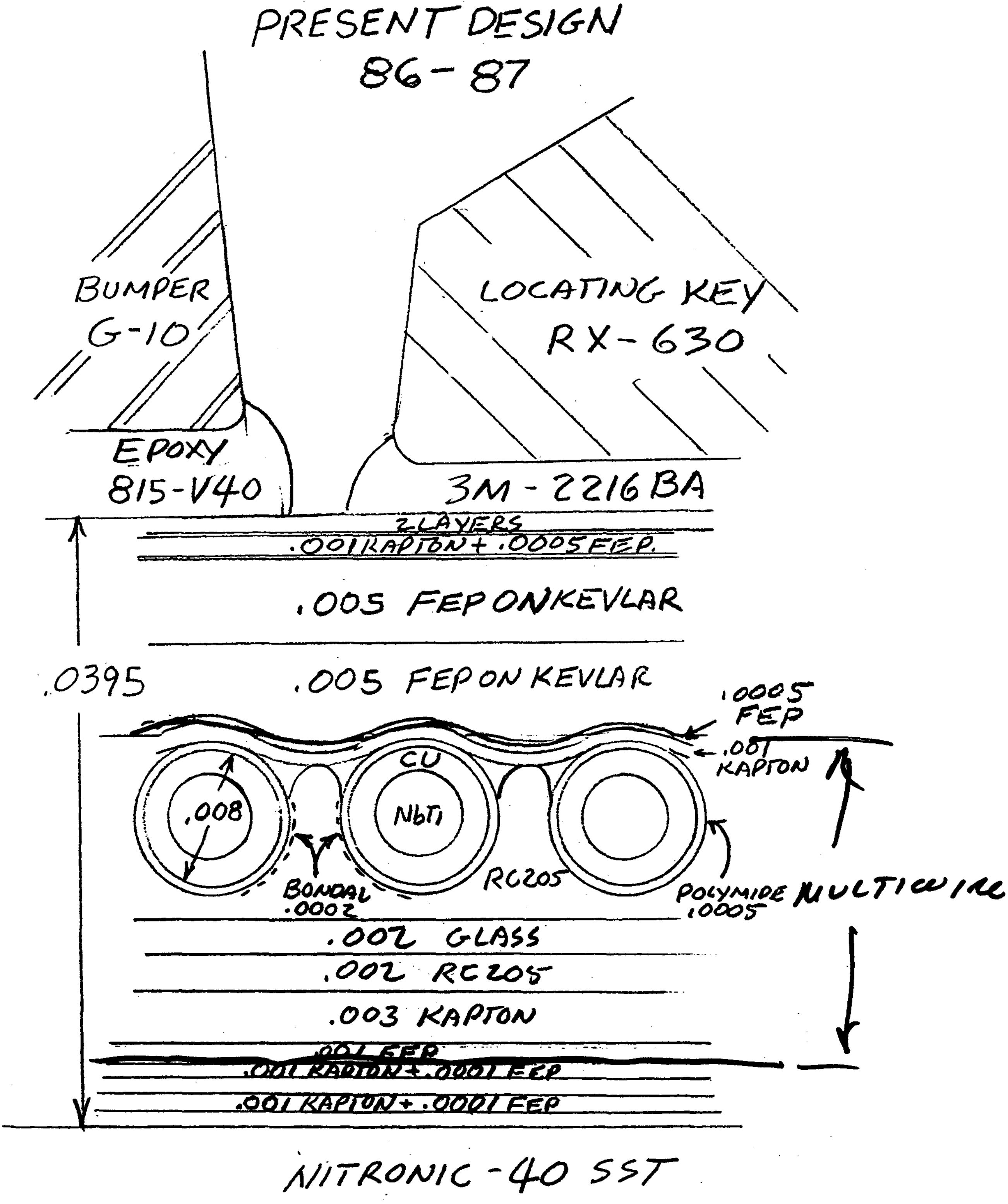
PRESENT DESIGN
86-87
BUMPER
G-10
LOCATING KEY
RX-630
EPOXY
815-V40
3M-2216 BA
2 LAYERS
.001 KAPTON + .0005 FEP
.005 FEP ON KEVLAR
.0395
.005 FEP ON KEVLAR
.0005
FEP
.001
KAPTON
CU
.008
NbTi
BONDAL
.0002
RC205
POLYMIDE
.0005
MULTIWIRE
.002 GLASS
.002 RC205
.003 KAPTON
.001 FEP
.001 KAPTON + .0001 FEP
.001 KAPTON + .0001 FEP
NITRONIC-40 SST

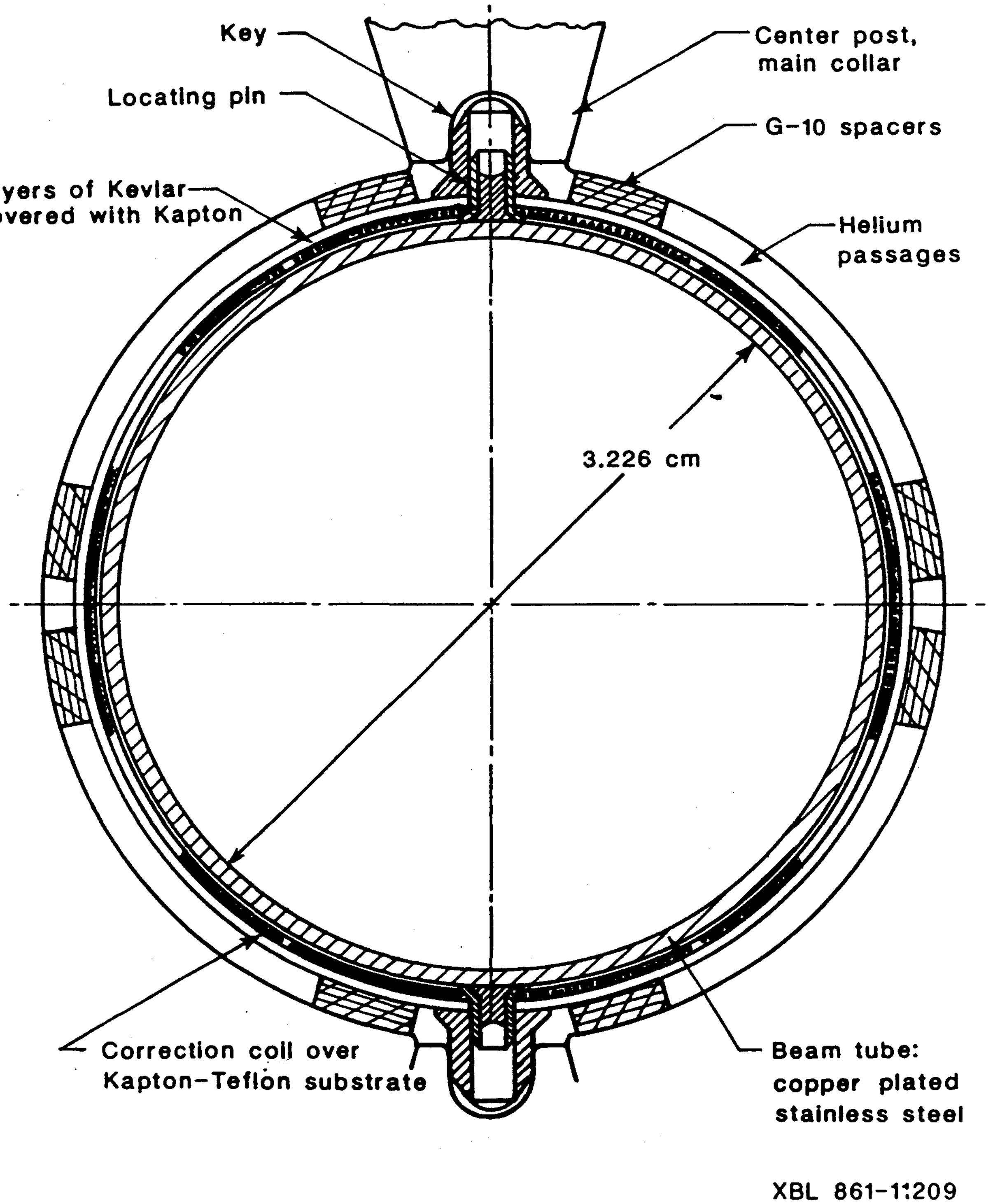
Key
Locating pin
Center post, main collar
G-10 spacers
Layers of Kevlar covered with Kapton
Helium passages
3.226 cm
Correction coil over Kapton-Teflon substrate
Beam tube: copper plated stainless steel
XBL 861-11209

22-329.06

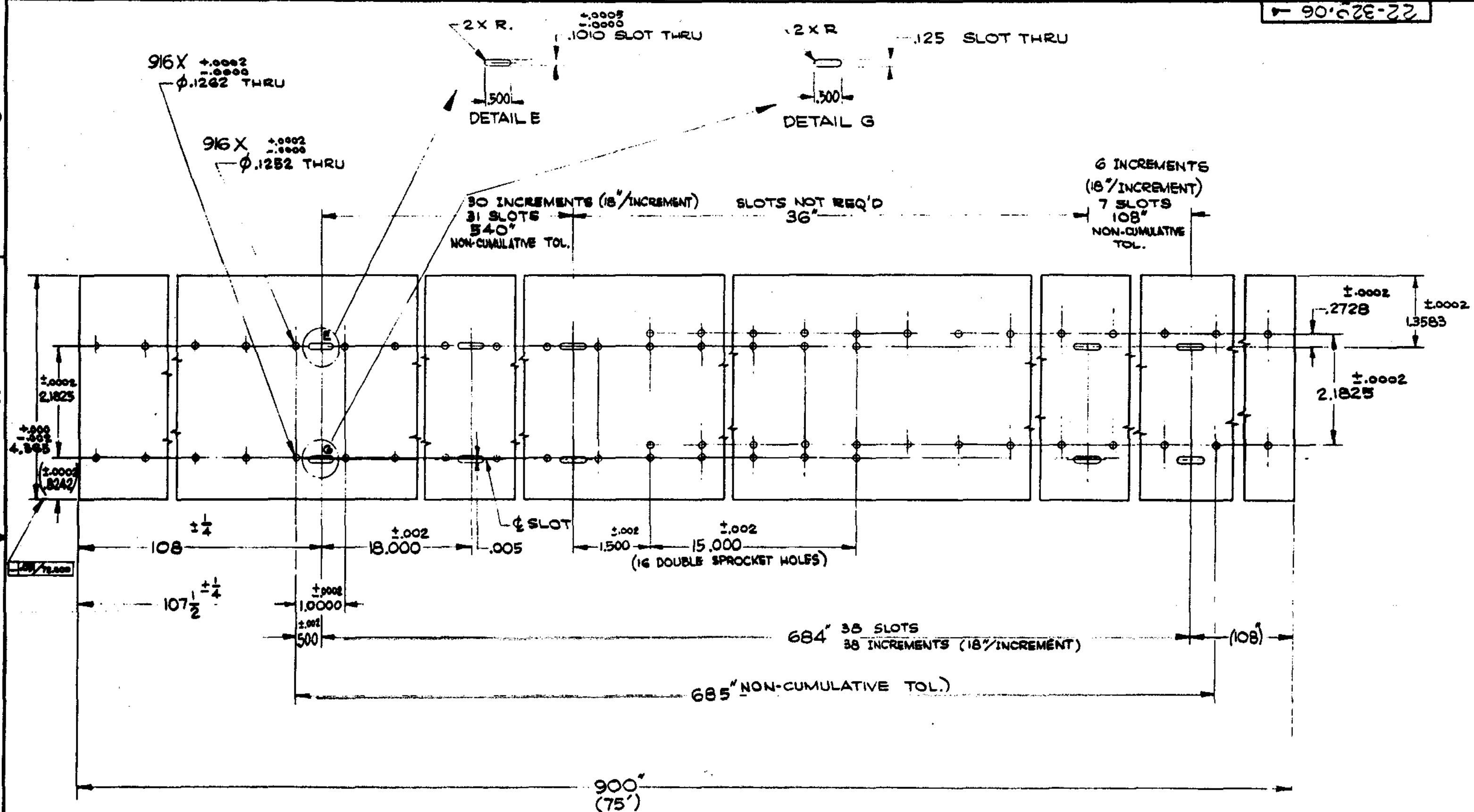

NOTE:

1. MATERIAL – 400 FN 031 TYPE "F" KAPTON FILM + ≦ .002 RC-205 MULTIWIRE ADHESIVE + .002" FIBERGLASS EPOXY PRE PREG. + .004-.005" RC-205 MULTIWIRE ADHESIVE + RELEASE LINER, SHELDAHL SUPPLIED LENGTH 6" ±1/32 X 75' LONG

FINAL

REV.	ZONE	DESCRIPTION	BY	DATE	CKR	APP
B	B6, D6	.005 WAS .010, .125 WAS .150		9/2/86		
A		MAJOR REVISION		8/6/86		

NO. REQ.	ACCT. NO.	I.L.R. NO.	ORDER NO.	DEPT.	JOB NUMBER	USED ON DWG. NO.	NO. PER ASSY
					22-329	22-329.02-5	1

TOLERANCE	DEC. ± .005 ANG. ± —
BREAK SHARP EDGES	MAX. — MIN. —
FRACTIONAL TOLERANCE	0-30" ±1/64 30"-60" ±1/32 OVER 60" ±1/8
FINISH	√
DATE	8/6/86
MATERIAL	NOTED
SCALE	FULL
WEIGHT	
DRAWN BY	L. Sandberg
CHECKED BY	J. SKARITKA
ENG. APP.	
SUPVR. APP.	

BROOKHAVEN NATIONAL LABORATORY
ASSOCIATED UNIVERSITIES, INC.
UPTON, N. Y. 11973

MAGNETS, DIPOLE
SSC 16.6M-LLN-007-012 BORE TUBE TRIM COIL
SUBSTRATE HOLE PATTERN

DRAWING NUMBER: 22-329.06-4 REV. B

F-10

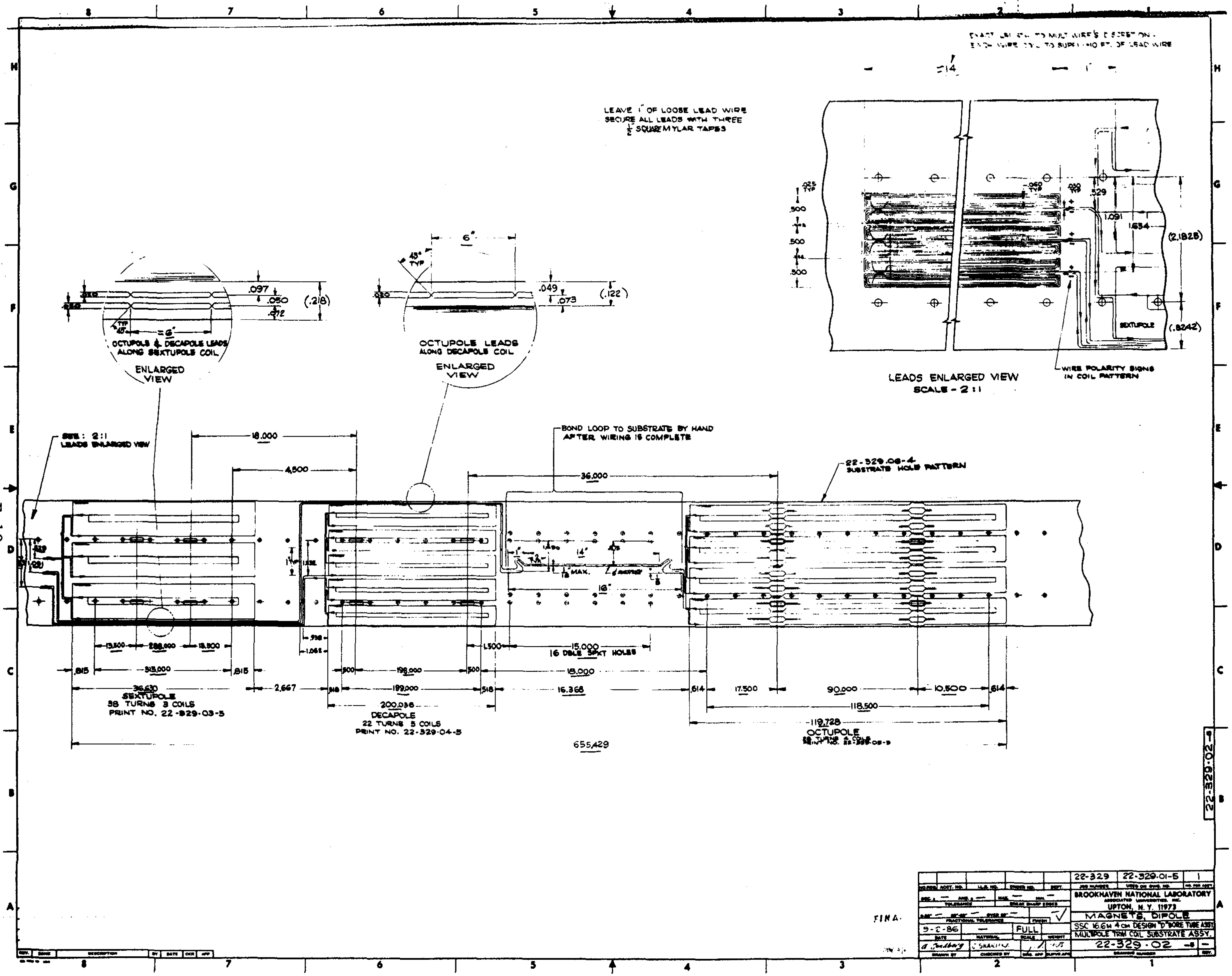

LEAVE 1" OF LOOSE LEAD WIRE
SECURE ALL LEADS WITH THREE
1/2" SQUARE MYLAR TAPES
OCTUPOLE & DECAPOLE LEADS ALONG SEXTUPOLE COIL
ENLARGED VIEW
OCTUPOLE LEADS ALONG DECAPOLE COIL
ENLARGED VIEW
LEADS ENLARGED VIEW
SCALE - 2:1
WIRE POLARITY SIGNS IN COIL PATTERN
SEXTUPOLE
SEE: 2:1 LEADS ENLARGED VIEW
BOND LOOP TO SUBSTRATE BY HAND AFTER WIRING IS COMPLETE
22-329.06-4 SUBSTRATE HOLE PATTERN
16 DBLE SPKT HOLES
SEXTUPOLE
38 TURNS 3 COILS
PRINT NO. 22-329-03-5
DECAPOLE
22 TURNS 5 COILS
PRINT NO. 22-329-04-5
OCTUPOLE
655.429
18.000
4.500
36.000
15.000
16.368
118.500
119.728
200.036
36.630
2.667
90.000
17.500
10.500
BROOKHAVEN NATIONAL LABORATORY
UPTON, N.Y. 11973
MAGNETS, DIPOLE
SSC 16.6M 4 CM DESIGN "D" BORE TUBE ASSY
MULTIPOLE TRIM COIL SUBSTRATE ASSY.
22-329
22-329-01-5
9-2-86
FULL
22-329-02
22-329-02

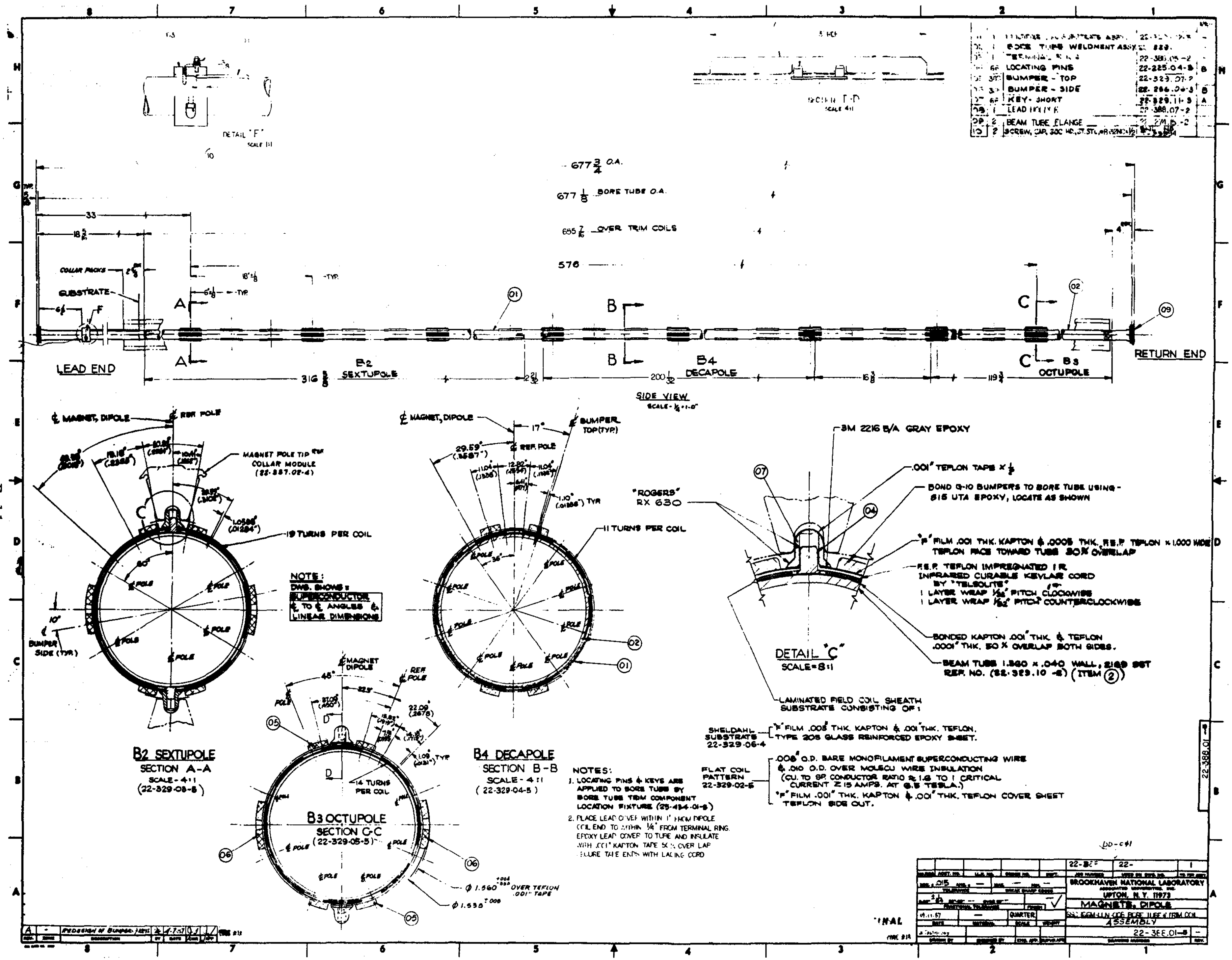

LOCATING PINS 22-225.04-3
BUMPER - TOP 22-329.07-2
BUMPER - SIDE
KEY - SHORT
BEAM TUBE FLANGE
SCREW, CAP, SOC HD
BORE TUBE WELDMENT ASSY
DETAIL "F"
677 3/4 O.A.
677 1/8 BORE TUBE O.A.
655 7/16 OVER TRIM COILS
576
33
18 5/8
COLLAR PACKS
SUBSTRATE
LEAD END
RETURN END
B2 SEXTUPOLE
B4 DECAPOLE
B3 OCTUPOLE
316 5/8
200 1/32
119 3/4
SIDE VIEW
SCALE - 1/4" = 1'-0"
℄ MAGNET, DIPOLE
REF POLE
MAGNET POLE TIP REF COLLAR MODULE (22-387.02-4)
19 TURNS PER COIL
NOTE: DWG. SHOWS SUPERCONDUCTOR ℄ TO ℄ ANGLES & LINEAR DIMENSIONS
BUMPER SIDE (TYP)
B2 SEXTUPOLE
SECTION A-A
SCALE - 4:1
(22-329.03-5)
BUMPER TOP (TYP)
11 TURNS PER COIL
B4 DECAPOLE
SECTION B-B
SCALE - 4:1
(22-329.04-5)
14 TURNS PER COIL
B3 OCTUPOLE
SECTION C-C
(22-329.05-5)
ϕ 1.560 OVER TEFLON .001" TAPE
ϕ 1.538
3M 2216 B/A GRAY EPOXY
.001" TEFLON TAPE x 1/2
BOND G-10 BUMPERS TO BORE TUBE USING 815 UTA EPOXY, LOCATE AS SHOWN
"ROGERS" RX 630
"F" FILM .001 THK. KAPTON & .0005 THK. F.E.P. TEFLON x 1.000 WIDE TEFLON FACE TOWARD TUBE 30% OVERLAP
F.E.P. TEFLON IMPREGNATED I.R. INFRARED CURABLE KEVLAR CORD BY "TELSOLITE"
1 LAYER WRAP 1/32 PITCH CLOCKWISE
1 LAYER WRAP 1/32 PITCH COUNTERCLOCKWISE
BONDED KAPTON .001" THK. & TEFLON .0001" THK. 50% OVERLAP BOTH SIDES.
BEAM TUBE 1.360 x .040 WALL, 2169 SST REF. NO. (22-329.10-6) (ITEM 2)
DETAIL "C"
SCALE = 8:1
LAMINATED FIELD COIL SHEATH SUBSTRATE CONSISTING OF:
SHELDAHL SUBSTRATE 22-329.06-4
"F" FILM .003 THK. KAPTON & .001 THK. TEFLON.
TYPE 205 GLASS REINFORCED EPOXY SHEET.
FLAT COIL PATTERN 22-329.02-5
.008 O.D. BARE MONOFILAMENT SUPERCONDUCTING WIRE & .010 O.D. OVER MOLECU WIRE INSULATION (CU. TO SP. CONDUCTOR RATIO ≈ 1.8 TO 1 CRITICAL CURRENT ≥ 15 AMPS. AT 6.5 TESLA.)
"F" FILM .001 THK. KAPTON & .001 THK. TEFLON COVER SHEET TEFLON SIDE OUT.
NOTES:
1. LOCATING PINS & KEYS ARE APPLIED TO BORE TUBE BY BORE TUBE TRIM COMPONENT LOCATION FIXTURE (25-434-01-6)
2. PLACE LEAD COVER WITHIN 1" FROM DIPOLE COIL END TO WITHIN 1/4" FROM TERMINAL RING. EPOXY LEAD COVER TO TUBE AND INSULATE WITH .001 KAPTON TAPE 50% OVER LAP SECURE TAPE ENDS WITH LACING CORD
BROOKHAVEN NATIONAL LABORATORY
UPTON, N.Y. 11973
MAGNETS, DIPOLE
ASSEMBLY
22-388.01-8

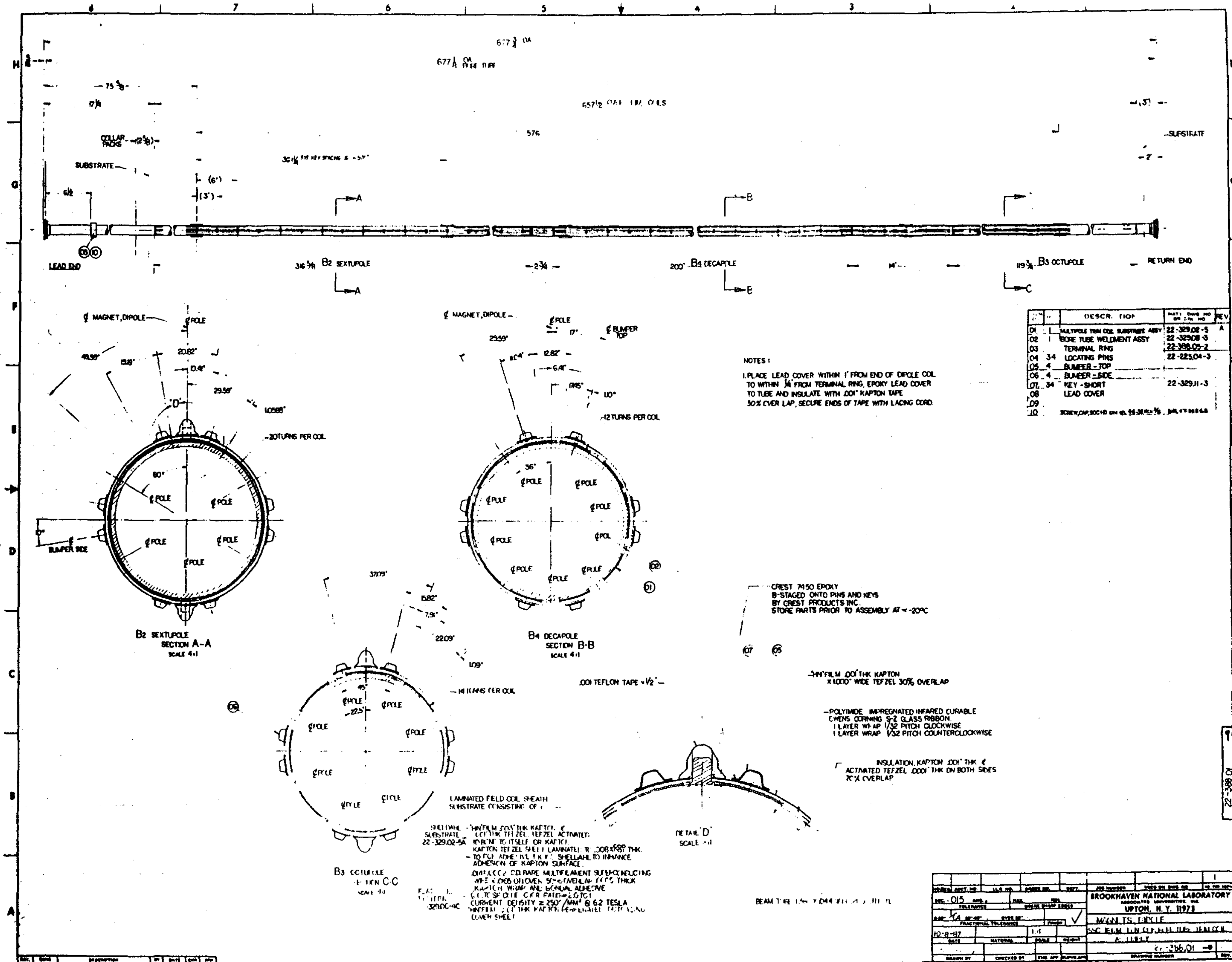

		DESCRIPTION	MAT'L DWG NO OR I.N. NO	REV
01	1	MULTIPOLE TRIM COIL SUBSTRATE ASSY	22-329.02-5	A
02	1	BORE TUBE WELDMENT ASSY	22-329.08-3	
03		TERMINAL RING	22-388.05-2	
04	34	LOCATING PINS	22-225.04-3	
05	4	BUMPER - TOP		
06	4	BUMPER - SIDE		
07	34	KEY - SHORT	22-329.11-3	
08		LEAD COVER		
09				
10		SCREW, CAP, SOC HD		

APPENDIX G

BNL 39615, "Development of the SSC Trim Coil Beam Tube Assembly,"

J. Skaritka et al., March 16, 1987

Presented at the 1987 Particle Accelerator Conference - March 16-19, 1987
Shoreham Omni Hotel, Washington, D. C.

BNL 39615

DEVELOPMENT OF THE SSC TRIM COIL BEAM TUBE ASSEMBLY*

J. Skaritka, E. Kelly, W. Schneider, R. Shutt,
P. Thompson, P. Wanderer, E. Willen
Accelerator Development Department
Brookhaven National Laboratory
Upton, New York 11973

D. Bintinger
SSC Central Design Group
Berkeley, CA

R. Coluccio, L. Schieber
Kolmorgen Co.,
PCK & Multiwire Divisions

Introduction

The Superconducting Super Collider uses ≈9600 dipole magnets. The magnets have been carefully designed to exhibit minimal magnetic field harmonics. However, because of superconductor magnetization effects, iron saturation and conductor/coil positioning errors, certain harmonic errors are possible and must be corrected by use of multipole correctors called trim coils. For the most efficient use of axial space in the magnet, and lowest possible current, a distributed internal correction coil design is planned. The trim coil assembly is secured to the beam tube, a UHV tube with special strength, size, conductivity and vacuum.

The following report details the SSC trim coil/beam tube assembly specifications, history, and ongoing development.

Required Specifications

The original design of the SSC trim coil is composed of a sextupole corrector which is distributed along the outside of the beam tube. The number of turns is maximized to decrease the required current in the trim coil. The absolute position of each conductor is controlled to ±0.05 mm along the length of the ≈17 m beam tube. This positioning tolerance was especially challenging because there was no conventional way to mass produce long complex multiturn coils using wire only ≈.2 mm in diameter to such precision. The variations due to accumulated tolerances of the wire position produce coil blocks of unequal conductor density and the required symmetry of the coil is lost.

To obtain the required precision with a method suitable for production, a technique developed by the Kolmorgan Corporation was adopted. In that technique, copper wires are placed directly onto an adhesive coated G-10 circuit board by an accurate, fast, fully automated process. We felt that we could exploit this established technology to produce complex coil patterns for the SSC.

This technique was adapted to produce a flat coil pattern on a flexible substrate that could be bent around the outside of the beam tube. The edges of the pattern must meet precisely because a varying gap or coil asymmetry would produce unwanted field harmonics. The coil is secured to the beam tube; the substrate must be slit to a precise size to fit the beam tube, which has an outside diameter tolerance of ±.02 mm over the entire 17 meter length.

The trim coil's substrate must withstand cryogenic temperatures and tolerate high radiation levels. The beam tube must be made from a high strength material of the required size which would not exhibit high eddy current loading during magnet quenches and which has an extremely low and uniform permeability. It must have an extremely pure layer of copper on its inside surface. The copper coating must have excellent adhesion to the beam tube without contaminates to poison the UHV. The copper must be uniformly applied over the full 17 meters.

Superconductor

The minimum current requirement for the SSC trim coil is 5 amps at the full 6.6 Tesla dipole field. From previous experience with CBA trim coils, a safety factor of at least 3 was considered prudent for the trim coil peak operating current. The critical current of the trim coil design was originally set ≥15 amps at 6.0 Tesla.

The bare wire diameter is .0082 ± .0002"; it is .0095 ± .0005" including the insulation. Monofilament wire with ≈1.65 to 1 copper to superconductor ratio with a current density of ≥2000 amps/mm^2 was selected. The monofilament was selected because it welded better to the multiwire substrate than did multifilament wire.

Beam Tube

The magnetic field length of each SSC dipole has been set at 16.7 meters. The overall length of the beam tube is ≈17 meters. The tube O.D. is 1.360 + .001-.000". The design of the beam tube was based on a maximum pressure of 20 atmospheres or ≈300 psi at quench. The initial wall thickness was set at .035 + .005-.000". Concern over Lorentz loading from eddy currents in the copper plating and increasing quench pressure dictated an increase in the wall thickness to .044 ± .004".

Various materials were considered for the beam tube, including stainless steels, such as 304LN, 304L and 316L. For 300 series stainless steel, any unannealed mechanical work hardening results in non uniform magnetic permeability; a uniform permeability of ≤1.005 at 4.5 K is required. Armco Corporation produces high nitrogen content alloys called the nitronic series. Two alloys, Nitronic 40 and 33, both have higher yield strengths and lower permeability than 300 series alloys. The Nitronic alloys do not have large changes in permeability caused by cold working.

Trent Tube of East Troy, Wisconsin with experience in very long Nitronic 40 welded tubing, was chosen to produce tubes.

Welded tubing was initially thought unacceptable because of UHV problems and ferrite content in the welds. In working closely with Trent and the BNL Material Science Group, we developed a weld, draw and anneal schedule which yielded a variation in permeability throughout the tube undetectable by a ferrite scope at 20 C. Recent magnetic measurements of completed SSC magnets show no adverse effects of the weld on magnetic field quality. The final choice of alloy was based on the fact that N33 was only available in billet form whereas N40 (ASM #21-6-9) was supplied as sheet, ready for the welding process. The major disadvantage of the Nitronic alloys are that they cannot be vacuum electron beam welded since the nitrogen will come out of solution in the weld puddle, producing porous and brittle welds.

When the tube is produced, a final cold overdraw and roll straightening is required to assure the tube's outer diameter to ±0.02 mm and straightness of 1 mm/2 meters.

The Development Program

Contracts were established with the Kolmorgan subsidary, Multiwire, to develop the wiring of superconductor using

*Work performed under the auspices of the U.S. Department of Energy

nonstandard equipment for the development of a cryogenically stable substrate, and to build the first .5 meter and 4.5 meter trim coils. Short sextupole trim coils ≈.5 meters long were wound and tested successfully using various assembly techniques.

A special substrate transport system was designed and built at BNL to expand the wiring capacity of one axis of the Multiwire wiring machine. 4.5 meter coils were wired and delivered to BNL using the new tooling. Since final assembly tooling was not available for the 4.5 m magnets, we removed the FEP backing on the substrate and used an epoxy impregnated glass wick to bond the trim coil to the beam tube. This assembly, unfortunately, resulted in an unsymmetrical coil with a substrate edge gap varying between .050" and .070". This error was observed in the magnetic field measurements. The operation of the coils was successful, however, with currents reaching ≈15 amps at 6.2 Tesla. The assembly tooling was completed in time for the 17 m magnet trims where the edge gap did close, showing a dramatic improvement in field quality.[1]

The Multiwire Process and Trim Coil Assembly

The Multiwire process was first developed by Mr. Page Burr in 1969 for the routing of copper wire on circuit boards. It was an alternative to printed circuit techniques. Our superconductor is insulated with a .0005" radial build up of polyimid "ML" insulation with a 1000 volt turn-to-turn breakdown. A very thin layer ≈.0002" thick of High Bond adhesive coats the insulation. The insulated wire is stored in a spool above a wiring head. A small motor on the wiring head drives the wire at a precise speed between a stylus and the circuit board adhesive. The stylus is vibrated at ≈25 KHz. The kinetic energy imparted to the wire while under the stylus causes the High Bond coating to chemically react with the circuit board adhesive, called RC205. The pressure and elevation of the head controls the depth of the wire into the RC205. Wiring speeds are between 8 to 15 meters per minute. In the past, Multiwire had produced various types of complex wiring patterns. The standard wiring machines have the capacity to wire a circuit board or coil pattern of 24" x 24".

A special substrate is required. It has to be cryogenically stable, it has to bond to the Kapton-insulated beam tube without distorting the wire positions, and it has to provide good bonding strength for the wires during the wiring, handling and assembly. The strength and electrical insulation are supplied by a .003" thick Kapton sheet. A .001" thick FEP teflon coating on one side provides the means of binding to the bore tube. The other side contains a .002-.003" matt of fiberglass bonded to the Kapton with a .002" layer of RC205 adhesive. On top the fiberglass matt is a layer of .005" RC205 for receiving the wires. The matt prevents the adhesive from cracking at LN2 temperature. The total substrate thickness is only ≈.014". This material is processed in 6" strips by the Sheldahl Co. of Northfield, Wisconsin.

After manufacture, the material is shipped to the Metlon Co. of Cranston, Rhode Island and slit to a width of 4.346 + .002 -.000" with a straightness of .005" over 24 inches.

Once slit and inspected, the substrate is shipped for precision punching by the Schneider and Marquard Co., Newton, New Jersey. Two sets of holes are punched at one inch increments along the length of the substrate. Location slots are punched along the substrate at 18 inch increments. The slots and holes are designed to allow any combination of odd or even harmonics from quadrupole to 14-pole correction coils. Present correction elements include an 8 meter long 19 turn sextupole, 5 meter long 12 turn decapole and 4 meter long 14 turn octupole.

After the substrate is punched, the material is sent to Multiwire. The hole and slot pattern is registered to the wiring head with the use of precision sprockets on the substrate transporter, which is mounted on the bed of the Multiwire wiring machine. The superconductor is applied to the substrate in a preprogrammed wire pattern (see multiwire flat pattern layout, Figure 1). After the wiring is finished, a protective .001" Kapton cover sheet is applied over the coil.

Once the wired substrate is received and inspected at Brookhaven, it is placed on a 60 ft. surface plate and the position of the location slots are checked and transferred to the beam tube. The beam tube has previously been wrapped and heat sealed with .001" FEP dispersion coated Kapton film to achieve a precise diameter. Precision locating fixtures have been used to apply location pins made from RX-630 to the wrapped beam tube. The pins transfer the precise and very flat plane of the surface plate to the beam tube

Special tooling is used to roll out and secure the wired substrate onto the beam tube. The location slots in the substrate fit snugly onto one row of location pins bonded to the beam tube. The substrate is wrapped around the beam tube and then securely wrapped with a double layer of FEP-impregnated Kevlar yarn. A final 50% overlap wrap of FEP-coated Kapton film is applied over the Kevlar. The Kapton assures a >5 KV breakdown between the trim and main coils.

The entire assembly is passed through a radiant oven to heat seal the various components of the assembly together. The location pins protrude through the top Kapton layer. Using the previously mentioned fixtures, locating keys are applied to the location pins and glued into position on 18 inch increments, on both sides of the tube. Bumper strips of G-10 are glued onto the Kapton outer wrap. These are used to space the beam tube inside the main coil at assembly.

The assembly is inspected and electrically tested for proper resistance, continuity, inductance and highpot breakdown (see the section drawing of the beam tube assembly, Figure 2).

Copper Plating

For the efficient transmission of beam image currents in the SSC, the beam tube must have a highly conductive surface applied to its inner diameter. This surface must have minimum photodesorption outgassing so that under the bombardment of synchrotron radiation the UHV of $\approx 10^{-10}$ Torr may be maintained to maximize the beam life. A high purity copper plating was selectd to form the conductive surface. During magnet quenching, eddy currents will be induced in the copper surface. Resulting high forces will tend to shear the coating off the tube wall. The copper's adhesive strength to the beam tube must be higher than the copper's yield strength. In addition, the surface must be smooth and void of high vapor pressure materials which outgas into the UHV.

Over the past two years, BNL has worked closely with the PCK Company to develop a copper plating that matches the above requirements. Beam tubes up to 18 feet in length have been plated, using a technique developed at PCK. This technique includes a non-consumable anode suspended in the beam tube, a copper bus applied to the outside of the beam tube and anode terminations protruding through manifolds at the tube ends. The anode is made up of a copper core inside a titanium tube with a thin layer of platinum on its surface.

A cleaning solution followed by a water rinse is first pumped through the beam tube. A solution of sulfuric acid is then pumped through the tube while a DC current is used to activate the inside surface. The activation solution is followed by a copper sulfate solution. Using various current densities, copper is applied to the stainless steel and built up to a uniform coating of .0025 ± .0005" along the entire length of the tube. After the copper is plated, a rinse is performed, followed by vacuum drying. The resulting copper surface has a uni-axial grain structure having the minimum number of grain boundaries. Resistivity ratios at zero field and 4.2K have been measured to be ≥900.[2] Photodesorption outgassing rates have been measured to be less than 5×10^{-9} Torr-liters/cm^2/sec. Photodesorption experiments have shown that the clean plated surface has a lower outgassing rate than stainless steel.[3]

Radiation Experiments

Concerns were raised about the effects of radiation on the beam tube assembly materials: Kapton, Kevlar, Glass, RC205 adhesive, and FEP Teflon. FEP was originally chosen as the main bonding agent of the trim assembly. Teflons in general are not recommended for use in high radiation environments. They have a low resistance to radiation as compared to other thermal plastics, rubbers, or polymers.

FEP-coated Kapton was chosen because it could be held to extremely close tolerance (±.0001") and as a standard Dupont product, it was readily available. This allowed close diameter tolerances which could not be achieved by use of epoxy as a bonding agent. FEP also had good bond strength at cryogenic temperatures.

A study at Brookhaven concluded that Teflon's radiation resistance is good if it is not irridiated in the presence of oxygen. Cryogenic temperatures also improve radiation resistance.[4] Since the SSC magnet offers this environment, it was decided that the benefits outweighted the risks. Alternate adhesives were also investigated; for instance, RC205 has various components of epoxy and rubbers, but the composite as a whole had no published radiation effects data.

Using the Brookhaven Linac Isotope Producer (BLIP) various component materials of the trim assembly were irradiated. The exposures were preformed at 3.5 and 20 µ amp-hours of proton beam current of energy ≈193 Mev. Although of relatively low energy, the ionization attributable to the proton beam is similar to a long-term exposure in the SSC machine. No effect on the Kapton substrate material other then a slight stiffening was found. Significant degration in the strength of G-10 at the higher bombardment was observed; the sample turned black and lost over 90% of its mechanical strength. Some degradation in RX630 was found but not enough to preclude its use. Initial observations showed an actual improvement in FEP bond strength but under high bombardments, the FEP became brittle. The peel strength of the superconductor from the RC205 adhesive did not change appreciably. However the interstitial bond strength of the RC205, glass and Kapton laminate deteriorated to a point that alternative adhesives must be investigated. The Kevlar yarn remained intact; however, under the higher bombardment, some loss of bond strength was noticed.

Future Developments

Work has begun on the evaluation of alternative adhesives that could be used in the trim coil assembly. An improved epoxy-based wire adhesive called PK102 will be tested for its radiation resistance. Different adhesives such as Tefzel are being investigated for the eventual replacement of the FEP Teflon.

Glass and carbon fiber yarns are being evaluated as alternatives to Kevlar. Alternative materials and designs are being evaluated to replace the G-10 bumpers on the outside of the trim coil assembly. Further work will continue to optimize the trim coil design to precisely match the SSC field requirements where needed.

Work is continuing on the development of a facility to plate beam tubes up to 17 meters in length.

Armco Nitronic 33 alloy stainless steel will be investigated as a lower cost, lower permeabilty alternative to the present Nitronic 40. New tooling will be developed at BNL to improve the trim coil/beam tube assembly tolerances. This tooling will also substantially reduce assembly time and cost.

Work will continue to emphasize industrial involvement in the development and improvement of the trim coil components and will seek to optimize procedures for the mass production of assemblies.

Technical Spinoffs

The first spin-off of this technology was the production of precisely made detector wire patterns for an IBM/BNL collaboration on a monopole detection experiment. Also, General Electric is working with Multiwire to develop a less expensive and more precise alternative for the production of superconductor trim coils for nuclear magnetic resonance imaging equipment. The Multiwire technique of precision wire placement can be applied to experimental instrumentation such as lumped correctors, measuring coils, and drift chambers for the SSC and other accelerators.

Conclusions

Over the past three years Brookhaven has been involved in a program which has led to the successful development of a precision field correction coil/beam tube assembly for the SSC. The initial results show that the assembly fulfills the various requirements of the SSC accelerator design in the areas of field strength, quality, copper plating, photodesorption, and assembly procedures.

Work is still needed to improve the radiation resistance of constituent materials. Efforts are under way to optimize and refine the materials and production techniques as well as quality control procedures to assure the efficient and trouble free operation of the 9600+ trim coil beam tube assemblies for the SSC project.

References

[1] P. Wanderer et al., Performance of R&D Sextupole Trim Coils for SSC Dipole, submitted to this conference.

[2] D. Bintinger, Measurement of Residual Resistivity Ratio for Copper Plated SSC Beam Tubes, SSC-N-184, May 1986.

[3] J.D. Jackson, Specification of Copper Plating of Beam Tube, SSC-N-298, February 1987.

[4] P. Wanderer, Radiation Resistance of Teflon, ISA Technical Note 363, April 1982.

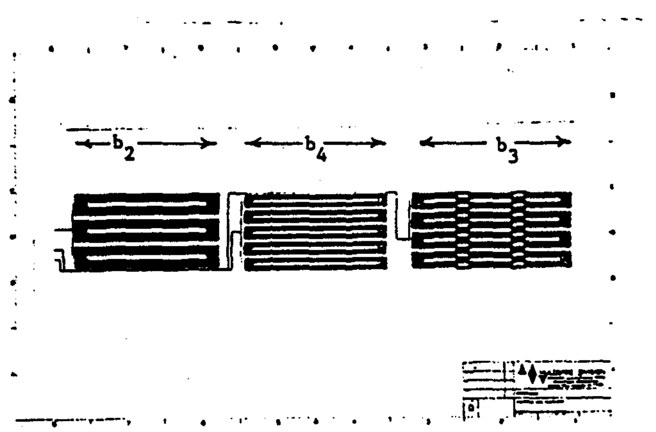

Figure 1. Multiwire Flat Pattern Layout.

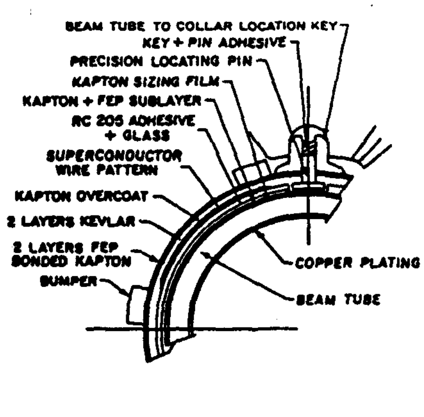

Figure 2. Beam Tube Assembly

APPENDIX H

"Results to Date: SSC Correction Coil Performance,"

Talk by Peter Wanderer

TRIM COIL TRAINING STUDIES: $T = 4.5K$

(assuming full-length trim)

Goal: $|\text{Trim-coil quench current}| > (4A + \text{margin})$

Quench: conductor becomes resistive because current too large or temperature too high, assuming fixed dipole field B_0.

Conductor temp. may increase if not well-secured [(e.m. force, $\propto I_{trim} \cdot B_0$) $\Rightarrow$ motion $\Rightarrow$ friction $\Rightarrow$ heat]

Typical program:

(A)
- Train trim coil to $+I_{max}$ ($I_{max} = I_{SS}$, time, ...)
- " " " " $-I$ " ("short-sample limit")
- Check training at $+I$
- " " " $-I$

Thermal cycle (4.5 K → room temp → 4.5 K)

Repeat (A)

Most severe test is $B_0 = 6.6\,T$ (20 TeV)
- largest force (at fixed I_{trim})
- smallest capacity of trim-coil conductor: $I_{SS} \tilde{\propto} 1/B_0$

Up to now - use $B_0 = 5.8\,T$ so that don't have to worry about dipole quenching.

As a first-order correction, estimate that

$I_Q(6.6T) = (5.8/6.6) \times I_Q(5.8T) \simeq 0.9 \times I_Q(5.8T)$

(This is too simplistic, since $-I_{max} \neq +I_{max}$)

Remark: Trim coil sensitive to heat leak from "warm finger" inserted in cold bore tube. Two 4.5 m & one 17 m trims tested w/o this finger installed.

TRIM COIL TRAINING IN 3.5m DIPOLE SLN015

I_{main} = 5.8 kA ($B_o \simeq 5.8T$) 4.5K

(Also: I_{trim} = 27A @ B_o = 3T, = 34A @ 2T, = 73A @ 0.3T)

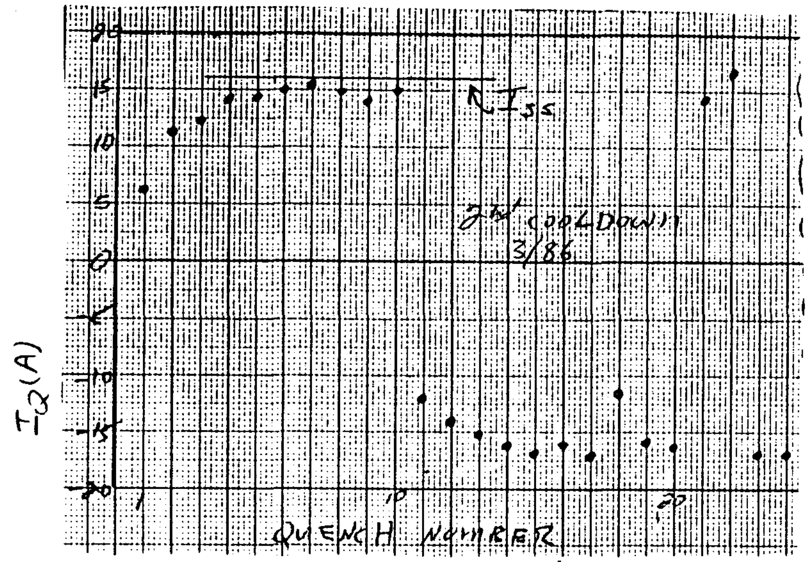

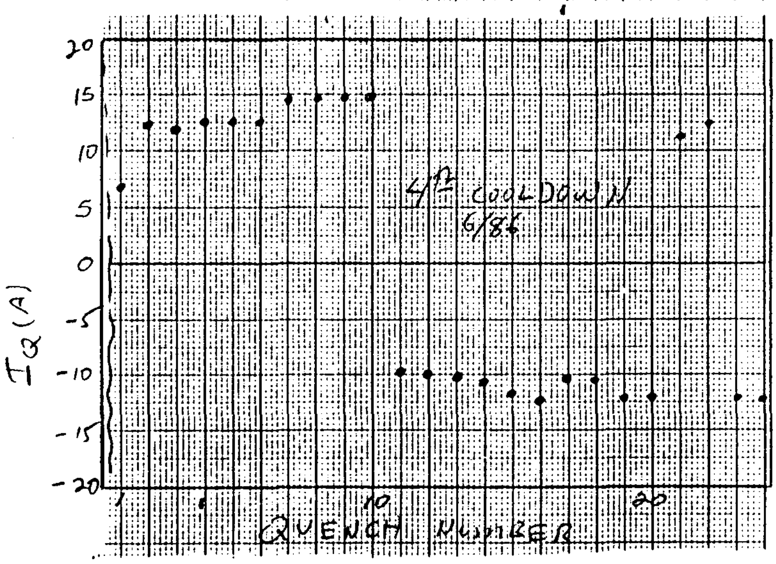

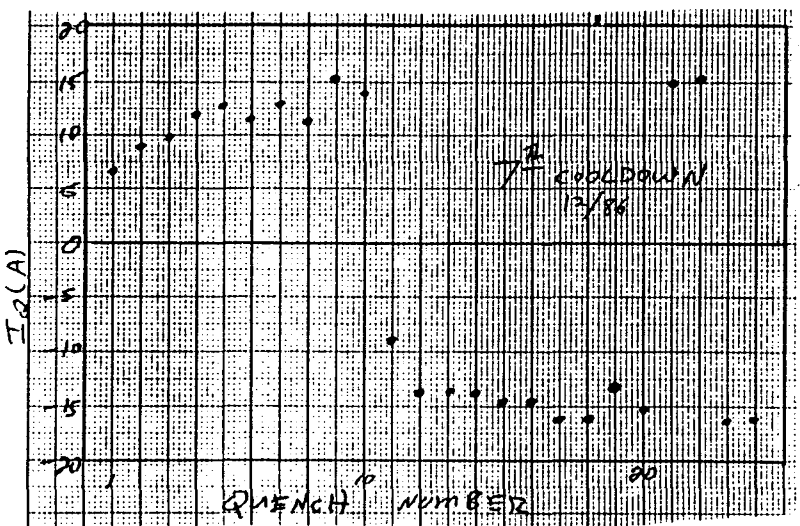

TRIM COIL TRAINING IN 4.5m DIPOLE {SLN013 SD13}

$I_{main} = 5.8$ kA ($B_0 \simeq 5.8$ T)   4.5 K

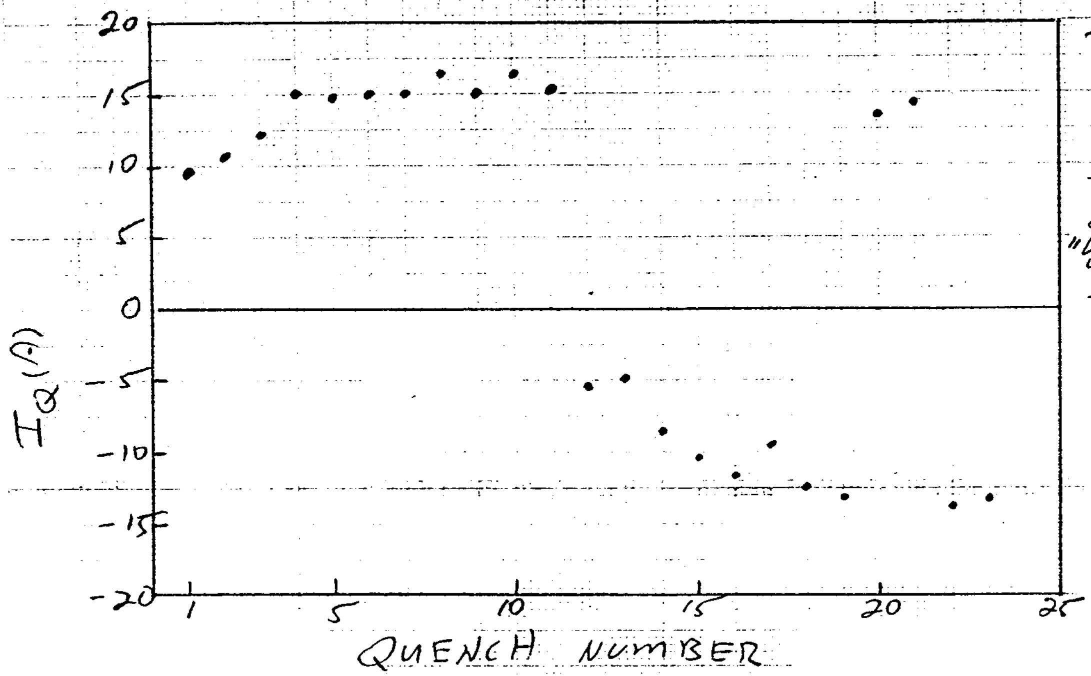

Tested @ BNL 1/87

72 previous quenches w/ "warm finger" in

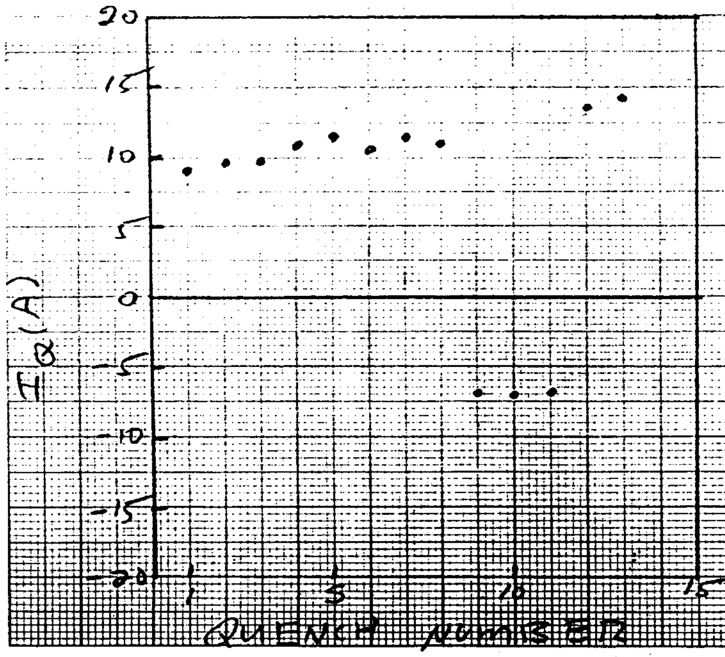

Tested March-April 87 @ Fermilab

Note: also established –
$I_{trim} \simeq 35$ A for $B_0 = 2$ T
$I_{trim} \simeq 75$ A for $B_0 = 0.3$ T

RW
12 Oct '87

(5)

TRIM COIL TRAINING IN 17m DIPOLE D00002

$4.0 < I_{main} < 5.5$ kA ($4.0 < B_0 < 5.5$ T) 4.5 K

(tested at Fermilab - no "warm finger")

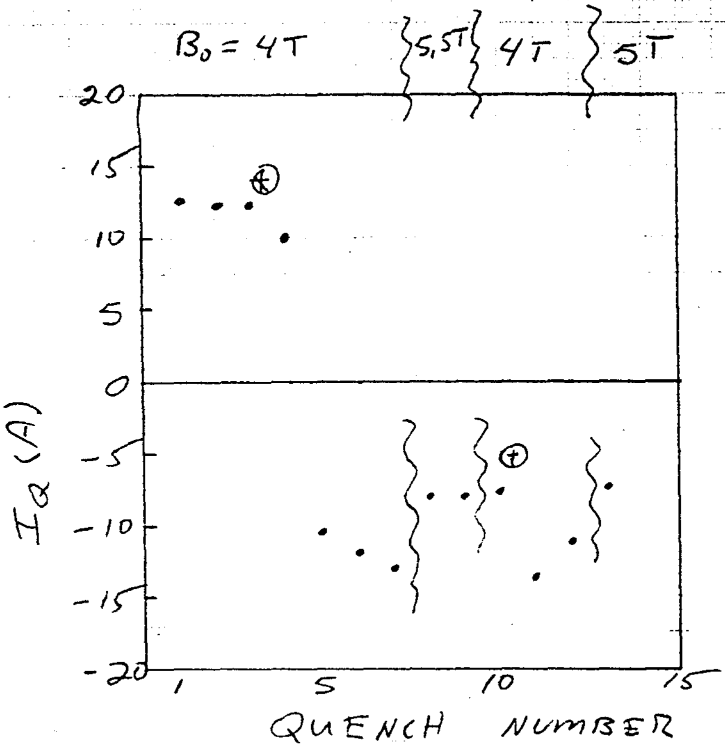

About ½ The quenches are "glitch related" ⇒ (?) shorted turns

⊕ Quench after 3 min at 12.1A

⊕ Quenched while ramping to 0A from 13A

P.W. 12 Oct '87

TRIM COIL TRAINING:

SUMMARY -

a) SLN015 - trains to $I_{ss} \gtrsim 15A$
- after thermal cycle, retrains from $\gtrsim 6A$
- must be trained in both polarities
- $+I_{max} \simeq -I_{max}$

b) SLN013/SD13 - about same as SLN015, except:
$-I_{max} \lesssim +I_{max}$

c) D00002 - ramp-rate & history dependance
⇒ have excuse for relatively poorer performance than 4.5m trims

CONCLUSION -

a) for full-length trim - need more margin.

b) for half-length trim - are the limits due to
i) I/I_{ss} - then need more margin
ii) $F \propto I \cdot B_o$ - not meeting operational needs now

either way, want to improve mechanical structure.

(remark: trim-coil quench doesn't cause dipole to quench.)

SHAPE OF TRIM COIL FIELD

Fourier analyze deviations from pure dipole
typically $(1/10^4) \times B_0$, at 1cm radius ("unit")

The fourier coefficients (e.g. quadrupole ~ $\cos 2\theta$, $\sin 2\theta$)
often closely linked to specific mechanical errors.

$$B_y + i B_x = B_0 \sum_{n=0}^{\infty} (b_n + i a_n)(x+iy)^n$$

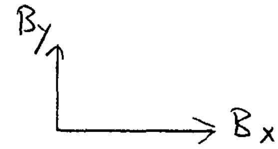

b_2 - sextupole field due to trim coil
b_8 - 18-pole field, allowed by sextupole symmetry
Is b_2/I correct?
Is b_8 small?

If trim coil not in center of dipole coil, b_2 feeds down as quadrupole (a_1 - vertical; b_1 - horizontal) or skew sextupole (a_2 - rotation).
Sensitivity ~ 0.1mm = 4 mils generates ~ 0.2 units (same for all 3 terms).

Oval trim coil ⇒ dipole term (cf Pat Thompson's note)

Scale: write fields in dipole "units".
At $B_0 = 2T$, $I_{trim} = 2A$, get 5 units of b_2.
Need 4-5 units (max) for nearly all values of B_0.

TRIM COIL CONSTRUCTION HISTORY - from the multipole perspective

① 1^{st} 3 4.5m trims

improve trim position on bore tube
⇒ improve feeddown-produced terms (a_1, b_1, a_2)

② 4^{th} 4.5m trim

reduce radial thickness of adhesive under substrate to design value, thus decreasing trim coil radius and closing gap between edges.
⇒ increase b_2/I a bit (radial change)
⇒ reduce octupole terms and (perhaps) higher-order terms caused by gap

③ full-length 17m trim
(remark: only central 60cm of D00001 trim measured)

(9)

TABLE I.

Multipole (units)	a_1	a_2	b_1
Dipole Tolerance (systematic ± random)	.2±.7	.1±.6	.2±.7
fourth 4.5m trim	.03	-.14	.01
First 17m (60cm section)	.09	-.39	-.06

TABLE II.

Multipole (units)	b_2	b_3	b_4	b_5	b_6	b_7	b_8
Dipole tolerance (systematic ± random)	±2.0	.1±.3	.2±.7	.02±.1	.04±.2	.06±.2	.1±.1
Four 4.5m trims (mean ± σ)	5.38± .08	.20± .04	.02± .02	.045± .03	.02± .01	.01± .01	.008± .002
First 17m (60cm section)	5.61	.035	-.02	-.008	.008	0	.009

Multipole (units)	a_3	a_4	a_5	a_6	a_7	a_8
Dipole tolerance (systematic ± random)	.2±.7	.2±.2	±.2	±.1	±.2	±.1
Four 4.5m trims (mean ± σ)	.26± .06	.10± .02	.02± .01	.02± .01	.02± .01	<.01
First 17m (60cm section)	.076	-.01	-.005	-.005	0	-.002

Table Captions

Table I. Low order multipoles from sextupole trim coils, scaled to a 2 A trim coil current in a 2 T dipole field. Multipoles are evaluated at 1 cm, in units of 10^{-4} of the dipole field.

Table II. Sextupole field and higher order multipoles from sextupole trim coils, scaled to a 2 A trim coil current in a 2 T field. Multipoles are evaluated at 1 cm, in units of 10^{-4} of the dipole field.

Dipole < 1×10^{-4} (4.5m trims)

APPENDIX I

"HERA Correction Coil Design and Performance,"

Talk by Peter Schmueser

Superconducting Correction Magnets for HERA p-Ring.

C. Daum, J. Geerinck NIKHEF-H Amsterdam
R. Heller, H. Möller DESY
P. Schmüser, Univ. Hamburg.
P. Bracké, HOLEC BV, Rotterdam

Correction dipoles

at 1 TeV 0.63 T·m horiz., 0.83 Tm vertical
(J. Rossbach, HERA 85-4)

Design 0.84 Tm

Correction quadrupoles (HERA 85-4)

$k = \pm 5.7 \cdot 10^{-4}\ m^{-2}$ at 1 TeV

$B_2 (r = 25mm) = 0.048 T$

$B_2 \cdot 12 m = 0.57 Tm$ (1 TeV)
0.47 " (820 GeV)

Sextupole strengths: determined by tracking (Wrulich)

$B_3 (r = 25mm) \approx 0.03 T$

$B_3 \cdot 12 m = 0.35 T \cdot m$

Straight sections:
10 superferric quadrupoles for each interaction region, built at DESY

Electron - Proton Collider

conventional e magnets

superconducting p magnets

e^-

30 GeV

58 mA

210 bunches

500 MHz

$\mathcal{L} = 2-3 \cdot 10^{31} cm^{-2} s^{-1}$

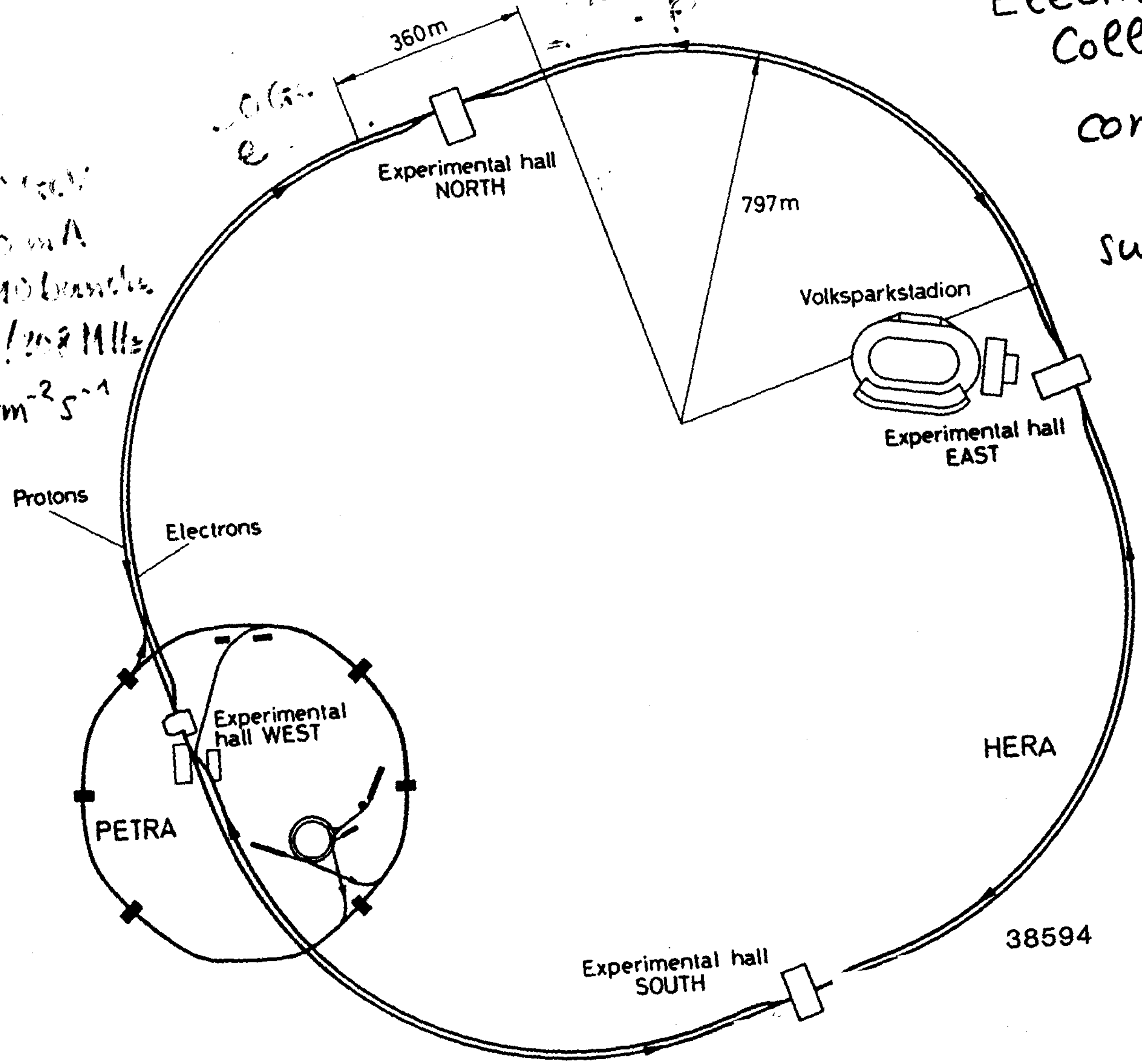

I-3

proton ring cell

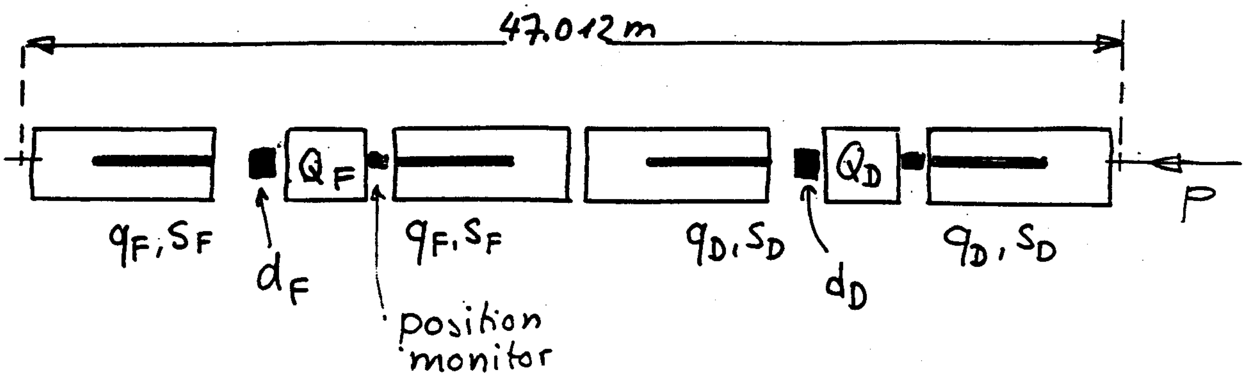

Sextupole/quadrupole coils :
mounted on cold beam pipe inside main dipole

currents ≤ 100A in high external field (≥ 5T)
— requires high-performance superconductor
— very good mounting on pipe to avoid quenches

length ≃ 6 m

correction dipoles :
superferric window frame magnets
two saddle-shaped coils impregnated with epoxy
length = 60 cm
mounted in quadr. cryostat

440 SQ coils
250 corr. dipoles
} Dutch contribution to the HERA machine

built by HOLEC BV, Ridderkerk near Rotterdam

S

SQ coil inside main dipole

outer diam 67.0 mm ; dipole inner diam. 75.0 mm

4mm annular slit for single-phase helium

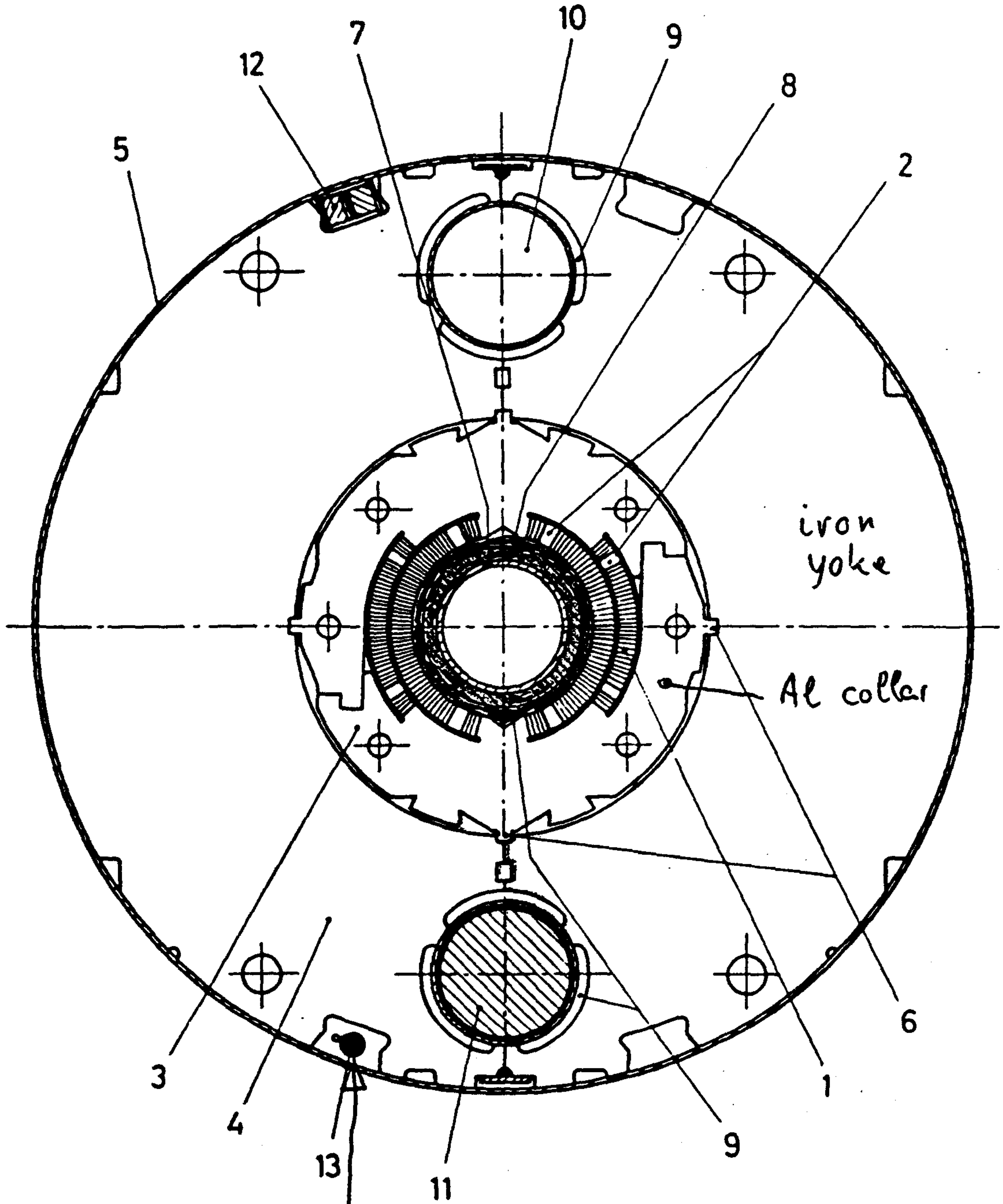

current bus for SQ coils

10 pairs of SC wires

Schematic layout of correction coils

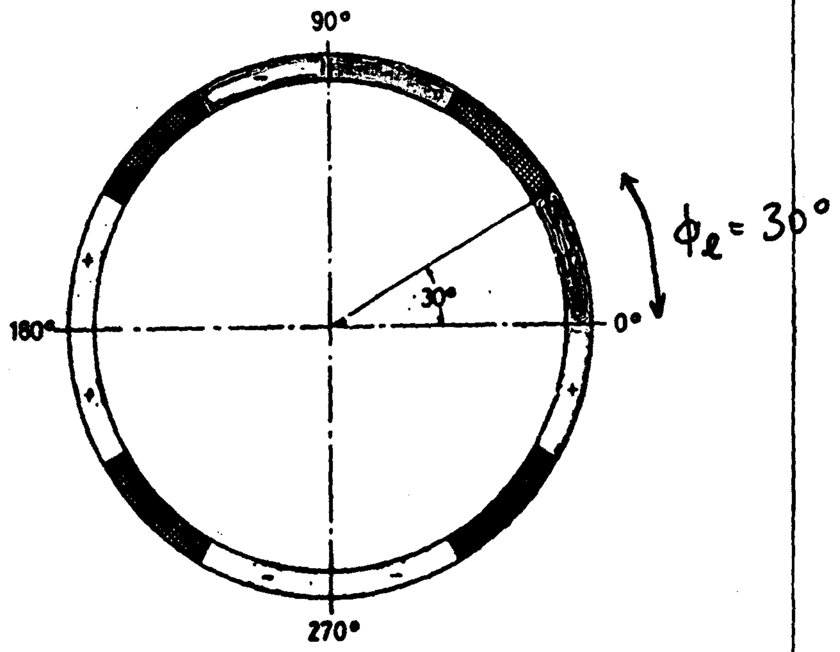

Quadrupole correction coil

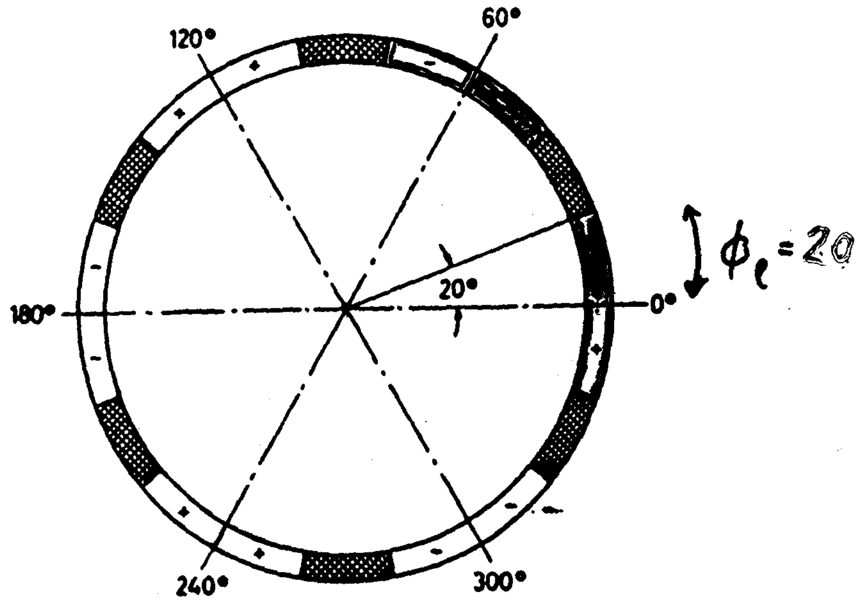

Sextupole correction coil

reference rad.
$r_0 = 25$ mm

Theoretical multipoles

Quadrupole	Sextupole
$b_2 \equiv 1$	$b_3 \equiv 1$
$b_6 = 0$	$b_9 = 0$
$b_{10} = -2.41 \cdot 10^{-2}$	$b_{15} = -1.48 \cdot 10^{-2}$
$b_{14} = 6.3 \cdot 10^{-3}$	$b_{21} = 2.9 \cdot 10^{-3}$
$b_{18} = 0$	$b_{27} = 0$
$b_{21} = -0.5 \cdot 10^{-3}$	

Field $< 10^{-2} \cdot B_0$

Quadrupole with $b_{10} \equiv 0$.

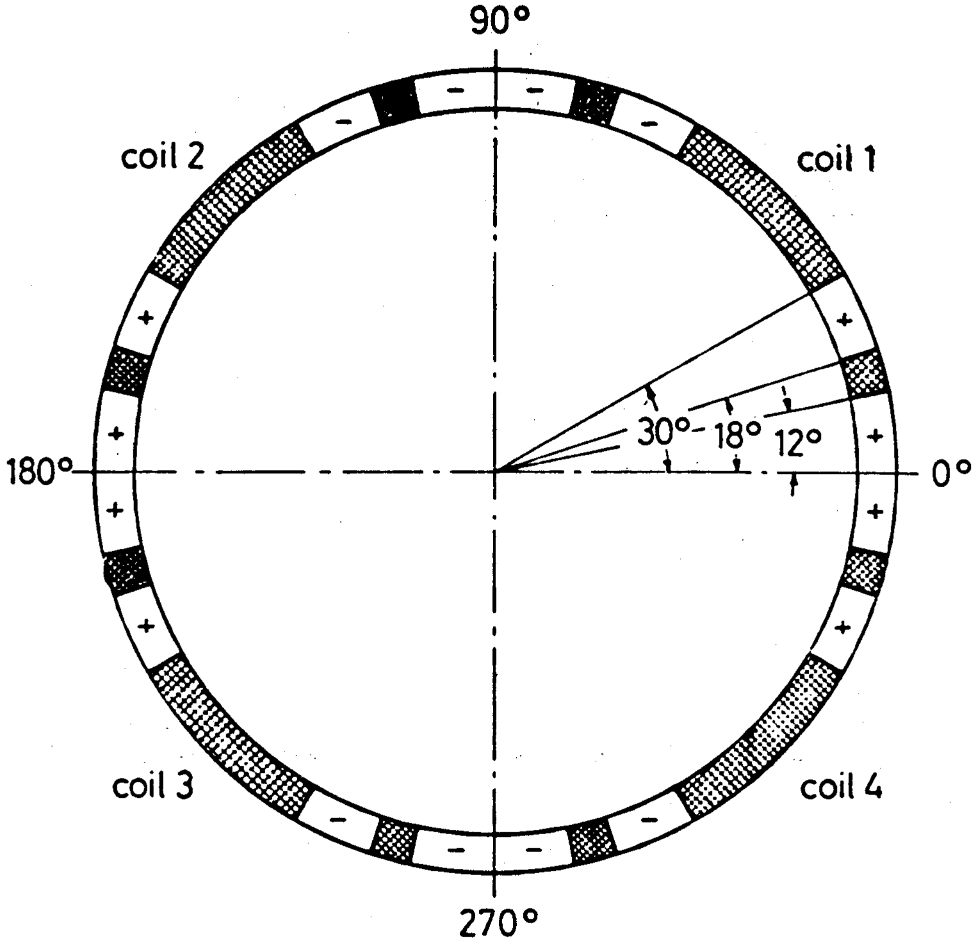

Quadrupole correction coil

Disadvantage: current factor of 1.27 higher
much harder to fabricate

Influence of systematic 20-pole ($n = 10$) in correction quadrupoles on the stable emittance

HERA injection optics
$Q_x = 31.18$, $Q_z = 32.15$

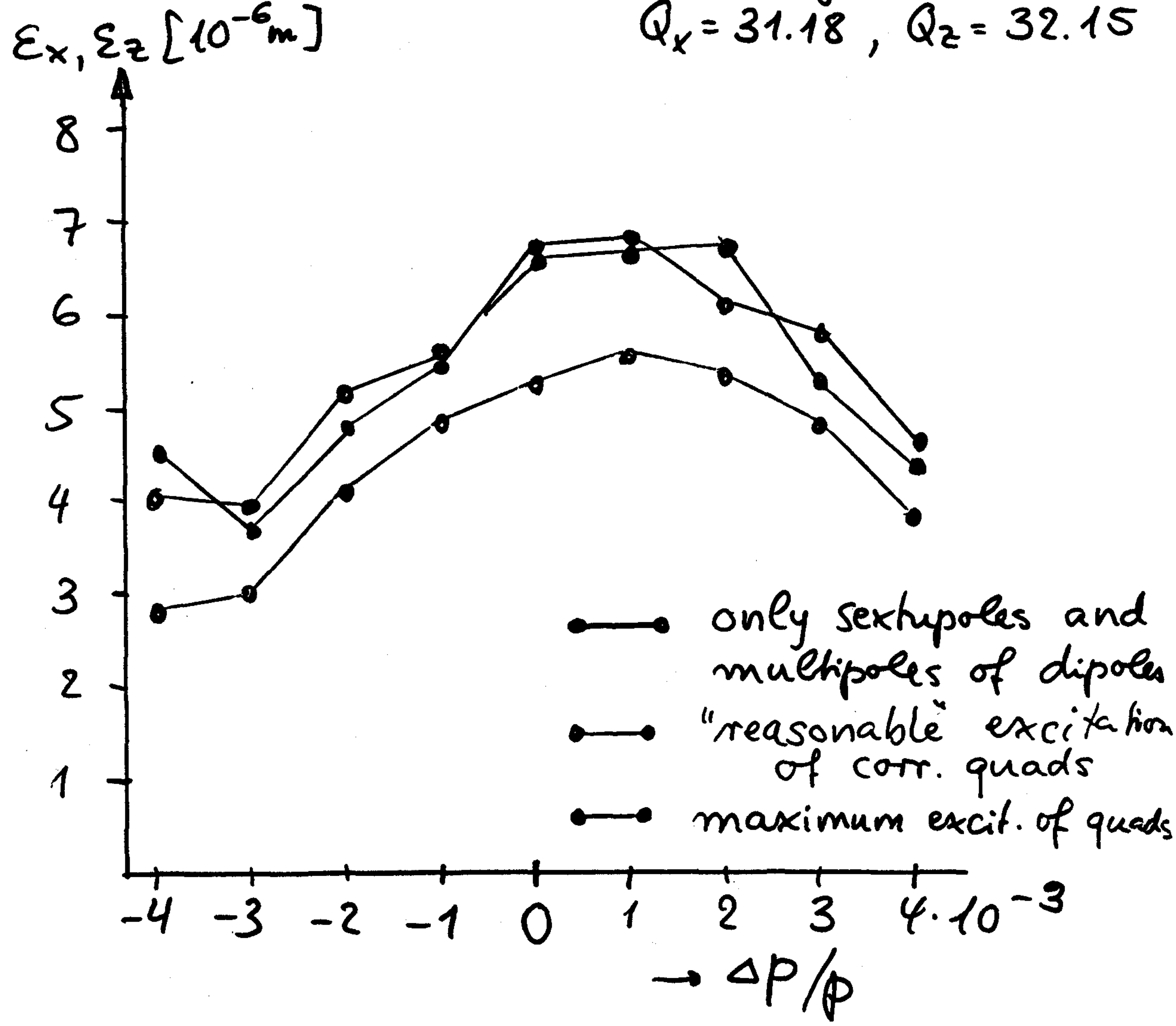

tracking calculations by R. Brinkmann (RACETRACK code)
16 particles for 100 turns

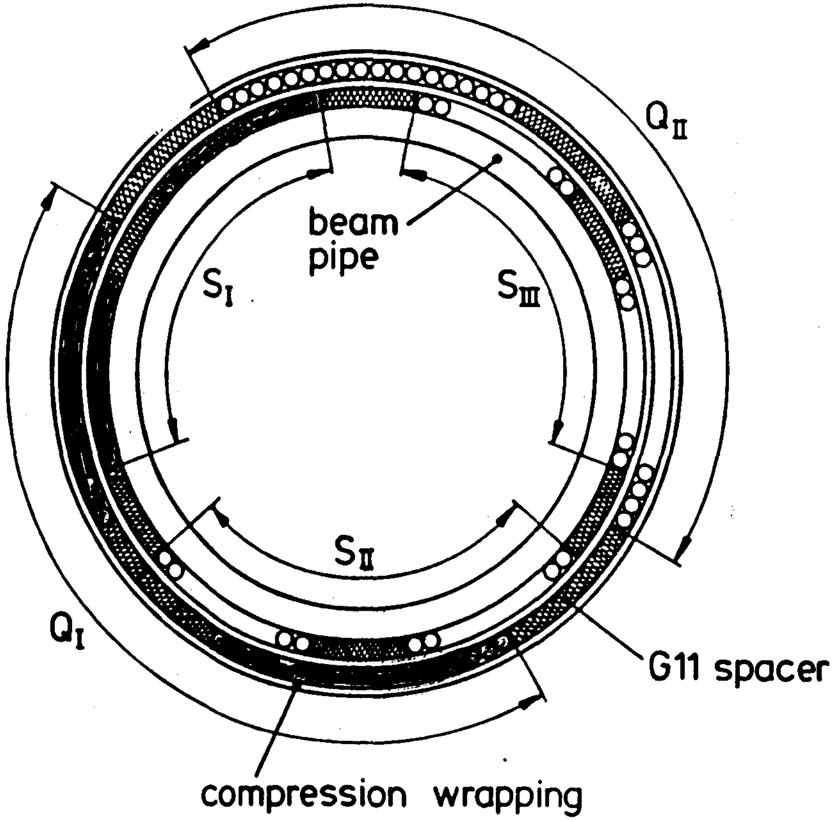

quadrupole
2 subcoils, 33 turns each

sextupole
3 subcoils, 21 turns each

beam pipe insulation:
2 layers glass-Kapton-glass tape
(0.15 mm thick)

after sextupole:
1 R glass compression wrapping
1 layer glass tape

after quadrupole:
2 R glass compress. wrappings
1 layer glass tape

beam pipe stainless steel
DIN 1.4429 ≙ 316 LN
outer dia 60.3 mm, wall 2.5 mm

Mechanical accuracies.

a) error in limiting angle ϕ_e

quad : $\phi_e = 30° + \delta$

$\Rightarrow b_6 \approx -0.7 \cdot 10^{-3} \cdot \delta$ $\quad \delta$ in mrad

$\delta = 5$ mrad : $|b_6| = 3.5 \cdot 10^{-3}$

sext : $\phi_e = 20° + \delta$: $|b_9| = 4 \cdot 10^{-3}$ for 5 mrad

b) distortion of symmetry: one current shell misaligned by angle δ

for quad coil, $\delta = 5$ mrad:

skew multipoles $a_1, a_2, a_3, a_4, \ldots \approx 1.5 - 3 \cdot 10^{-3}$

$\Rightarrow$ require angular accuracy < 5 mrad

specif. : $\pm 0.2° = \pm 3.5$ mrad.

c) deformation of beam pipe

elliptical deformation

$\Delta R = 0.2$ mm $\Rightarrow$ $b_4 = 4 \cdot 10^{-3}$ in quad

$b_5 = 5 \cdot 10^{-3}$ in sext.

specified inner radius: 30.5 ± 0.05 sextupole

31.9 ± 0.05 quadr.

measured ellipticity : $\Delta R \lesssim 0.1$ mm.

d) influence of winding short:

for quad : typical $n = 3, 4, 5, \ldots$ poles

of $\approx 1 \cdot 10^{-2}$

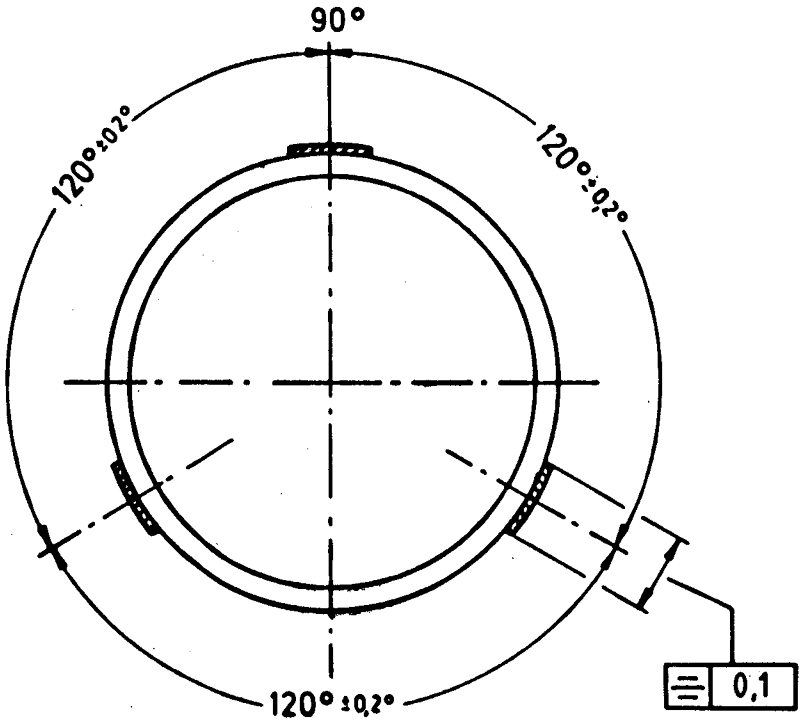

G11 - Zwischenstücke Sextupol

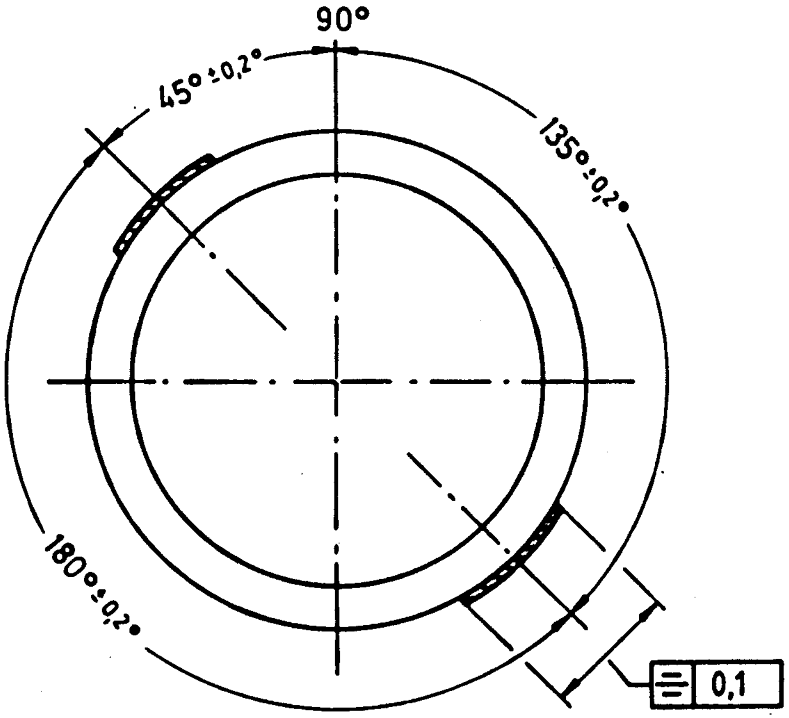

G11 - Zwischenstücke Quadrupol

Alignment of SQ coils on beam pipe.

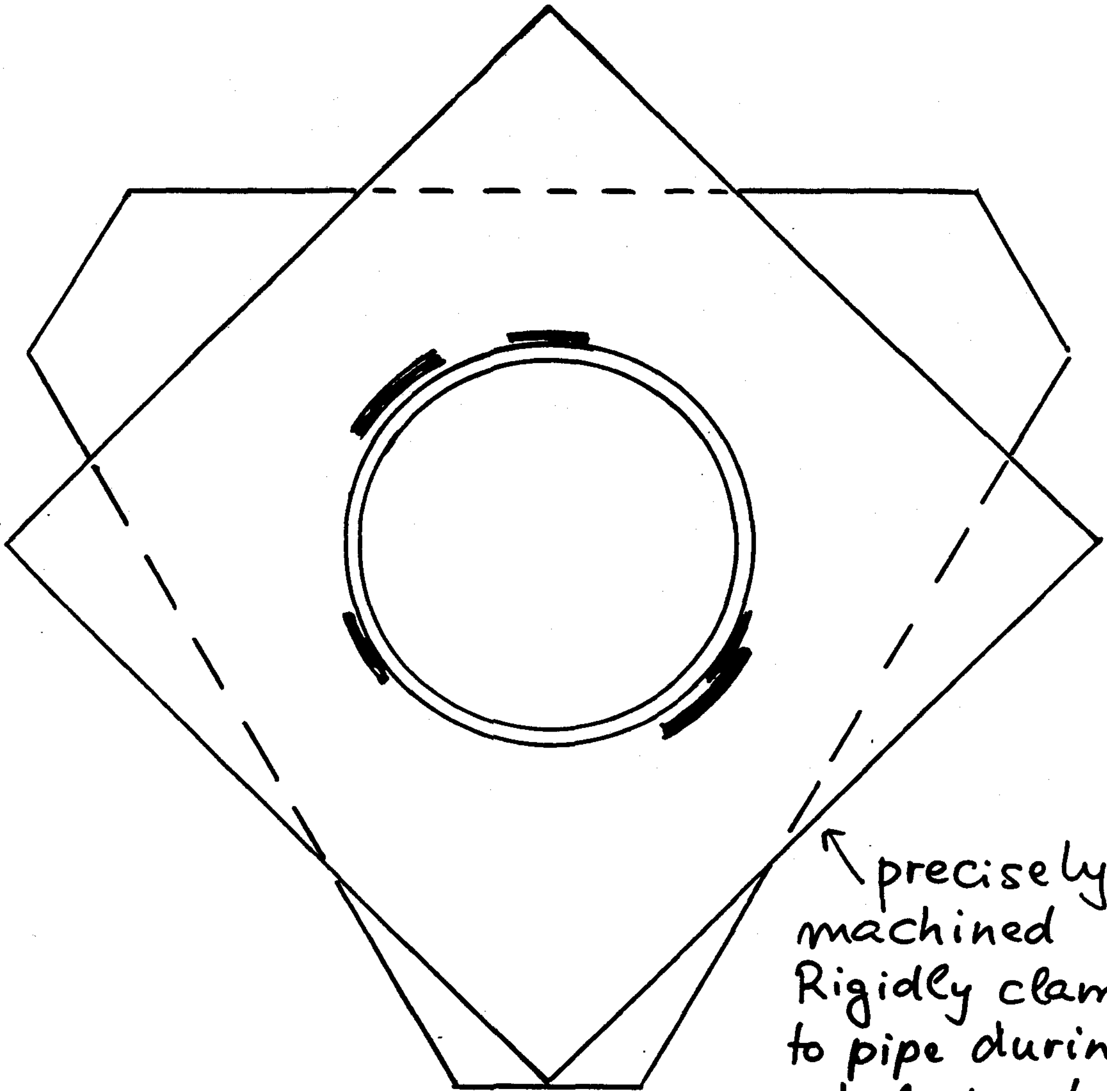

— G11 spacers between the 3 sextupole sub coils

— G11 spacers between the 2 quad. sub coils

spacers should align coils to ±0.2°
over whole length of 6m

Tool for glueing of G11 spacers
(SICOMET cyan-acrylat-glue)

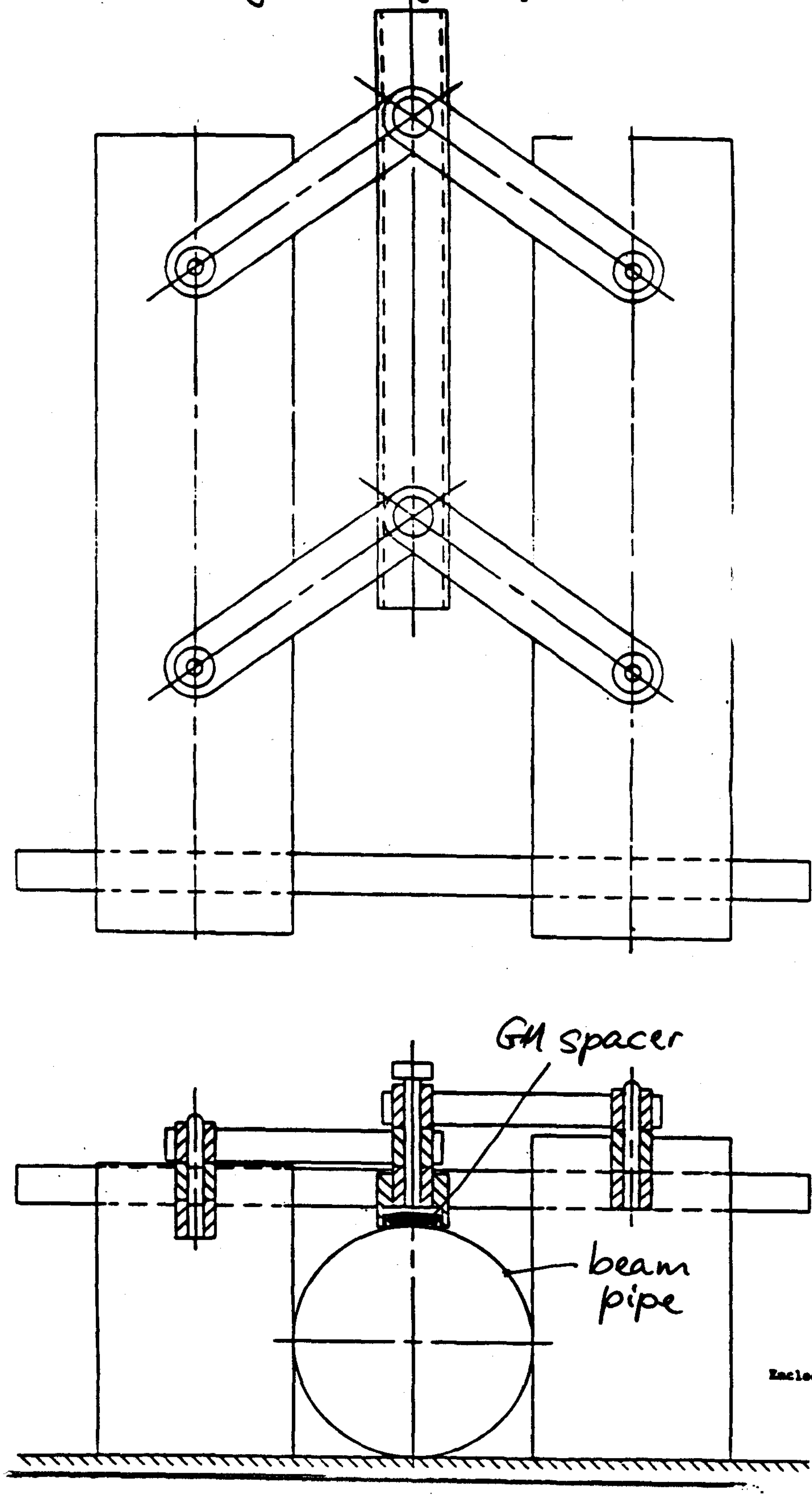

Enclosure 7

Fig. 6

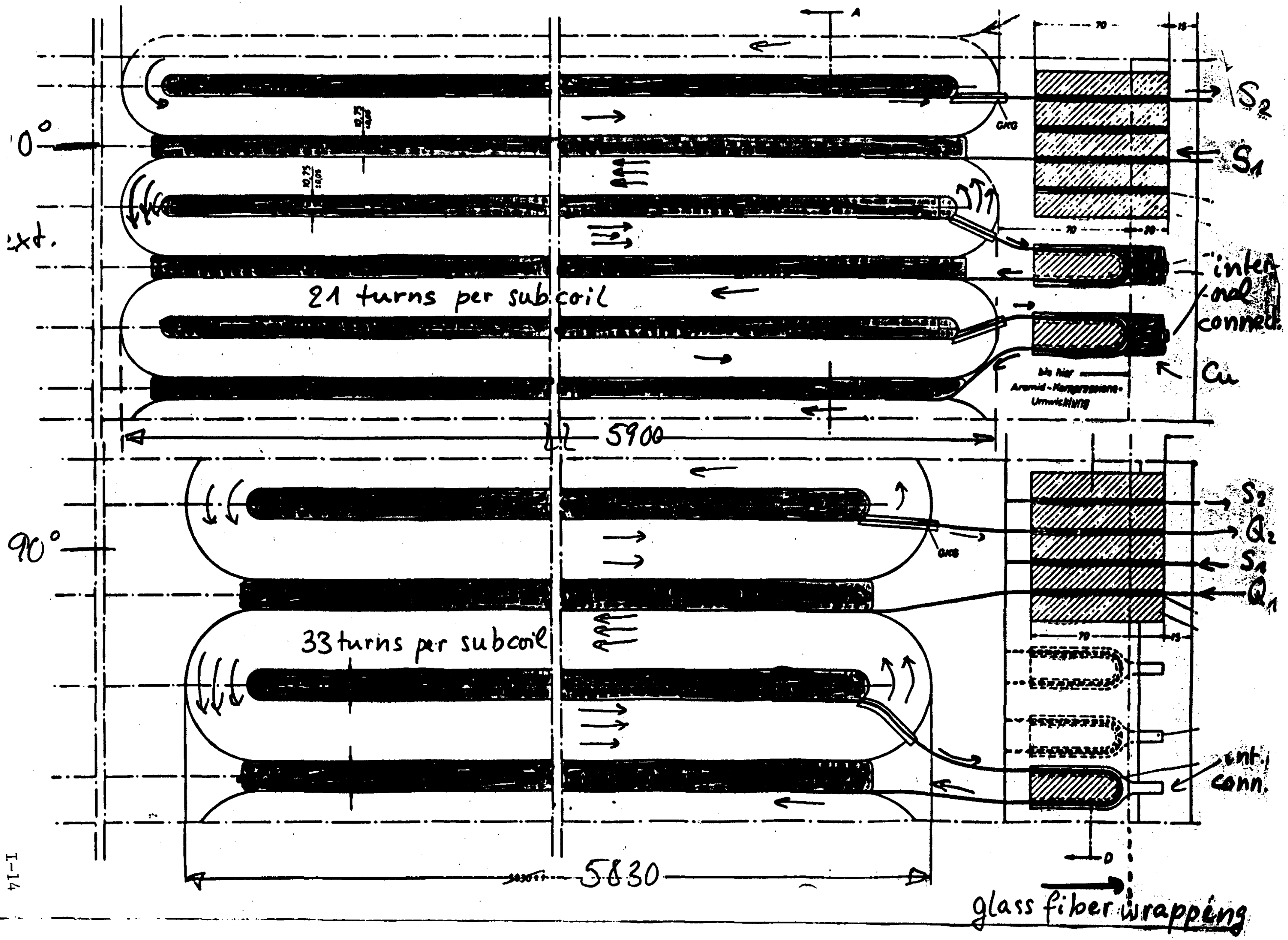

0°
ext.
21 turns per subcoil
5900
S2
S1
internal connect.
Cu
bis hier Aramid-Kompressions-Umwicklung
GKG
70
15
20
90°
33 turns per subcoil
5830
S2
Q2
S1
Q1
int. conn.
glass fiber wrapping

Baking mould for subcoils

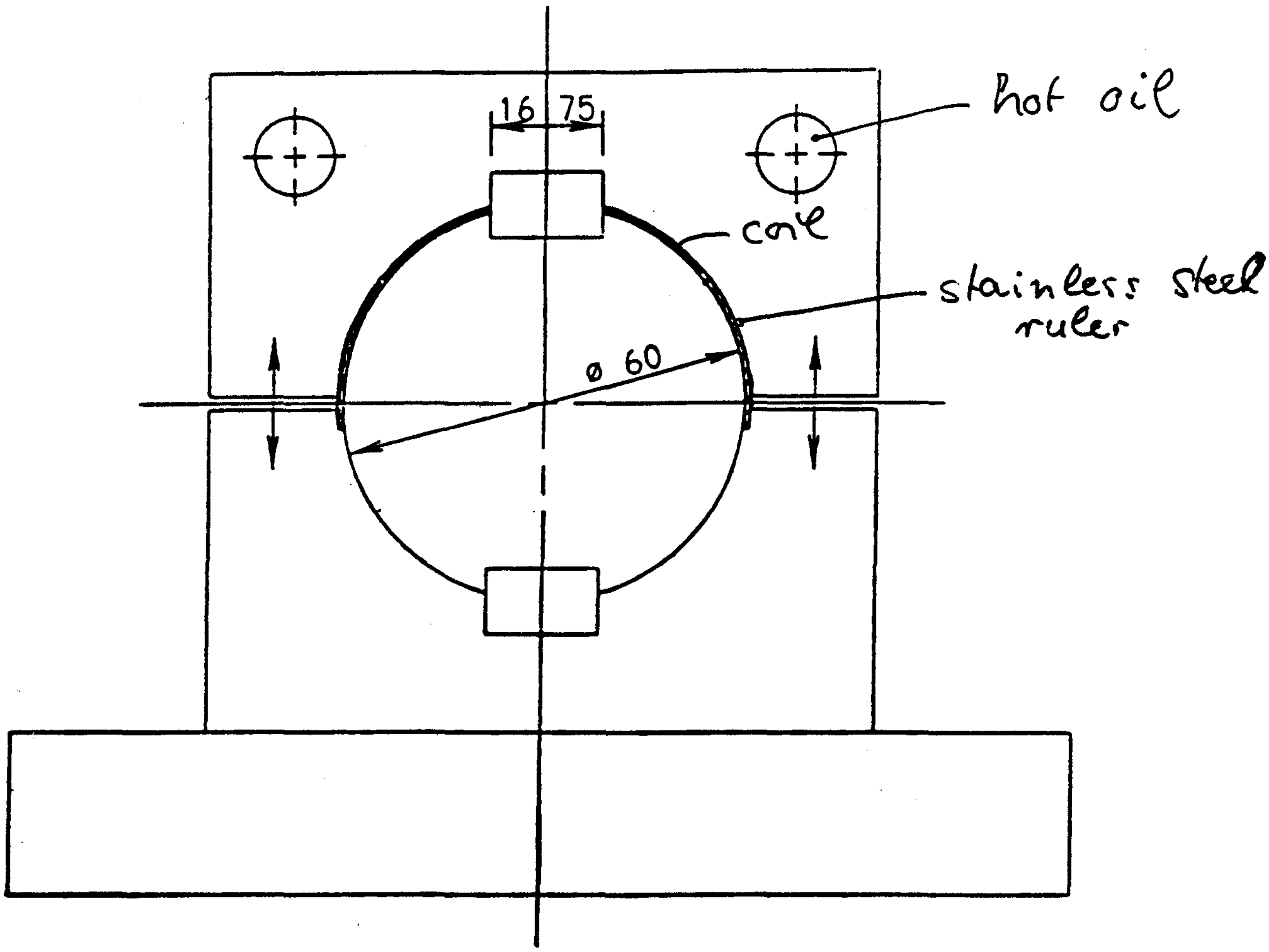

Fig. 4

Sextupol-Teilspule nach dem Ausbacken

(Maßstab 2:1)

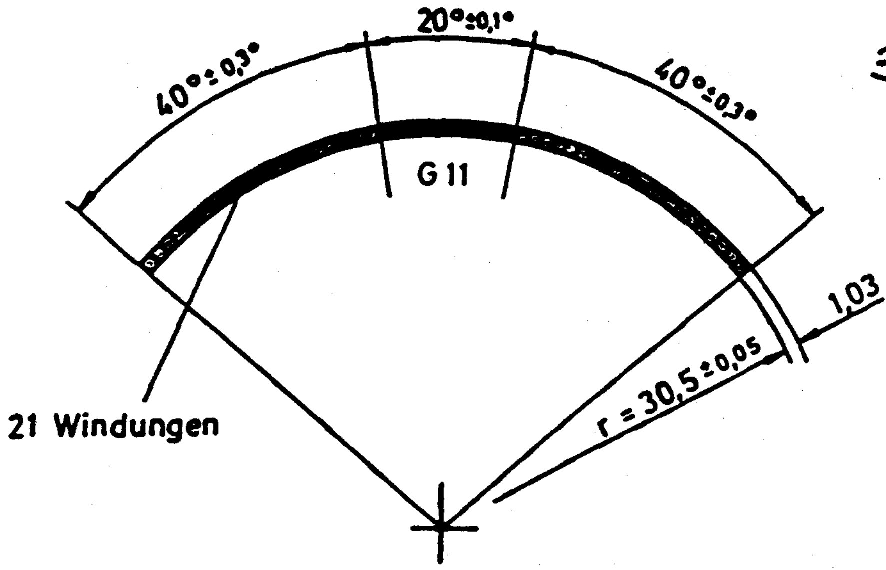

3 S-subcoils wound and baked in curved form

Quadrupol-Teilspule nach dem Ausbacken

(Maßstab 2:1)

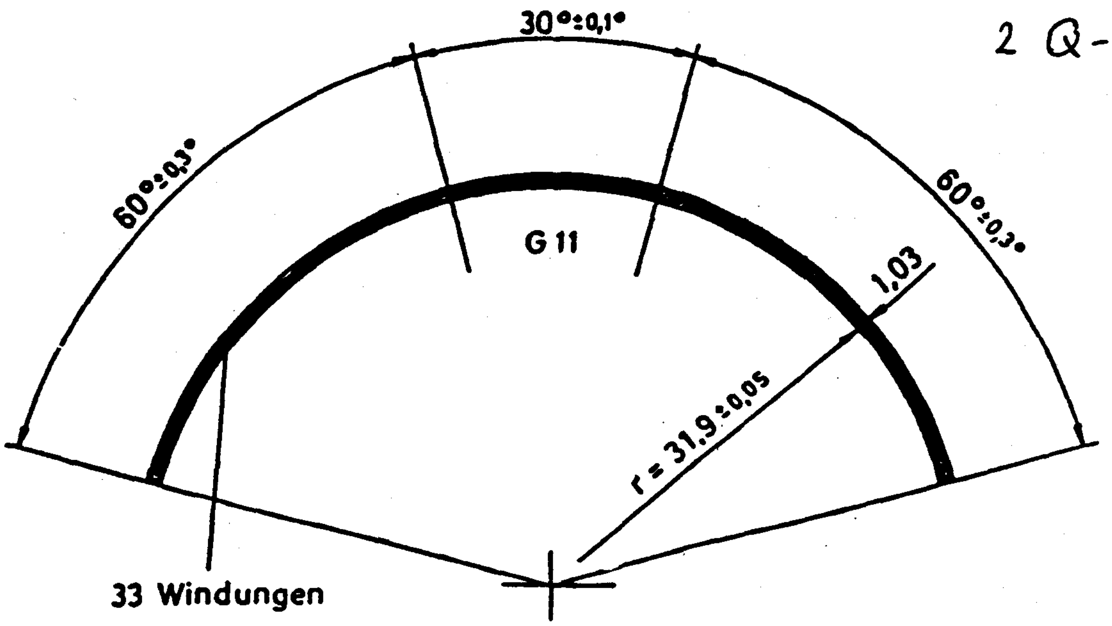

2 Q-subcoil

diameter of insulated conductor after baking:
1.03 mm ; tolerance ≤ 0.01 mm.

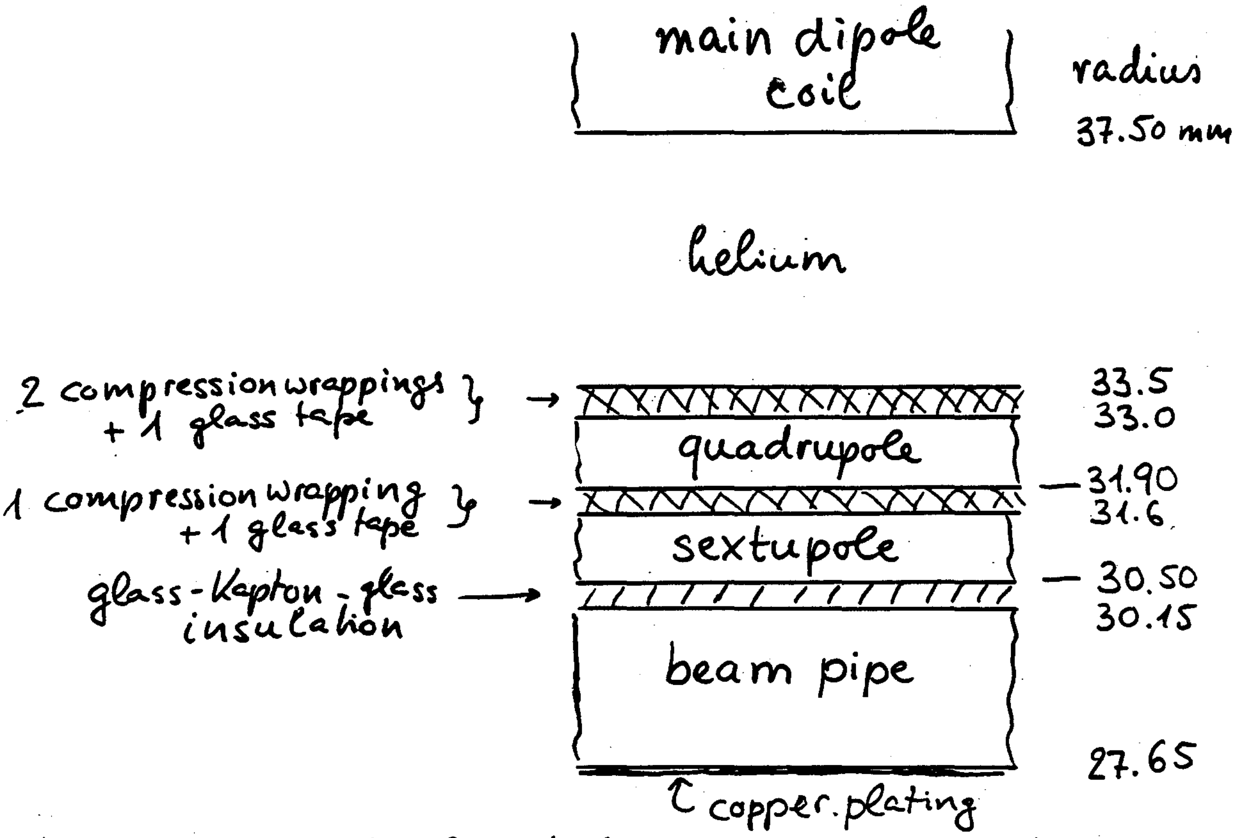

beam pipe: stainless steel DIN 1.4429 ≙ 316 LN
outer dia. 60.3 ± 0.1 mm, thickness 2.5 mm
$\chi_{mag.}$ $1.6 \cdot 10^{-3}$ at 4.2K
copper plated on inside (≈ 12 μm)

glass-Kapton-glass tape: 25 μm Kapton, total thickness 150 μm, 2 layers

compression wrapping: preimpregnated unidirectional R glass fiber (Stratipreg by Vetrotex.)
800 tex = 800 g / km, fiber dia 10 μm, $\rho = 2.55\ g/cm^3$
ultimate tensile strength 3600 N/mm²
winding stress 800 N/mm²
Force 250 N on 0.31 mm² fiber bundle, pitch 2.5 mm

Superconductor

		BBC numbers
single strand dia.	0.70 ± 0.01 mm	
NbTi filament dia.	< 20 μm	12 μm, 1230 filaments
Cu / NbTi ratio	$1.8 {}^{+0.2}_{-0.1}$	
twist pitch	about 25 mm	
RRR	> 100	
I_c at 5.5 T, 4.60 K	> 250 A	
5.5 T, 4.2 K	> 285 A	310 - 320 A at 4.2 K 5.5 T

Insulation

Kapton layer of 50 μm
(wound from 25 μm tape, 48% overlap)
glass fiber layer of 0.1 mm thickness
coated with B stage epoxy

insulated wire: dia. $1.03 {}^{+0.06}_{-0}$ mm

Wire compressed to 1.03 mm in baking mould

(ISOLA for first 60 coils
then SMIT DRAAD, Nijmegen)

Epoxy: Epikote 215 / Versamid 140 1:1
baking 2 hours at 150°C

shear test at LN_2 temperature

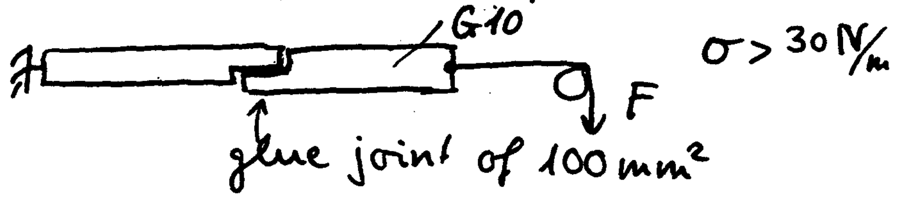

N° 417

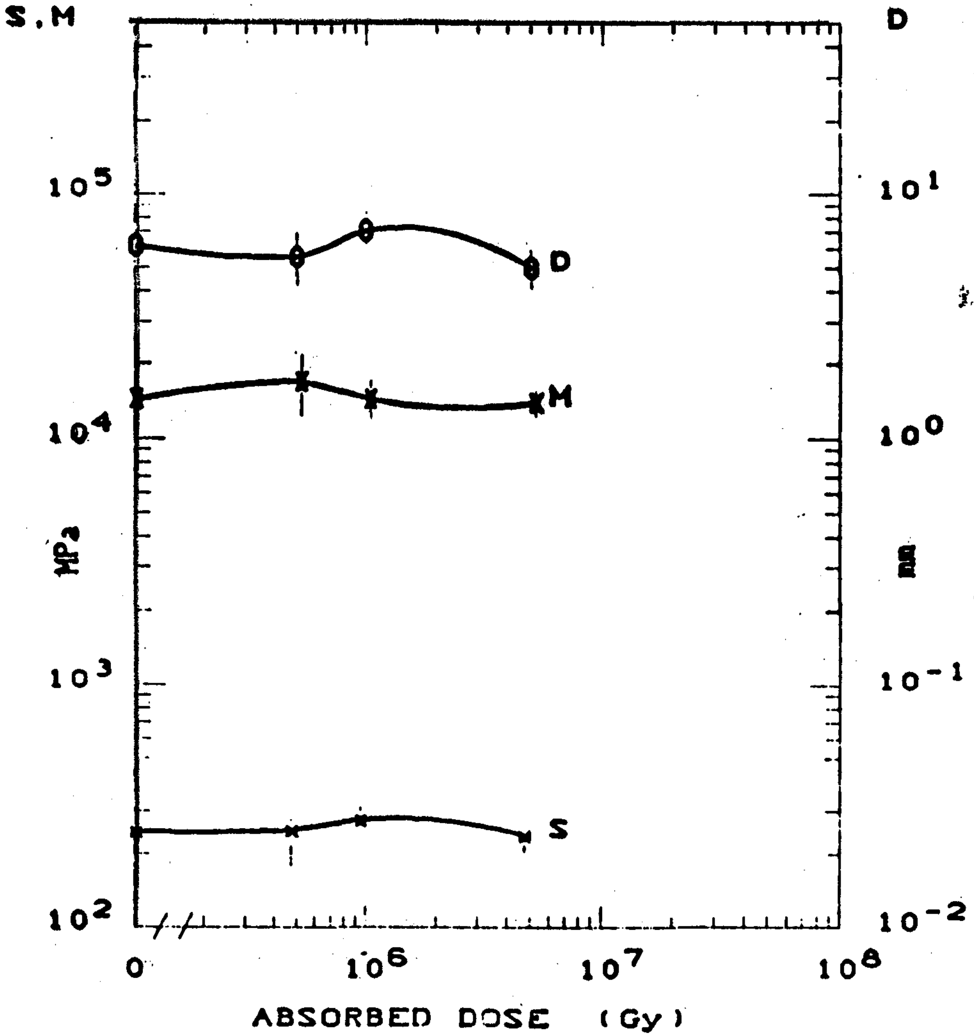

MATERIAL: ARENKA 900

SUPPLIER: ENKA (D)

REMARKS : · ARAMID FIBER +EPIKOTE 215/VERSAMID 140.
ratio 1:1
baking at 150° C, 2 hours

CURVE	PROPERTY	INITIAL VALUE
S	FLEXURAL STRENGTH AT BREAK	248.0 MPa
D	DEFLEXION AT BREAK	6.1 mm
M	MODULUS OF ELASTICITY	14400.0 MPa

Compression wrapping.

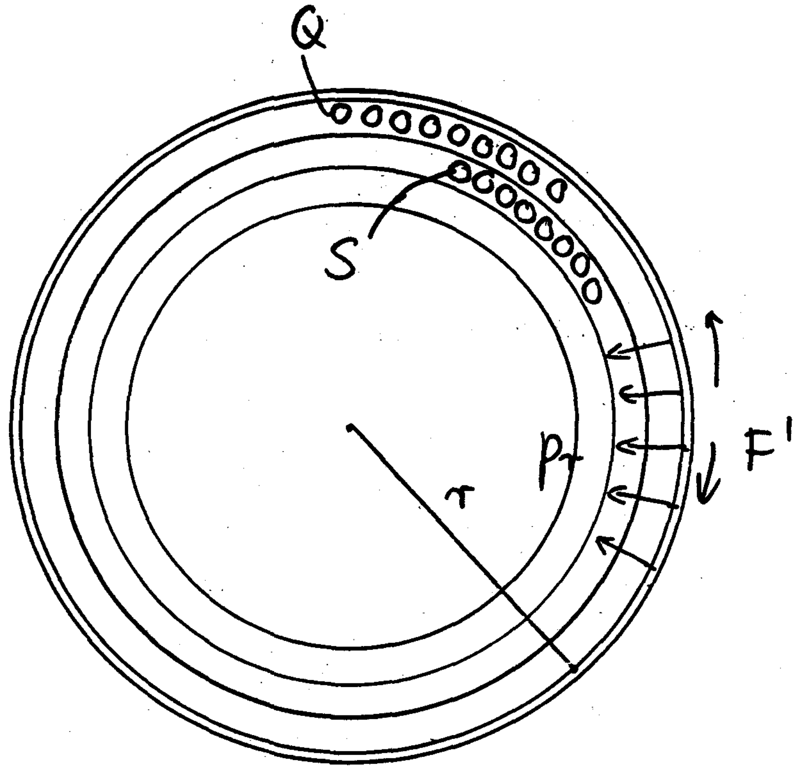

Call F' tangential force in wrapping per unit length of the beam pipe, r its radius

radial pressure $p_r = \frac{F'}{r}$

For the two wrappings after the quad. coil:

$F' \simeq 2 \cdot 250N / 2{,}5 mm = 200 N/mm$

$r \simeq 33 mm \rightarrow p_r \simeq 6 N/mm^2$

Lorentz force on a 1mm long and wide piece of conductor at 5 Tesla, I = 300 A (quench test):

$p_{Lor} \simeq 1.5 N/mm^2$

pressure on the beam pipe has been determined directly by measuring diameter reduction of pipe

2 pipe sections (330 mm long) accurately ground on the inside to a precision of ± 1 μm in diameter.

pipe 1 : wrapped with 3 layers of R glass

diameter reduction Δd:

$\Delta d_{meas} = (30.5 \pm 1)\ \mu m$

$\Delta d_{computed} = 31.7\ \mu m$ (accuracy ~ 5%)

pipe 2 : equipped with insulation, sextupole section, 1 wrapping, quadr., 2 wrappings like original coils

diameter reduction $\Delta d = 25\ \mu m$

There is only very little plastic flow during bakeout.

Stress in beam pipe due to wrappings

$\sigma = 86\ N/mm^2$ room temp.

$\approx 74\ N/mm^2$ L He "

p_r (quad) $= 4.2\ N/mm^2$ L He

p_r (sext) $= 6.4\ N/mm^2$ "

Stress-strain relation of aramid fibers

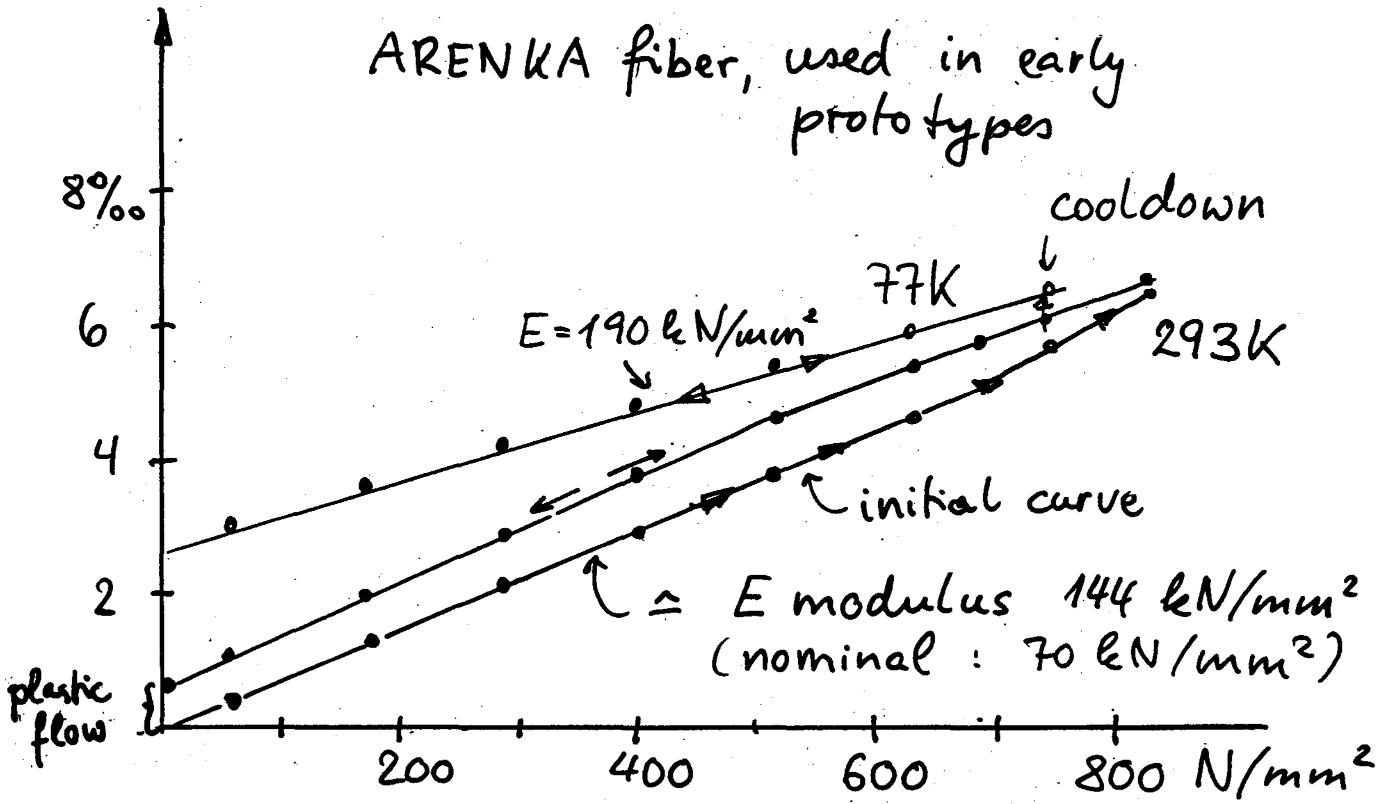

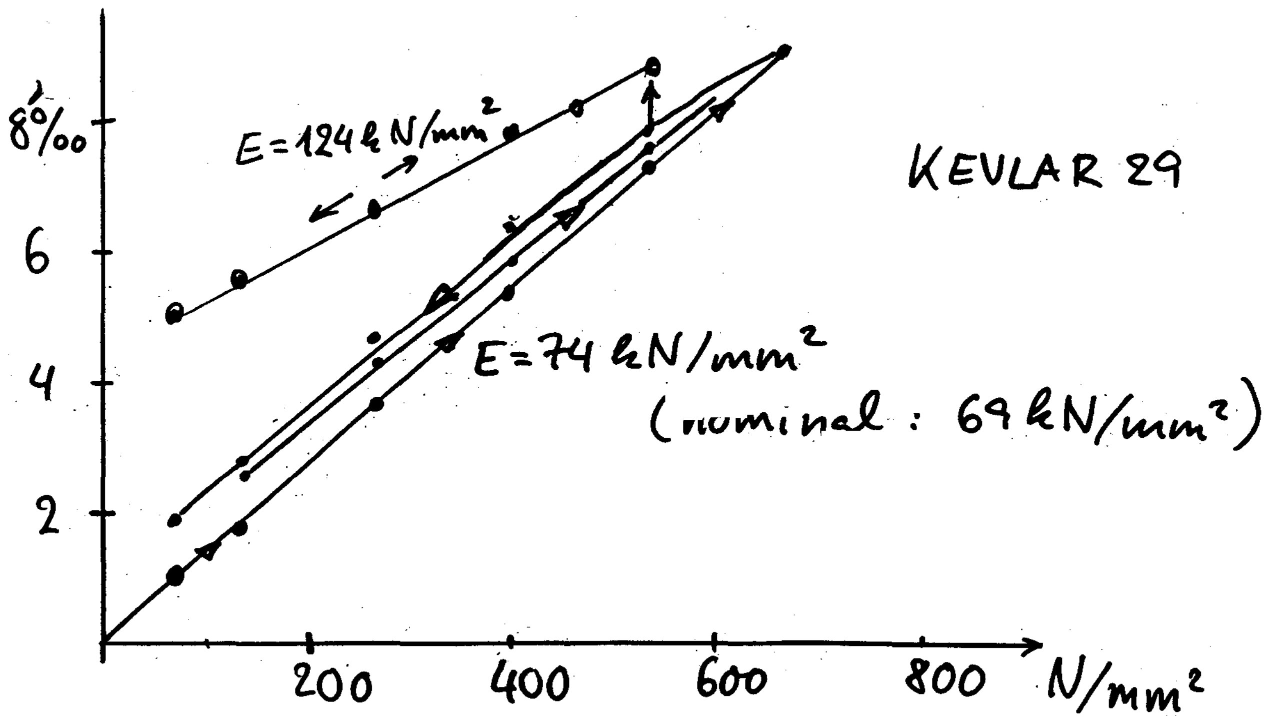

R glass (VETROTEX)

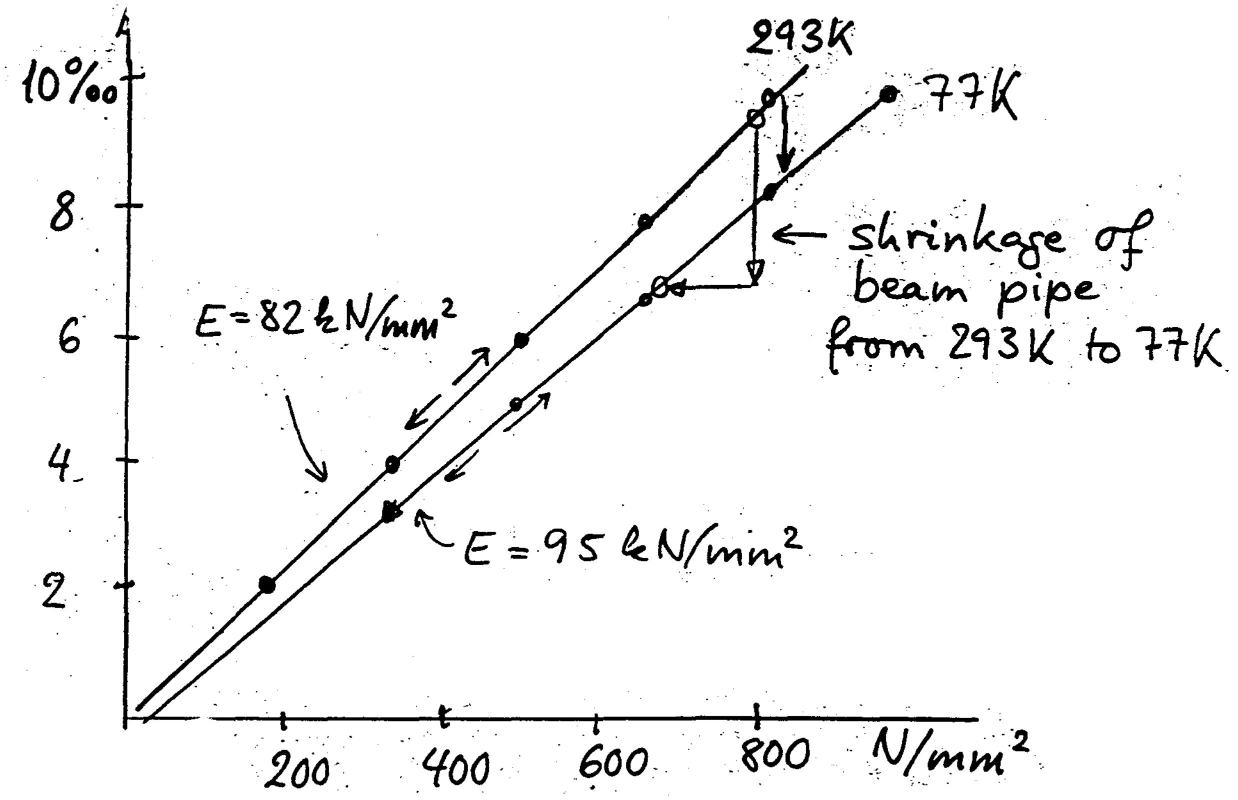

aramid fiber: plastic flow
elongation at cool down
more than 80% of tension lost
only advantage: easy to apply

R glass fiber: stronger than aramid (3600 N/mm² vs 2700 ")
no plastic flow
shrinks during cooldown
only about 15% of tension lost
disadvantage: preimpregnated fiber needed.

fiber mounted with ~ 800 N/mm² in stainless steel tube
after cooldown to 77K:
aramid: rather loose (~ 10% of 800 N/mm²) R glass: ~ 85% of 800 N/mm²

Production of Correction coils.

joint development of methods and tooling by DESY and HOLEC
4 early prototype and 6 "development" coils built under DESY order

20 "preseries" coils built Sept., Oct. 86

Series production started in Nov. 86
rate now ~8 coils per week

Quality control at HOLEC:
measurement of mechanical dimensions
high voltage test (2500 V dc)
measurement of field harmonics at room temperature
DESY: quench test in external field of 5.08 T
check of important dimensions, quality of workmanship.

Field measurement,
2.05 m long radial pickup coil, used in 3 longitudinal positions.
Quad. or sext. excited by 11 Hz current, 0.7A
Induced signal amplified via lock-in technique
Fourier analysis on personal computer

Measured multipole coefficients for 134 corr. coils

quadrupole: $b_{10}/b_2 = -2.41 \cdot 10^{-2}$ expected
$(-2.35 \pm 0.08) \cdot 10^{-2}$ meas.

$b_{14}/b_2 = 6.3 \cdot 10^{-3}$ exp.
$(6.1 \pm 0.5) \cdot 10^{-3}$ meas.

sextupole: $b_{15}/b_3 = -1.48 \cdot 10^{-2}$ exp.
$(-1.37 \pm 0.08) \cdot 10^{-2}$ meas.

$$\Delta b_n = (b_n)_{meas.} - (b_n)_{exp.}$$

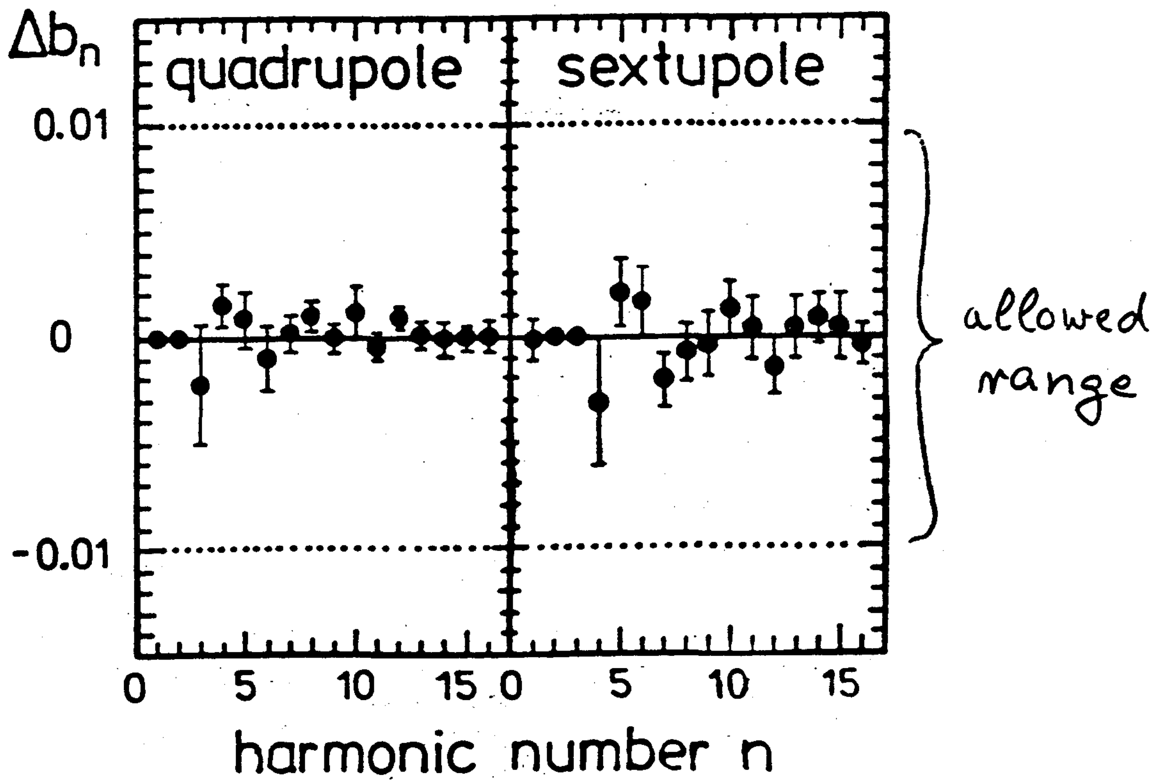

misalignment angle quad vs. sext.:
specified $2 \cdot 0.2° = 7$ mrad
measured 1.42 ± 2.59 mrad

Conclusion: field quality much better than specified.

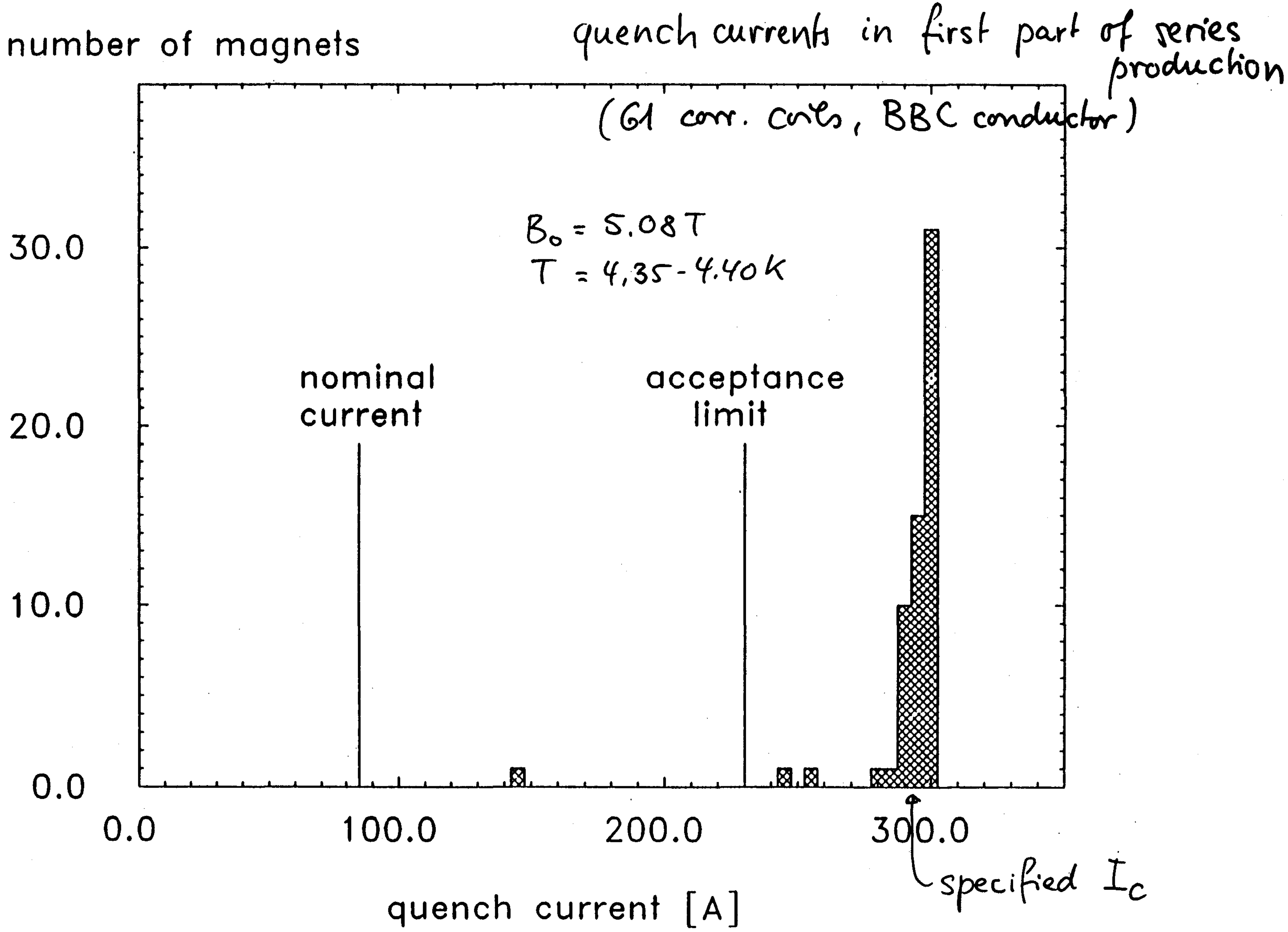

number of magnets
quench currents in first part of series production
(61 corr. coils, BBC conductor)
B_0 = 5.08 T
T = 4,35 - 4.40 K
nominal current
acceptance limit
30.0
20.0
10.0
0.0
0.0
100.0
200.0
300.0
specified I_c
quench current [A]

I-26

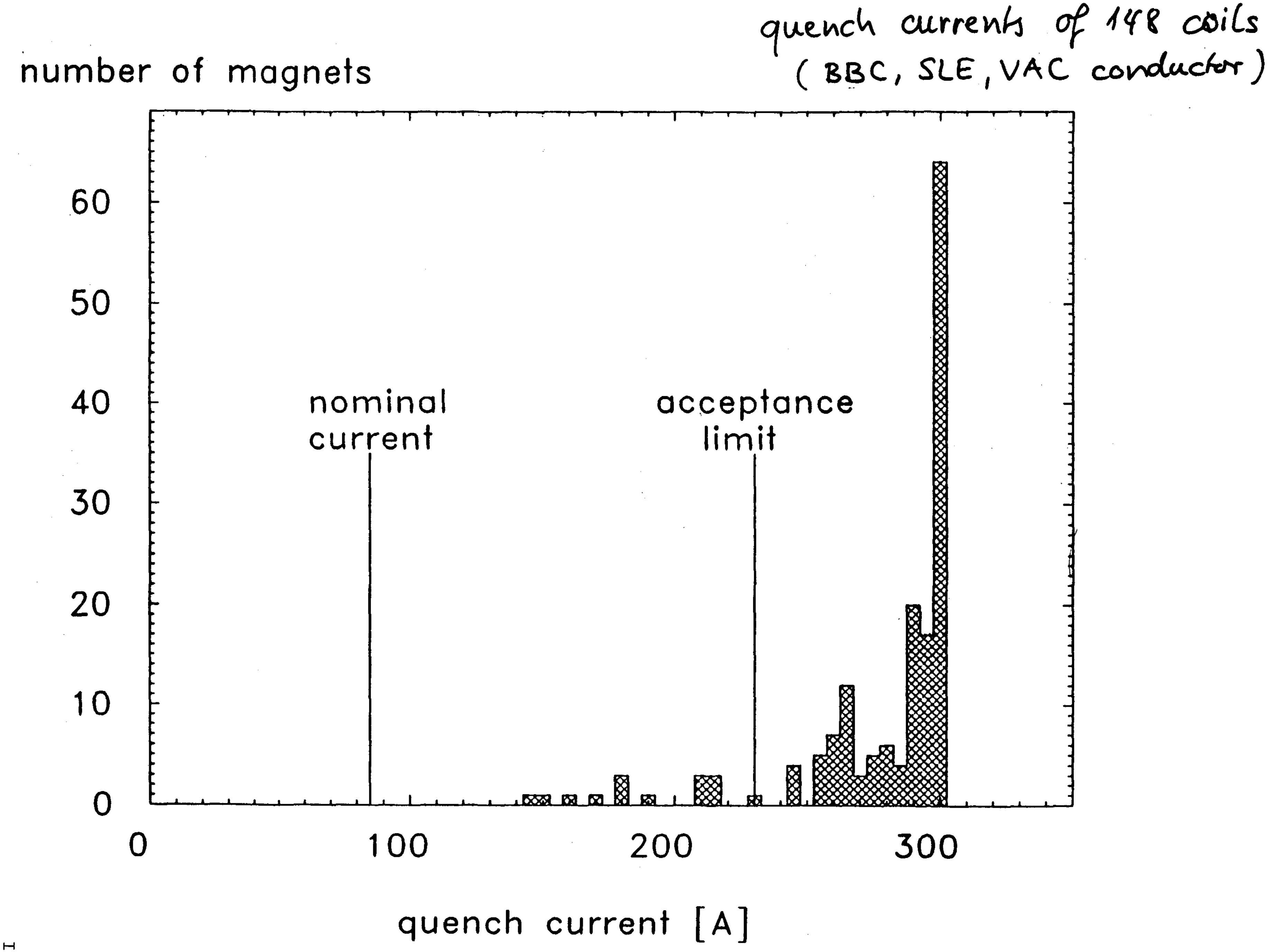

quench currents of 148 coils
(BBC, SLE, VAC conductor)
number of magnets
60
50
40
30
20
10
0
nominal current
acceptance limit
0
100
200
300
quench current [A]

Training behaviour

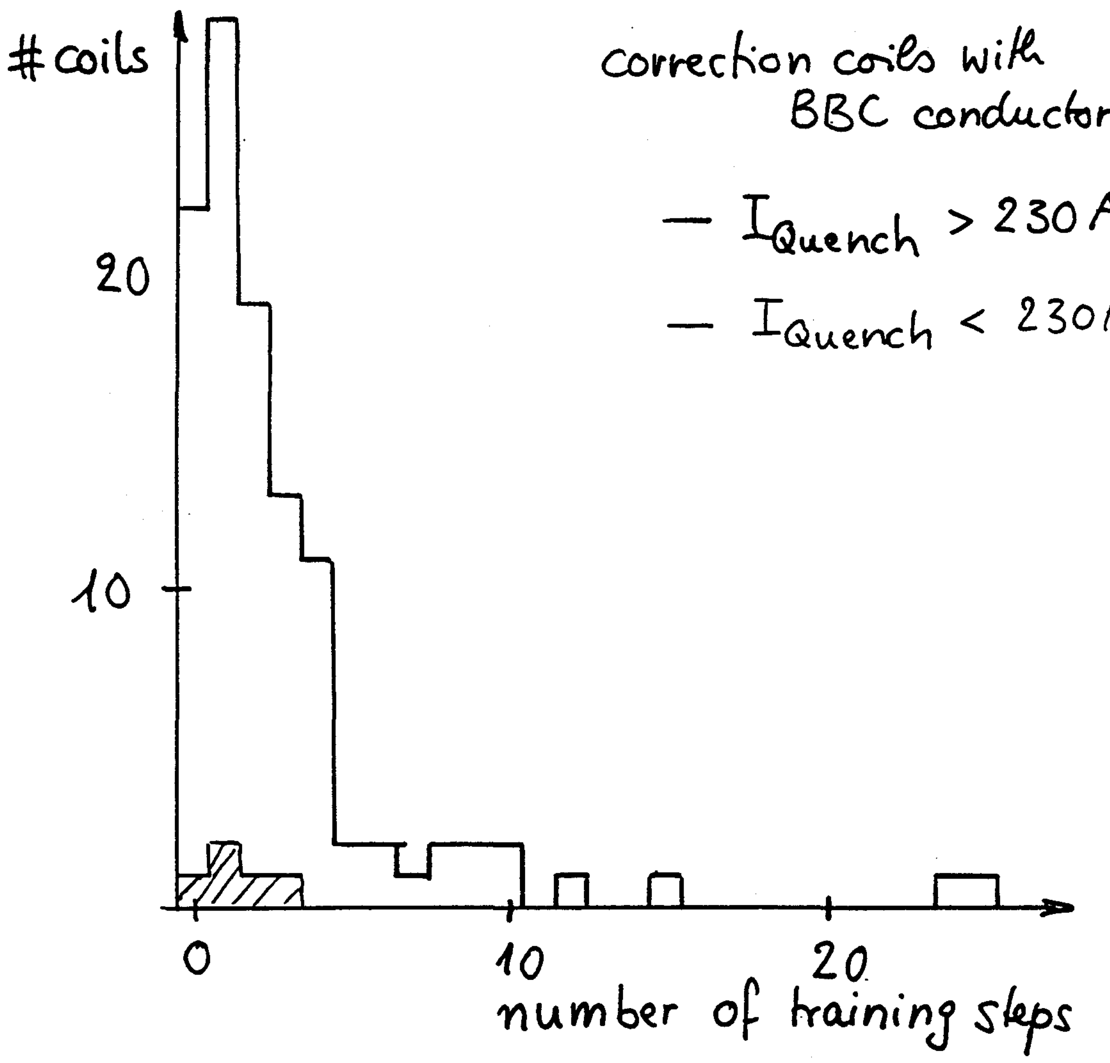

Conclusion: low performance not caused by conductor motion

One coil with many training steps was tested a second time: no further training.

One development coil was tested one year later: no training, $I_{quench} \approx I_c$
$\Rightarrow$ no fatique in wrapping and glue joints

Simultaneous excitation of quadrupole and sextupole coils.

All coils from the series production can be excited to the minimum I_{quench} of sext. or quad. when connected in series.
In most cases $I_{series} \approx I_{critical}$.

Different for early prototype coil with aramid fiber compression wrapping

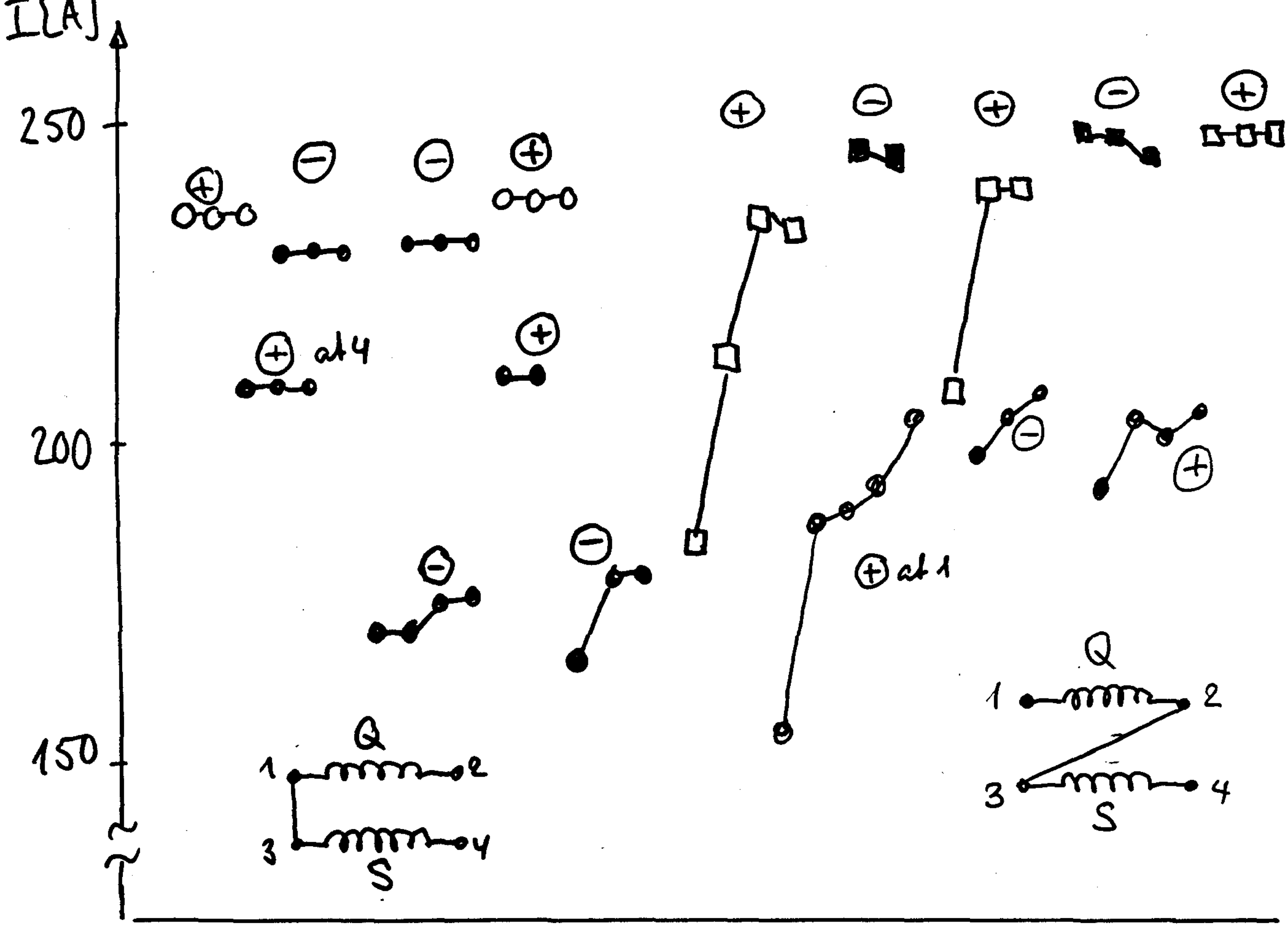

Test in field of 4.35 Tesla, T= 4.35 K
Conductor of lower I_c.

Deformation of beam pipe due to Lorentz forces

$B_0 = 4.5\,T$, $I_{sext} = 65A$, $I_{quad} = 85$

wall thickness of pipe 2mm

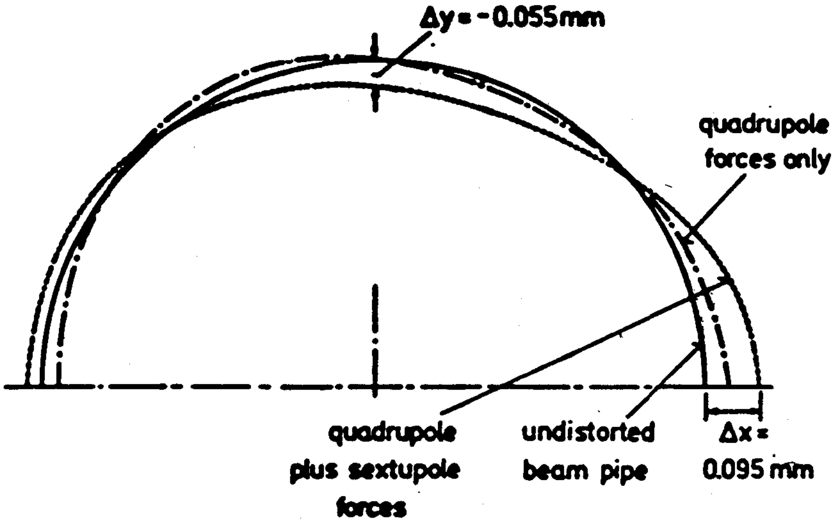

Fig. 11 - Distortion of the beam pipe caused by the magnetic forces.

max. stress in stainless steel 110 N/mm²

Now wall thickness 2.5mm

$\Rightarrow \left(\frac{2.5}{2}\right)^3 = 1.95$ times stiffer

820 GeV : $\Delta x_{max} \approx 0.05$ mm

$\sigma_{max} \simeq 75\,N/mm^2$

Quench of main dipole: induced voltages in correction coils

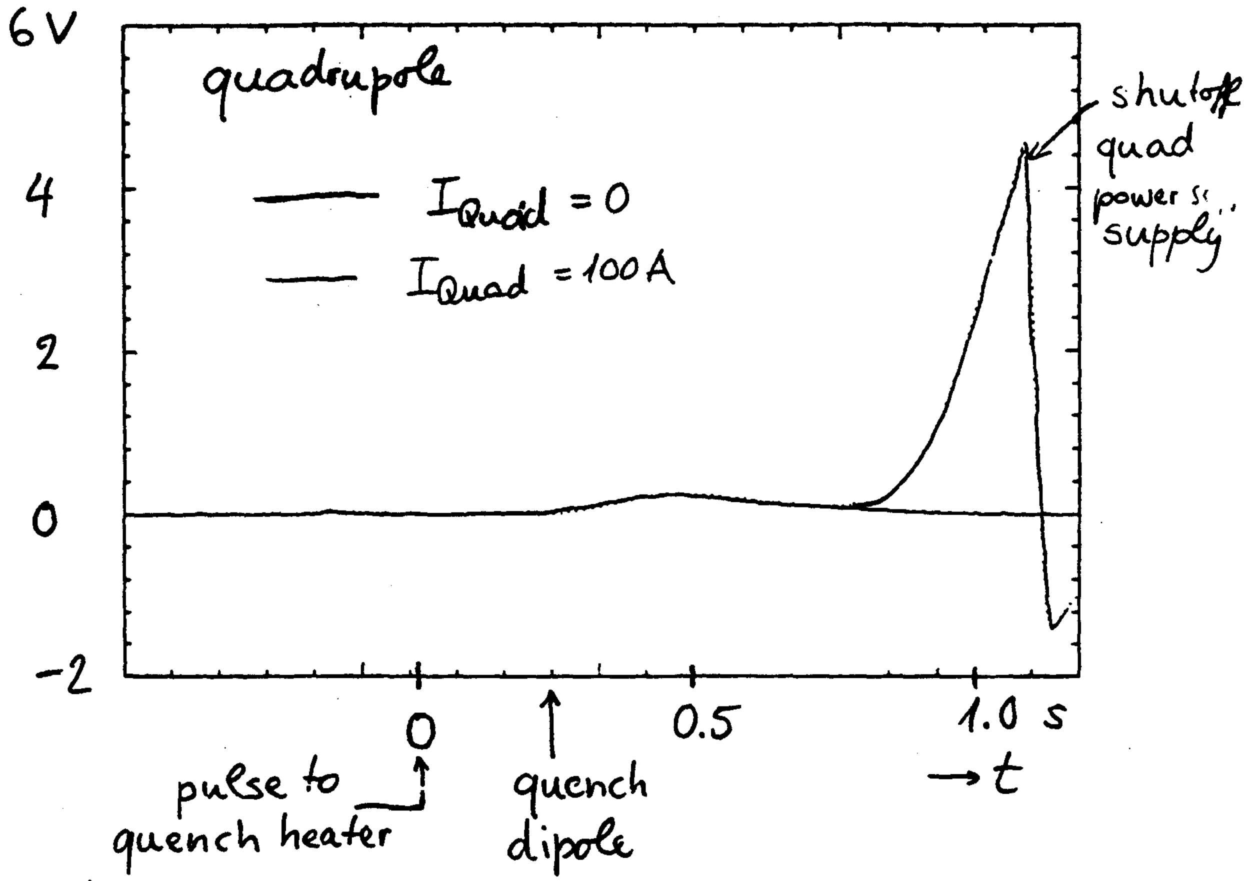

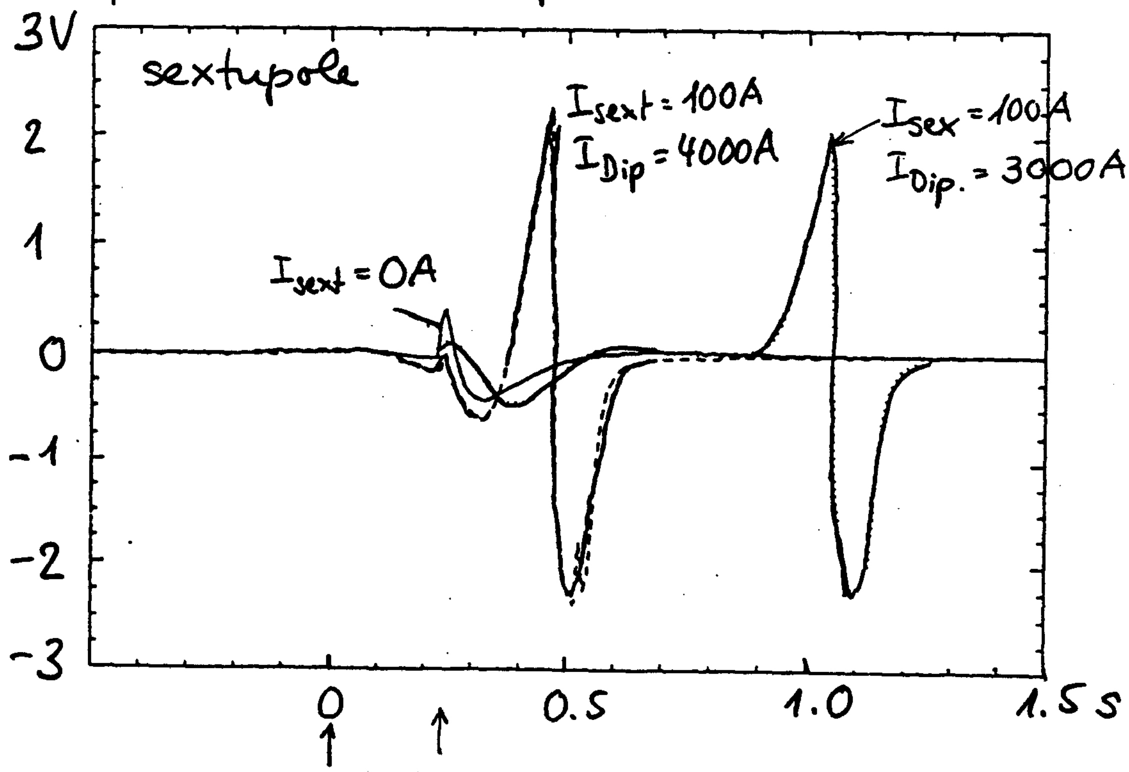

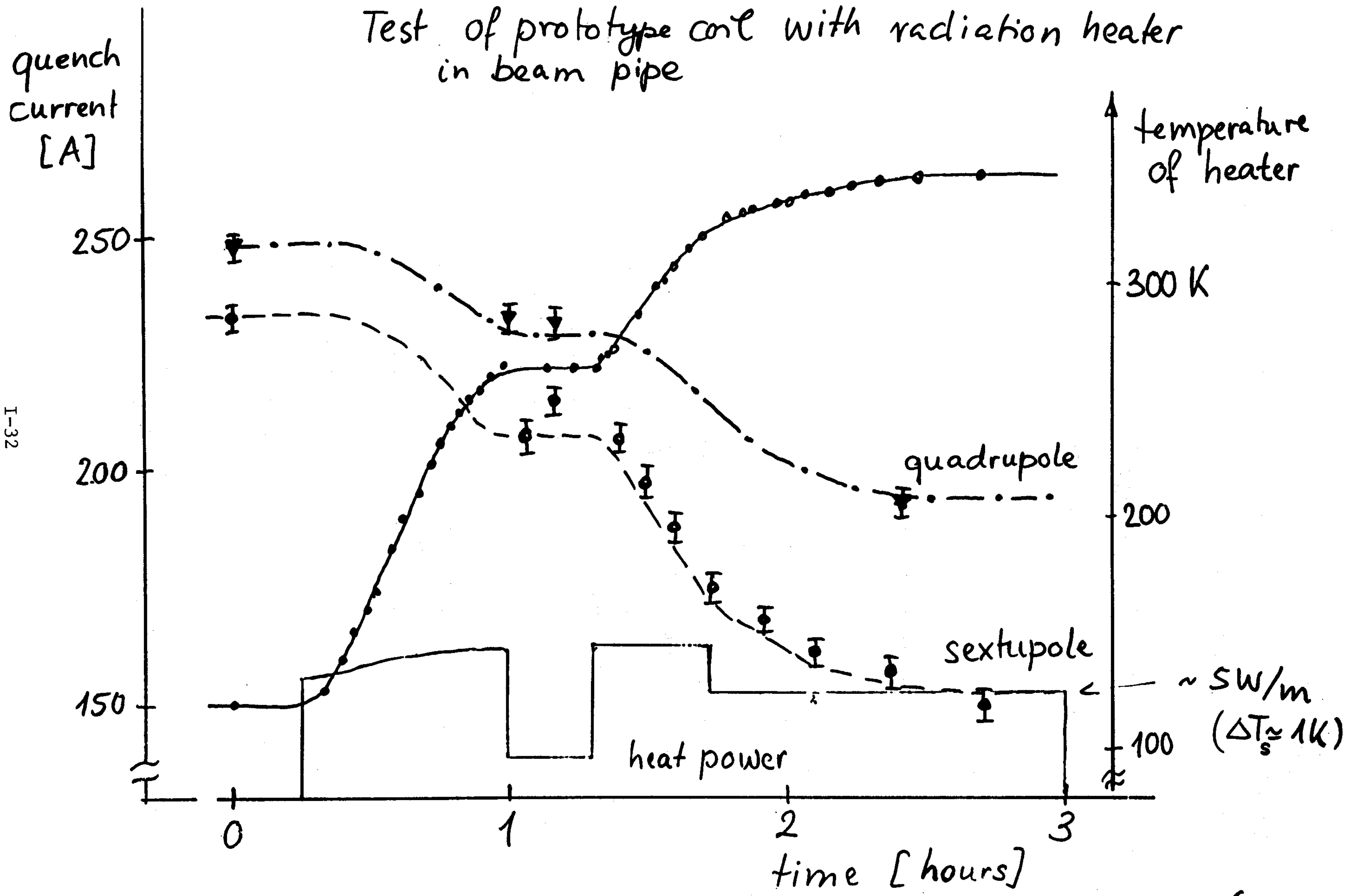

image currents : < 0.05W/m for copper plated pipe (Trines)

Angular alignment of SQ coil in dipole.

Methode:

excite main dipole with ac current (500 Hz)
compare induced signals in subcoils SI, SIII

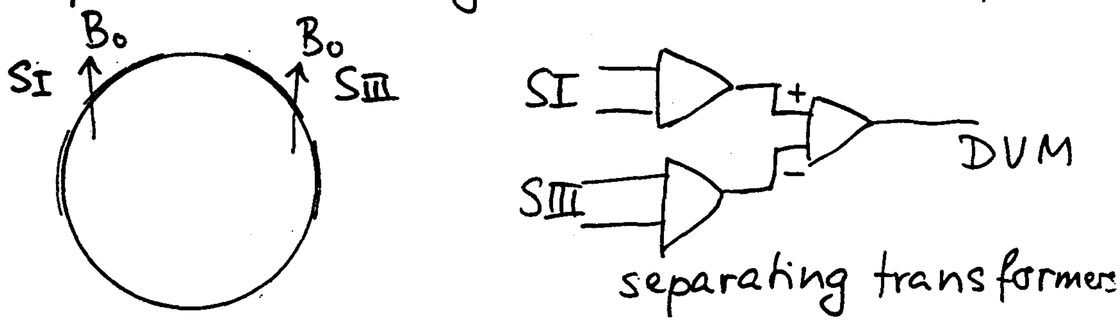

beam pipe rotated by precision screws with measuring devices on both ends to reduce twist in pipe.

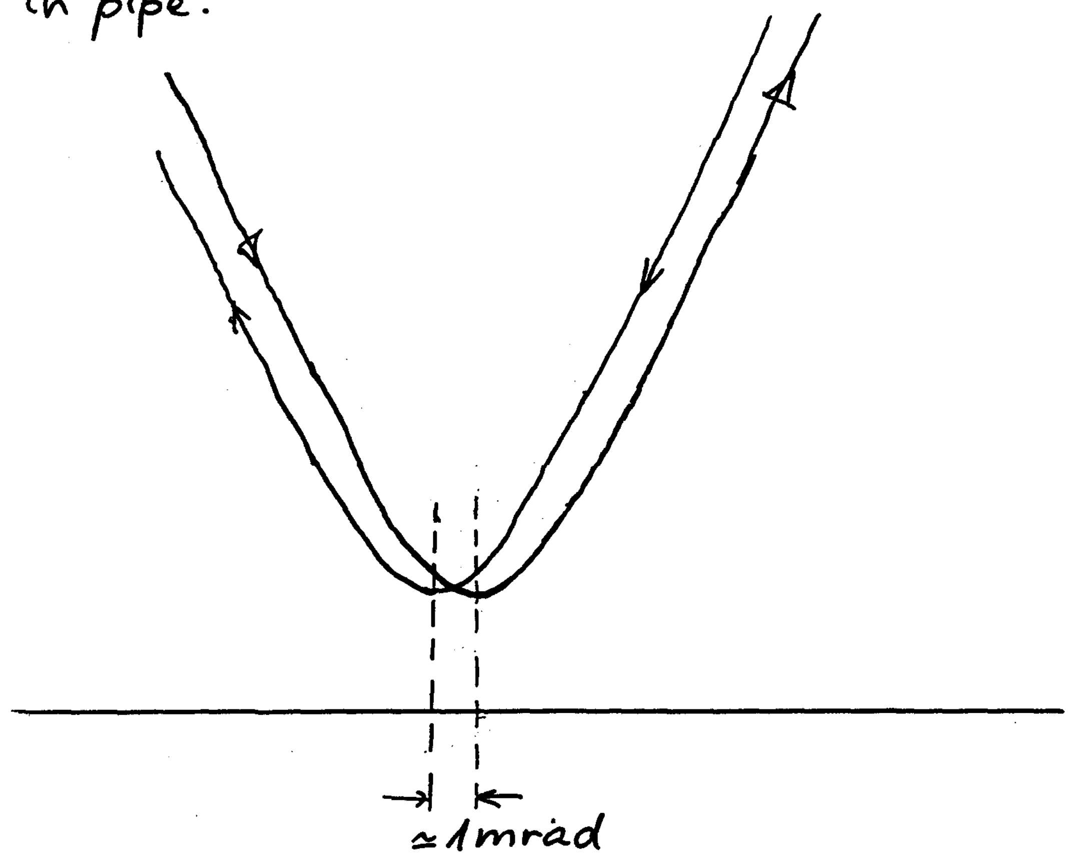

alignment accurate to about 1 mrad
well below allowed limit.

Measurement on coil B38
sext. good, quad. low

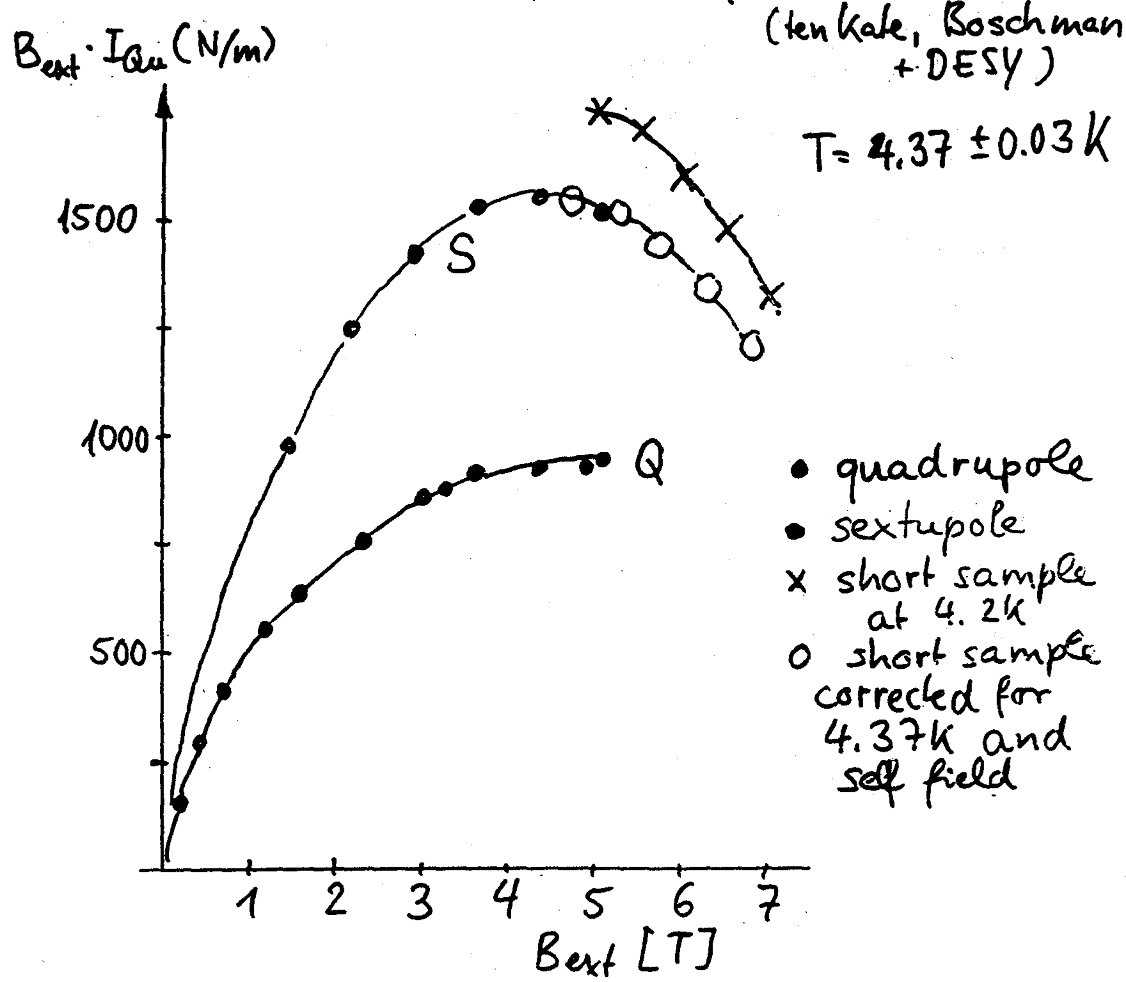

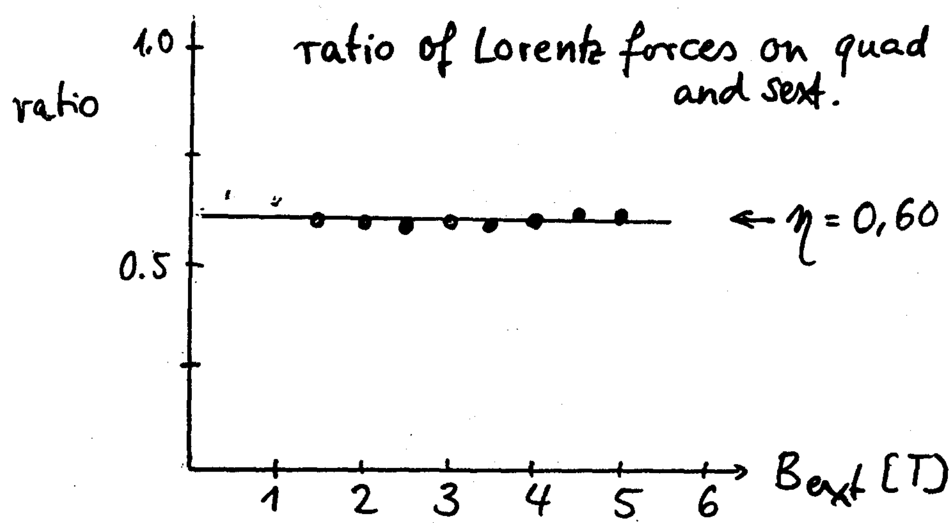

Conclusions: sext. reaches short sample I_c;
quad has bad spot with $\eta = 0.60$

APPENDIX J

"Radiation Damage to Organic Materials,"

Talk by Roger Clough

RADIATION RESISTANT POLYMERS

R. L. Clough

Sandia National Laboratories
Albuquerque, New Mexico 87185

For Publication in John Wiley & Sons
Encyclopedia of Polymer Science and Engineering

RADIATION DAMAGE TO ORGANIC MATERIALS

Degradation Mechanisms and Degradation Behaviors

Influence of Environmental Factors [O_2, dose rate, ...]

Accelerated Aging Methodologies for Predicting Long-Term Degradation Rates

Inherent Radiation Stability of Different Polymer Types

Approaches To Stabilizing Polymers Against Radiation

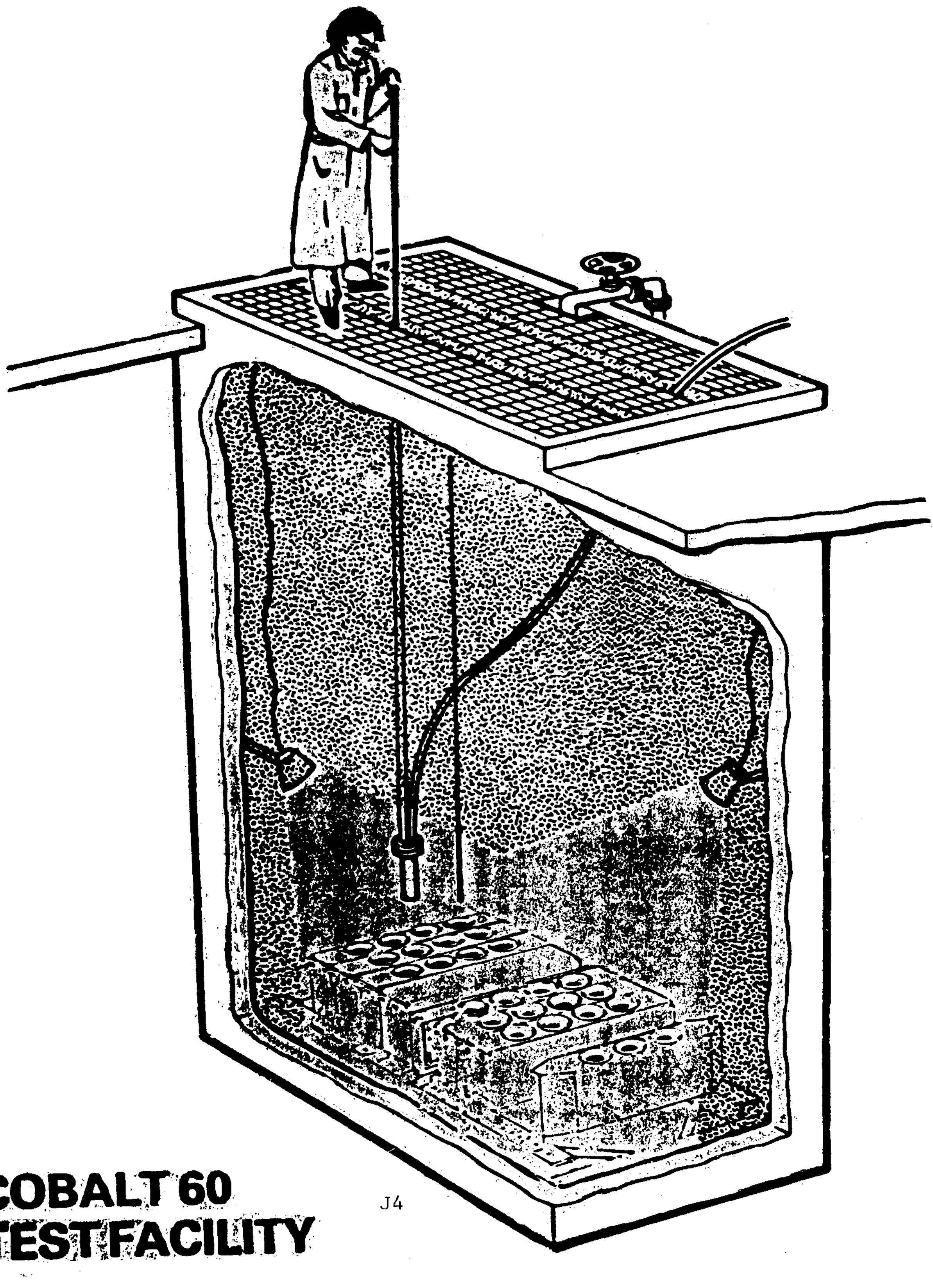

COBALT 60 TEST FACILITY

J4

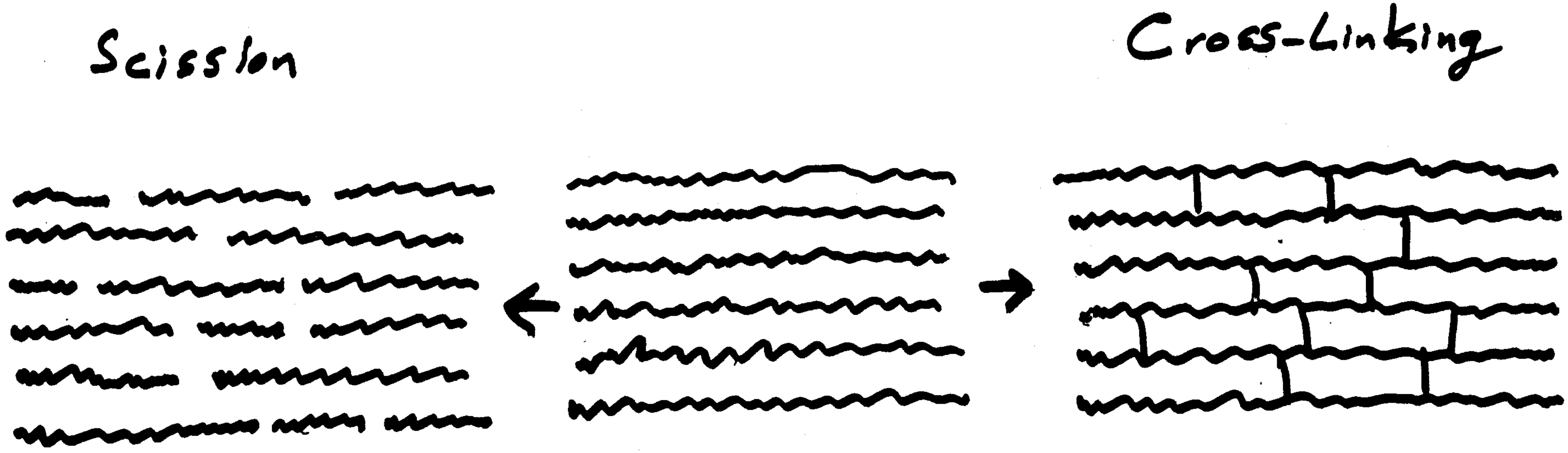
Scission
Cross-Linking

TABLE 1.

CLASSIFICATION OF POLYMERS ACCORDING TO THEIR PREDOMINANT DEGRADATION MODE WHEN IRRADIATED UNDER INERT ATMOSPHERE CONDITIONS

Polymers Which Undergo Primarily Chain Scission	Polymers Which Undergo Primarily Crosslinking
polyisobutalene	polyethylene
poly-α-methylstyrene	polypropylene
polyvinylidenechloride	polystyrene
polyvinylfluoride	poly(vinylchloride)
polytrichlorofluoroethylene	poly(vinyl alcohol)
polytetrafluoroethylene	polyacrylonitrile
polyvinylformal	polybutadiene
polyvinylbutyral	polychloroprene
polymethylmethacrylate	poly(styrene-co-acrylonitrile)
polymethacrylamide	poly(styrene-co-butadiene)
polyoxymethylene	poly(butadiene-co-acrylonitrile)
poly(propylene sulfide)	natural rubber
poly(ethylene sulfide)	chlorinated polyethylene
cellulose	chlorosulfinated polyethylene
polyalanine	polyamides
polylysine	polyesters
DNA	polyurethanes
	polysulfones
	polyacrylates
	polyacrylamides
	polydimethylsiloxane
	polymethylphenyl siloxane
	phenol-formaldehyde
	urea-formaldehyde
	melamine-formaldehyde

J7

RADIATION - ELEVATED TEMPERATURE DEGRADATION OF PVC
IN AIR AND UNDER N_2

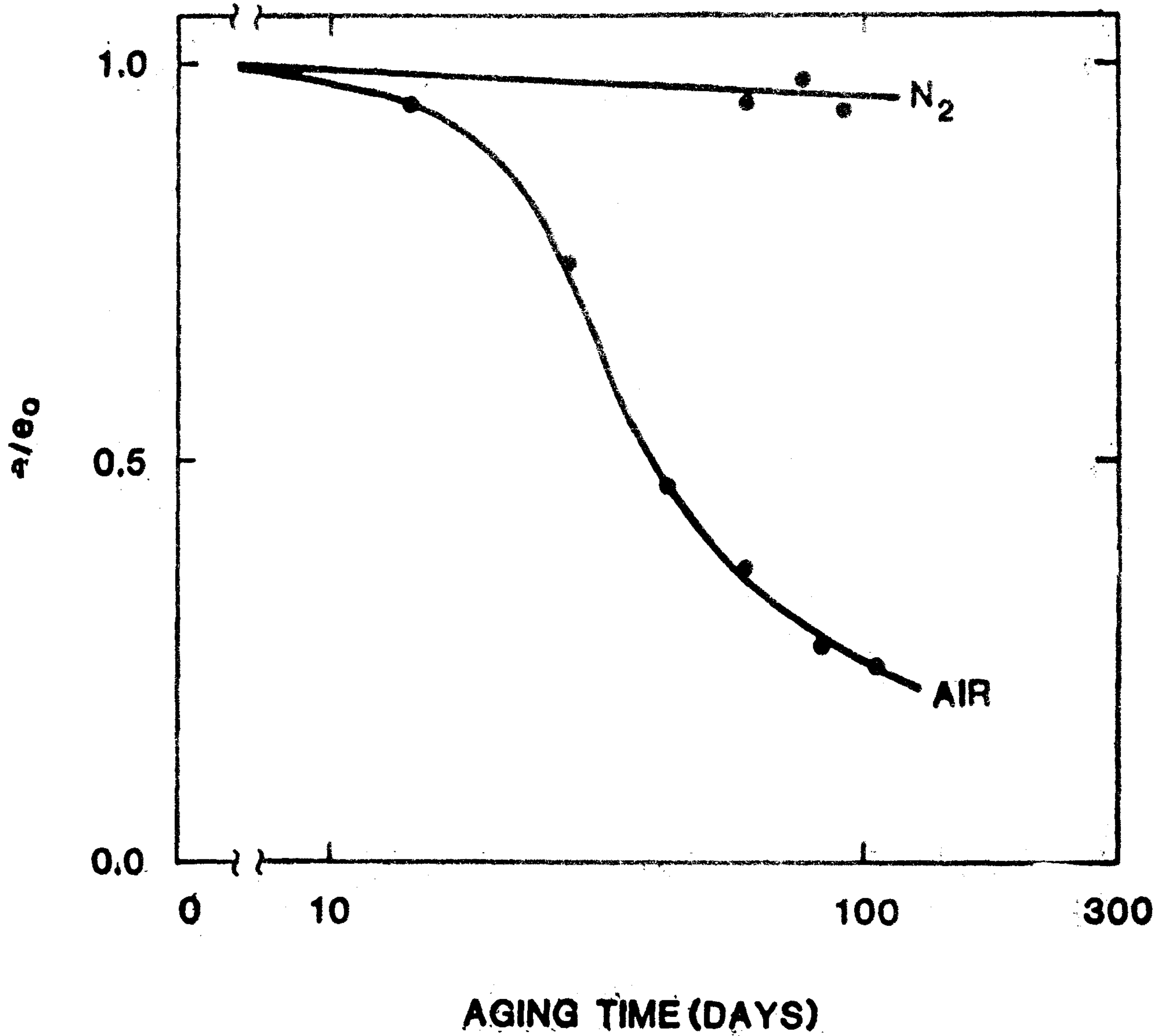

DOSE RATE EFFECTS IN POLYVINYL CHLORIDE DEGRADATION

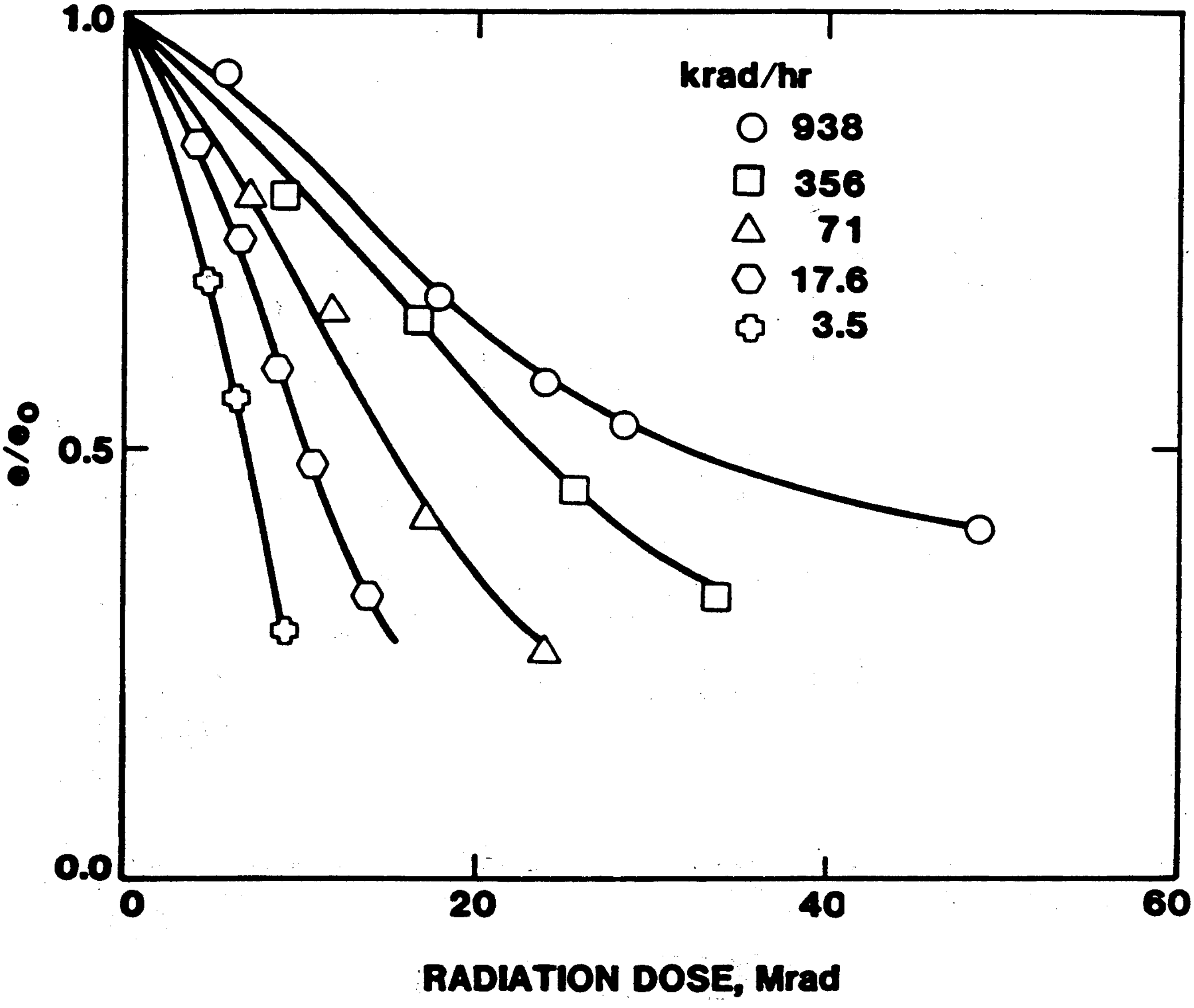

RADIATION SENSITIZATION OF POLYETHYLENE TO THERMAL DEGRADATION

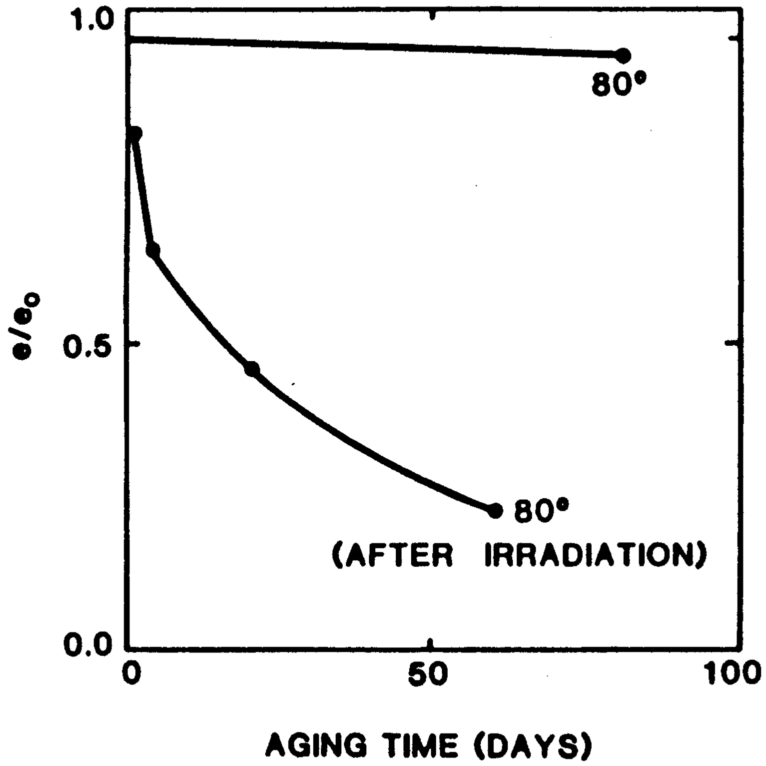

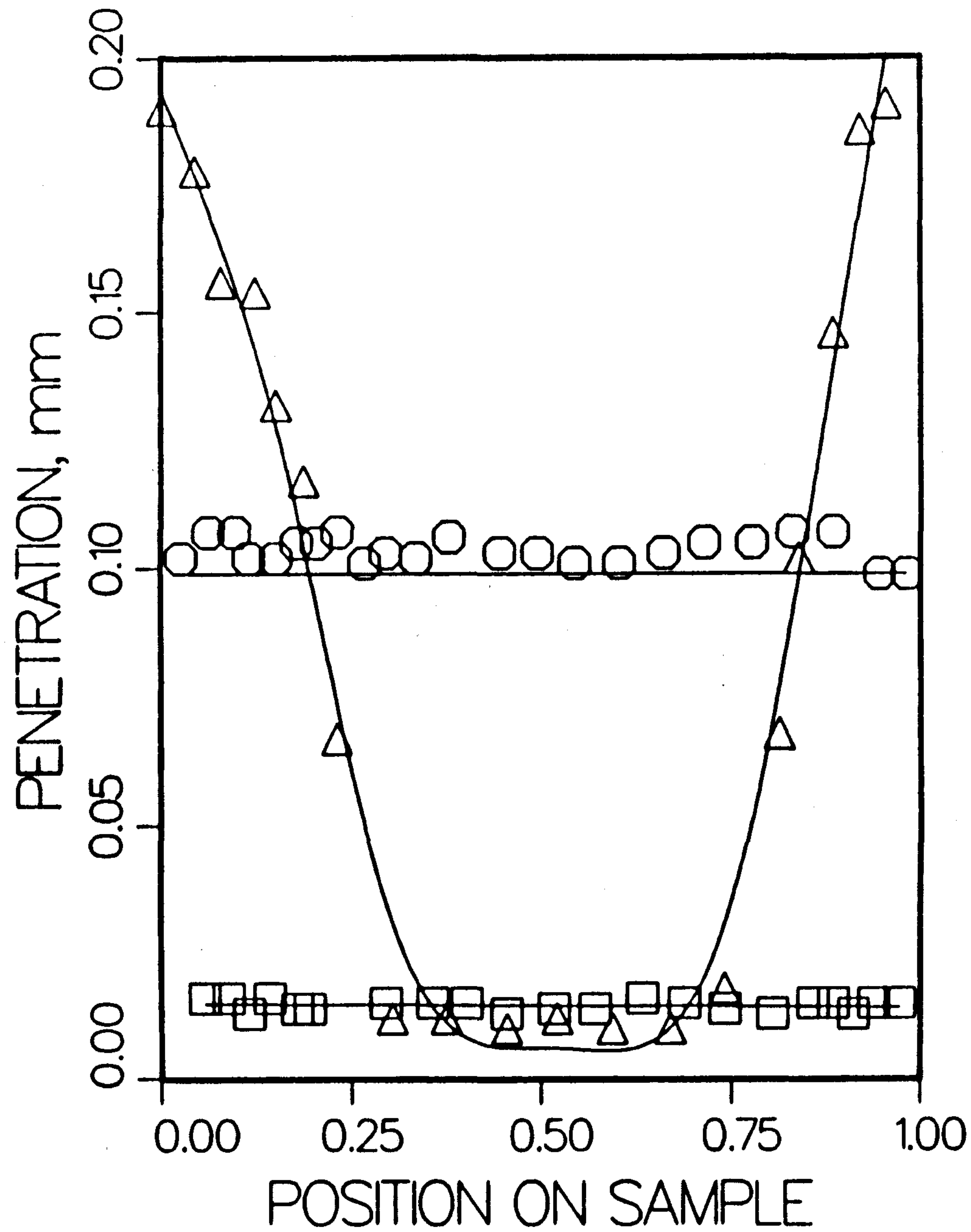
PENETRATION, mm
0.00
0.05
0.10
0.15
0.20
0.00
0.25
0.50
0.75
1.00
POSITION ON SAMPLE

J10

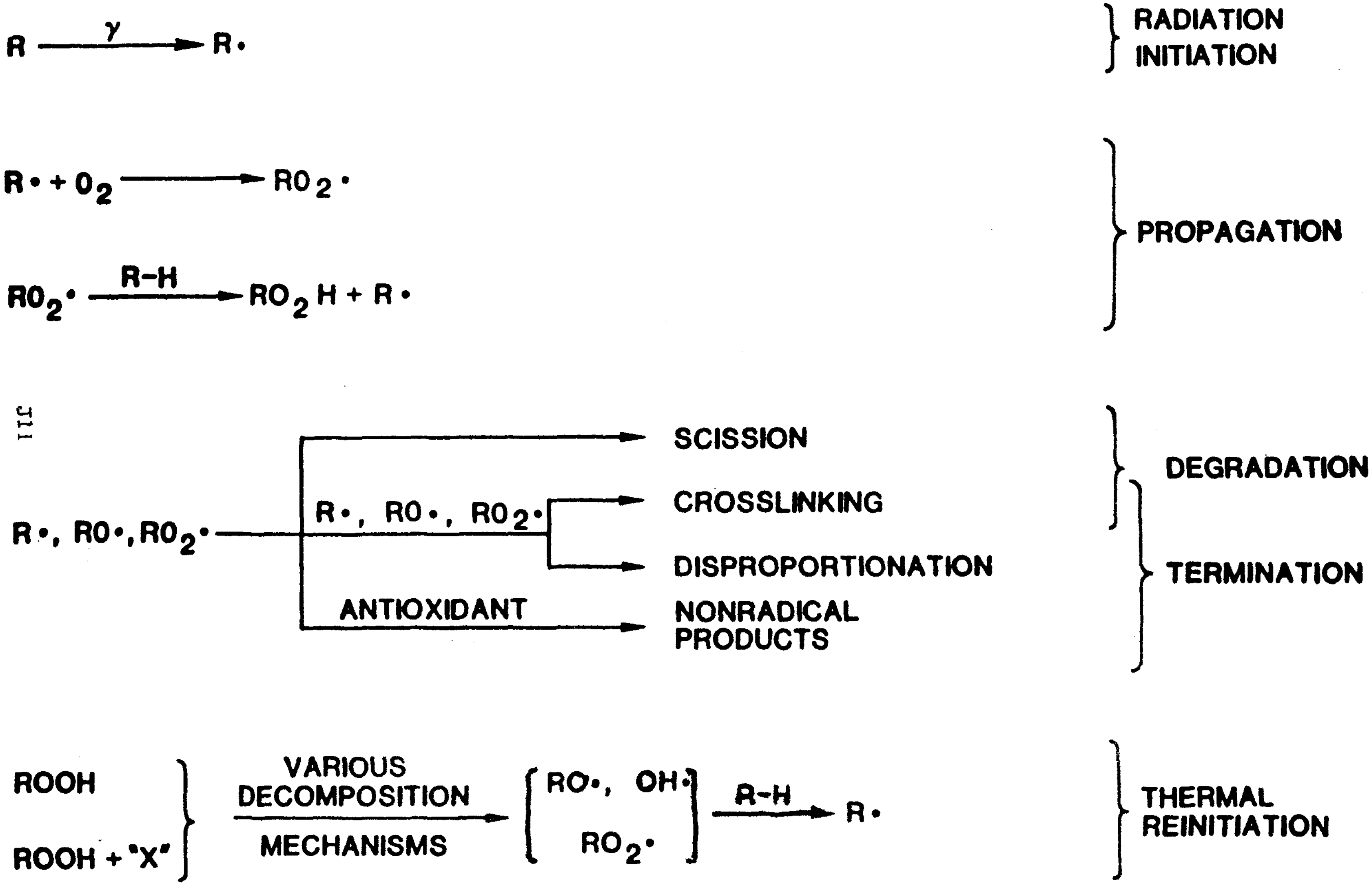

R → R· (γ)
RADIATION INITIATION
R· + O2 → RO2·
RO2· → RO2H + R· (R-H)
PROPAGATION
R·, RO·, RO2·
SCISSION
R·, RO·, RO2·
CROSSLINKING
DISPROPORTIONATION
ANTIOXIDANT
NONRADICAL PRODUCTS
DEGRADATION
TERMINATION
ROOH
ROOH + "X"
VARIOUS DECOMPOSITION MECHANISMS
RO·, OH·
RO2·
R-H
R·
THERMAL REINITIATION

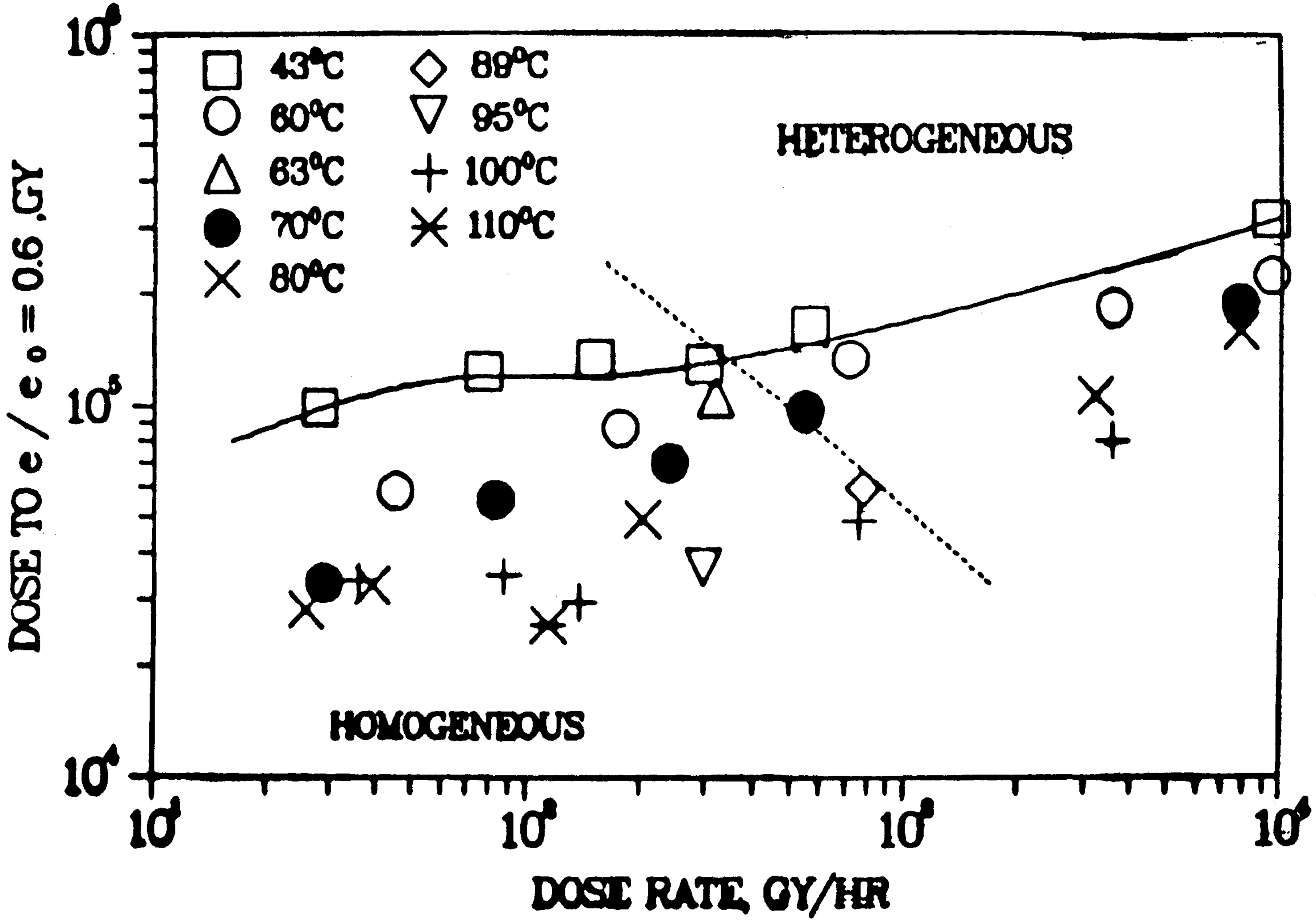

43°C
60°C
63°C
70°C
80°C
89°C
95°C
100°C
110°C
HETEROGENEOUS
HOMOGENEOUS
DOSE TO e / e o = 0.6, GY
DOSE RATE, GY/HR
10^6
10^5
10^4
10^1
10^2
10^3
10^4

SHIFTED PVC DATA FITTED TO MODEL

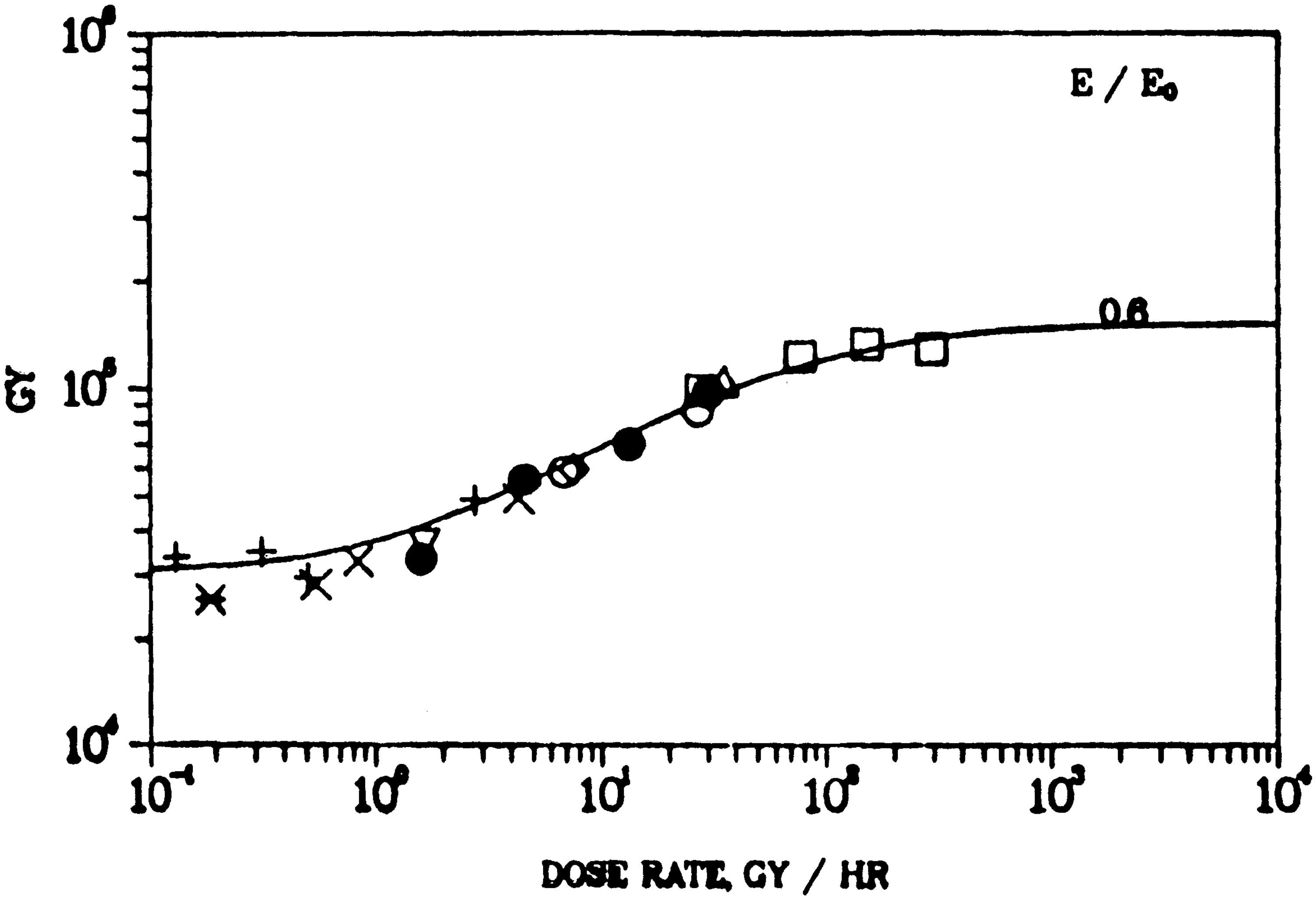

from: R. L. Clough and K. T. Gillen, "Gamma-Radiation Induced Oxidation and Mechanisms of Its Inhibition," in P. Klemchuk and J. Pospisil, eds., Oxidation Inhibition In Organic Materials, CRC Press, 1988.

TABLE IV

RELATIVE RADIATION STABILITIES* OF POLYMERS, UNDER TWO DIFFERENT SETS OF CONDITIONS, AS INDICATED BY THE DOSE (in rads) REQUIRED TO REDUCE MECHANICAL PROPERTIES TO 50% OF THEIR ORIGINAL VALUE.**

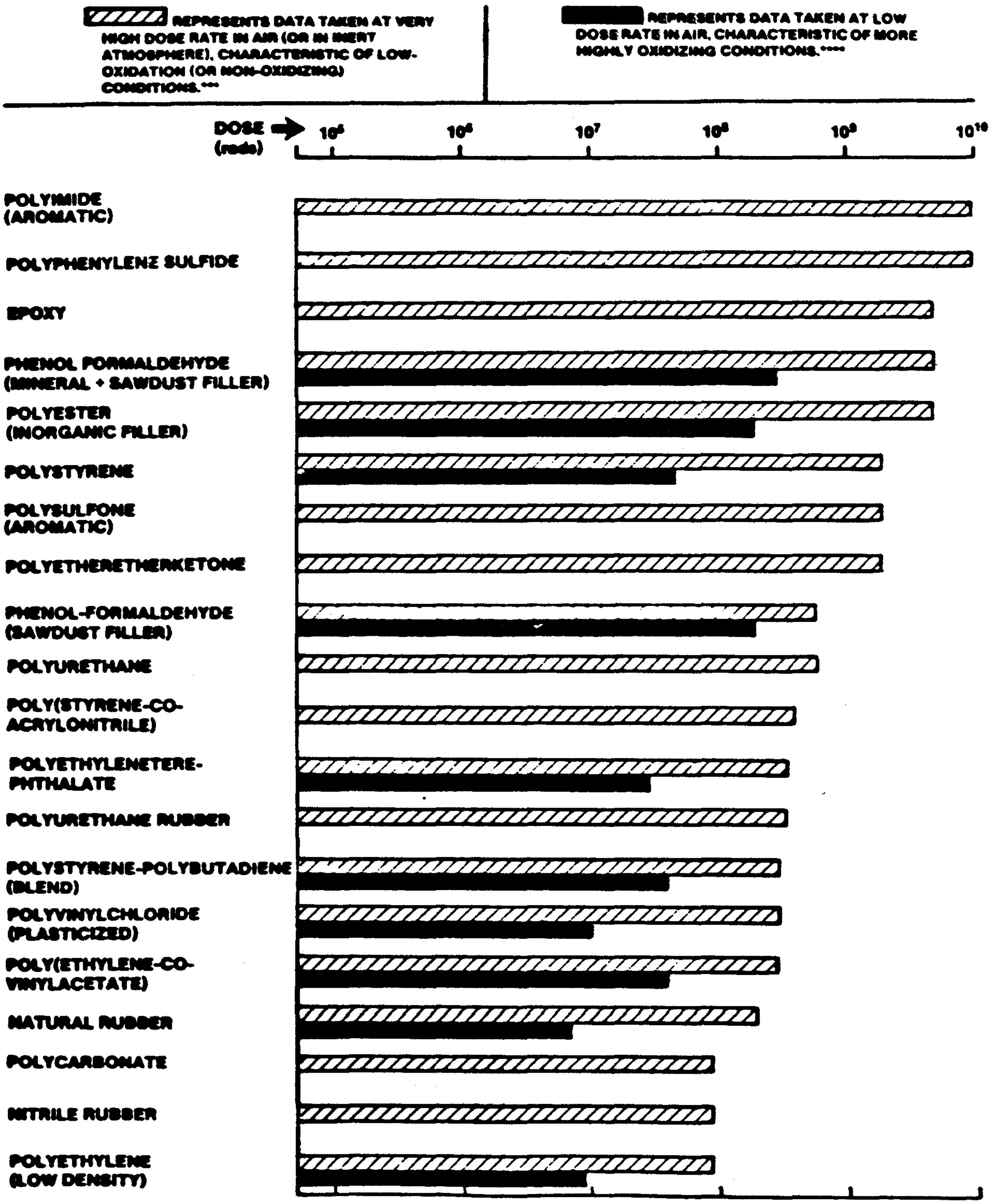

TABLE IV (continued)

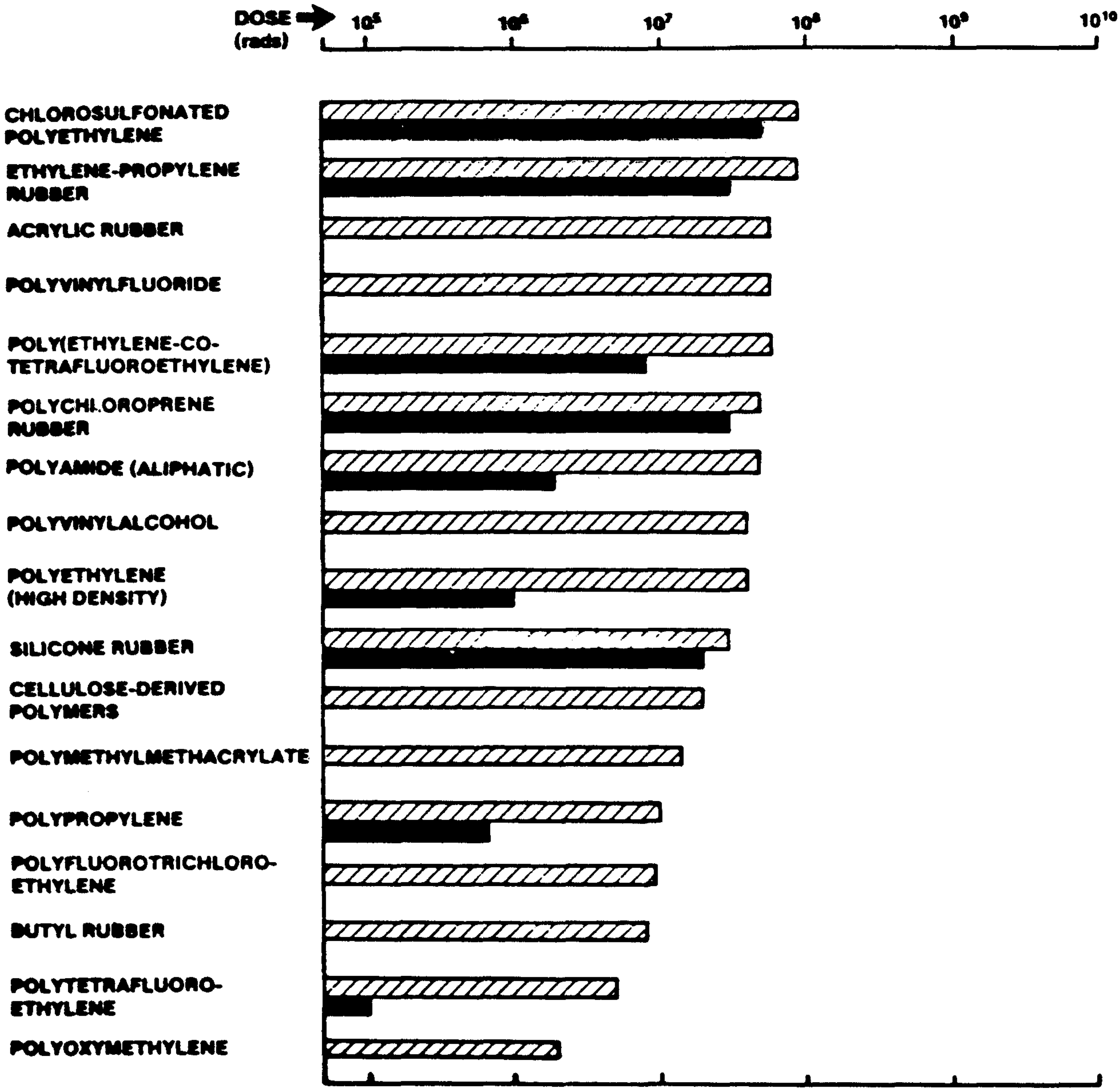

* This table is intended as a rough guide, to be used as an aid in selection of materials for further testing. The data were taken from numerous literature sources, and represent approximate radiation tolerances of individual polymeric materials under two specific environmental conditions. As discussed in the text, other factors not taken into account in the data will have a major influence on radiation resistance due to differing oxidation effects. These factors include: other dose rates, temperature, post-irradiation time, formulation and sample thickness.

** In most cases, the mechanical property considered was tensile elongation at break. Where elongation data were unavailable, some other important mechanical property, such as bend strength, was considered.

*** Data were taken at a variety of high dose rates, primarily in the range of 10^6 - 10^7 rads/h or above.

**** Data were taken within or near the dose rate range of 5×10^2 - 5×10^3 rad/h, in air. Sample thicknesses were primarily in the range of 0.4 - 1.5 mm. Samples were irradiated at or somewhat above room temperature. Mechanical properties were measured shortly after the irradiation was completed.

TABLE 5.

Dose Required to Reduce Tensile Elongation to Half the Initial Value, for Polyethlene Containing Various Stabilizers at a Concentration of 0.25%* (Ref. 87)

Stabilizer	Dose (Gy, x 10³)
Nothing	6
2-Mercaptobenimidazole	6
Trilaurylphosphite	6
Ionox 330**	8
2-Mercaptobenzothiazole	13
N,N'-Di-(β-Naphthyl-p-phenylenediamine) (DPPD)	15
Santonox R**	23
Santowhite Powder (refined)**	24
Phenothiazine: Ionol** 50:50	32
Phenothiazine: Ionol** 30:70	36

*For samples containing two stabilizers, the combined concentration equaled 0.25%.

**A hindered phenol derivative.

GENERAL APPROACHES TO DEVELOPING A RADIATION-RESISTANT POLYMERIC MATERIAL

* Must, of course, consider many application-specific parameters besides radiation tolerance: processability, cost, toxicity, physical properties . . . . .

J17

1. Judicious choice of polymer type, based on literature information

2. Appropriate modification of polymer structure

   - Copolymers
   - Grafting

3. Incorporation of additives

- Energy deactivator antirads (generally polycyclic aromatics)
- Antioxidants
- Radical mobilizers
- Antiozonants

J18

4. Modification of irradiation parameters

5. Post-irradiation treatments

6. (Combination of the above)

7. PREDICTIVE AGING EXPERIMENTS

PHOTOCONDUCTIVITY EXPERIMENT

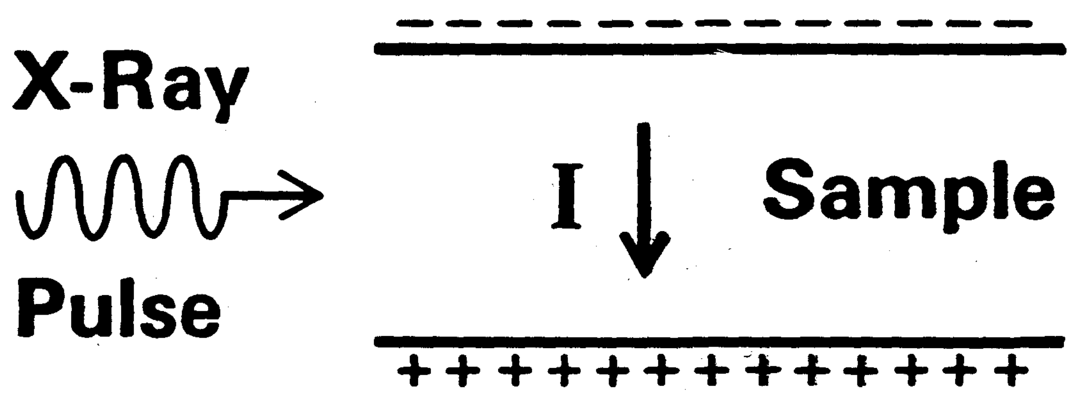

Conditions:

Dose rate = 30 rads/sec
E = 290 KV/cm^3

DC PHOTOCURRENT OF PET-TNF

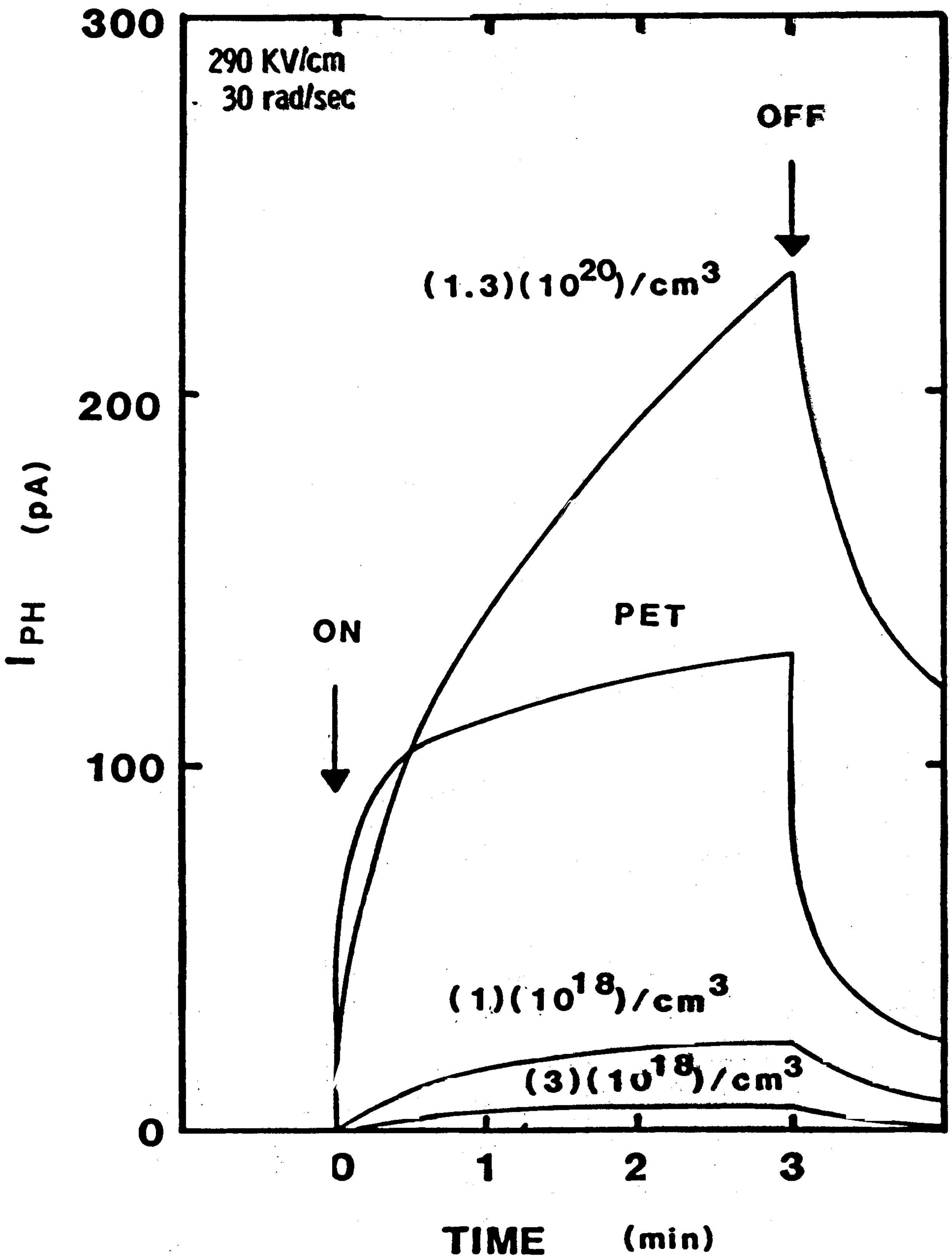

J20

CHEMICAL STRUCTURES OF MYLAR AND TNF

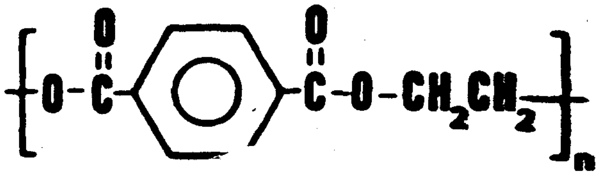

MYLAR

(POLYETHYLENE TEREPHTHALATE)

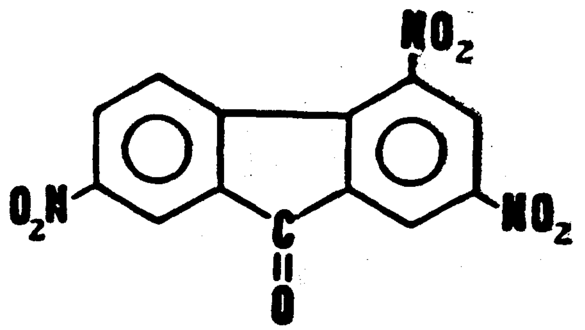

TNF

(2,4,7-TRINITRO-9-FLUORENONE)

RADIATION EFFECTS ON POLYMERS

APPLICATIONS

Nuclear Plants (U.S. ≅ 100, Worldwide ≅ 550)

Nuclear-Powered Ships

High-Energy Physics Installations (CERN, etc.)

Space Vehicles

Radiation-Sterilization of Disposable Medical Equipment

Polymer Processing: Cross-linking of Rubbers and Coatings

Misc: Defence, Nuclear Waste, Radiation Biochem, ...

APPENDIX K

"Results of Radiation Damage Experiments at BNL,"

Talk by Al Prodell

Appendix includes summary of experimental results.

Brookhaven Linac Isotope Production (BLIP)

BLIP is operated in conjunction with the AGS SEB under the following conditions:

Linac pulse of 200 Mev protons –

about 22 mA for 420 μsec repeated 5 times/sec

Once every 2.5 sec, AGS takes a pulse – so that

12/13 of the protons are directed to BLIP

Effective beam current = 42 μA

Beam profile – ~~half-width~~ FWHM ~ 2.1 cm

BLIP Target Holders

Foil Sample – diameter up to 3.81 cm

thickness up to 0.15 cm

Standard Sample – diameter up to 7.3 cm

thickness up to 2.26 cm

1 Gy = 100 rads = 10^4 ergs/gm = 6.24×10^9 Mev/gm

Assume, on the average, for 200 Mev protons, $\frac{1}{\rho}\frac{dE}{dx} = 3.5$ Mev $\frac{cm^2}{gm}$

Need 1.8×10^9 p/cm^2 for 1 Gy or

$$\frac{1.8 \times 10^9 \; p/cm^2}{6.28 \times 10^{12} \; p/\mu A\text{-sec}} = 2.87 \times 10^{-4} \; \frac{\mu A\text{-sec}}{cm^2}$$

For 40 MGy : 114.8×10^2 μA-sec/cm^2

For a target of 6.85 cm^2 and a beam current of 42 μA, exposure time is 1872 secs ~ 0.52 hrs or exposure is 21.84 μA-hrs.

Actual dose ~ 80 MGy, because beam area turned out to be ~ 3.5 cm^2

RADIATION SAMPLE RESULTS

Selected sample of trim coil substratum and components were prepared and assembled into film sample holders. The sample holders were sealed by electron beam welding to form targets. The targets were installed in the (Blip) Brookhaven Linac Isotope producer Beam Line. The sample targets were exposed to approximately 20 micro amp hours of proton beam at an energy of 193 MeV. The following tables present the qualitative results of the radiation effects on these samples. A qualitative rating system was devised *'s indicate any possible use as a trim coil material, 0 indicates no possible use in the samples condition at the time of exposure, --- indicates no results or a lost sample. Three and four * ratings indicate good to excellent results.

A summary of three and four star samples are also presented. Most of these materials will be proposed to be used as components in radiation resistant Multiwire trim coil assembly.

RAD Sample Results

Rating	Sample	Target	Description	Remarks
*	1	1A	Tefzel Sheet .001	Discolored near center, slightly brittle, LN_2 okay shrinkage, no loss in strength
**	2	1B	Tefzel on Kapton Dupont 400ZN031	No damage, some cracking after multiple cycling. Fair to good adhesion. Some de-lamination after severe bending.
***	3	1C	Disks of Kapton bonded by Tefzel	Very well bonded, some cracking, flakes de-laminating, but ductile at LN_2 temp. stays bonded.
---	4		Tefzel coated Kevlar	(Not in disk form could not be tested).
**	5	1D	Halar sheet	Sample appeared non ductile but did not discolor like Tefzel. Slightly brittle.
0	6	1E	Uncured and unsupported PK102 Adhesive only	Without backing material the sample completely, easily fractured, and disintegrated.
---	7	---	---	---
****	8	1I	Disks of Kapton bonded by Crest epoxy	No apparent damage. Excellent bonding.
(** as coating only) (0 bond)	9	1F	Disks of Kapton bonded by 3M2216BA6GRAY epoxy	Disks quickly delaminated, but adhesive was well bonded to Kapton, ductile at LN_2.

RAD Sample Results

Rating	Sample	Target	Description	Remarks
**	10	1G	Tefzel coated Kevlar on Kapton disk	Once cover sheet is removed, the bond between the Kevlar of yarns will crack and fail. No effect on LN_2 cycle thermostatic.
*	11	1J	Substratum disk Non cured PK102 and wire	Adhesive cracked at moderate bonding. Very poor wire bonding. Adhesive de-laminated from Kapton.
----	12	1K	Sheldahl 757-7-1	Lost at Blip.
0	13	1L	Sheldahl 757-7-6	Discolored, surface foamed up. Very brittle.
*	14	1M	Sheldahl 757-7-6A	Some bobbles, severe bending, adhesive will crack and flake off. Adhesive is well bonded after thermal cycling, but cracks when warm.

RAD Sample Results

Rating	Sample	Target	Description	Remarks
**	15	1N	Sheldahl 757-7-8	No noticable cracks or adhesive delamination. No dis-coloration. High differntial contraction.
***	16	1O	Sheldahl 757-7-9	Slightly bonded together, coated black. No visible effects or damage, (Possible Kapton adhesive alternative).
***	17	1P	Sheldahl 757-7-10	Disks slightly bonded together, but delaminated. No visible damage. No sign of differential contraction evi-dent. (Possible Kapton adhesive alternative).
0	18	1H	Halar bonded Apical (Kapton) disks	Sample de-laminated and adhesive cracked into pieces, slightly ductile.
** (glue only)	19	1Q	Sheldahl 757-7-11	Disks glued together but separates when flexed, adhesive is intact. *Glue intact.*

RAD Sample Results

Rating	Sample	Target	Description	Remarks
**	20	1R	Sheldahl 757-7-12	If it had adhesive it turned white-yellow. Little or no effect. *No effect. Glue intact.*
---	21	1S	Kapton disks bonded together with Barcel PV adhesive	Lost at Blip.
***	22	1T	Light PV coated S-2 glass by Barcel	Execellent; no visible damage, but some glass fiberious delamination. When cold the glass cracked, but the Kapton stayed adhered to glass.
****	23	1U	Heavy PV coated S-2 glass by Barcel	No effects, glass is slightly brittle. Excellent adhesive.
***	24	1V	Tefzel coated Kapton	Some cracking when bent, but layers stayed bonded together. Did not show bond change when temp. cycled.
0	?	1W	Kapton disks bonded together	Fell apart when slightly bent or creased.

RAD Sample Results

Rating	Sample	Target	Description	Remarks
***	25	1X	Bonded strips of Kapton and Tefzel. Dupont 120ZN616	Some delamina- when bent severely creased. Sample did not delami- nate and was still ductile at LN_2 temp.
0	26	1Y	Fully cured RC205 substratum, bonded to stainless steel	>60 mr/hr surface is flaking off exposing glass. De- laminations from steel very brittle, cracks on bending. De- laminated when thermal cycled.
***	27	1Z	Non cured Wired RC205 substratum	Adhesive darkened. Fair adhesion, did not crack. Wire peel strength ≈ 5 oz./wire survived LN_2 cycle. Some delamination when creased.
*	28	2A	Non cured RC205 substratum	Very brittle, no temp. cycle effect, blackened sample cracked and pulled apparently easily.

RAD Sample Results

Rating	Sample	Target	Description	Remarks
0	29	2B	Fully cured Wired RC205 substratum bonded to stainless steel	Blackened, delaminated cracks, very hot > 90 MR/HR. When bent. Little effect of cold shock. Wire peels strength < 2 oz./wire.
---	30	2C	Wired PK102 on Kapton	Lost at Blip.
****	31	2D	Multiwire #6, 6s substratum, PK102 on Kapton	Discolored, good adhesion, to Kapton survives severe bending. Good results.
****	32	2E	Multiwire #3 wired. Substratum PK102 and glass on Kapton	Kapton delaminates Somewhat from glass composite is still ductile. Good peel strength 5-7 oz./wire. Glass could be added to PK102. Survives LN_2 cycling. Very well.
0	33	2F	Multiwire #3 unwired substratum PK102 and glass on Kapton	Extremely brittle, Partially disinte-grated.

RAD Sample Results

Rating	Sample	Target	Description	Remarks
**	34	2G	Outgassed PK102 substratum high volital wire wired	Cover sheet well bonded. Wire peak strength 5-6 oz./ adhesive. Did become foam like.
0	35	2H	PK102 between layers of Kapton	Survived outgassing, brittle, adhesive becomes disintegrated when flexed.
****	36	2I	PK102 adhesive and wired substratum bake	Good cold properties. Sample still ductile. Some cracking but adhesive did not crack off. Good bonds even after severe bending. Wires bonded well, but peel strength ≈ 3 oz./wire.
**	37	2J	PK102 on Kapton substratum Unwired	Some chipping after bending. Quite ductile. Survived creasing, some cracks of Tefzel, but survived LN_2 shocks.

RAD Sample Results

Rating	Sample	Target	Description	Remarks
	38			
	39			
0	40	2K	Multiwire #3 glass press baked. Substratum PK102	Cracks apart after bending, substratum discolored alot or foaming. Delamination 3 oz./wire peel.
*	41	2L	Multiwire #4 wired substratum. Fully cured PK102	Wire peeled off on bending. Wire pole, stayed together, cover sheet still bonded.
0	42	2M	Multiwire #4 unwired substratum Fully cured PK102	Foamed, disintegration, came apart on bending and creasing.
***	43	2N	*Multiwire #6 fully cured substratum, no outgassing with Tefzel on Kapton	Cover sheet stayed intact. Wire peel ≈ 3 oz./ wire. Sample discolored. Poles survived abrasions. Fair cold effects, some wire delamination.

RAD Sample Results

Rating	Sample	Target	Description	Remarks
***	44	2O	Multiwire #5 stratum baked without cover sheet with Tefzel on on Kapton	Adhesive delaminated from Kapton on bending into fine chards. Good low temp. Ductility. PK192 adhesive stayed on Kapton.
**	45	2P	Multiwire #5 substratum wired bakeout without cover sheet with Tefzel on Kapton	Good adhesive to Kapton. Low wire adhesive peak 2-1.5 oz./wire. Some delamination on cold shocking. Fair to good results.
*	46	2Q	Rogers TMM-3 standard	Gray disk. Very brittle, but does not chard. Fairly weak.
**	47	2R	Rogers TMM-3 toughened	Very brittle, discolored. Stronger than 2Q, gray partial disk.
0	48	2S	Rogers T6-9 standard	Disintegrated and melted into a cat's eye, sharp brittle. *Sample exploded target*.
0	49	2T	Rogers T6-9 toughened	Brittle to the touch. Disintegrated.

RAD Sample Results

Rating	Sample	Target	Description	Remarks
**	50	2U	Rogers fleximide	Some delamination, but survived LN_2 cycling, some discoloration.
**	51	2V	Tefzel on glass	Very little cold ductility, but was intact.
****	52	2W	Disk of Rogers Envex	Excellent. No visible effects.

Summary of RAD Results

Rating	Sample	Target	Description	Remarks
3*	3	1C	Kapton layers bonded with Tefzel	To be used in trim coils. *
4*	8	1I	Crest 7450	*
3*	17	1P	Sheldahl 757-7-10	
3*	22	1T	Light PV coated glass by Barcel	
4*	23	1U	Heavy PV coated (double coated) glass by Barcel	*
3*	25	1X	Dupont 120ZN616 Kapton bonded with Tefzel	*
3*	27	1Z	Non cured and wires RC205	
4*	31	2D	Multiwire #6 PK102 on Kapton	*6/3
4*	32	2E	Multiwire #3 PK102 glass on Kapton	*6/3
4*	36	2T	PK102 adhesive wire and bakeout	*6/3
3*	43	2N	Multiwire #6 baked and outgassed Tefzel on Kapton	*6/3
3*	44	2O	Multiwire #5 baked without cover sheet and Tefzel on Kapton	
4*	52	2W	Rogers Envey	*

APPENDIX L

"Proposals for New Materials,"

Talk by John Skaritka

CHANGES

1. FEP TEFLON WILL BE REPLACED BY TEFZEL ON ALL LAMINATED ADHESIVE MEMBERS

   REASONS A.. SUPERIOR RADIATION RESISTANCE

   B. SUPERIOR ADHESION AFTER MULTIPLE THERMAL CYCLING.

   C. LOWER THERMAL BONDING TEMP. THEN FEP

2. KEVLAR WILL BE REPLACED BY GLASS

   A. A NEGATIVE THERMAL CONTRACTION COEFFICIENT

   B. SUPERIOR RADIATION RESISTANCE

   C. REDUCED COST.

3. .008" MONOFILIMENT SUPER CONDUCTOR WILL BE REPLACED BY .014" MULTIFILIMENT WIRE.

   A. REDUCE MAGNETIZATION

   B. IMPROVE MECHANICAL INTEGRITY

   C. GREATER POTENTIAL CORRECTION

4. POLYMIDE FILM COATED WIRE WILL BE REPLACED BY .0005" KAPTON WRAPED WIRE

   A. EXPERIMENTS HAVE SHOWN SUPERIOR PROFORMANCE TO FILM COATED WIRE.

   B. WILL TAKE UP MOTIONS DUE TO DIFFERENTIAL CONTRACTION WITH OUT IMPARTING A STICK SLIP REACTION.

5. FEP COATED (KEVLAR) WILL BE REPLACED BY A POLYIMIDE ADHESIVE

   A. SUPERIOR RADIATION RESISTANCE

   B. LOWER THERMAL BONDING TEMP.

6 RC 205 BASED SUBSTRATUM WILL BE REPLACED BY A PK102 BASED SUBSTRATUM.

   A. SUPERIOR RADIATION RESISTANCE

   B. SUPERIOR THERMAL STABILITY

   C. SIMPLIFICATION OF DESIGN

   D. REDUCED COST

   E. TRANSLUCENT SUBSTRATUM WILL ALLOW SUPERIOR QC PROCEDURES.

7. RX-630 LOCATION KEYS AND PINS WILL BE REPLACED BY POLYIMIDE BASED ENVEX.

A. SUPERIOR RADIATION RESISTANCE

8. 815V40 AND 3M 2216BA WILL BE REPLACED BY CREST 7450 EPOXY

A. SUPERIOR RADIATION RESISTANCE

B. SUPERIOR STRENGTH AND MECHANICAL PROPERTIES AT LOW TEMPS.

C. EASY ASSEMBLY AND HIGH SPEED PRODUCTION.

9. G-10 BUMPERS WILL BE REPLACED BY EXTRUDED KAPTON BUMPER STRIPS COATED WITH CREST 7450 EPOXY

A. SUPERIOR RADIATION RESISTANCE

B. EFFICIENT ASSEMBLY FOR HIGH SPEED PRODUCTION.

C. ALLOWS MALFORMATIONS IN DIPOLE COIL WITHOUT CRUSHING BEAMTUBE

10. KAPTON COVERSHEET WITH FEP LAYER WILL BE REPLACED BY POROUS "N" KAPTON LAYER.

A. SIMPLIFICATION OF COIL PREPORATION

11. WHERE POSSIBLE THE FEP COATED KAPTON WILL BE REPLACED BY "N" FILM.

A. SIMPLIFICATION AND REDUCED COST.

FUTURE DESIGN

FEB. 88

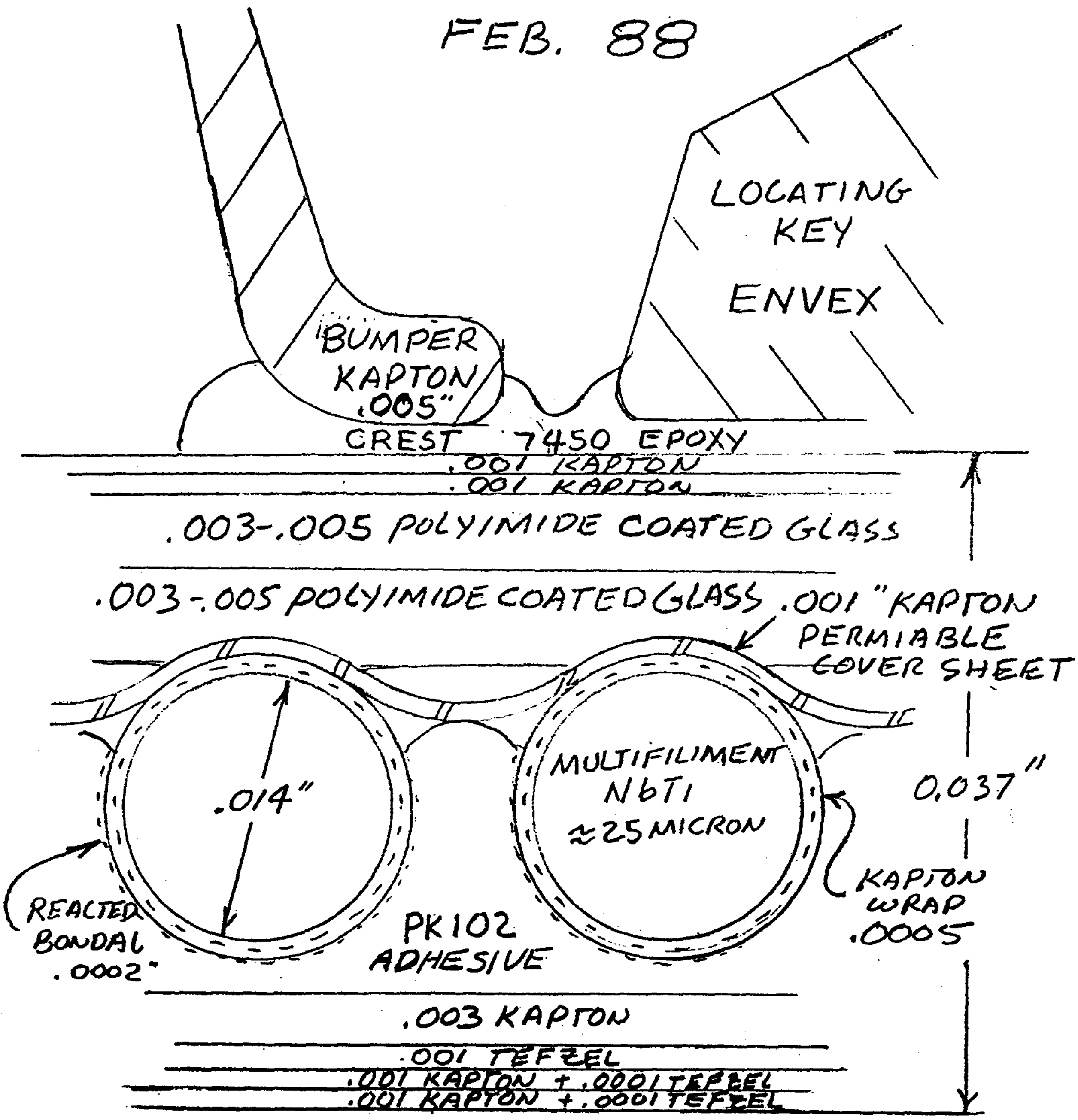

NITRONIC - 40 SST

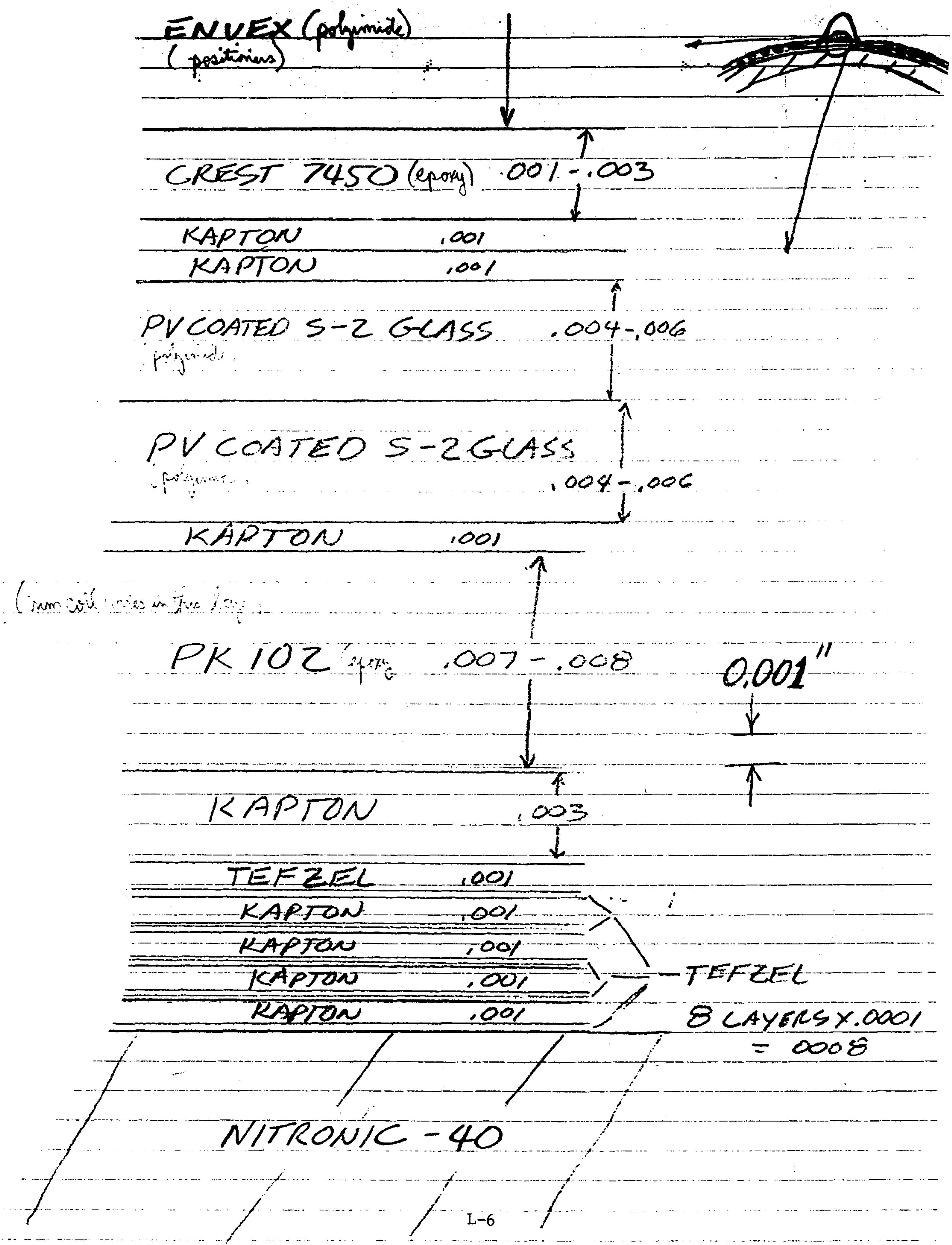

ENVEX (polyimide)
(positioners)
CREST 7450 (epoxy) .001 - .003
KAPTON .001
KAPTON .001
PV COATED S-2 GLASS .004-.006
polyimide
PV COATED S-2 GLASS
polyimide
.004 - .006
KAPTON .001
PK 102 epoxy .007 - .008
0.001"
KAPTON .003
TEFZEL .001
KAPTON .001
KAPTON .001
KAPTON .001
KAPTON .001
TEFZEL
8 LAYERS X .0001
= .0008
NITRONIC - 40

THESE MAY NOT BE THE FINAL CHANGES.

FUTURE IMPROVEMENTS COULD BE THE USE OF

1. LOW TEMPERATURE THERMOPLASTIC POLYIMIDES WHICH CAN BE USED TO REPLACE TEFZEL. OUTGASSING OF SOLVENTS ARE PROHIBITED IN THIS APPLICATION

2. POSSIBLE ULTRASONIC BONDABLE THERMOPLASTIC POLYIMIDE COULD BE USED TO REPLACE THE PK102

THE ABOVE OPTIONS SHOULD BE INVESTIGATED AS POSSIBLE IMPROVEMENTS TO TRIMCOILS PRODUCED IN 1989

☆ INSTRUMENTATION THAT WILL DETECT FLAWS SUCH AS A POOR ADHESIVE BOND LINES AND AIR GAPS IN THE COIL ASSEMBLY WILL ALSO BE INVESTIGATED.

☆ OBSERVATIONS OF RADIATION EFFECTS ON THE VARIOUS MATERIALS TESTED WILL BE PART OF THE SUMMARY REPORT. ☆

A PROGRAM IS UNDERWAY TO MAKE THE TRANSITION BETWEEN OUR PRESENT TRIM COIL DESIGN AND THE OPTIMISED DESIGN.

1. A SERIES OF .6 METER SEXTUPOLE COILS WILL BE PRODUCED WHICH WILL SHOW A GRADUAL TRANSITION BETWEEN OUR PRESENT DESIGN AND THE OPTIMISED DESIGN.

2. ONCE A .6 METER OPTIMISED MODEL IS PROVEN SUCCESSFUL, SEVERAL 1.8 METER COILS WILL BE PRODUCED AND TESTED AT FULL FIELD. THESE COILS WILL BE BUILT BY FEBUARY. 88

3. AFTER THE FIELD STRENGTH TRAINING BEHAVIOR AND FIELD QUALITY IS PROVEN ACCEPTABLE 17 METER TRIMS WILL BE BUILT AND TESTED IN FULL LENGTH DIPOLES

NOTE: ANY OTHER IMPROVEMENTS WILL BE TRIED OUT IN .6 AND 1.8 METER LENGTHS AND PROVEN BEFORE 17 METER TRIMS ARE ATTEMPTED.

APPENDIX M

"Cryogenic Performance of Materials,"

Talk by Mort Katz

DU PONT FLUOROPLASTIC RESINS

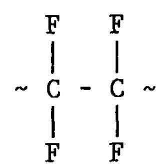

TEFLON® PTFE

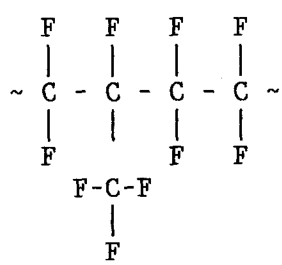

TEFLON® FEP

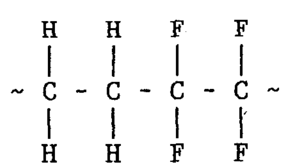

TEFZEL®

TYPICAL PROPERTIES OF TEFLON® RESINS

	TEFLON® TFE	TEFLON® FEP	TEFZEL® ETFE
M.P. °C.	327	253-282	270
Upper Service, °C.	260	200	150-177
Coefficient of Friction	.04-.08	.06-.10	.4
Dissipation Factor, 60-10^9 Hz	.00002- .00045	.00004- .0012	.0006- .005
Flex. Mod., PSI at RT	40-90 x 10^3	95 x 10^3	200 x 10^3
Izod Impact, ft.-lb./in.	3	No Break	-
Specific Gravity	2.14-2.21	2.12-2.17	1.70
T.S., PSI at RT	3000-5000	3000-4000	6500
U.E., % at RT	250-450	300	-
Diel. const. 60-10^9 Hz	2.1	2.1	2.6
Vol. Resistivity, ohm-cm	10^{18}	10^{18}	-

TEMPERATURE DEPENDENCE OF CHARPY IMPACT STRENGTH

(ASAHI)

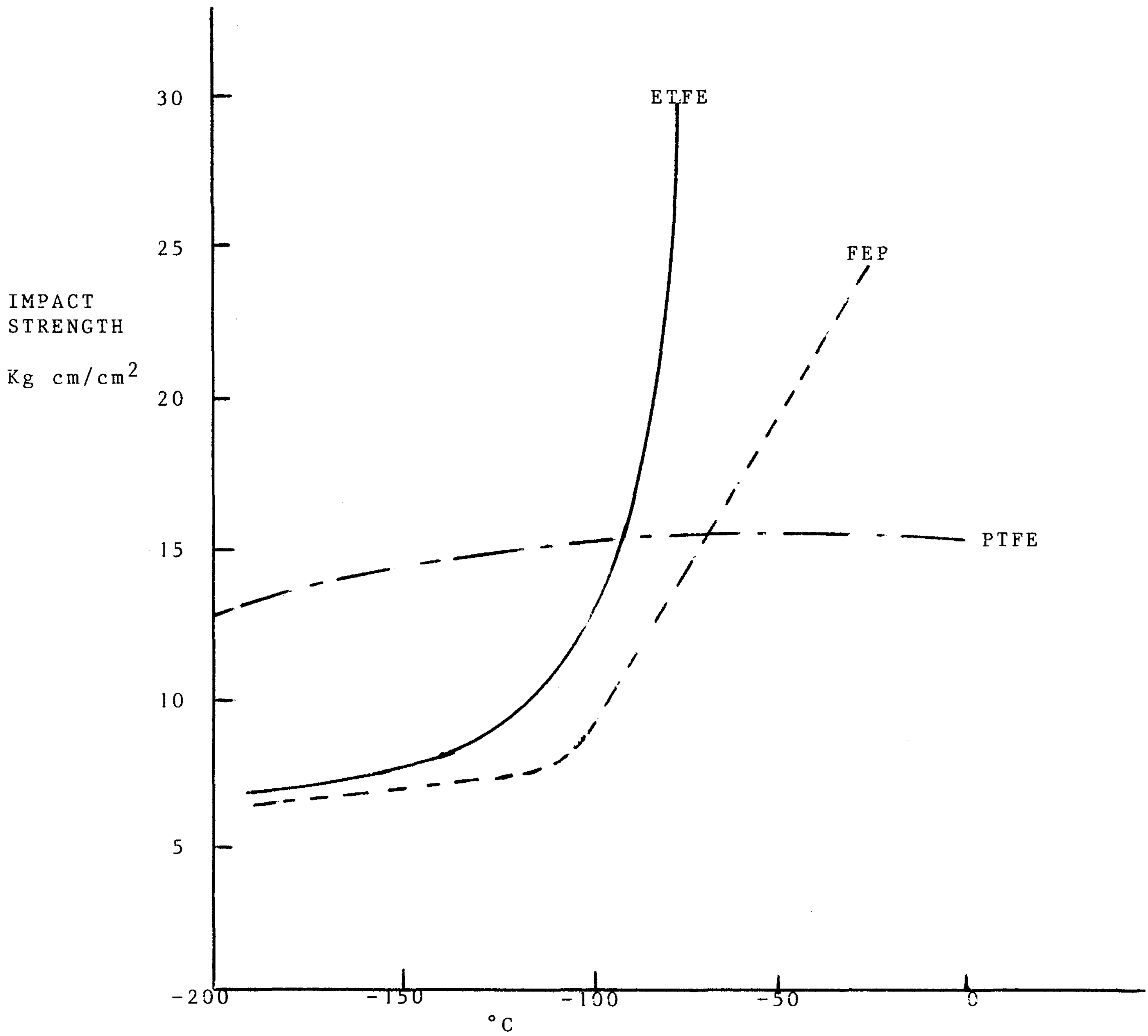

CRYOGENIC MECHANICAL PROPERTY OF SELECTED BULK MATERIALS

MATERIAL	ULTIMATE TENSILE STRENGTH AT 77K, MPa (PSI)
VESPEL® 211	100 (14,500)
VESPEL® 92Y77	105 (15,000)
DELRIN®	140 (21,000)
TEFZEL®	83 (12,000)
INSULATION PAPER	45 (6,500)

MEAN ELECTRIC STRENGTH OF POLYMERS

POLYMER	AC DIELECTRIC STGRENGTH (MV/m(rms))			DC DIELECTRIC STRENGTH		
	LIQ. N_2	LIQ.He	VACUUM 5°K	LIQ. N_2	LIQ.He	VACUUM 5°K
PE	401	233	440	580	294	535
TEFLON® PTFE	294	189	350	430	255	510
TEFLON® FEP	209	230	468	310	400	720
KAPTON®	371	300	630	540	420	882

DC BREAKDOWN VOLTAGE AND ELECTRIC FIELD
AT 12K UNDER 1.38 MPa OF HELIUM PRESSURE

MATERIAL	MEAN (kV/mm)	STD. DEV. (kV/mm)	PUNCTURE/ FLASHOVER
KAPTON®	358.7	85.63	4/32
TEFLON® FEP	312.9	31.7	18/18
MYLAR®	308.4	38.4	5/31
NOMEX®	92.5	14.5	35/0
PINK POLY	216.1	30.9	33/0
VALERON	303.9	31.6	30/5

DISSIPATION FACTOR OF 125 MICRON KAPTON® WITH VARYING FREQUENCY AND STRESS AT 77K

Frequency (Hz)	Stress (MPa)	Dissipation Factor
1×10^2	0	.015
1×10^2	48	.018
1×10^2	96	.020
1×10^3	0	.009
1×10^3	48	.009
1×10^3	96	.010
1×10^4	0	.010
1×10^4	48	.010
1×10^4	96	.015

ELECTRICAL POST IRRADIATION TESTS PERFORMED

TEST	ENVIRONMENT	TEMPERATURE (K)
IN-SITU RESISTIVITY	HELIUM	4.9-300
POST IRRADIATION RESISTIVITY	DRY N_2	300
BREAKDOWN	AIR	300
DIELECTRIC LOSS FACTOR	AIR	300

RESULTS OF ELECTRICAL MEASUREMENTS[a]

MATERIAL	RESISTIVITY (TΩ m)		RESISTIVITY (TΩ m)		BREAKDOWN MV/m		DISSIPATION FACTOR (1 kHz)	
	C	I	C	I	C	I	C	I
Stycast 2850	10	3.5	140	50	32[b]	32[b]	0.024	0.023
Epon 828	15	7.5	100	60	24[b]	23[b]	0.026	0.028
G-10 CR	7	5	70	70	22[b]	22[b]	0.022	0.024
EF 527			120	0.05	31	11	0.025	
Nomex 410	35	15	130	140	38	39	0.008	0.008
Kapton® F			150	190	70[b]	57[b]	0.008	0.008

[a] C = Control, I = Irradiated

[b] Surface flashover, not breakdown

TABLE I

EFFECT OF GAMMA EXPOSURE ON "KAPTON"* POLYIMIDE FILM

PROPERTY	CONTROL (1 MIL FILM)	Co^{60} SOURCE (OAK RIDGE) 10^6R 1 HR	10^7R 10 HRS	10^8R 4 DAYS	10^9R 42 DAYS
Tensile Strength (K psi)	30	30	31	31	22
Elongation (%)	80	78	78	79	42
Tensile Modulus (K psi)	460	475	490	475	421
Volume Resistivity, 200°C (OHM-CM)	4.8×10^{13}	6.6×10^{13}	5.2×10^{13}	1.7×10^{13}	1.6×10^{13}
Dielectric Constant (1 KC)	3.46	3.54	3.63	3.71	3.50
Dissipation Factor (1 KC)	.0020	.0023	.0024	.0037	.0029
"Mylar"* Polyester Film				$<$50% of initial tensile & elongation	$<$10% of initial tensile & elongation
"Teflon"* FEP-Fluorocarbon Film				$<$10% of initial tensile & elongation	

*Reg. U. S. Pat. Off.

TABLE I

(Continued)

EFFECT OF GAMMA EXPOSURE ON "KAPTON"* POLYIMIDE FILM

Co^{60} SOURCE (LANGLEY RESEARCH CENTER)

PROPERTY	CONTROL	2×10^9R AIR	2×10^9R VACUUM
Tensile Strength (K psi)	21.7	17.2	24.4
Elongation (%)	87	36	84

TABLE II

EFFECT OF ELECTRON EXPOSURE ON "KAPTON"* POLYIMIDE FILM 2 MEV ELECTRONS (VAN DE GRAAF)

PROPERTY	CONTROL (2 MIL FILM)	1×10^9R	2×10^9R	3×10^9R
% of Initial Tensile and Elongation Retained	100%	89%	78%	75%
Volume Resistivity 23°C (OHM-CM)	6×10^4	6×10^{14}	5×10^{14}	3×10^{14}
Dielectric Strength (V/mil)	1700	1610	1720	1695
Dielectric Constant (1 KC)	3.5	3.4	3.9	4.2
Dissipation Factor (1 KC)	.0062	.0310	.0259	.0388

*Reg. U. S. Pat. Off.

TABLE III

EFFECT OF NEUTRON EXPOSURE ON "KAPTON"* POLYIMIDE FILM
MIXED NEUTRON AND GAMMA RADIATION (BROOKHAVEN PILE)

	5×10^9 R	10^{10} R
Temperature 175°C Flux 5×10^{12} N/cm^2/sec.	Film Darkened	Film Darkened and embrittled

TABLE IV

EFFECT OF ULTRAVIOLET EXPOSURE ON "KAPTON"* POLYIMIDE FILM
(LEWIS RESEARCH CENTER)

	CONTROL	1000 HRS. VACUUM
Tensile Strength (K psi)	21	21
Elongation (%)	106	78

*Reg. U. S. Pat. Off.